

FRACTURING OIL SHALE WITH EXPLOSIVES  
FOR IN SITU RECOVERY

by

J. S. Miller<sup>1</sup> and Robert T. Johansen<sup>2</sup>  
Bartlesville Energy Research Center, Bartlesville, Okla.

## ABSTRACT

Three different explosive fracturing techniques developed by the Bureau of Mines for preparing oil shale for in situ recovery on eight experimental sites near Rock Springs, Wyo., are discussed. The fracturing procedures included (1) displacing and detonating nitroglycerin in natural or hydraulically induced fracture systems, (2) displacing and detonating nitroglycerin in induced fractures followed by wellbore shots using pelletized TNT, and (3) detonating wellbore charges using pelletized TNT.

The research on oil shale formations demonstrated that nitroglycerin displaced into natural or hydraulically induced fractures could be detonated with the resulting explosion propagating through the explosive-filled fracture. Sufficient fragmentation was obtained to sustain an in situ combustion experiment by these procedures. Detonating nitroglycerin in fracture systems and pelletized TNT in wellbores of various well patterns at 100-ft depth developed extensive rock fragmentation, thereby achieving interwell communication suitable for in situ recovery experimentation. The remaining explosive fracturing technique used

---

<sup>1</sup> Petroleum engineer.  
<sup>2</sup> Research supervisor.

charges of pelletized TNT in repetitive wellbore shots at depths ranging from 340 to 386 ft in various well arrays. Results from the shooting caused fragmentation of rock around the wellbore and provided some interwell communication. However, the resulting flow capacity between wells was deemed insufficient to support an in situ recovery experiment when compared with results from shallower tests at other sites.

### INTRODUCTION

The research was started in 1964 as a part of the energy research program of the Bureau of Mines. The goal of the research described here was to develop means for fragmenting the oil shale with explosives and to expose sufficient rock surface area to achieve in situ combustion recovery of shale oil. These studies are relevant to the rising concern for our capability to meet this Nation's mounting energy demands at reasonable costs and an acceptable level of social and environmental impact.

The concept involves the injection and detonation of a liquid chemical explosive in natural or previously induced fracture systems or the use of a pelletized explosive to enlarge and extend these fractures to provide fragmentation and interwell communication. This study is one of few known research efforts to evaluate results of detonating sheetlike layers of explosive intending to increase flow capacity in confined rock formations. The literature contained little information on this subject to serve as guidelines for the design of the experiments. Some related work, however, had been conducted by a few individuals and oilfield

service companies. Briefly, the earlier work resulted in moderate successes, near failures, injuries, and numerous premature detonations that destroyed wells and property. One report (16)<sup>3</sup> recorded an account of a combined shot of 5,000-qt

---

<sup>3</sup> Underlined numbers in parentheses refer to items in the list of references at the end of this report.

---

nitroglycerin (NGI) displaced into the formation from a wellbore loaded with glass marbles in the Turner Valley field during February 1946. Oil flow was not increased, and no further shooting was done following the experiment.

Brewer (2) indicated that the Tar Springs, Jackson, and Benoist Formations in the Illinois Basin responded when the voids in these low-permeability formations were filled with explosives and detonated. Further, the Cleveland and Red Fork sands in Oklahoma were reported to have responded to NGI shots in the formation. Data on individual tests and detailed results were not publicized.

Included in U.S. patents relating to explosive fracturing are those of Zandmer (18, 19), Brandon (1), Hanson (8), and Hinson (10). Results of the patented Stratablast process were reported at a meeting of the American Petroleum Institute in April 1965 (17). The multiple component systems used were generally hypergolic fluids that explode when combined in the formation. In 1970, an article (11) reviewed the "new look" at stimulation by explosives and gave a state-of-the-art account of the modern explosive techniques for improving production.

The extensive oil shale formations in parts of Wyoming, Colorado, and Utah cover an area of approximately 16,000 square miles (Fig. 1). These rocks of the

Green River Formation originated as limey muds deposited in predominantly lacustrine environments. Through geologic processes these lake floor deposits were transformed into marlstone containing organic kerogen, which requires considerable heat to change it into a liquid shale oil. Because the host rock has little natural porosity and permeability, fractures must be induced through which the injected air can establish and maintain a combustion zone and to provide a means to recover the retorted shale oil.

Surveys (6) show that oil shale deposits in the United States testing 25 gal or more per ton contain about 600 billion bbl of oil. These deposits range in depths from surface outcrops to 2,000 ft. If a lower limit of richness is set at 10 gal/ton, the available volume of oil would be increased 25-fold to about 2 trillion bbl. The development of a technique for efficient shale oil recovery would significantly influence the Nation's total oil supply.

Development of mining and aboveground retorting of oil shale has only recently advanced beyond the experimental stage. In addition, aboveground oil shale processing is accompanied by ecologic disturbances with the attendant water supply and pollution problems of effluents and disposal of spent shale. Underground retorting potentially offers a more feasible solution to the problem. Bureau of Mines laboratory and field research on the use of chemical explosives to fracture the rock lends encouragement for developing means to accommodate the airflow requirements to maintain combustion, and for displacing retorted shale oil to producing wells.

Explosive fracturing was applied to the Green River Formation on eight sites near Rock Springs and Green River, Wyo.; three of which are described in

this paper. Descriptions of procedures and explosive fracturing evaluation methods relating to the sites have been reported (4, 14, 15). The methods used to fragment the formation differed from site to site because of the differences in depth to the richer shale beds at the various sites, differences of ground water levels, the extent of natural or induced fractures encountered, and the type of explosive used to fracture the shale.

#### FIELD TEST, ROCK SPRINGS SITE 4

##### Purpose

The first research program designed for the recovery of shale oil by in situ combustion was planned for Rock Springs site 4. Little information has been published about in situ retorting methods for production of shale oil (5, 7, 9). The experiment was designed to establish sufficient fracture permeability through expanding natural fractures, inducing hydraulic fractures, and by chemical explosive fracturing (12).

##### Procedure

The site was developed on a five-spot pattern about 25 ft square, as shown in Fig. 2. The wells were rotary drilled with water and completed with 50 ft of 7-in casing and cemented to the surface. A 6 1/4-in hole was drilled below the casing to a total depth of 100 ft in the oil shale. Two additional wells were drilled off pattern as observation wells. A Fischer assay determined the oil yield of the section to range from 19.0 to 26.5 gal/ton. Two sand-propped hydraulic fracture treatments were applied for emplacing NGI in the formation.

In the first two tests of a series of three explosive fracturing experiments, well 3 was used for the injection and displacement of 100 and 300 qt of NGI in the depth intervals from 70 to 74 ft. Continuous sampling of surrounding test wells showed that the NGI migrated to a second well during each injection. Detonators were set in each well, and the explosive charges were detonated simultaneously.

To further improve interwell communication, a hydraulic fracturing treatment was performed at a depth of 79 to 84 ft in well 5 to assure the displacement and detonation of the 300 qt charge of NGI.

The effectiveness of the three fracturing techniques was determined by measuring airflow rates between selected wells before and after each test.

#### Results

The first explosive fracturing test detonated 100 qt of NGI displaced into the formation from well 3 at a depth interval from 70 to 74 ft. Following detonations in wells 3 and 4, fracture intervals in the wellbores connecting the injection well 3 and other wells were determined by airflow measurements.

Comparing these airflow intervals with those permeable zones induced by conventional hydraulic fracturing indicated that explosive fracturing created additional communication paths to wells 2 and 5 at the 73-ft level; however, the injection capacity of well 3 was reduced 64 percent. This reduction in injection capacity may have resulted from too wide a dispersion of the liquid explosive, so that the shot did not have sufficient strength to lift and fracture the overburden rock permanently, or the fractures may have been plugged by fine oil-shale particles or mud.

The detonation of the first 300 qt charge of NGI resulted in ground movement recorded at a particle velocity of 2.5 in/sec. Air-entry intervals that existed after the first 100 qt shot were not apparent after the 300 qt shot; however, new zones were opened to airflow. The injection capacity was increased by 500 percent.

The volume of the fractures created by the 300-qt NGI shot in well 3 was estimated by water fillup to be 800 cu ft. This was the amount of water removed from the wells in the test area by pumping and bailing.

Surface-elevation changes (Fig. 3), brought about by the explosive work, ranged from 1.20 in at well 1 to 1.92 in at well 3 in the five-spot test pattern to 0.84 and 0.60 in, respectively, at off pattern wells 6 and 7. The contours of surface elevation change indicated that the change was almost proportional to the distance from the NGI injection well 3.

Void volume based on the elevation-change contours and the area enclosed by the dashed line in Fig. 3 was calculated to be nearly 150 cu ft. The total area affected by explosive fracturing could not be determined because of the lack of elevation-measuring stations outside of the contoured area.

Detonation of the second 300-qt NGI charge (well 5) resulted in a particle velocity of 2.2 in/sec measured at the surface, indicating complete detonation. Airflow tests were made, and the air-injection capacity was increased about 800 percent. These air-injection rates were judged to be sufficient to support a planned in situ combustion experiment.

Although the nature and extent of fractures created in the oil shale by the various fracturing techniques are not completely known, some generalizations can be made.

Horizontal fractures were opened to all wells in the original five-spot pattern with no apparent vertical communication established, except in the area between wells 3 and 5 where greater rock breakage with horizontal and vertical fracturing resulted from the explosive fracturing.

In general, hydraulic fracturing with sand propping provided adequate void space for emplacement of the NGI in these explosive-fracturing tests in the oil shale. Explosive fracturing caused significant increases in fracture permeability when a sufficient NGI charge was detonated.

Results from a subsequent in situ combustion experiment on this site (3), to produce shale oil from oil shale, indicated that combustion could be sustained in an explosively fractured zone.

#### FIELD TEST, ROCK SPRINGS SITE 5

##### Purpose

Explosive-fracturing research at Rock Springs site 5 was designed to develop additional expertise in creating sufficient fragmentation and permeability in the oil shale to support in situ retorting. Results obtained from previously completed field applications indicated that detonation of a liquid explosive in natural or hydraulic fractures effectively lifted the overburden, extended existing fractures, and fragmented the oil shale formations (4, 13). At this stage of the research, it was not possible to either precisely describe or adequately evaluate the fractures. Consequently, to achieve maximum fracturing, a combination method of explosive fracturing was used: (1) Displace and detonate a liquid chemical explosive in a

natural fracture system, and (2) use pelletized TNT in a series of wellbore shots as the principal means to fragment the oil shale for in situ retorting.

### Procedure

#### Site Preparation

A five-spot pattern of test wells (Fig. 4) was drilled to an approximate depth of 57 ft and completed with 7-in casing cemented to the surface. The wells, deepened to 100 ft with a 6 1/4-in bit, were tested to determine the extent of air communication between the center well (well 5) and the surrounding wells. These tests indicated fractures ranging from 1 to 3 ft in height between depths from 67 to 90 ft.

#### Explosive Fracturing

To fragment the oil shale, three types of explosives were used: desensitized NGI, 60-percent dynamite, and pelletized TNT.

Figure 5 shows the positions and sequence of all shots on Rock Springs site 5. A 340 qt charge of NGI was displaced from well 5 into the natural vertical fracture system (SHOT A, Fig. 5), and was detonated successfully. This detonation was intended to lift the overburden and create space for fragmenting more shale by use of other explosives through repetitive simultaneous wellbore shooting. Elevation measurements were obtained on the casing heads of each well before and after detonation to determine residual crowning of the overburden rock.

During the second step of the fracturing experiments at this site, 60 percent dynamite was detonated in the five wells to relieve stress conditions in the block of oil shale. Each of the wells in the 25- by 25-ft five-spot pattern was loaded with

45 lb charges of 60 percent dynamite on detonating cord with electric caps attached, and detonated simultaneously (SHOT B).

Theoretically, to fragment the block of oil shale, by detonating wellbore charges of pelletized TNT, the area around center well 5 should be enlarged or "sprung." This would be accomplished by repeated wellbore shots from bottom to top of the test zone. The broken and enlarged area surrounding the wellbore would serve as a free face to enhance effects from later simultaneous wellbore shots across the pattern.

Six shots (C, D, G, H, I, K) using approximately 1,000 lb of TNT, were detonated in well 5 at depths ranging from 67 to 88 ft. The first three shots were not stemmed; consequently, water and debris were blown to the atmosphere. The last three shots were sand tamped to the surface to fragment the maximum amount of oil shale around the wellbore and permit the contained explosive gases to extend the induced fractures.

Two shots (E-E, F-F), using a total of 536 lbs of TNT, were detonated in wells 3 and 4 between depths of 71 and 87 ft.

After cleanout in wells 1 and 2, 150-lb charges of TNT were placed in each hole to depths of 85 and 83 ft, respectively, and detonated (SHOT J-J).

Wells 2 and 4 were cleaned out and a total of 250 lb of TNT filled the holes to depths of 76 and 77 ft, respectively, and were detonated (SHOT L-L).

Wells 1 and 3 were prepared for reshooting by charging 150 lb of TNT in each wellbore at depths of 77 and 74 ft, respectively, and were detonated (SHOT M-M).

This explosive fracturing series was concluded by loading the four outside wells 1, 2, 3, and 4 with charges of 296, 225, 185, and 185 lb of TNT and shooting simultaneously at depths of 75, 72, 69, and 73 ft, respectively (SHOT N-N).

### Results

Although the numerous methods used to evaluate underground fractures created by confined explosive fracturing techniques in oil shale under this site revealed much information, the data obtained from the evaluation tests showed that the oil shale formation exposed to the effects of explosive fracturing was extensively fragmented. The data also indicated that the fragmented zone was roughly ovaloidal in shape, approximately 95 ft in diameter and 70 ft thick. Extensive fracture systems were detected by airflow tests at a distance of 90 ft from the center well of the five-spot pattern.

## FIELD TEST, GREEN RIVER SITE 1

### Purpose

This fracturing program was intended to devise an effective method to fracture the formation with wellbore shots. More specifically, Green River site 1 was developed to test chemical-explosive-fracturing procedures for establishing communication between wells at greater depths and well spacings than had been previously attempted in oil shale.

### Procedure

Green River site 1 was located 5 miles west of the Rock Springs sites 4 and 5. The oil shale zone of interest, at approximately 340 to 385 ft, was selected after studying the analysis of cores cut from an earlier well. As determined by Fischer assay, oil yield of the cored section averaged about 21.0 gal/ton.

The completed site contained 10 pattern wells for explosive-fracturing research. Six wells were drilled on 50-ft spacing to form a rectangle with three wells on a side. The remaining four wells were drilled on 25-ft spacing to form a five-spot pattern (Fig. 6); all wells were completed similarly to the earlier described test wells.

Caliper and gamma ray logs were run to detect caving and borehole irregularities, and to correlate the oil shale formations. Airflow tests were made to measure initial communication between injection well 6 and the remaining wells in the pattern.

The first series of explosive tests on the site was performed on the wells in the five-spot pattern. The amount of TNT used in each well was calculated from total-depth and caliper-log measurements. The accumulated water was bailed prior to lowering the priming devices and filling the wellbores with TNT.

The pelletized TNT was poured slowly into the wells until the TNT column rose above the water level to assure that the TNT had not bridged in the well. The wells were loaded with a total of 3,540 lb of TNT, as indicated in Table 1. Each well was sand tamped from the top of the explosive to approximately 150 ft in the casing before the explosive was detonated.

TABLE 1 . - Shooting data, first shot, small five-spot pattern, Green River site 1

Well No.	Total depth of well, ft	Total depth of casing, ft	Explosive height, ft	Sand tamp depth, ft	Explosive used, lb
2....	389.5	342.0	<sup>1/</sup> 355.0	150	420
3....	374.5	343.0	347.0	150	<sup>2/</sup> 600
4....	386.5	341.0	345.0	150	1,020
5....	382.5	341.0	<sup>3/</sup> 327.0	150	<sup>2/</sup> 600
6....	383.5	342.0	355.0	150	<sup>2/</sup> 900

<sup>1/</sup> Explosive bridged in casing.

<sup>2/</sup> Explosive did not detonate.

<sup>3/</sup> Explosive bridged; washed out; no additional explosive added.

An explosive-fracturing test was then performed on the remaining five wells in the large pattern; a total charge of 3,600 lb of TNT was used in this shot, as indicated in Table 2.

The five-spot pattern wells were cleaned to bottom to remove rubble from the wellbores. During the cleanout, it became evident from the recovery of debris, that the explosive had not detonated in wells 3, 5, and 6. Caliper logs run in these wells verified the findings.

Wells 3, 5, and 6 were reloaded with 1,860 lb of TNT and shot (Table 3). After cleanout and after caliper logs were obtained, airflow tests were run on the five-spot pattern wells to determine the relative extent of fragmentation and improvement in communication between wells.

The final explosive-fracturing test performed on this site was a simultaneous shot detonated in the wells of the five-spot pattern. Wire-line measurements were obtained to determine total depth, and caliper logs were run to determine wellbore enlargement from which to calculate the amount of TNT to fill each well. Water was swabbed and boiled from each well, the primers were run to total depth, and a predetermined amount of TNT was poured in each well. A total charge of 7,140 lb of TNT was loaded in these wells and was detonated (Table 4).

#### Results

Data obtained from evaluation tests indicated that the oil shale was fractured and/or fragmented from the explosive work. Three of these tests indicated either formation damage and/or increased fracturing of the shale existed between wells.

TABLE 2. - Shooting data, first shot, large pattern,  
Green River site 1

Well No.	Total depth of well, ft	Total depth of casing, ft	Explosive depth, ft	Sand tamp depth, ft	Explosive used, lb
7.....	373.5	341.0	346.0	150	600
8.....	375.0	337.0	342.0	150	600
9.....	384.5	337.0	342.0	150	840
10.....	373.5	340.0	345.0	150	<sup>1/</sup> 600
11.....	403.5	342.0	308.0	150	<sup>2/</sup> 960

<sup>1/</sup> Explosive did not detonate.

<sup>2/</sup> Explosive in casing. Casing damaged; no clean out.

TABLE 3. - Shooting data, second shot, small five-spot pattern, Green River site 1

Well No.	Total depth of well, ft	Total depth of casing, ft	Explosive depth, ft	Sand tamp depth, ft	Explosive used, lb
2....	-	-	-	150	(- <u>1</u> /)
3....	379.0	343.0	345.0	150	600
4....	-	-	-	150	(- <u>2</u> /)
5....	382.0	341.0	346.0	150	540
6....	381.0	342.0	346.0	150	720

1/ Set bridge plug at 290.0 feet.

2/ Set bridge plug at 337.0 feet.

TABLE 4. - Shooting data, third shot, small five-spot pattern, Green River site 1

Well No.	Total depth of well, ft	Total depth of casing, ft	Explosive depth, ft	Sand tamp depth, ft	Explosive used, lb
2....	381.0	342.0	346	190	780
3....	384.0	343.0	345	200	1,920
4....	379.0	341.0	351	252	1,800
5....	383.0	341.0	346	197	1,320
6....	378.0	342.0	$\frac{1}{350}$	200	1,320

$\frac{1}{}$  Stopped pouring explosive because of bridging with excessive water influx.

## CONCLUSIONS

Results of explosive fracturing tests in oil shale show that NGI will detonate and that the explosion will propagate in water-filled natural fractures and sand-propped, hydraulically induced fractures in oil shale. The shale was fragmented by this method, and a successful underground retorting experiment to recover shale oil was performed.

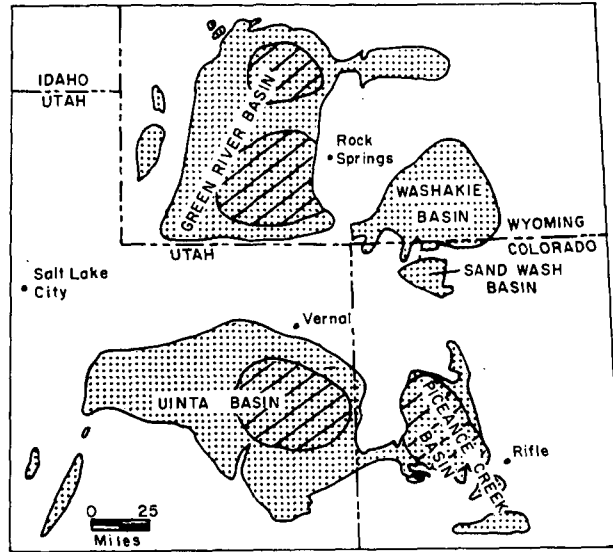
A combination of displacing NGI into a natural fracture system and using pelletized TNT in wellbore shots fragmented oil shale between wells at relatively shallow depths ranging from 60 to 100 ft. Extensive fragmentation extending to a radius of approximately 48 ft and extensive fractures to a radius of 90 ft were disclosed by various evaluation methods.

Further, pelletized TNT performed satisfactorily in wellbore shots in wells ranging between 150 and 385 ft in depth. Fractures were created between wells as indicated by airflow tests, but numerous other evaluation techniques tried did not indicate the extent of rock fragmentation.

## REFERENCES

1. Brandon, C. W. Method of Explosively Fracturing o Productive Oil and Gas Formation. U.S. Pat. 3,066,733, Dec. 4, 1962.
2. Brewer, B. Stimulation of Oil Production by the Use of Explosives After Hydraulic Fracturing. Producers Monthly, v. 21, No. 4, February 1957, pp. 22-23.
3. Burwell, E. L., H. C. Carpenter, and H. W. Sohns. Experimental In Situ Retorting of Oil Shale at Rock Springs, Wyo. BuMines TPR 16, June 1969, 8 pp.
4. Campbell, G. G., W. G. Scott, and J. S. Miller. Evaluation of Oil-Shale Fracturing Tests Near Rock Springs, Wyo. BuMines RI 7397, 1970, 21 pp.
5. Carpenter, H. C., E. L. Burwell, and H. W. Sohns. Evaluation of an In Situ Retorting Experiment in Green River Oil Shale. J. Petrol. Technol., v. 24, No. 1, January 1972, pp. 21-26.
6. Childs, O. E. The Status of the Oil Shale Problem. Colo. School Mines Quart., v. 60, No. 3, July 1965, pp. 1-6.
7. Grant, B. F. Retorting Oil Shale Underground--Problems and Possibilities. Colo. School Mines Quart., v. 59, No. 3, July 1964, pp. 39-46.
8. Hanson, A. W. Assignor to the Dow Chemical Co. Plastically Deformable Solids in Treating Subterranean Formations. U.S. Pat. 3,159,217, Dec. 1, 1964.
9. Hill, G. R., and P. Dugan. The Characteristics of a Low Temperature In Situ Shale Oil. Colo. School Mines Quart., v. 62, No. 3, July 1967, pp. 75-90.

10. Hinson, F. R. Method and Apparatus for Treating an Earth Formation Penetrated by a Well. U.S. Pat. 3,191,678, Apr. 2, 1962.
11. Howell, W. D., J. L. Eakin, J. S. Miller, and C. J. Walker. Nitro-glycerin Tests Prove New Application. World Oil, v. 171, No. 6, November 1970, pp. 96-98. This article appeared as part of "New Look at Stimulation by Explosives," by R. E. Snyder (World Oil, v. 171, No. 6, November 1970, pp. 81-98).
12. Miller, J. S., and W. D. Howell. Explosive Fracturing Tested in Oil Shale. Colo. School Mines Quart., v. 62, No. 3, July 1967, pp. 63-73.
13. Miller, J. S., W. D. Howell, J. L. Eakin, and E. R. Inman. Factors Affecting Detonation Velocities of Desensitized Nitroglycerin in Simulated Underground Fractures. BuMines RI 7277, 1969, 19 pp.
14. Miller, J. S., and H. R. Nicholls. Methods and Evaluation of Explosive Fracturing in Oil Shale. BuMines RI 7729, 1973, 22 pp.
15. Miller, J. S., C. J. Walker, and J. L. Eakin. Fracturing Oil Shale With Explosives for In Situ Oil Recovery. BuMines Bull. 666, 1974.
16. Nicklen, C. O. History-Making Blast Set Off February 4. Oil Bulletin, Bull. 432, Calgary, Canada, Feb. 8, 1946, pp. 1-2.
17. Oil and Gas J. Space-Age Explosive May Revive Well-Shooting. V. 64, No. 38, Sept. 19, 1966, p. 82.
18. Zandmer, S. M. Method of Treating Oil and Gas Wells. U.S. Pat. 2,246,611, Oct. 12, 1936.
19. \_\_\_\_\_. Pressure Reduction Chamber and Unloading Valve for Explosives. U.S. Pat. 2,504,611, Feb. 25, 1946.



**LEGEND**

-  Area of Green River Formation
-  Area of 25 gal/ton, or richer, oil shale more than 10 ft thick

FIGURE 1. - Location of Oil Shale Deposits in Utah, Colorado, and Wyoming.

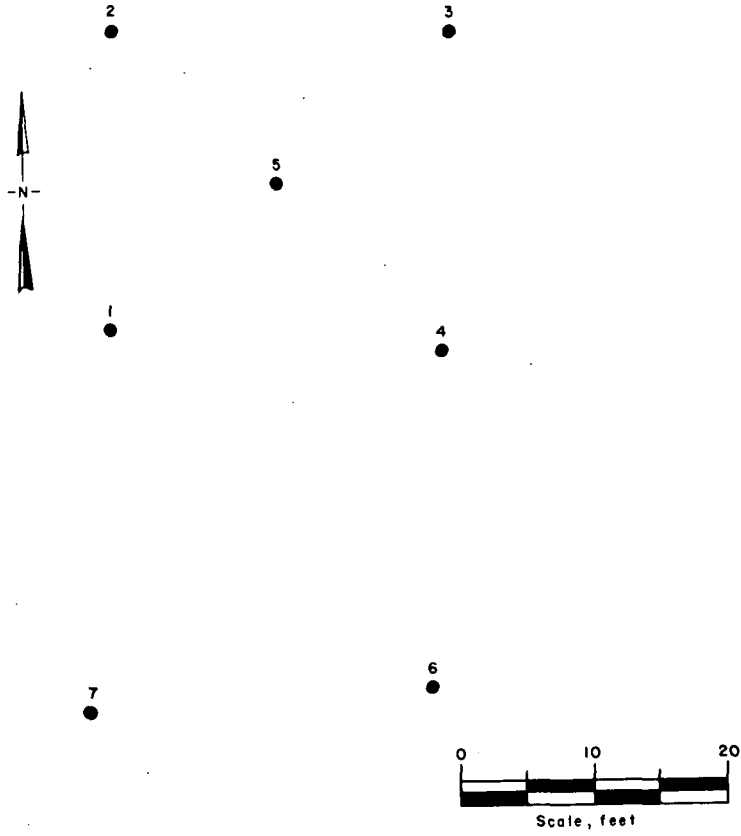


FIGURE 2. - Location of Wells, Rock Springs Site 4.

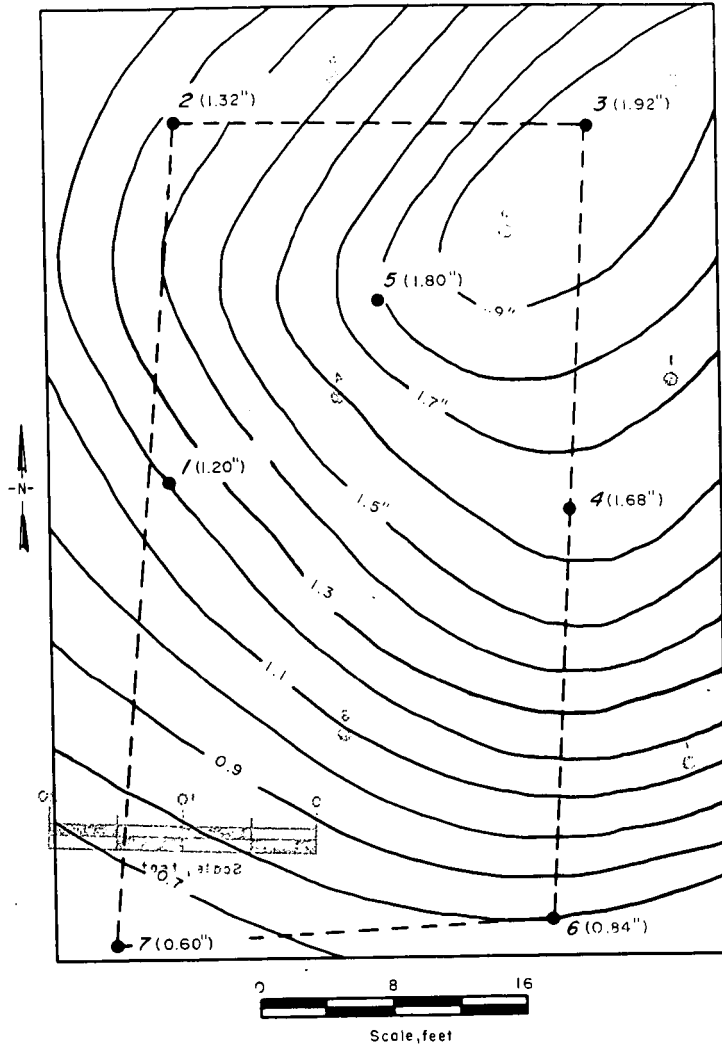


FIGURE 2. - Location of Wells, Rock Springs Site 4.

FIGURE 3. - Contours of Change in Surface Elevation Resulting From 300-Qt NG1 Shot, Rock Springs Site 4.

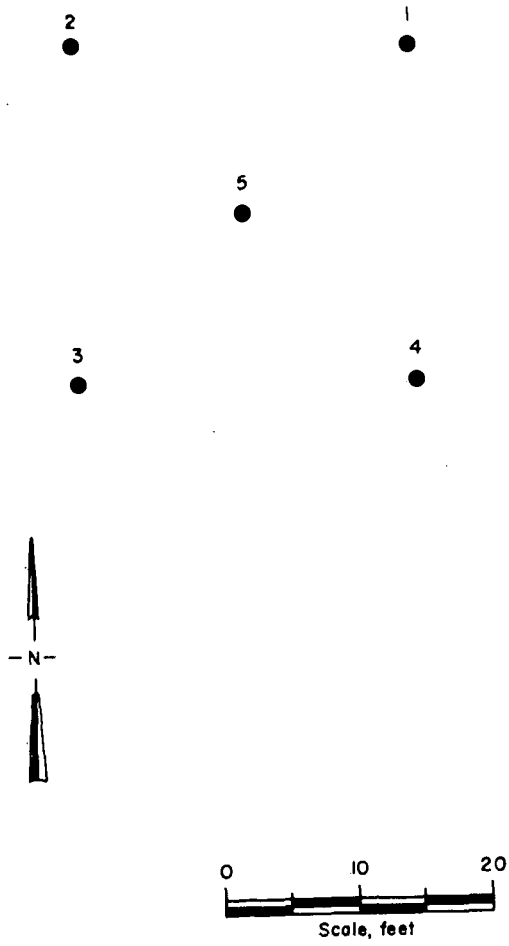


FIGURE 4. - Location of Wells, Rock Springs Site 5.

6

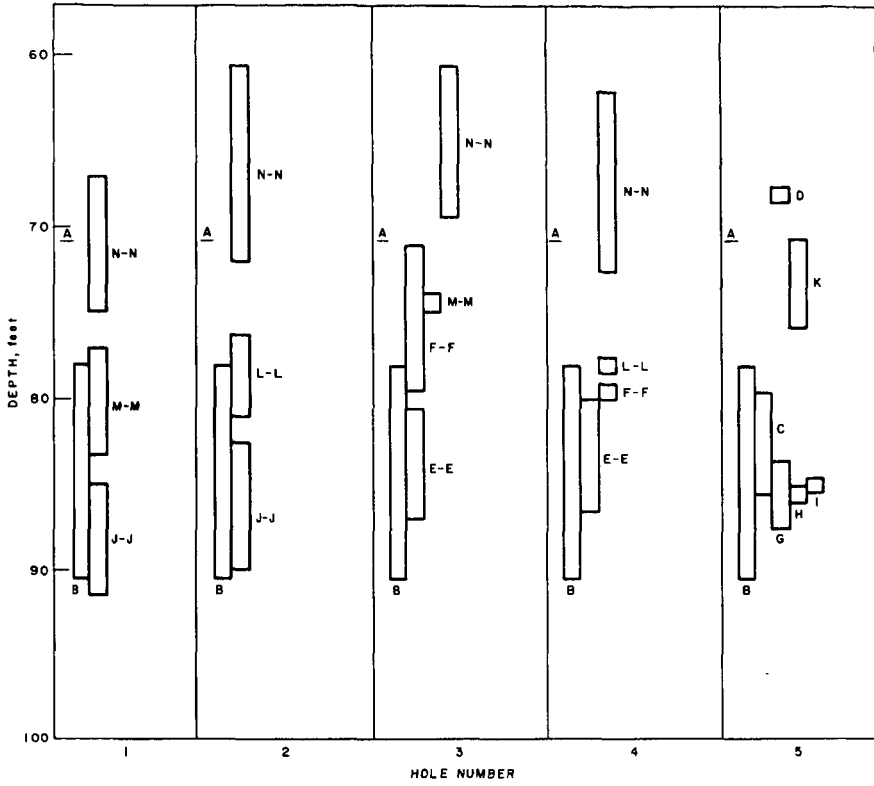


FIGURE 5. - Position of Explosive Charge in Sequence of Wellbore Shots in Five-Spot Pattern, Rock Springs Site 5.

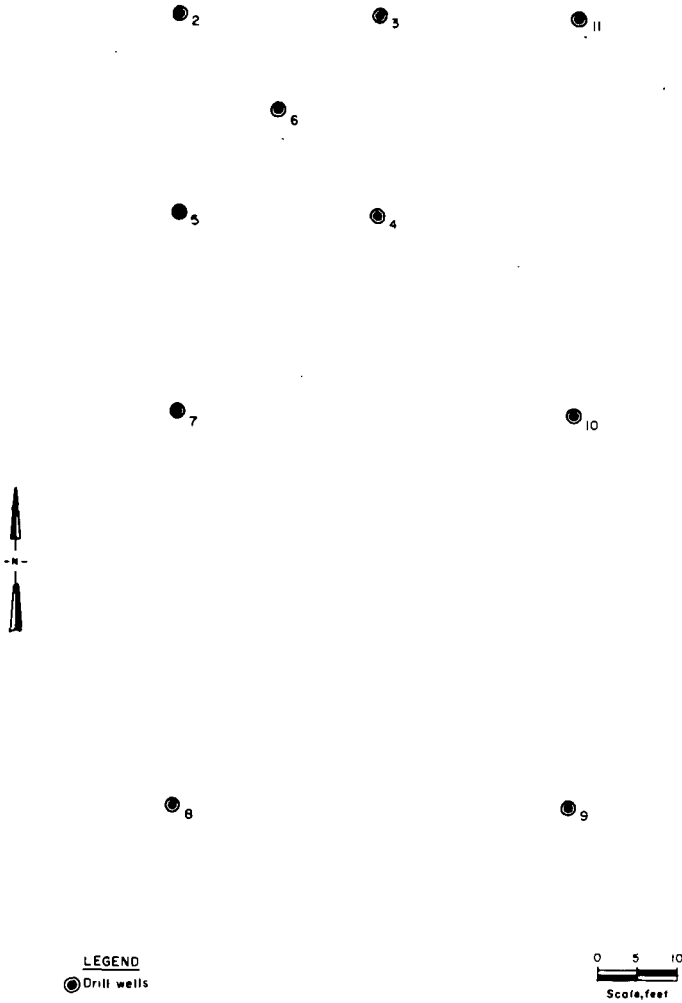


FIGURE 6. - Location of Wells, Green River Site 1.

## PULSED NMR EXAMINATION OF OIL SHALES--ESTIMATION OF POTENTIAL OIL YIELDS

F. P. Miknis, A. W. Decora, and G. L. Cook

U.S. Department of the Interior, Bureau of Mines  
Laramie Energy Research Center, Laramie, Wyoming 82070

### INTRODUCTION

For the past 4 years the Laramie Energy Research Center has been investigating the application of nuclear magnetic resonance (NMR) as a method of rapidly and reliably predicting potential oil yields of oil shales. With the present interest in the government's oil-shale test-lease program, the need for a rapid and reliable oil-shale assay method is more urgent. The potential of wide-line NMR for this purpose has already been demonstrated by Decora, McDonald, and Cook.<sup>1</sup> Another type of NMR, pulsed or transient NMR, is being explored as a method for rapidly providing this information. The pulsed NMR method is more rapid than the wide-line NMR method because no time is spent sweeping the field or frequency to record the signal. Other advantages of pulsed NMR over wide-line NMR are the elimination of line-broadening effects, no need for signal integration, greater sensitivity in a given measuring time, and ease of spectrometer operation. In addition, direct measurements of the spin-spin,  $T_2$ , and spin-lattice,  $T_1$ , relaxation times by pulsed NMR can provide other useful information about oil shales.

In this paper we present the results of some pulsed NMR assays on oil-shale samples. Two groups of oil-shale samples from two different cores were analyzed by pulsed NMR in a routine assay-type operation. Statistical analyses are presented to show that the NMR data linearly correlate with the Fischer assay oil-yield data.

### EXPERIMENTAL PROCEDURES

#### Oil Shales Studied

Two oil-shale cores were studied. The first came from a proposed test-lease core and had been recently Fischer assayed. A total of 141 samples, designated as Group I samples, was selected from this core to represent the entire depth (1,300 to 2,700 feet) and oil-yield ranges (0-70 gal/ton) of the cored interval.

The second core was cut below the B groove of the Mahogany zone. The total length of the core was 1,100 feet and the oil-yield range was 0 to 60 gallons per ton. The first 300 samples from this core, designated as Group II samples, were analyzed by pulsed NMR parallel with the Fischer assay oil-yield determination on the same core sections.

#### Sample Preparation

To prepare Group I samples for the first study, the sample remaining after Fischer assay was riffled to reduce the sample size to about 75 to 100 grams. This sample was then crushed to a fine powder on a disc grinder, and a representative portion (0.5 g) of the powdered sample was taken for the NMR measurements.

Group II samples for the second study were of the same particle size (8 mesh) as was used in the Fischer assay method. No further crushing was done to the samples prior to the NMR

measurements. The samples were, however, riffled to a smaller sample size from which a representative portion (2.5-4.5 g) was taken for the NMR measurements. The riffling of these samples was an attempt to minimize errors in the NMR method, which could arise from nonrepresentative sampling.

### Instrumentation

Pulsed NMR measurements on the Group I samples were made on a Bruker 322S variable frequency pulsed spectrometer housed at the Marathon Oil Co. Research Center in Denver, Colo. These measurements of the free induction decay (FID) amplitude following a 90° pulse were made at a resonant frequency of 60 MHz, a pulse length of 2.5 μsec, a pulse repetition rate of 1 sec and using diode detection. About 30 FID amplitude measurements (requiring about 30 sec) were made for each oil-shale sample, and the average values of these measurements were used to determine the relationship with Fischer assay oil yields by regression analyses. The FID amplitudes were corrected to unit sample weight prior to the regression analyses.

FID amplitudes for the Group II shales were measured on a similar instrument housed at the Laramie Energy Research Center. A resonant frequency of 20 MHz, a pulse length of 6 μsec, a pulse repetition rate of 1 sec, and phase sensitive detection were used for these measurements. Because the Group II samples were coarser than the Group I samples, a larger sample tube (15 mm diameter) was used. As was done for the Group I samples, about 30 FID amplitude measurements were made for each Group II sample from which an average value was obtained and corrected to unit weight prior to the regression analyses.

### Linear Regression Analyses

Linear first-order regression analyses were first performed on the FID amplitudes and Fischer assay oil yields for standard samples chosen from both groups. There were 30 standard samples chosen from Group I and 36 from Group II. Based on the slopes and intercepts of the best least-squares data fits, oil yields were calculated for the remainder of the samples in both groups. Regression analyses were then performed on the oil yields calculated from NMR measurements and oil yields determined by Fischer assay. The index of determination (square of the correlation coefficient,  $r$ ) is the parameter we use to judge the "goodness of fit" in the regression analyses. A value of 1.00 for this parameter implies a perfect fit of data points to a straight line.

## THEORETICAL CONSIDERATIONS

The basis for the pulsed NMR assay method lies in the assumption that the organic hydrogen content of an oil shale is related to the shale's potential oil yield. The FID amplitude, following a 90° pulse, is proportional to the total number of resonant nuclei in the sample, just as is the area under the absorption curve in wide-line NMR. Because the resonant nuclei in this case are protons, the FID amplitude is proportional to the hydrogen content of the oil shale.

The basic NMR measurement is shown in figure 1(a). A sample introduced into a magnetic field,  $H_0$ , achieves a net magnetization,  $M$ , proportional to the amount of hydrogen in the sample. If an rf pulse,  $H_1$ , is applied at right angles to  $H_0$ ,  $M$  can be rotated from its equilibrium position and begins to precess about  $H_1$ . If the intensity and duration of  $H_1$  are properly chosen,  $M$  can be rotated into the  $xy$  plane at which time  $H_1$  is turned off. The condition for a 90° rotation is

$$\pi/2 = \gamma H_1 \tau_p, \quad (1)$$

where  $\gamma$  is the magnetogyric ratio of the proton,  $H_1$  is the strength of the pulse, and  $\tau_p$  is the pulse

duration. Following the termination of  $H_1$ , the individual magnetic moments begin to interact with each other and lose phase coherence as in figure 1(b). The net result is that the signal intensity decreases to zero in a characteristic time,  $T_2$ , the spin-spin relaxation time.

In the pulsed NMR assay method, measurements are made on  $M_x$  immediately after the  $90^\circ$  pulse, to obtain the maximum signal from all the protons in the sample. These measurements may include signal contributions from inorganic protons (adsorbed water, mineral hydrogen, tightly bound hydroxyl groups, etc.) as well as the organic protons in the oil shale. To improve precision of the method effort is made to distinguish between the different types of protons in the sample. By the very nature of the pulsed NMR measurement it is difficult to make this distinction, except in the case of adsorbed water for which an example is shown on figure 2. Here the effect on the FID of drying the shale sample to remove water is illustrated. The signal that persists in the undried samples for times greater than about 50  $\mu\text{sec}$  shows the effect of adsorbed water because upon drying, the signal is significantly reduced. This indicates that organic hydrogen relaxation times are shorter than those of adsorbed water and suggests that signal contributions due to adsorbed water can be corrected for by subtracting FID amplitude measurements at 50  $\mu\text{sec}$  from those made at 20  $\mu\text{sec}$ . The corrected FID amplitude was assumed to more closely represent the organic hydrogen content of the oil shale. This procedure was followed for the Group II shales but not the Group I shales.

Another parameter that may aid in minimizing signal contributions due to inorganic protons is the spin-lattice relaxation time,  $T_1$ . This is the characteristic time during which equilibrium is restored along the applied field direction, after the application of a pulse.  $T_1$  determines the frequency at which the  $90^\circ$  pulse sequence can be repeated and ultimately determines the rapidity of the pulsed assay method. Typically, one should wait at least  $5 T_1$  to allow for equilibrium to be restored before applying a second, third, etc.,  $90^\circ$  pulse.<sup>2</sup> For oil shales the  $T_1$  values for the organic material are quite short (10-300 msec) whereas some of the inorganic protons apparently have longer  $T_1$  values. Evidence to illustrate this is presented in the next section of this paper.

## RESULTS AND DISCUSSION

### Pulse Repetition Rate

Shown on table 1 are the results of a preliminary study made to determine how  $T_1$  values of inorganic and organic protons affect the pulsed assay method. Here, two FID amplitude measurements were made on 10 oil-shale samples containing substantial amounts (up to 53 percent) of nahcolite ( $\text{NaHCO}_3$ ). The first NMR measurement was made with a pulse repetition rate of 1 sec, and the second was made with a repetition rate of 30 min. The results on table 1 show that the NMR measurements of 1 sec correlate better with the oil-yield determinations; whereas, those made at 30 min correlate better with the total hydrogen. The total hydrogen includes both organic and inorganic hydrogen and was determined by the combustion method. These results suggest that a fast repetition rate tends to minimize some effects due to inorganic protons.

### Fischer Assay Repeatability

Previous work<sup>1</sup> related NMR signals to Fischer assay oil yields using single measurements. Repeatability measurements for each of these experimental methods was not determined. Because the reliability of the NMR assay method is dependent on that of the Fischer assay, a series of tests was made to determine the reliability of the Fischer assay oil yields. Seventy-five samples (three each of 25 Group I samples) were Fischer assayed, and average oil yields and standard deviations were calculated for each of the 25 samples. These results are presented in table 2. If one defines

the dispersion coefficient as the standard deviation divided by the average value, then the calculated "average" dispersion coefficient is 0.138 for the 25 samples and represents the uncertainty in Fischer assay oil yields.

TABLE 1. - Correlations between oil yields and total hydrogen for different pulse repetition rates

Regression	Pulse rate	Index of determination $r^2$
Oil yield (gal/ton) versus free induction decay amplitude	1 sec	0.97
Total hydrogen (wt pct) versus free induction decay amplitude	1 sec	.95
Oil yield (gal/ton) versus free induction decay amplitude	30 min	.90
Total hydrogen (wt pct) versus free induction decay amplitude	30 min	.98

TABLE 2. - Summary of data for Fischer assay repeatability test

Sample No. SBR71-	Average F.A., gal/ton	Standard deviation, S	Dispersion coefficient, K
10164	38.7	11.2	0.289
10178	35.2	3.1	.088
10335	15.5	1.3	.083
10446	18.2	1.1	.059
10648	14.2	6.7	.472
10262	24.7	5.7	.230
9522	21.7	6.6	.303
9993	9.4	.7	.074
10296	17.9	1.0	.056
10650	11.9	.5	.039
10352	30.7	.8	.025
10026	22.0	.6	.028
9947	8.8	.5	.061
10162	9.5	4.2	.436
10115	14.1	.3	.019
10531	22.1	1.3	.059
9587	21.4	.8	.038
10444	28.5	1.0	.033
10603	6.4	2.4	.381
10452	28.7	5.8	.202
10254	21.5	1.6	.073
10137	18.8	.26	.014
10564	21.9	6.9	.317
10217	29.0	.82	.028
10224	27.0	1.2	.045

### Group I Oil-Shale Samples

Results of linear regression analyses made with the 30 standard samples chosen from Group I were used to calculate oil yields of the remaining 111 samples. The correlation between the measured Fischer assay oil yields and calculated oil yields is shown on figure 3. The value of 0.93 for the index of determination is remarkably good, considering the small sample size (0.5 g) used in the NMR measurements compared to the much larger size (100 g) typically used for Fischer assay. It appears that the procedure for preparing the NMR samples effectively duplicated the quality of the larger Fischer assay samples. Furthermore, these results were obtained for a single FID amplitude measurement, suggesting an insignificant adsorbed water contribution from these samples.

### Group II Oil-Shale Samples

The Group II shales were run in a more routine assay type of operation than the Group I shales. In this case the oil-shale samples were run by NMR before, during, or after the Fischer assay of the same samples. Thus the reported Fischer assay oil yields were not known prior to making the NMR measurements. Thirty-six samples were processed at any given time by the NMR method. When Fischer assay data became available, linear regression analyses were made on the FID measurements and reported oil yields. The results for each run are shown on table 3. The poorer index of determination for run 1 was due to improper tuning of the pulsed spectrometer, and in subsequent runs this problem was remedied as evidenced by the better correlations in runs 2-9. These data also indicate that day-to-day tuning of the pulsed spectrometer on a standard sample can be accomplished readily and with good reliability.

TABLE 3. - Indexes of determination for the pulsed NMR assay method

Run	$r^2$ (Index of determination)
1	0.78
2	.91
3	.96
4	.94
5	.93
6	.97
7	.96
8	.98
9 <sup>1/</sup>	.92

<sup>1/</sup> This run totaled 12 samples; all other runs contained 36 samples each.

The 36 samples of run 3 were chosen as "standards" to determine how well the pulsed NMR measurements could predict oil yields for the remaining samples. The correlation between the measured and calculated oil yields is shown on figure 4. Again a good correlation was obtained between the predicted and measured oil yields. The data for the 36 samples in run 1 were not included in the correlation on figure 4. It should be emphasized that the correlations on figures 3 and 4 assume complete reliability in the Fischer assay. No uncertainties in the Fischer assay data were incorporated in our regression analyses, although the data on table 2 show that the Fischer assay method is subject to errors. This could account for some of the scatter in figures 3 and 4. Another reason for the scatter in these figures is probably due to sample size and sampling procedures. The indices of determination, however, indicate that our sampling procedures tended to give NMR samples representative of the total samples.

### Time Savings

Thus far, data have been presented to show that pulsed NMR measurements can be used to predict potential oil yields of oil shales. We have not stressed an important advantage of the pulsed NMR assay method over the Fischer assay method--namely, the savings in time offered by the NMR method. To obtain a gallon-of-oil-per-ton-of-shale figure by the Fischer assay method for a single sample averages out to about 100 min per sample. This results from the number of measurements required by the Fischer assay method. Here one must weigh the sample retorts and collectors, retort the sample (60 min), reweigh the retorts and collectors, centrifuge (10 min) and measure the volume of oil and water produced, and finally determine the specific gravity (30 min) of the shale oil. In all these steps, there is chance for error, particularly when different people are doing the assays. The NMR measurements can be obtained directly in gallons-of-oil-per-ton-of-shale units with a suitable calibration line. To obtain an oil yield by NMR requires about 2 min per sample, including the time spent in riffing and weighing the sample. In the NMR method, a simple voltage measurement is made, and if coupled to a programmable calculator or minicomputer, an instantaneous assay can be obtained. Thus a factor of 50 in rapidity of assay is easily obtainable with NMR methods over the conventional Fischer assay.

### CONCLUSIONS

The free induction decay amplitude measured on oil-shale samples by pulsed NMR linearly correlates with Fischer assay oil yields. This has been shown from analyses of 405 samples from two different oil-shale cores. In cores for which adsorbed water may be an important contributor to the NMR signal, it was necessary to make two NMR measurements of the free induction decay amplitude to correct for these interferences.

### ACKNOWLEDGMENTS

The work upon which this report is based was done under a cooperative agreement between the Bureau of Mines, U.S. Department of the Interior, and the University of Wyoming.

Reference to specific equipment does not imply endorsement by the Bureau of Mines.

### REFERENCES

1. Decora, A. W., F. R. McDonald, and G. L. Cook. Using Broad-Line Nuclear Magnetic Resonance Spectrometry to Estimate Potential Oil Yields of Oil Shales. BuMines RI 7523, 1971, 30 pp.
2. Farrar, J. C., and E. D. Becker. Pulse and Fourier Transform NMR. Academic Press, New York, N. Y., 1971, p. 21.

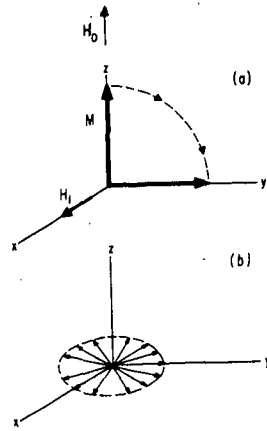


FIGURE 1.-A 90° Pulse Sequence.

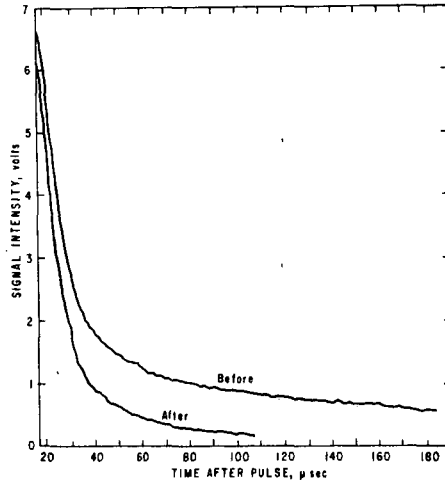


FIGURE 2.-Effects of Drying Oil Shale Samples on Free Induction Decay.

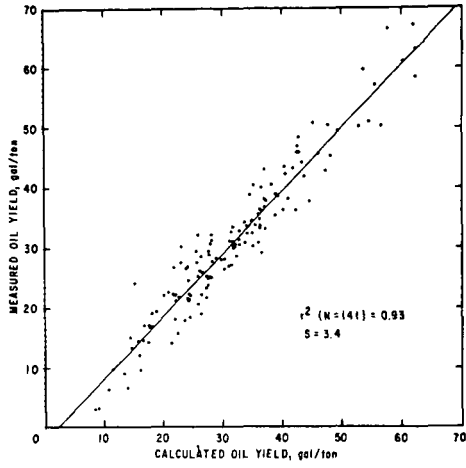


FIGURE 3.—Measured Oil Yields Vs. Calculated Oil Yields, Group I.

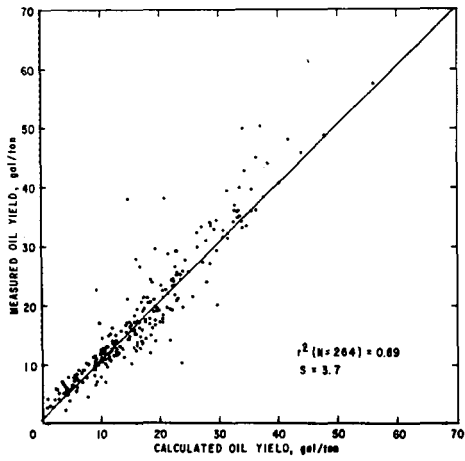


FIGURE 4.—Measured Oil Yields Vs. Calculated Oil Yields, Group II.

## THE EFFECTS OF BIOLEACHING ON GREEN RIVER OIL SHALE

W. C. Meyer and T. F. Yen  
Departments of Geological Sciences  
and Chemical Engineering  
University of Southern California, University Park  
Los Angeles, California 90007

## INTRODUCTION

Bioleaching, utilizing a sulfuric acid medium generated by the sulfur oxidizing capabilities of Thiobacillus spp. has proved to be useful in releasing hydrocarbons from petroliferous rocks from the Mahogany Ledge of the Green River formation. As yet, however, these methods do not yield a high percentage of the kerogen trapped within the rock. The purpose of this paper is to investigate the texture and mineralogy of the Green River shale to ascertain the nature of kerogen entrapment and the physical effects of bioleaching. Such an understanding should ease the development of a method to increase the effectiveness of bioleaching in releasing kerogens for commercial extraction.

Shale Description

The Green River shale is a highly indurated, fine-grained, varved, calcareous sedimentary rock deposited in the Eocene fresh-water lake Gosuite. The rock varies in color from tan to black, depending on organic content. Rock of this type is technically a marl, but in this paper it will be called shale in convention with common usage.

Varves in the Green River shale consist of carbonate summer laminae, and fine grained winter laminae composed of clay and organic components. Thin sections of the shale show distinct banding of dark components enclosed in a light colored matrix composed of polymineralogic crystal aggregates, and small single crystals that, when large enough to identify, are predominantly dolomite. This crystalline matrix superimposes a granular texture over the entire rock.

Clays and associated (adsorbed) organics appear to be localized in small blob-like aggregates ( $\approx 20\mu$ ) which string out to form the dark winter laminae. These organo-clay concentrations vary from diffuse dark brown bands to narrow opaque strings, but are always parallel to the varved textural grain. Light colored bands appear to be composed entirely of small matrix crystals and a few relatively coarse possibly detrital grains, with little evidence of clays or organics. The clays and visible organics are intimately associated, either because they were deposited simultaneously, or have become linked by processes of chem-adsorption. It would seem reasonable that the first step in liberating adsorbed or mechanically trapped kerogens would be the disaggregation of the crystalline matrix to release clays.

## MINERAL COMPOSITION

X-ray Methods

All x-ray analyses were made using a Norelco diffractometer using  $\text{CuK}\alpha$  radiation with a nickel filter, 0.006 inch slit at 40 kv and 20 MA. The optimum rate was found to be 1000 cps at  $1^\circ 2\theta/\text{min}$ .

Disordered powder mounts were used for whole-rock mineral analyses. Separate preparations were made for analysis of clay mineralogy, using the method devised by Jackson (5). The indurated nature of the shale made complete disaggregation impossible, but digestion of 50 gms of crushed shale in warm sodium-acetate solution (part of Jackson's method) released enough carbonate-free clay to analyze with no difficulty.

In order to separate different clay species, clay mounts were treated according to the method proposed by Carrol (3) to promote shifts in position of diagnostic x-ray peaks. This treatment includes dissication, glycolation, and heating to 350°C and 550°C respectively.

### Whole Rock

Whole-rock mineral content can be divided into major and minor constituents based on relative peak intensities (Table I). The shale contains too many mineral species to be easily matched by addition of necessary comparative internal standard, therefore quantitative determination of mineral abundance were not made.

TABLE I

#### Whole Rock Mineralogy

<u>Major</u>	
Quartz	SiO <sub>2</sub>
Dolomite	CaMg(CO <sub>3</sub> ) <sub>2</sub>
Calcite	CaCO <sub>3</sub>

#### Minor

Analcite	NaAlSi <sub>3</sub> O <sub>8</sub> · H <sub>2</sub> O
Montmorillonite	Al <sub>4</sub> (Si <sub>4</sub> O <sub>10</sub> ) <sub>2</sub> (OH) <sub>4</sub>
Orthoclase	KAlSi <sub>3</sub> O <sub>8</sub>
Plagioclase	Na(Ca)Al <sub>0-2</sub> Si <sub>2-3</sub> O <sub>8</sub>
Pyrite	FeS <sub>2</sub>

#### Clay Mineralogy

Montmorillonite	Al <sub>4</sub> (Si <sub>4</sub> O <sub>10</sub> ) <sub>2</sub> (OH) <sub>4</sub>
Illite	K <sub>0-2</sub> Al <sub>4</sub> (Si <sub>8-6</sub> Al <sub>0-2</sub> )O <sub>20</sub> (OH) <sub>4</sub>

Quartz and dolomite were found to be the predominant minerals in these samples. Calcite is also present, probably representing residual primary carbonate that has not undergone diagenesis. Dolomite and calcite appear to form the granular matrix observed in thin section. Feldspar, including albite rich plagioclase and orthoclase, occur primarily as detrital grains making up part of the primary sediment deposit. Pyrite probably formed in the sediment before or during lithification when organic-rich bottom sediments provided the reducing environment favorable to formation of this mineral.

Analcite, abundant here and in some other members of the Green River formation, is thought to have formed authigenically shortly after deposition of the primary sediment (1). It is possible that some of the plagioclase content of the shale may have been formed by reaction of analcite and quartz (2). The temperature required for this conversion is about 190°C, somewhat higher than would be expected in these deposits, but in the presence of concentrated brine, conversion temperature would be lowered (1).

To see what effect bioleaching has on mineralogy, the x-ray pattern of raw shale was compared to that of a sample that had undergone a 38.4% weight loss during bioleaching. The mineral composition of both samples

are identical, however, peak intensities of carbonate minerals are strongly reduced suggesting they have been dissolved and partially removed. Peak size is not linearly related to the amount of mineral present, so quantitative induration of carbonate removal is not indicated by comparing peak heights.

To quantify the amount of carbonate removed by bioleaching, whole-rock weight percentages of organic carbon, carbonate ion, and mineral carbonate were determined on duplicate one-half gram samples (270 mesh) using the Leco gasometric analyser (6). Calculation of mineral carbonate uses a constant (8.33) derived from the relative weight of calcium at carbonate ion in calcite. Since it was not possible to quantitatively evaluate the ratio of calcite to dolomite in the mineral carbonate fraction, the calcite constant was used for calculations. This causes the calculated weight percentages of mineral carbonate to be slightly lighter than actual values. Organic carbon was sufficiently abundant to necessitate halving the normal sample weight (0.25 g) for analysis.

Carbon and carbonate data are expressed as weight percent. Raw shale proved to be about 33% mineral carbonate by weight, and 10% carbon contained in organic compounds. Assuming an average hydrocarbon chain is  $C_{16}$  in the Green River material, the added hydrogen would bring the total weight of organic constituents to approximately 11%.

To ascertain if bioleaching is removing the available carbonate, samples of crushed (16 mesh) bioleached material were analysed for residual carbonate. The sample used for this experiment had lost 36.5% of its weight during leaching, and it was found to have approximately 2.3% residual mineral carbonate indicating that bioleaching is quite effective.

#### Clay

A peak at 18.8 Å in the clay and whole-rock mounts suggest montmorillonite, reported from Green River samples by previous investigators (1), is the dominant clay group in the studied samples. This peak occurs at somewhat higher angstrom values than is normal for montmorillonite, but the presence of abundant organics often causes aberration in x-ray patterns, explaining the observed shift (7).

Montmorillonite is a poorly crystallized mineral and is often not detectable by x-ray unless present in excess of 15% of the sample (3). The presence of a montmorillonite peak in the whole-rock pattern suggests, therefore, this mineral may be present in significant quantities. Water is readily absorbed into the montmorillonite structure causing swelling. If the quartz and dolomite are removed from the shale, the expansive forces of swelling montmorillonite may be useful in disaggregation of the residual fraction.

Illite is the second abundant clay mineral, and may represent primary clays, degraded mica, or potassium enriched primary clays of other species. Garrels and Mackenzie (4) show that, through time, most clay species will alter to montmorillonite, illite, or chlorite. The age of the Green River formation (Eocene) would be more than sufficient for alteration of primary clays.

It is not possible to accurately determine what percent of the shale is clay without data on the whole-rock distribution of elemental oxides. A process of elimination by comparison with mineralogy would reveal how much of these elements are contained in clays, but as yet the appropriate

analyses have not been performed.

#### VISIBLE EFFECTS OF BIOLEACHING

Scanning electron micrographs were taken of shale samples treated for various periods of time to see the effects of bioleaching. Samples were cut to convenient size and polished to a flat surface with #600 grit prior to treatment. Control samples of polished unleached shale (Fig. 1), and unleached fractured rock surface (Fig. 2) were photographed to ascertain if any material was being removed by crystal plucking during polishing. Neither control showed evidence of pitting due to mechanical processes, so it seems safe to conclude that pitting observed in treated samples is due to chemical action.

Shale bioleached for two days shows a pitted, spongy-appearing surface texture caused by solution of mineral material (Fig. 3). Bioleaching for one week caused no apparent increase in the number of pits per unit area, but an increase in pit size was noted. Two weeks exposure to bioleaching medium seemed to further increase pit size but did not result in formation of additional pits (Fig. 4).

In order to quantify the effects of bioleaching, photomicrographs of shale samples bioleached for varying time (Figs. 1-4) were used to count and measure the cross sectional dimensions of solution pits as an indication of the amount of material removed by solution. This data shows that solution pits form rapidly after exposure to the leaching medium. The number of pits on each sample ranged from 29 to 33 independent of time. Average pit size (calculated as surface area using the two maximum diameters for each pit) did vary directly with time, increasing from a minimum of  $24.8 \mu^2$  after two days, to a maximum of  $54.3 \mu^2$  after two weeks, indicating that the volume of carbonate removed is a fraction of time exposed to the bioleaching medium.

Paired microphotographs of the same area can be used as a stereopair if they are taken at slightly different tilt angles. Using an equation modified from that devised for interpretation of aerial photographs, these photographs can be used to determine pit depth. On an average the pit depth is in the order of  $2.2 \mu$  (Fig. 5).

The irregular bottom of this pit is a typical effect of solution. The shelf-like false bottom, and the small penetration of the true bottom indicate that continued solution would result in farther deepening. This fact, coupled with the absent lateral enlargement with time should result in neutral and lateral interconnection of soluble sites causing an increase in porosity and permeability. This will prove to be an important mechanism to facilitate exposure of fresh surface to the leaching medium and form conduits for the migration of liberated hydrocarbons.

#### CONCLUSIONS

Kerogens in the Green River shale are trapped in an inorganic mineral matrix composed primarily of quartz and dolomite (calcite). Liberation of hydrocarbons will depend upon the degree to which this matrix can be disaggregated, exposing kerogen for extraction. Thin sections show organic components within this rock are associated with the clay fraction, possibly through a process of chemical adsorption. Expansive properties of montmorillonite, the dominant clay component, may be useful in final disaggregation of the shale after removal of mineral matrix.

Biobleaching effectively removes carbonate minerals from the shale eliminating matrix material, and thereby developing porosity and permeability which are effectively nil for untreated shale. This brings more rock surface in contact with the leaching medium, increasing solution of matrix and enlarging pathways for migration of liberated hydrocarbons. Carbonate removal during biobleaching proceeds rapidly upon exposure to the leaching medium, and continues as a function of time.

#### ACKNOWLEDGEMENT

This work is supported by NSF Grant No. GI-35683.

#### REFERENCES

1. Bradley, W. H. and H. P. Eugster, U. S. G. S., Prof. Paper, 49b-B, p. 1-71, 1969.
2. Campbell, A. S. and W. S. Fyfe, Am. J. Sci., 263, 807 (1965).
3. Carroll, D., Geol. Soc. Amer., Spec. Pub., No. 126, p. 1-80, 1970.
4. Garrels, R. M. and F. T. Mackenzie, Evolution of Sedimentary Rocks, W. W. Norton, Inc., N. Y., 1971, p. 235.
5. Jackson, M. L., "Soil Chemical Analyses---Advanced Course," Madison, M. L. Jackson, 1956, p. 31-59.
6. Kolpack, R. L. and A. S. Bell, J. Sed. Pet., 38, 617 (1968).
7. Seyfreid, Personal Communications, 1973.

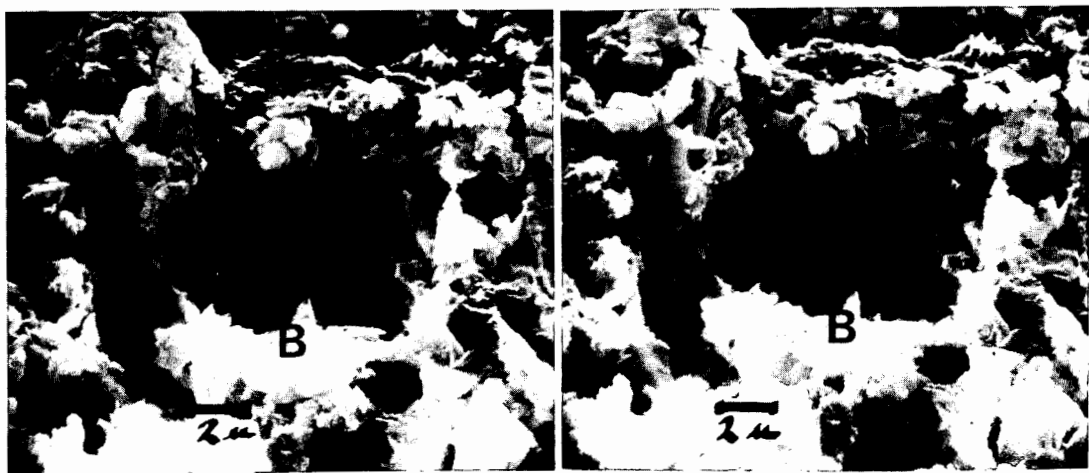


Fig. 5 Polished, leached two weeks, 0° tilt (Left)  
 Polished, leached two weeks, 7° tilt (Right)

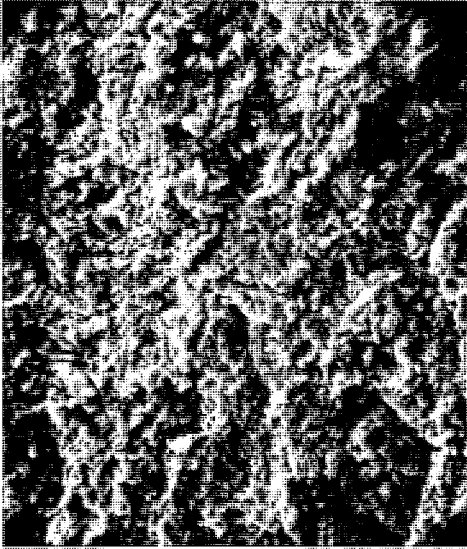


Fig. 1 Polished, unleached

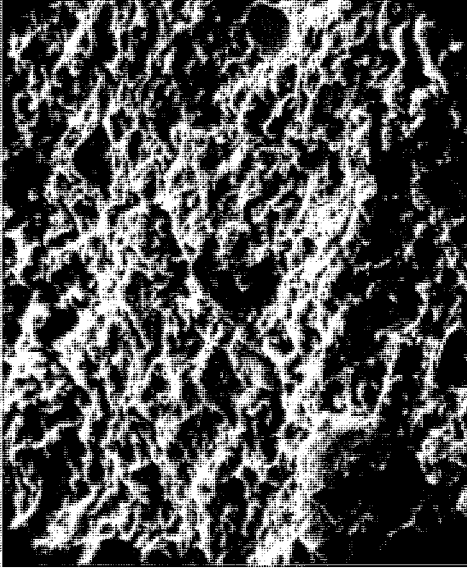


Fig. 2 Fractured, unleached

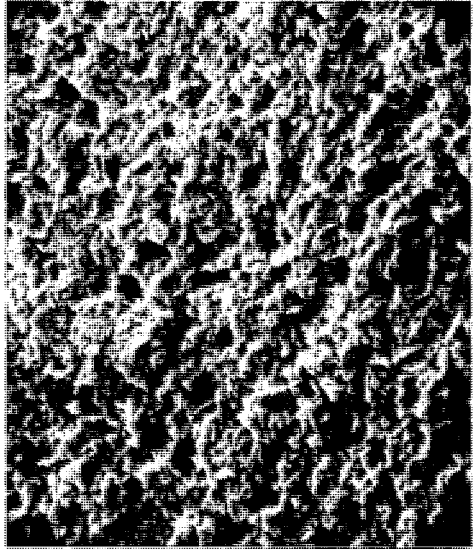


Fig. 3 Polished, leached two days



Fig. 4 Polished, leached two weeks

INVESTIGATIONS OF THE HYDROCARBON STRUCTURE OF KEROGEN FROM  
OIL SHALE OF THE GREEN RIVER FORMATION

J.J. Schmidt-Collerus and C.H. Prien  
University of Denver  
Denver Research Institute  
Denver, Colorado 80210

I. INTRODUCTION

Colorado Oil Shale of the Green River Formation contains about 16 per cent insoluble organic matter, the so-called "kerogen." This represents about 80 per cent of the total organic matter present. The remaining 20 per cent soluble organic matter represents the "soluble bitumen."

The problem of the nature and constitution of both "kerogen" and soluble bitumen and their relationship to each other is of considerable interest both with respect to the question of the origin, genesis and geochemistry of oil shale and the problem of degradation mechanisms during pyrolysis.

The paper discusses investigations on the structure of kerogen conducted at the Center for Fundamental Oil Shale Research of the University of Denver. Among several approaches for the structural elucidation of oil shale kerogen investigated to date, the MPCM-method developed at the Center proved most effective.

By using the combination of micro-pyrochromatography and mass spectrometry it could be shown that "kerogen" consists of a three-dimensional organic matrix of high molecular weight. The hydrocarbon portion of the matrix itself appears to consist of polycyclic "protokerogen" subunits or nuclei (of tetralin, terpenoid, phenanthrenoid and steroid type structure) interconnected by long chain alkanes and isoprenoids to form the three-dimensional network of the kerogen matrix. Studies on synthetic model compounds of the "protokerogen" type support this concept.

However, the matrix of "kerogen" in the conventional term also contains a substantial amount of entrapped long chain alkanes, normal and branched fatty acids and other uncondensed "protokerogen" subunits not removed by the normal extraction process. The presence of these compounds, which appear to have been overlooked, may considerably influence the results of structural investigations reported in the literature.

Morphological and physicochemical studies also indicate that Green River Oil Shale contains at least two major types of kerogen: alpha-kerogen and beta-kerogen. These are probably of different origins.

The chemical structure of the protokerogen subunits identified by macropyrolysis, chemical cleavage and by the MPCM-method used in conjunction with reaction chromatography are described. The possible relationship between kerogen structure, the soluble bitumen and the biogenesis and geochemical origin of oil shale are discussed.

\*Head, Chemistry Section, Chemical Division, Denver Research Institute and Professor of Chemistry, University of Denver.

\*\*Head, Chemical Division, Denver Research Institute and Professor of Chemical Engineering, University of Denver.

## II. MATERIALS AND METHODS

### A. Oil Shale Samples.

Samples were taken from freshly mined raw shale of the Green River Formation which were part of a 100 ton lot from the underground room-and-pillar mine of the Colony Development Corporation in the East Middle Fork of the Parachute Creek in Colorado. The material was crushed to - 1/4 inch size and riffled. Samples used for the extraction, separation and analysis experiments were ground to -100 mesh.

### B. Extraction of Soluble Bitumen.

The ground raw shale was exhaustively extracted by percolation at 50°C with a number of organic solvents with successively increasing polarity over several weeks. This was followed by treatment with acetic acid to remove inorganic carbonates and liberate any weaker acids present. The acid leached material was again exhaustively extracted with the same solvent sequence.

### C. Concentration of Kerogen.

Two methods were used for the separation of kerogen from the inorganic matrix: 1. Density gradient separation and 2. Chemical Separation by Acid Leaching. The density gradient method yielded a kerogen concentrate with about 3 percent ash content. However, the yield was rather low. The acid leaching method gave a concentrate with about 12 percent ash content. This material was used during most of the preliminary investigations.

### D. Analytical Methods.

A number of different approaches were investigated for the degradation of kerogen to larger but tractable and identifiable fragments. Among these the most promising one was a combination of micro-pyrolysis with pyrochromatography and mass spectrometry, designated as the MFGM method. A schematic outline of this method is shown in Figure 1.

This controlled pyrolysis method combined with reaction chromatography and mass spectrometry was used successfully for the separation and identification of predominantly primary pyrolysis fragments. Such fragments can be identified and yield useful information for the evaluation of the structure of kerogen subunits and that of kerogen itself.

## III. PROCEDURE

A modified "Fischer Technik" Induction Micro Pyrolysis instrument was used. This unit could be operated either in conjunction with a condenser unit or with a GC-MS unit consisting of a Beckman GC-4 unit and a AEI Model MS 12 mass spectrometer. The kerogen concentrate was applied to the pyrolysis needles in the form of a very thin coating. The needle was paced into a micro pyrolysis chamber equipped with an injection syringe tip which was inserted into the injection port of the GC instrument or into a micro-condenser unit. After ignition the volatile material was analyzed directly by the GC-MS unit or collected in the condenser for pre-separation of major fractions. To obtain sufficient material for the latter procedures e.g. GPC or micro column chromatography, up to 200 individual pyrolysis reactions had to be carried out. The pre-fractionation scheme used is shown in Figure 2. Some of these fractions (in particular the neutral hydrocarbon fractions) were subsequently analyzed by the GC-MS method.

Similar pyrolytic fragmentation experiments were carried out in conjunction with reaction chromatography using either selenium dehydrogenation or hydrogenation reactions. In this way one obtains either aromatized or completely saturated derivatives of the primary pyrolysis fragments; most of them representing "protokerogen" moieties.

Comparison of these derivative structures with the original primary fragments using these methods allows a better structural evaluation of the subunits of the hydrocarbon matrix of oil shale kerogen.

The pyrolysis fragmentation pattern of major subunits obtained by the MFGM method and the mass spectral fragmentation patterns of a number of such subunits could be corroborated using identical or closely related synthetic reference compounds.

#### IV. DISCUSSION

The results of these studies carried out over a period of several years led to the following conclusions:

1. Microscopic analysis and micro-spectrophotometric analysis of isolated "kerogen" particles indicates the presence of at least two types of kerogen components in the oil shale of the Green River Formation: The major component (designated as alpha-kerogen), represents an alginite like material of low aromatic content; the second component is present in the form of darker reddish-brown particles (beta-kerogen) with a much higher content of aromatic (probably polycondensed) material. The latter represents about 5 percent of the total kerogen present.

2. Under controlled micro-pyrolysis alpha-kerogen yields several types of subunits:

- a) normal and branched alkanes,
- b) alkyl derivatives of decalins and tetralins, (mostly o-substituted) and
- c) alkyl substituted tricyclic terpenoid or phenanthrenoid type derivatives.

In addition there are present a smaller number of higher molecular weight ring-compounds of probably steroid origin.

Some of the major subunits obtained by the MFGM method are summarized in Table I.

3. From these subunits and others obtained by micro-pyrolysis from kerogen one can rationalize a number of possible aspects concerning the structure of alpha-kerogen:

- a) The hydrocarbon part of the kerogen appears to be relatively uniformly structured i.e. consisting of nuclei of subunits (representing built-in "protokerogen" units), interlinked by normal or branched alkane bridges or long chain ether bridges. The major part of the subunits consist of alkyl substituted decalins or tetralins. A smaller proportion of these subunits may consist of ring systems containing hetero atoms.
- b) The bulk of the skeleton is hetero structural i.e. several hundred different types of subunits form a three-dimensional organic matrix. However there are repeatedly occurring predominant subunits of two and three-membered ring-systems. These have characteristic structural features which may be very informative about the origin of the "protokerogen" subunits. Thus the kerogen of the Green River Formation does not represent a material of randomly connected carbon atoms (scrambled eggs) but appears to be structured.
- c) One can make an attempt to put the principal subunits together and thus arrive at some reasonable reconstructed original structure of the kerogen molecule. From the structure of the subunits obtained it appears that they were interlinked by di- and tri-substituted subunits. The structure of the hydrocarbon skeleton of kerogen could therefore be visualized by a generalized structure shown in Figure 3.

4. A somewhat anomalous phenomenon observed in isolated kerogen concentrates provided additional information on the possible structure of kerogen. Exhaustively extracted kerogen stored under nitrogen for two years, yielded upon re-extraction with n-hexane 5-6 percent of material which upon analysis proved to be a mixture of normal and branched saturated hydrocarbons from C<sub>10</sub> to C<sub>25</sub>. Since the material was stored at ambient temperature (25°C), it must be assumed that these hydrocarbons have diffused to the surface of the kerogen particle from the interior of the kerogen matrix. Subsequent investigations not only corroborated this assumption but also indicated that in addition to these hydrocarbons there are entrapped within the organic matrix a number of other residual "prokerogen" components such as normal and branched fatty acids, alicyclic acids and/or their alkyl derivatives, cyclic subunits such as alkyl derivatives of decalins and tetralins, terpenoids etc. These compounds can be extracted from the matrix if one "swells" the kerogen particle by treatment with alkaline alcoholic solutions or by heat. The entrapped

fatty acids present in the matrix may explain their presence in the pyrolysate obtained under inert gas e.g. helium.

5. These experiments may indicate that these compounds may be the residual subunits from which the kerogen was formed by hetero condensation; it can be assumed that this condensation process is still progressing, although at a very slow rate, as part of the diagenetic process; however, because of the high viscosity of the substrate and the reduced diffusion rate the condensation reaction is strongly reduced. Thus a more complete structure of the isolated kerogen material could be visualized as shown schematically in Figure 4.
6. The entrapped material is very similar in composition to that of the soluble "bitumen". The latter is diffusely distributed in the oil shale between the kerogen particles and the inorganic mineral matrix. This portion of the organic matter in the oil shale of the Green River Formation may therefore also represent "protokerogen" containing material which is as yet not condensed to kerogen. Since the Green River Formation is a relatively young geologic formation it may explain the presence of the relatively high percentage ( 20 percent ) of still soluble lower molecular weight compounds in the organic matter of the oil shale.

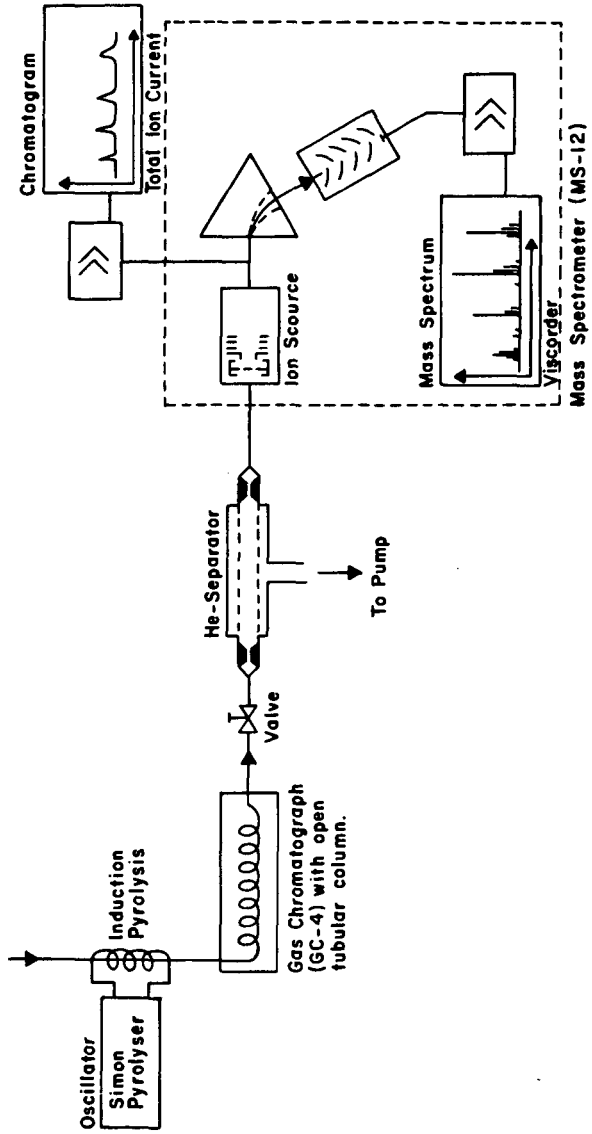
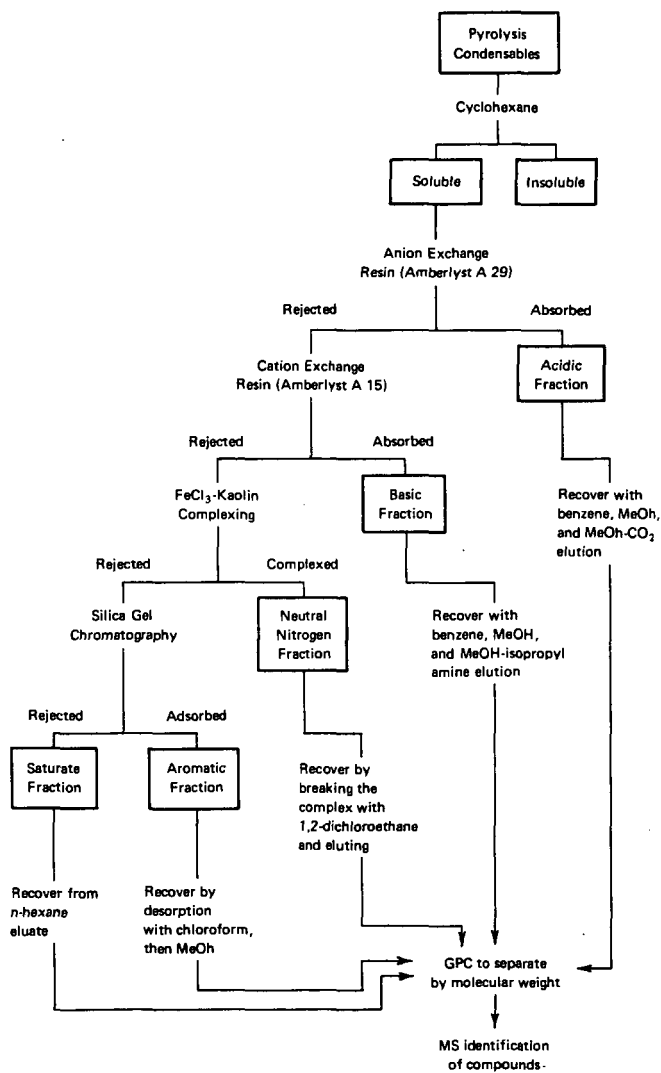


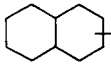
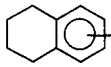
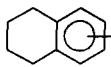
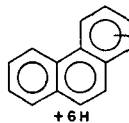
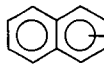
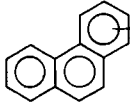
Figure 1. Schematic of the MPG System



**Figure 2.** Separation Procedure for Pyrolysis Condensable Fraction by Functionality

Table I.

## Principal Fragmentation Products of Kerogen Concentrate

No.	Name	Formula	Identified in Fraction
1	<u>Aliphatic Hydrocarbons</u>	n-C <sub>10</sub> to n-C <sub>34</sub>	85-7
		b-C <sub>10</sub> to b-C <sub>36</sub>	122-1
2	<u>Alicyclic Hydrocarbons</u>		
	Cyclohexanes	 C <sub>10-13</sub> H <sub>21-27</sub>	123-1
	Decalins	 C <sub>5-8</sub> H <sub>11-17</sub>	123-1
3	<u>Hydroaromatic Hydrocarbons</u>		
	Dialkyltetralins	 C <sub>2-5</sub> H <sub>5-11</sub>	122-1 123-1
		 C <sub>8-12</sub> H <sub>17-25</sub>	122-1
Hexahydro-phenanthrenes	 C <sub>1-3</sub> H <sub>3-7</sub> + 6H	123-1	
4	Dialkylbenzenes	 C <sub>8-13</sub> H <sub>17-27</sub>	123-1
5	Dialkylnaphthalenes	 C <sub>3-4</sub> H <sub>7-9</sub>	123-1 123-4
6	Alkylphenanthrenes	 C <sub>1-3</sub> H <sub>3-7</sub>	121-4 123-2

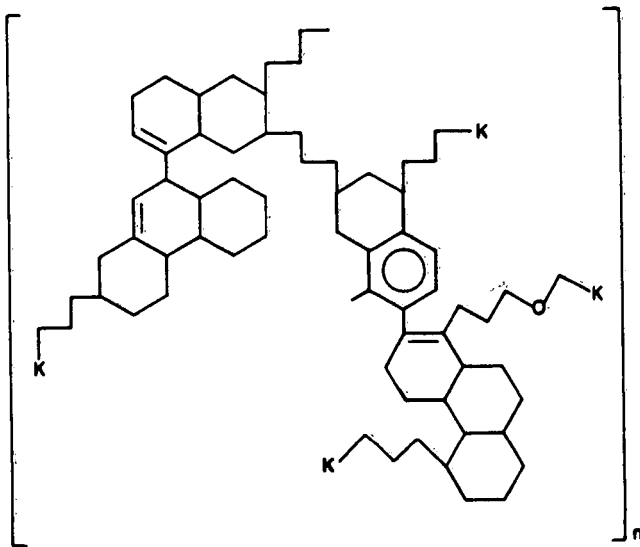


Figure 3. Generalized Structure of Kerogen of the Green River Formation

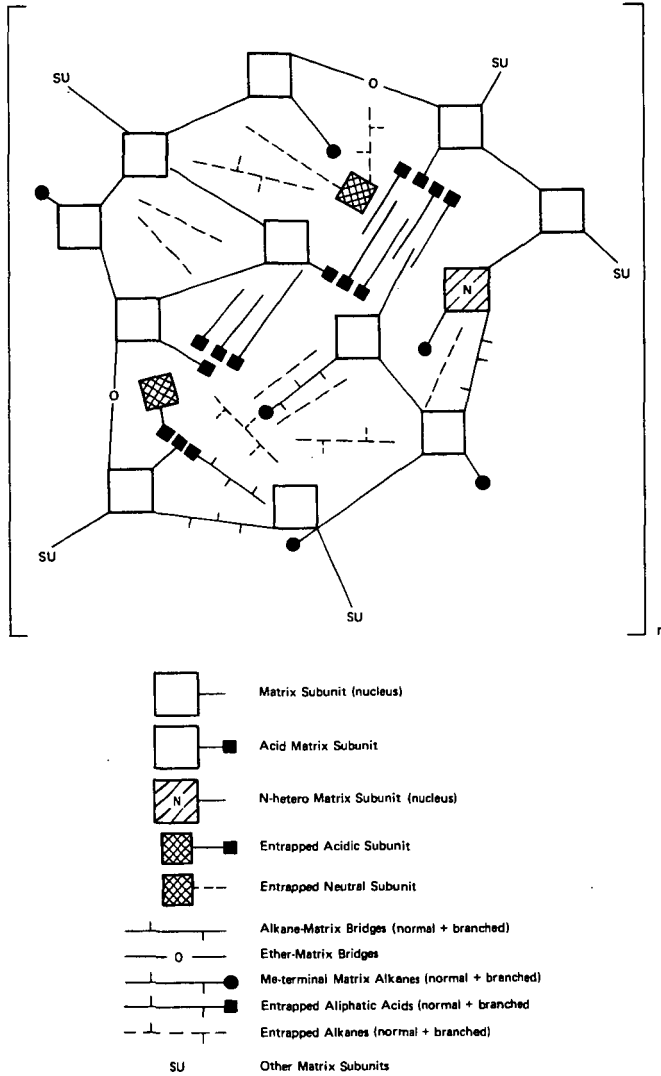


Figure 4. Schematic Structure of Kerogen Matrix

## A NEW STRUCTURAL MODEL OF OIL SHALE KEROGEN

T. F. Yen

Departments of Medicine (Biochemistry),  
 Chemical Engineering, and Environmental Engineering  
 University of Southern California  
 Los Angeles, California 90007

Kerogen is usually defined as the insoluble fraction of organic components of oil shale in contrast to the soluble fraction which is called bitumen (1). Structural elucidation of kerogen is difficult due to the following:

- (a) Kerogen is a large complex molecule belonging to the multipolymer class (2).
- (b) The insoluble nature of the kerogen is closely related to the non-uniform 3-dimensional gel nature of a giant crosslink network.
- (c) Inhomogeneity due to biogenesis.

All of these have challenged a number of researchers (3,4,5); so far the molecular structure of kerogen remains unsolved.

A method has been developed for the structural elucidation of amorphous and mesomorphic carbonaceous organic materials (6). It is possible to obtain a number of structural parameters from x-ray diffraction (7). The kerogen concentrate of Green River oil shale was obtained from W. E. Robinson of the Bureau of Mines. The bitumen-free sample was subjected to the usual acid leaching procedure to remove the carbonate and silicate minerals with ca. 10% of the ash content remaining; from the elemental analysis, %C is 66.4 and %H is 8.8.

The powdered sample of kerogen concentrate was packed in an aluminum holder and mounted in a goniometer. A Norelco diffractometer was used to measure the intensities ranging from  $2\theta = 8$  to  $100^\circ$ . The reduced intensity data were obtained by:

- (a) Adjusting the data for polarization by  $(1 + \cos^2 2\theta)/2$ .
- (b) Fitting the data to electronic units, A, by normalization of the amplitude to the region of  $0.40 \leq (\sin \theta)/\lambda \leq 0.50$ .
- (c) Substrating tabulated values of incoherent scattering, C.
- (d) Dividing each value by the proper value (for isolated carbon atoms) of the independent coherent scattering, E.

This reduced intensity, (A-C)/E of the Green River oil shale kerogen concentrate over the angular range of  $(\sin \theta)/\lambda$  of 0.02 to 0.50 is shown as the solid line in Fig. 1.

The first band in the low angle region does not appear as a doublet. The distance of the single peak centers at  $(\sin \theta)/\lambda = 0.11 \text{ \AA}^{-1}$  definitely corresponds to a  $\gamma$ -band ( $\sin \theta/\lambda = 0.10 \text{ \AA}^{-1}$ ). There is no peak or shoulder of the 002-band at  $(\sin \theta)/\lambda = 0.14 \text{ \AA}^{-1}$ . Based on this information alone, it is concluded that there is little or no aromatic carbon skeletons in the kerogen matrix. This is further substantiated by the fact that the controlled oxidation-derived products from oil shale contain no aromatic protons (8). The low angle peak in the x-ray graph of Fig. 1 is shifted slightly to the high-angle side (from 0.10 to  $0.11 \text{ \AA}^{-1}$ ). This fact may indicate that in the saturated structure there are some isolated double bonds.

The next two strong bands which center around  $(\sin \theta)/\lambda = 0.25$  and  $0.42 \text{ \AA}^{-1}$  are generally, classified as [10] and [11] reflections, respectively. These two bands correspond to the first and second nearest neighbors (2.1 and 1.2  $\text{\AA}$ ) in cyclic compounds for both aromatics and naphthenics. Since these fall in the 2-dimensional reflective region, a number of theoretical calculations has been made (9,10). The simplest procedure will be the profile matching procedure. From calculated patterns of 10 and [11] regions, only the contour of [11] of the kerogen fits the saturated-ring (naphthenic) from Fig. 1. For example the dash-dotted line (Fig. 1) is perhydro-agbi-dibenzoperylene and the dash line (Fig. 1) is perhydro-anthracene. The maxima of both patterns check quite well with the maximum of the pattern of kerogen. If there is an aromatic-ring structure in kerogen, it is anticipated to have a 2 or 3 unit-shift in  $\sin \theta/\lambda$  to the high angle region. An example is provided by the dotted line (Fig. 1) which corresponds to a polycyclic aromatic compound, anthracene. It is evident that the pattern of aromatic compounds does not match that of the oil shale kerogen.

Another important feature for these 2-dimensional patterns is the bandwidth. As the ring number increases, usually the bandwidth decreases (6). The profile for both [10] and [11] bands of the kerogen do indeed correspond to a 3-ring naphthenic (dash line, Fig. 1) better than a 7-ring naphthenic (dash-dotted line, Fig. 1). In this instance matching should be emphasized on the band shape (x-axis), not on the vertical y-direction since the intensities are relative. From this alone it is plausible to conclude that the saturated clusters within oil shale kerogen are small, in the 3-4-ring range.

In the  $\gamma$ - and 002-band region we have so far failed to locate the sharp doublet of [110] and 200 bands, as these are prerequisites for wax-like long chain alkane-containing compounds (11). Usually these two peaks, 4.15 and 3.74  $\text{\AA}$ , occur close to the  $\gamma$ -band in polymethylene chain-like-containing materials. These crystalline reflections are in all pure long chain paraffins. The absence of these two bands suggests there is no free end or flexible long-chain polymethylene in the kerogen of Green River oil shale. This is supported by the fact that we have not observed any  $725 \text{ cm}^{-1}$  band which is so characteristic of the  $-(\text{CH}_2)_n-$ , ( $n > 4$ ) structure in our infrared work, even at a lower temperature. However one cannot rule out the possibility of condensed or isolated cycloparaffin in which the flexibility has been inhibited.

Finally the multiple weak peaks between the  $(\sin \theta/\lambda = 0.28-0.35 \text{ \AA}^{-1})$  range in Fig. 1 of the kerogen could suggest the presence of diamond-like crosslink structures. One such example is the [102] band of hexagonal diamond crystallite. Of course, there are also possibilities of other contaminations.

To summarize, the present x-ray diffraction method strongly supports the following for Green River oil shale kerogen:

(a) There is little or nil aromatic carbon skeleton in kerogen. Aromaticity for this kerogen approaches zero. There is a possibility of the presence of isolated double bonded carbon structure (12).

(b) The bulk of the carbon structure is naphthenic containing 3-4 rings. It is possible that these are clusters and are linked by heterocyclic atoms and short-chain bridges.

(c) There is no free-end and flexible long-chain linear polymethylene structures in this kerogen. This does not rule out the possibility of the presence of the crosslink structure of elaterite (2) which could be condensed polycycloparaffin. Such a structure could be foreseen as poly-

mantane-like (1), since alkyl adamantanes are easily converted by Lewis acid from a great number of precursors including steroids and terpenoids.

(d) The C/O atomic ratio of kerogen is 18. The distribution of oxygen functional groups in this kerogen is predominantly of ether type (53%) and ester type (25%)(13). The crosslink sites of the structure of (b) is anticipated to be largely oxygen.

(e) The age of the Eocene formation of Green River oil shale kerogen is considered to be youthful (18). The diagenesis is expected to be still in progress. Actually the difference of bitumen versus kerogen is of degree, not of kind. The analogy is similar to the difference between asphaltenes and the insoluble carbonenes and carboids in source rocks. In this sense the structure of kerogen can be reflected from the structure of bitumens.

(f) The structure of kerogen is a multi-polymer consisting of monomers which are the molecules so far identified from bitumen. These molecules in bitumen are steranes, triterpanes and isoprenoids, such as squalene, lycopene, cyclic carotenoids of  $C_{40}$  (15), etc. The monomers also can be inferred as the mild oxidation products when the kerogen is subjected to oxidation by aqueous permanganate (8). In this instance the products are mono- and di-carboxylic acid homologs.

(g) There is as anticipated, not only the primary bonding but secondary and tertiary bonding as well. The inter- and intramolecular hydrogen bondings as well as the charge-transfer bonding plays an important role. Molecular entrapment of which the molecular force is in the van der Waals range, become important. This is especially true since the nature of kerogen is comparable to a molecular sieve and can retain small molecules present in bitumens.

In conclusion, a hypothetical structural model is proposed to summarize the above statement (Fig. 2).

#### ACKNOWLEDGEMENT

This work is supported by NSF Grant No. GI-35683.

#### REFERENCES

1. T. F. Yen, "Terrestrial and Extraterrestrial Stable Organic Molecules," in Chemistry in Space Research, (R. F. Landel and A. Rembaum, eds.), Elsevier, New York, 1972, pp. 105-153.
2. T. F. Yen, Energy Sources, 1, (1973).
3. M. Djuric, R. C. Murphy, D. Vitorovic, and K. Bilmann, Geochim. Cosmochim. Acta, 35, 1201 (1971).
4. A. L. Burlingame, P. A. Haug, H. K. Schnols, and B. R. Simonet, Adv. Org. Geochem. Proc. Int. Congr. 4th, Pergamon, 1969, pp. 85-129.
5. C. H. Prien, Lectures delivered at USC, 1973.
6. T. F. Yen, J. G. Erdman, and S. S. Pollack, Anal. Chem., 33, 1587 (1961).
7. T. F. Yen, ACS, Div. Petrol. Chem., Preprints, 17, F102-F114 (1972).
8. D. K. Young, S. Shih, and T. F. Yen, This Preprints (1974).

9. S. Ergun, W. Donaldson, and R. W. Smith, Jr., X-ray Diffraction Data for Aromatic, Hydroaromatic, and Tetrahedral Structures of Carbon, Bull. 620, U. S. Bureau of Mines, 1965.
10. R. Diamond, *Acta Cryst.*, **10**, 359 (1957).
11. T. F. Yen, *Nature Phys. Sci.*, **233**, 9-13, 36 (1971).
12. T. F. Yen and J. G. Erdman "Asphaltenes (Petroleum) and Related Substances: X-ray Diffraction," in Encyclopedia of X-rays and Gamma-rays, (G. L. Clark, ed.) Reinhold Publishing Corp., New York, 1963, pp. 65-68.
13. J. I. Fester and W. E. Robinson, "Oxygen Functional Groups in Green River Oil-shale Kerogen and Trona Acids" in Coal Science, ACS, pp. 22-31, 1966.
14. D. E. Anders and W. E. Robinson, *Geochim. Cosmochim Acta*, **35**, 661 (1971).
15. E. J. Gallegos, *Anal. Chem.*, **43**, 1151 (1971).
16. A. L. Burlingame, P. Haug, T. Belsky, and M. Calvin, *Proc. Nat. Acad. Sci.*, **54**, 1406 (1965).
17. A. Ensminger, A. VanDorsselaer, C. H. Spyckerekke, P. Albrecht, and G. Curisson, 6th International Meeting on Organic Geochemistry, September, 1973.
18. T. F. Yen and S. R. Silverman, *ACS, Div. Petrol. Chem. Preprints* **14** (3), E32-E39 (1969).

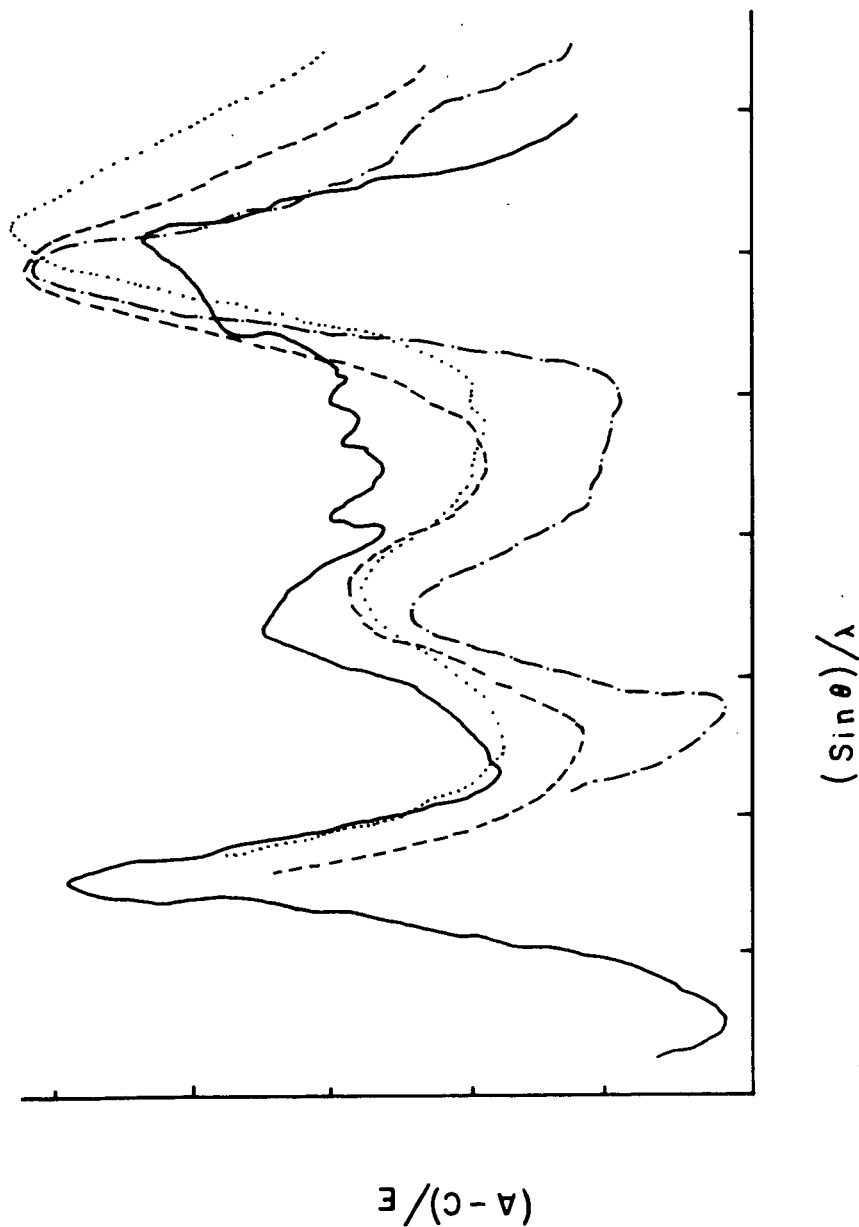


Fig. 1. X-ray Spectrum of Green River Oil Shale Kerogen and Calculated Intensities of some Hydrocarbons. Solid line is kerogen; dotted line is the calculated intensities of anthracene; dash line is those of perhydroanthracene; the dash-dotted line represents those of perhydro-dibenzo(a,g,b,i)perylene.

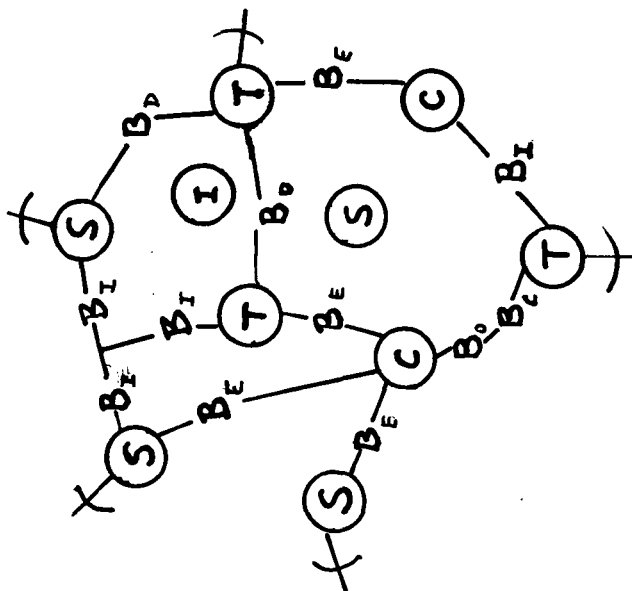
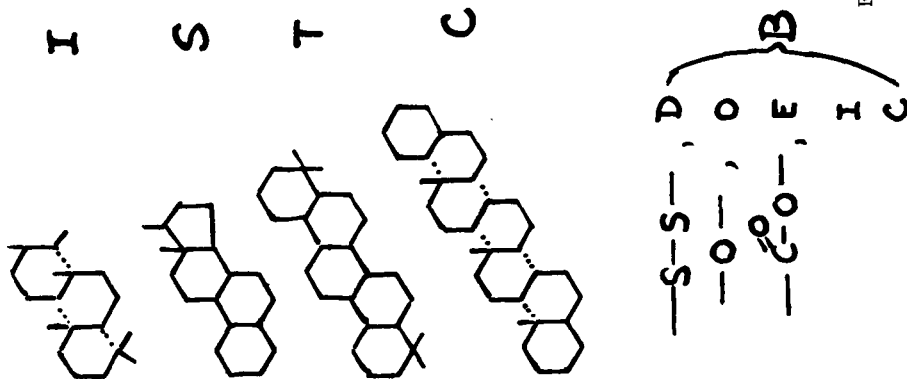


Fig. 2. Hypothetical Structural Model of Green River Oil Shale Kerogen. The left are the monomers of the multipolymer. I, represents isoprenoids; T, terpenoids; C, carotenoids; and B, bridges (molecules have been isolated from Green River oil shale, see Ref. 13-17). Bridges can be disulfide (D), ether (E), ester (E), isoprenoid (I), and carotenoid (C) linkages. The entrapped molecules in the matrix of the network is not bonded.

POLYCONDENSED AROMATIC COMPOUNDS (PCA) AND CARCINOGENS IN THE SHALE ASH  
OF CARBONACEOUS SPENT SHALE FROM RETORTING OF OIL SHALE OF THE GREEN  
RIVER FORMATION

J. J. Schmidt-Collerus, Francis Bonomo, and C. H. Prien  
University of Denver, Denver Research Institute  
Denver, Colorado 80210

I. POTENTIAL OF A COMMERCIAL OIL SHALE INDUSTRY  
IN THE U.S.A.

Although there are large oil shale deposits outside of the United States (e.g. Manchuria, USSR, Brazil, etc.), the United States contains some of the largest deposits of oil shale considered to be most promising for potential oil shale production. Among the U.S. deposits, those found in Colorado, Utah and Wyoming (representing oil shale of the Green River Formation) are known to be the richest ones in the nation and are contained predominantly in three large basins: The Piceance Creed Basin in Colorado, the Uintah Basin in Utah and the Green River Basin in Wyoming. Among these the Colorado deposits are considered to be the richest in high grade oil shale.

The oil shale deposits occur beneath 25,000 square miles of land of which 17,000 square miles (11 million acres) are believed to contain oil shale of potential "commercial" value. The Green River Formation deposits include high grade shales (averaging 25 or more gallons of oil per ton of rock) representing about 600 billion barrels of oil and an additional 1,200 billion barrels in places of low grade oil shales (with an average yield of 15-20 gallons per ton). The total in-place reserves of equivalent shale oil in the Green River Formation is estimated to amount to more than three trillion barrels.

In addition to the actual oil shale there are large reserves of sodium minerals present in the Piceance Basin, particularly nahcolite ( $\text{NaHCO}_3$ ), trona ( $\text{Na}_2\text{CO}_3 \cdot \text{NaHCO}_3 \cdot 2\text{H}_2\text{O}$ ), halite ( $\text{NaCl}$ ) and a sodium-aluminum mineral, dawsonite ( $\text{NaAl}(\text{OH})_3\text{CO}_3$ ), which occur in zones at greater depths of the basin (1800-2000 ft.).

Thus, oil shale represents a sizable portion of the nation's energy sources. While the development of these resources was hampered in the past by inadequate technologies and strong competition with domestic and foreign crude oils, the increasing demand of energy sources in general and the political situation of the present time in particular, have brought the possibilities of a commercial exploitation of these deposits into sharper focus. This appears evident from the announcement of some industrial companies such as Colony Development Corporation, Union Oil and

Occidental Oil to venture into commercial production and the more recently announced leasing of government-owned land to Gulf Oil and Standard Oil of Indiana.

Based on statements made by some of the companies interested in the commercial exploitation of the waste oil shale deposits it would appear that at present the state of the art in mining and processing technologies for oil shale have reached the stage to be potentially feasible for commercial application although some of the operations will require disposal areas and availability of considerable water resources.

A 50,000 barrel/day plant using surface retorting of shale averaging 30 gallons per ton will require 72,000 tons per day of raw shale as feed and will discard 61,000 tons per day of spent shale. Most mining of the shale will probably be done by the room-and-pillar method, with perhaps 10-15% being treated by open pit mining; strip mining is not being considered at the present time. Their possible contribution to an oil shale industry, however, must be considered.

The extraction of the oil from the oil shale, i.e. the so-called "retorting process" can (in principle) be carried out by "above-ground" retorting using oil shale mined by one of the afore-mentioned methods or by the so-called "in-situ" or in-place underground retorting of the oil shale deposits.

There are three basic "methods" for above-ground retorting. In each case the shale rock is heated to 900-1000°F and the oil vapors obtained are removed and cooled to yield a semi-viscous liquid which is shale oil. The latter is subsequently upgraded to yield either a pipeline crude or various partially refined products (fuel oil, naphtha, etc.). The main processes of this type are the following:

1. Tosco II/Colony Retort
2. Vertical Retorts such as
  - a. Union Rock Pump Retort
  - b. Bureau of Mines Gas Combustion Retort
  - c. Petrosix Externally-heated Retort, and
  - d. Paraho Vertical-kiln Retort.

All but the Union retort use downward gravity flow of shale.

3. Lurgi Retort using fluidized bed.

The "in-situ" processing of oil shale is an attractive alternative to mining and above ground retorting. Its main advantage claimed is the elimination of the mining and kiln retorting, the elimination of the necessity of disposal of spent shale and large scale water requirements. However, in-situ retorting has not been technically or economically successful to date and requires considerably more research - although most recently Occidental Oil Company has announced that it has demonstrated successfully an in-situ method which according to the report may be developed within the near future. The shale oil obtained from the retorting of oil shale stems from the cracking of the organic matter contained in the marlstone type sedimentary rock of the oil shale. The major portion of this organic matter is an insoluble high molecular weight organic material called "kerogen." In the case of the oil shale of the Green River Formation kerogen represents a three-dimensional organic matrix composed of more complex cyclic organic subunits called "proto-kerogen" linked together by longer alkane or ether type compounds bridging these subunits. Entrapped within this matrix are residues of protokerogen components which have as yet not combined with each other by diagenesis due to increase in viscosity and the admixture of considerable amounts of inorganic mineral matter. The mixture of the two major components forms the rather compact rock called oil shale. Heating the rock (retorting) to 900-1200°C will break up the organic matrix and form lower molecular weight organic hydrocarbons which yield the major constituents of the shale oil produced.

The technology of oil shale mining and production in the United States and the economics of the energy requirements are such that a commercial industry is eminent. However, some of the processes will require considerable amounts of water for their operation and will also lead to disposal problems. The water requirements will vary with the process involved. For a typical 50,000 barrel/day plant the water consumed would be 20 acre feet/day which is about 3 barrels of water per barrel of shale oil produced. Some 45% of this water is used for wetting and compaction of the discarded spent shale, 25% for retorting and upgrading and 30% for mining, crushing, etc. All water diverted is eventually consumed in the process. A one million barrel/day operation would require approximately a total of 175,000 acre ft. of water per year.

Furthermore, the initiation of a commercial oil shale operation for instance in the Piceance Basin will also generate solid waste of considerable proportion. On the basis of evaluations made by government and industry the estimated amount of spent shale generated at the end of 1979 (i.e. only five years hence) will be approximately 183,000 tons per day or over 60 million tons per year and by 1987 when the production is considered to exceed one million barrels/day, the spent shale produced will be about 1,280,000 tons/day or approximately 420 million tons of spent shale per year. In some types of operations an estimated 50-60 percent of the retorted residue could be replaced into the mine and 40-50 percent will have to be disposed on the surface.

## II. POTENTIAL ENVIRONMENTAL IMPACT

Because of the necessity of solid waste disposal encountered in some processes, the water requirements and the possible socio-economic implications such an industry may have, it is not surprising that the potential problems of environmental impact of commercial operations were raised by an ever-increasing environmental-conscious segment of the population. This led eventually to the compilation of a six-volume Environmental Impact Statement prepared by the U.S. Department of the Interior, the finalized form of which was published in 1973. This document covers practically every facet of potential environmental impacts which could ensue from commercial oil shale operations and countermeasures proposed, the effectiveness of which have been already demonstrated experimentally in pilot studies. However, in many other aspects the "Impact Statement" does not (and probably was not intended to) provide final solutions but rather outlines potential problems and can by necessity provide only guidelines to possible solutions because in many cases there just is as yet not available sufficient hard core experimental data. There exists therefore in many areas covered by the Impact Statement the need of experimental implementation and/or corroboration and of course this is also indicated in the document.

This appears to be certainly true with respect to some aspects of the problem areas with which the research program conducted under this NSF Grant is concerned, i.e. the potential environmental effects stemming

from the generation and disposal of carbonaceous spent shale. The data obtained from these investigations are to be considered preliminary at the present and represent a mere point of departure. However, with the foreseeable development of actual larger scale demonstration plants (in the order of 50,000 barrels of oil per day) these investigations appear to be timely and hopefully may contribute some new experimental data useful for a better evaluation of the potential environmental problems. The basic philosophy of the present research program is therefore to investigate these problems experimentally (in cooperation with the industry and government agencies interested in shale oil production), and make the results of these investigations available to all interested private and other government organizations and also publish them in the open literature.

What then are the possible environmental impacts which could conceivably result from the generation and disposal of carbonaceous spent shale?

The major by-products from an oil shale operation are (a) the solid spent shale, (b) the process water generated during the retorting (pyrolysis) process and (c) process gases.

The composition and properties of the solid waste will depend on the type of retorting process used and the conditions of retorting. In some of the retorting processes the resulting spent shale still contains up to five percent carbon residue from the original organic matter present. This carbonaceous organic matter is in part present as organic compounds which are soluble in organic solvents. It stands to reason that due to the pyrolytic process used during retorting part of this organic matter consists of polycondensed organic matter (POM) which may include polynuclear or polycondensed aromatic hydrocarbons (PAH) and aza-azarines (AA) in addition to other types of higher molecular weight organic compounds.

While in itself the formation of such compounds in small quantities is practically ubiquitous wherever pyrolysis of organic matter occurs and could therefore be regarded as more or less inconsequential, systematic and long range investigations carried out over the last few decades have shown that chronic exposure to certain polluting inorganic trace elements as well as trace amounts of polycondensed aromatic pollutants can have a detrimental effect on the ecology including man.

The fact that such organic compounds may be present (even in trace quantities) in carbonaceous spent oil shale cannot be overlooked for the simple reason of the magnitude of their production.

Obviously not every commercial operation will produce carbonaceous spent shale. However, there is considerable evidence that some of the processes ready for larger scale operations will produce carbonaceous spent shale. Consequently the disposal of this type of solid waste involves not only inorganic trace elements and water leachable salts but also considerable amounts of residual organic matter containing polycondensed aromatic hydrocarbons.

On the basis of the estimated spent shale generated in 1979 alone, this could include up to 3.1 million tons of carbonaceous matter which may contain as much as 6,000 tons of solubilizable and in part volatile organic compounds. It is conceivable that even a small portion of these organic compounds may have (in the long run) some undesirable impact on the ecosystem because of potential leaching and accretion of this material in the aquifer, their potential concentration during recycling operation of impounded water and their possible translocation into the vegetation and/or partial transfer into the surrounding atmosphere. Some of this rationale applies not only to above ground operations but also to potential "in-situ" operations. The potential impact from these trace organic matter from carbonaceous spent shale has not been investigated to date systematically and in greater detail. It is the main objective of the present research program to fill this gap. The exposition of the more detailed potential problems involved, and methods of approach utilized, and the preliminary experimental results obtained to date are presented in the First Annual Report to be submitted to NSF and various other interested agencies.

### III. PRELIMINARY RESULTS

The major activities and preliminary results of these investigations (carried out to date) can be summarized as follows:

A. Samples of soil, water, vegetation and air from various pristine (i.e. as yet undisturbed) areas of potential future oil shale operations were collected and analyzed for their content of polycyclic organic matter in particular polycondensed aromatic hydrocarbons including those of known

carcinogenic properties such as 3,4 benzo[a]pyrene. This was done to establish a base line for future comparative studies.

B. Samples of carbonaceous spent shale from various retorting processes used in pilot plants (operated at various times) were collected and also analyzed for their content of polycondensed aromatic compounds.

Neither of the two studies mentioned above have as yet been completed and more detailed comparisons must await additional experimental data.

The results of these preliminary investigations indicate the following:

1. Carbonaceous spent shale with up to 5% organic carbon content, contains higher molecular weight and lower molecular weight organic material soluble in organic solvents. The benzene soluble fraction ranges from 0.02 to 0.2 percent, depending on the retorting conditions and the age of the spent shale.

2. The benzene soluble portion contains polynuclear organic matter (POM) such as polycyclic aromatic hydrocarbons (PAH) and aza-azarines. The PAH compounds contain (among other components) also 3,4 benzo[a]pyrene.

3. The percent amount of benzene soluble material in carbonaceous spent shale is about one order of magnitude higher than in the soils from pristine areas but about one order of magnitude lower than that found in airborne particulate matter, e.g. collected in industrial areas. However, on a volume basis (cubic meter of material) spent shale is higher in soluble material (12 order of magnitudes).

4. In a traverse of a gulch projected as a disposal area the extractable material in soil is in general also one order of magnitude lower than in the spent shale ash, but varies with the density of vegetation growing at the particular sampling site; this is due to the fact that endogenic PAH compounds generated by the vegetation will eventually end up in the soil.

5. The content of benzo[a]pyrene in the benzene extracts is about three order of magnitude higher than that in the extracts of soil and/or plant material from the pristine environment and 3 to 30 fold as high as in vegetables (e.g. salad with approximately 10 micrograms/kg dry weight) and smoked food (1-10 micrograms/kg dry weight).

6. Preliminary data also indicate that saline water from leached carbonaceous shale may be at least three to four order of magnitudes higher in PAH content than ground water or surface water from pristine areas.

7. Polycyclic aromatic compounds can apparently be leached from the carbonaceous spent shale by water to a considerable extent in the presence of water soluble inorganic salts.

8. Whether the amount of PAH compounds with known carcinogenic properties present in carbonaceous spent shale constitutes a serious hazard to the environment will need more extensive studies and additional experimental data to allow comparison with urban and industrial environments to which man is exposed at the present time. Therefore the final answers will have to await forthcoming results from extended investigations.

9. Studies on the oxidation of carbonaceous shale ash have been initiated. There are as yet not sufficient data available to lead to any definite conclusions.

## HYDROGASIFICATION OF OIL SHALE

S. A. Weil, H. L. Feldkirchner, and P. B. Tarman

Institute of Gas Technology  
Chicago, Illinois 60616INTRODUCTION

In the early 1960's, the Institute of Gas Technology (IGT) carried out an extensive research program for the American Gas Association (A. G. A.) on the direct hydrogasification of, primarily, Colorado oil shale (3). IGT used laboratory and bench-scale equipment. In the bench-scale tests, using cocurrent hydrogen/shale contacting, we were able to gasify about 65% of the organic carbon in the oil shale. About 15% was converted to light aromatic liquids, and about 20% remained in the spent shale. The major variable controlling the conversion of organic matter to gas was the hydrogen/shale ratio.

Economic studies indicated that the cost of pipeline gas from oil shale was promising. However, there were two major disadvantages in cocurrent operation:

- Approximately 20% of the available energy in the raw shale was not recovered, and it was questionable whether the residual organic matter could be economically recovered as process fuel.
- Most of the heat used in preheating the shale to reaction temperature would be lost as sensible heat in the hot spent shale, which would discharge at 1100°-1300°F.

This study was initiated, therefore, to investigate the technical and economic feasibility of producing synthetic pipeline gas from oil shale by hydrogasification, using countercurrent gas-solids contacting and excess hydrogen. It was expected that the use of excess hydrogen with controlled, countercurrent shale heating and cooling would result in increased organic carbon removal from the shale and improved heat recovery - resulting in improved overall process efficiency compared with previous processes. The use of excess hydrogen would require hydrogen recycle, but would probably permit operation at lower pressures and thus reduce plant capital equipment costs (relative to processes using cocurrent gas-solids contacting and near-stoichiometric hydrogen/shale ratios). Preliminary economic studies based on a 20-25 gal/ton Fischer Assay oil shale indicate that raw material costs would be much greater than reactor costs. Thus, it would be desirable to convert as much of the organic matter content of the shale as possible. This would also be desirable in view of long-range energy conservation principles.

Initially, we carried out material and energy balance, heat transfer, and other process design calculations to determine the general areas for the most efficient operation. Next, we conducted a series of tests using a thermobalance to determine the effects of temperature, pressure, hydrogen partial pressure, and the rate of shale heat-up on the rate and ultimate level of kerogen conversion. Ways to minimize undesirable mineral carbonate decomposition reactions were also studied. Finally, a series of tests was conducted in a 4-inch-diameter reactor to determine the effects of process variables on the yields of gaseous, liquid, and solid products and their rates of production from oil shale kerogen. In this paper, we present test results relating process variables to product yields and product properties.

## THERMOBALANCE STUDIES

### Experimental

The test program to study the effects of temperature, hydrogen pressure, particle size, and heat-up rate on the rate and extent of kerogen removal from the shale was carried out with a thermobalance, as diagrammed in Figure 1. The design and operation of the equipment have been described earlier (2).

In most of the runs, the shale sample (as pebbles) was contained in a stainless-steel wire-screen basket 1/4 to 3/8 inch in diameter and 3 inches in height. The reactor section was brought to the desired initial temperature with a stabilized gas flow stream at about 10 SCF/hr. The sample was lowered into the reactor and the power into the heating elements adjusted to achieve the desired heat-up rate. The heat-up rates used included slow (about 15° F/min), fast (about 35° F/min), and very rapid, in which case the sample was lowered quickly into a preheated reactor. In the last case, it is estimated that about 40 s were required for the sample to attain reactor temperature. After a prescribed time or upon reaching a prescribed temperature, the sample was raised into a cool region above the reactor, effectively stopping further reaction.

The sample was weighed before and after each run, and the residue was analyzed for carbon, carbonate, hydrogen, and ash. During the run, the sample weight and temperatures (using four thermocouples which surrounded the sample) were continuously recorded.

After selection, the shale rocks were crushed, sieved, and divided by riffing into small samples. The shale samples were 2.5 to 3 g in weight and -6+10 in U.S. Standard sieve size. Random samples chosen for chemical analysis gave the following average composition. (See Table 1.)

Table 1. SHALE COMPOSITIONS

Composition	Rich Shale,	wt %	Lean Shale,
	52 gal/ton		11 gal/ton
Organic Carbon	21.06		5.40
Hydrogen	2.84		0.99
Carbon Dioxide	12.54		18.17
Sulfur	0.83		0.45
Calcium	6.3		8.8
Magnesium	3.3		4.8
Ash	60.0		74.0

It is estimated that the rich shale has 40.3% potentially volatile material of which 12.5% is CO<sub>2</sub> and 27.8% is other volatile components (OVC). Of the CO<sub>2</sub>, 53% is from the CaCO<sub>3</sub> and 47% is from the MgCO<sub>3</sub>.

#### Results of Rich-Shale Studies (Total Conversion)

The weight loss vs. time curves and the shale residue compositions were determined for a wide variety and range of conditions. The major variables were hydrogen pressure, gas composition, heat-up rate, initial temperature, and maximum temperature.

A typical time-temperature-weight loss relation is shown in Figure 2. Characteristics common to all heat-up rate runs are the onset of significant weight loss at 700°F and a rapid rate of weight loss between 800° and 1000°F, followed by a much slower rate until about 1100°F when the rate increases again significantly. The thermobalance measures only weight changes, so the curve represents weight loss due to CO<sub>2</sub> as well as to kerogen removal. In any given run, only the final amounts of each component are known. Other runs were made at the same operating conditions and temperature histories except that the samples were withdrawn from the reactor at different temperatures. From their residue analyses, additional points were added to Figure 2 to show an estimate of the weight loss due to volatile components other than CO<sub>2</sub> (OVC) and of that due to CO<sub>2</sub>. These results show that there is a sharp drop in the rate of kerogen removal above about 1000°F. Furthermore, although there is still organic carbon left, there is not much more weight loss beyond 1200°F. The above behavior appears to apply to all of the runs made.

Under almost any conditions, the organic carbon recovery in a hydrogen atmosphere was at least 87%. The maximum recovery in a helium atmosphere was 77%.

From the variations of time-temperature paths, the following qualitative characteristics were found to be true in a hydrogen atmosphere.

- a. Direct exposure (hence, very rapid heat-up) to temperatures of 1300°F or higher leaves about 13% of the original carbon in the residue regardless of exposure time.

- b. Soaking of the shale sample for 1 hour or more at 700° or 800° F (or very slow heat-up) improves kerogen conversion at higher temperatures.
- c. Soaking at low temperatures without heating above 1000° F results in as much kerogen recovery as direct exposure to high temperatures (13% of original carbon remaining ).
- d. Higher hydrogen pressures resulted in lower residual organic carbon.

Figure 3 shows the residual organic carbon for the range of hydrogen pressures and heat-up rates studied. In all of these runs, the final temperature was 1300° F. It is apparent that the high-temperature kerogen recovery is extremely pressure sensitive.

The carbonate decomposition does not become significant until 1000° F and, as would be expected, is greater for longer periods at temperatures above 1000° F. There appears to be a qualitative correspondence between residual organic carbon and residual CO<sub>2</sub>. For example, it is noticeable in comparing the helium runs with the pure hydrogen runs which have the same time-temperature path to 1300° F. The former resulted in 23% residual carbon and 80% residual CO<sub>2</sub>. The latter resulted in 7% residual carbon and 34% residual CO<sub>2</sub>. In two areas, this rough correspondence does not hold; at low hydrogen pressure or very rapid heat-up rates, the conditions are relatively poor for kerogen recovery and very good for carbonate decomposition. Also, kerogen recovery is enhanced relative to CO<sub>2</sub> generation when the shale is soaked in hydrogen at temperatures below 1000° F and above 700° F. Figure 4 shows that low carbonate decomposition (less than 20% of original) can be achieved in simple heat-up paths, but at the expense of leaving 8% of the shale's organic carbon. To obtain lesser amounts of carbons, the most favorable path for minimal CO<sub>2</sub> generation is that of long soaking at 800° F before heating to higher temperatures. In that case, a residual carbon of only 3% of the original carbon can be achieved with 65% carbonate decomposition, as compared to almost 100% carbonate decomposition to achieve the same residual carbon by uniform heat-up.

An alternative method of suppressing carbonate decomposition is possible because the decomposition pressure of CaCO<sub>3</sub> is low enough to be overcome by a trace of CO<sub>2</sub> in the gas phase. When 2% CO<sub>2</sub> was added to the feed gas (10-*psia* CO<sub>2</sub>), the carbonate decomposition was much less than in the corresponding pure hydrogen runs.

It should be noted, however, that while the carbonate decomposition was repressed, the kerogen recovery was also reduced relative to the pure hydrogen runs. Thus, the net improvement was not as striking as implied by the CO<sub>2</sub> repression (Figure 4).

## Results of Rich-Shale Studies (Kinetics)

### Low-Temperature Kerogen Recovery

In the heat-up runs, there appears to be a significant decrease in weight-loss rate when the sample reaches about 1000°F and has lost about 25% of its original weight (Figure 2). In constant-temperature runs below 1000°F, there appears to be a limiting weight loss, again about 25% of the rich shale. In this discussion, this portion of the recovered kerogen (and any other materials that comprise this weight loss) is referred to as the low-temperature weight loss or kerogen recovery.

In Figure 5, the low-temperature weight-loss rates for several heat-up runs are shown as functions of the extent of weight loss. The range of operating conditions includes 15° to 35°F/min temperature-rise rates and 20 to 500 psig pressures. In all cases, the low-temperature rate can be extrapolated to zero in the region of 23 to 25% weight loss. The actual rate goes through a minimum in this region (which also corresponds to 1000° - 1100°F), the subsequent rise being due to the CO<sub>2</sub> generation that begins at these temperatures and increases very rapidly. (See Figure 2.)

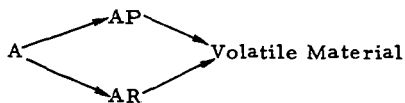
In Figure 6, similar data are presented at higher conversions for the constant-temperature runs at 800°, 900°, and 1000°F. Again, the rate of weight loss appears to become zero at about 25% weight loss. However, at 700°F the extrapolated weight loss at a zero loss rate was significantly lower than in the other runs, being about 11% rather than 25%.

It is apparent that, at temperatures of at least 800°F and, at most, 1000°F, a definite fraction of the kerogen is capable of being removed and will be removed if enough time in a hydrogen atmosphere is allowed. Furthermore, if any more kerogen were to be recovered at temperatures below 1000°F, it would require an additional time that is an order of magnitude greater than that needed for the low-temperature kerogen recovery.

In the case of the rich shale, the low-temperature weight loss, on the average, is 25.0% and (as are all kinetic data) is based on thermobalance data rather than on chemical analysis. There was no way to identify the components in this 25% from the data taken.

The randomness of the extrapolated values about 25%, regardless of temperature, makes it safe to assume that no portion of that 25% is CO<sub>2</sub>. Of the other volatile components, 25% of the 28% in the original feed may constitute the low-temperature kerogen, leaving 3%. This value is supported by the results of runs in which the shale was at temperatures high enough to achieve full low-temperature weight loss (900° - 1000°F), but inadequate to go any further. In these, the final OVC was 3.3 to 3.4%.

Attempts to devise a kinetic scheme for the low-temperature kerogen recovery in hydrogen have been made, but have not been successful. The constant-temperature data appear capable of description by a linear combination of first-order exponential terms as might result from a mechanism such as -



where AP and AR represent two different intermediate species. However, the determination of the appropriate kinetic parameters from the data proved to be very sensitive, and a satisfactory fit of the data has not been achieved.

#### High-Temperature Kerogen Recovery

The thermobalance data permit examination of the kinetics at low temperatures ( 1000°F ) because of the fortuitous fact that no CO<sub>2</sub> is generated in that region. Above 1000°F, the CO<sub>2</sub> generation precludes any kerogen-generation rate data. Any analysis of the high-temperature kerogen recovery must be based solely on the residue analyses.

Among the runs with rich shale in hydrogen, a surprisingly large number resulted in residual organic carbons of about 2.7% of the original sample. These included -

- a. Instantaneous heat-up runs that did not have a reasonable time below 1000°F
- b. Runs at low hydrogen pressures
- c. Constant temperature runs below 1000°F

Runs in which temperatures higher than 1000°F were reached in hydrogen atmospheres left this amount or less residual carbon. It is very reasonable to identify the 2.7% residual carbon of the rich shale with the residual of the low-temperature kerogen recovery. Possibly fortuitously, the low-temperature OVC residual of 3% is approximately the same fraction of the original OVC as the 2.7% residual carbon is of the original carbon.

Eighteen runs at 500 psig with the rich shales resulted in residual carbon contents significantly lower than 2.7%. Simple relationships between the residual carbon and temperature history were sought, but not found. One characteristic of the results is that comparable conversions can be obtained in shorter time periods if the sample is uniformly heated from 600° to 1300°F than if it is dropped into 800°F or higher, held there, and then heated to 1300°F. This, together with the fact that we could not obtain high conversion (of the potential 2.7% high-temperature product) with long times at high temperatures, implies competing reactions are involved - one to the product or its precursor and the other to residual carbon. To even qualitatively explain both heat-up and constant-temperature run results, it is necessary to assume that the basic competing reactions are fast and that the ultimate conversion is determined within a few minutes of exposing the shale to reaction temperatures (probably above 600°F).

### Results of Lean-Shale Studies

Because of the small fraction of organic carbon in the original sample and the correspondingly small amount of carbon in the residue, it is difficult to be sure of the significance of differences in the residual carbon among the runs. Certainly, qualitatively, there are many similarities with the results with the rich shale. Among these are -

- a. A residual carbon which is about twice as great in an inert gas (helium) as in hydrogen is obtained.
- b. Without low-temperature exposure, 89% of the organic carbon can be recovered compared with 87% for the rich shale.
- c. Seven percent of the carbon remains in fast heat-up runs and 3% in slow heat-up runs. The rich shale showed 7.3% and 3.6%, respectively.
- d. CO<sub>2</sub> generation is suppressed by CO<sub>2</sub> in the feed gas, but with a penalty in kerogen recovery.

There is other behavior which is different. Most noticeable is a much lower CO<sub>2</sub> generation rate in the lean shale. Only very long exposures at high temperatures resulted in CaCO<sub>3</sub> decomposition. In most of the runs only 65% of the MgCO<sub>3</sub> decomposed, while in the rich shale all the MgCO<sub>3</sub> always appears to decompose if the sample reaches 1300°F.

In the fast heat-up runs of the lean shale, there appears to be a smaller fraction of kerogen recovery above 1000°F than one would expect from the rich-shale work, implying a difference in the low-temperature kerogen kinetics.

### BENCH-SCALE TESTS

A flow diagram of the bench-scale unit is shown in Figure 7. The unit consists primarily of a hydrogasification reactor with associated equipment for feeding oil shale and hydrogen and measuring their flow rates and for collecting and measuring the quantities of residual shale, liquid products, and product gas. Simple controls were used a) to maintain reactor temperatures at the desired values, b) to maintain feed rates at constant values, c) to maintain constant reactor pressures, and d) to collect representative samples of the feed and product gases.

The reactor (Figure 8) consists of a cold-pressure shell, with a 24-inch-ID and about 23 feet long, containing an Incoloy 800 internal reactor tube (4-inch ips, Schedule 40) which is heated by a seven-zone electric heater. The details of the design and operation of this reactor have been described previously (1). Each individually controlled zone is 31 inches long and has an ID of about 7 inches. The reactor pressure and the bed-pressure drop are recorded continuously as are the reactor temperatures. A total of 32 thermocouples is attached to the outer tube wall. Several internal thermocouples were installed during the test program. These temperatures were recorded continuously along with temperatures on other major pieces of equipment.

Shale was fed by a screw feeder from a pressurized hopper, which was filled before testing with sufficient shale for the entire run. The cold shale entered the top of the reactor and was preheated by countercurrent contact with the hot product gas. The residue shale was discharged from the bottom of the reactor into a pressurized residue receiver by a second screw feeder. The residue shale was cooled by countercurrent contact with cold feed hydrogen. In a few later runs at high hydrogen rates, the feed hydrogen was preheated.

The feed hydrogen entered the bottom of the reactor at a point above the discharge screw through a dip tube (Figure 8). The exit gas left through a dip tube extending down into the top of the reactor. In later runs, a bayonet filter constructed of sintered metal was installed on the end of the dip tube to remove dust and eliminate plugging of the outlet lines which had occasionally occurred. The feed shale dropped down through a third dip tube which served to keep any heavy liquids in the exit gas from condensing on the feed shale and plugging the tube at the feed screw outlet.

Hydrogen feed gas and hydrogen purge gas were both metered by orifice meters. The shale was fed constantly at the desired rate, and the rate of shale discharge was manually adjusted to give a constant shale-bed level. The shale-bed level was indicated by a nuclear-type level indicator and was recorded continuously. A more accurate measure of the rate of shale feed and discharge was obtained by weighing the shale initially charged to the feed hopper and that present in the feed hopper and residue receiver at the end of the run. Feed and residue shales were analyzed by methods described in Appendix B of IGT Research Bulletin No. 36 (3). The exit-gas volume was measured by a conventional iron-case-type meter. Aliquot samples of the exit gas were collected during the steady-state part of each run. Gas samples were analyzed by mass spectrometer and gas chromatograph. The exit-gas specific gravity was monitored continuously by a recording gravimeter. The product liquids were collected in two different knockout pots and analyzed by conventional ASTM procedures. The first knockout pot (operated at high temperature) contained a short cyclone section, which removed dust and heavy tar. The exit gas was then cooled in a three-stage condenser to condense out low-temperature liquids. These liquids were collected in a low-temperature knockout pot. Both pots were drained, and the collected liquids were weighed every 1/2 hour during the steady-state portion of each run.

All of the tests conducted in the pilot plant were with a single batch of Colorado oil shale from the U. S. Bureau of Mines mine at Rifle, Colorado. Mine run material was crushed to -1/4-inch size at the mine and sieved elsewhere into various fractions. We selected a -6+10 U. S. Standard sieve size material for most of these tests because it was the largest size which we could successfully feed with our existing equipment. This material had a Fischer Assay oil yield in the 20-25 gal/ton range.

#### Analysis of Oil Shale

A typical analysis of the oil shale used in the tests reported here is given in Table 2.

Table 2. TYPICAL ANALYSIS OF COLORADO OIL SHALE  
USED IN BENCH-SCALE TEST PROGRAM

Moisture, wt %	0.30
Composition, wt % (dry basis)	
Organic Carbon	11.30
Mineral Carbon Dioxide	17.55
Hydrogen	1.72
Nitrogen	0.35
Oxygen (By Difference)	1.73
Sulfur	0.54
Ash	<u>66.81</u>
Total	100.00

Screen Analysis, U.S. Standard Sieve Size

	<u>wt %</u>
+6	0.1
+8	12.5
+16	79.9
+30	6.9
+60	0.3
+100	0.1
+200	0.1
-200	<u>0.1</u>
Total	100.0

### Effects of Operating Temperature

The first series of tests was conducted to study the effects of reaction zone temperature on the yields and properties of gaseous, liquid, and solid products. These tests were conducted with relatively short (9 to 12 feet) beds and flat temperature profiles. The results of these tests are summarized graphically in Figures 9 and 10.

As expected, gaseous hydrocarbon yields and mineral carbonate decomposition increase with increases in temperature (Figure 9). The results are very encouraging. In all tests, over 90% of the organic carbon was recovered as gaseous and liquid products. At 1200° F, over 80% of the organic carbon was converted to liquids; at 1400° F, over 60% was converted to gas.

The effect of temperature on kerogen conversion is not pronounced although some increase can be noted in the neighborhood of 1300° F. The test at 1200° F was conducted with a shale space velocity considerably higher than that used in the tests at 1300° and 1400° F. More organic carbon removal could probably have been obtained at 1200° F if more residence time had been provided. This higher space velocity probably also caused a relatively lower mineral carbonate decomposition.

The effects of temperature on the lighter (<400° F) liquid product properties are shown in Figure 10. Although less hydrocarbon liquids are formed at the higher temperatures, those formed would be more difficult to gasify. First, the saturates plus olefins content of the IBP <400° F fraction decreases from about 92 volume percent to about 40 volume percent as the temperature increases from 1200° to 1400° F. Also the C/H weight ratio of the entire liquid product increases from an average of about 7.5 to about 11 as the temperature increases from 1200° to 1400° F. Thus, at the higher temperatures, an increasing portion of the liquid product is aromatic. The lighter aromatics, such as benzene, toluene, and xylene, are, of course, very difficult to gasify. The heavier aromatics, however, will produce additional hydrocarbon gases with further reaction. It should be pointed out that the hydrocarbon-type analysis could only be performed on the <400° F fraction of the oils. It should also be pointed out that in no run did the <400° F fraction constitute more than 35% of the total oil.

The liquid products produced in these tests were of substantially better quality than those produced by conventional retorting. In all these tests, at least 89% boiled below 730° F, whereas in conventional retorting processes reported in the literature less than 50% boiled below 800° F.

Because bed heights of about 9 to 12 feet (3-1/2 to 5 heating zones) were used, the feed shale fell through a long heated zone (of 1000° F or more) before reaching the shale bed. This gave an initial rapid heat-up of the shale feed rather than the slow heat-up which would be preferred based on laboratory thermobalance tests. However, based on heat transfer calculations, we estimate that the shale particles reached an average temperature of no greater than about 900° -1000° F by the time they reached the shale bed. Further heating to final bed temperature ranged from about 20° to 30° F/minute, which is more favorable to higher yields.

### Effects of Operating Pressure

A second series of tests was conducted to study the effects of reaction zone pressure on the yields and properties of each product. These tests were conducted with a relatively steep temperature gradient in the bed (to prehydrogenate the shale) and bed depths ranging from 12.9 to 15.5 feet (5 to 6 zones). In Figure 11, the product yields are shown as functions of pressure. The product gas yield is only slightly affected by pressure. The liquid products, however, increase with increases in pressure. Thus, the organic carbon remaining in the residue shale decreases with pressure: More than twice as much remains at 125 psig than at 500 psig. The reason for the lower gas yields and higher amounts of residual organic carbon in these runs (compared with previous runs at a 1400° F maximum temperature) is a shorter residence time at high temperature. In these tests, we used a steeper temperature gradient in the upper part of the bed to prehydrogenate the feed shale.

The effects of pressure on hydrocarbon types in the liquid products (<400° F fraction) and the C/H ratio in the total oil are shown in Figure 12. There are only slight effects in the range studied. The olefins fraction decreases and the saturates fraction increases with increases in pressure, but the effect is slight. There is no discernible effect of pressure on the fraction of aromatics. The C/H ratio of the total liquid products also is not significantly affected by pressure. This agrees with the fact that the olefins fraction also remains nearly constant. One would expect a lower C/H ratio at higher pressures because of hydrogenation of the oils. The absence of any oil hydrogenation is probably caused by the low temperatures in the empty space above the bed and within the upper part of the bed, so that the primary liquid products are not hydrogenated.

### Mineral Carbonate Decomposition

In tests conducted to show the effects of temperature on the hydrogasification behavior of oil shale, mineral carbonate decomposition ranged from about 26% (at 1200° F maximum reactor temperature) to about 85% (at 1400° F maximum reactor temperature). High mineral carbonate decompositions are undesirable for several reasons. First, the product gas is diluted with carbon oxides, requiring extensive shifting and scrubbing and/or methanation of the product gas. Second, valuable feed hydrogen is consumed by reverse shifting of the carbon dioxide evolved in the carbonate decomposition. Third, the decomposition reaction is endothermic, thus removing sensible heat from the system. Oil shale typically contains large amounts of dolomite ( $\text{CaCO}_3 \cdot \text{MgCO}_3$ ) as well as calcite ( $\text{CaCO}_3$ ). Approximately 36% of the mineral carbon dioxide is present as  $\text{MgCO}_3$  in Colorado oil shales, according to the literature (4). We analyzed our oil shale and found the feed material to be about 47%  $\text{MgCO}_3$ . From previous studies (3) and from our laboratory thermobalance studies, we found that calcite decomposition can be suppressed by adding  $\text{CO}_2$  to the feed gases. However, magnesium carbonate decomposes very rapidly at temperatures above about 1000° F — even in the presence of high partial pressures of  $\text{CO}_2$ .

Therefore, later in the test program, we added  $\text{CO}_2$  to the feed gas (at about the 5-mole-percent level) in an attempt to reduce total mineral carbonate decomposition (suppress calcite decomposition) since we had been successful in doing so in laboratory thermobalance tests. Mineral carbonate decomposition was reduced about 25% by the addition of  $\text{CO}_2$  to the feed gas.

#### In-Situ Methanation of Carbon Oxides

We noticed, during the bench-scale test program, that carbon oxides were apparently being methanated in the reactor since more hydrocarbons and less carbon oxides were present in the products than would be indicated by carbon and carbon oxides balances. We then carried out two tests with no oil shale present in the reactor and with feed gases containing from about 4 to 6 mole percent carbon dioxide at temperatures and pressures in the region employed in the oil-shale hydrogasification tests. In the first test, we simply passed the feed gas through the reactor tube packed with sand. We found that about 59% of the carbon dioxide was converted to gaseous hydrocarbons (methane and ethane). Since it was possible that the metal reactor tube was catalyzing the reaction rather than the solids, we conducted a second test with an empty reactor tube (to ensure that the methanation observed in our bench-scale tests were indicative of what would happen in a large-scale plant, where the reactor would be refractory-lined and reactor gases would not contact a metallic wall). In this test, only about 18% of the  $\text{CO}_2$  was converted to gaseous hydrocarbons, indicating that the metal tube wall was only partially contributing to the observed methanation. Since the gas residence time and gas contact with the metal wall were greater in the latter test than in the first test, it appears that even less of the observed methanation in the bench-scale tests is due to catalysis by the wall.

We also made thermodynamic equilibrium calculations to see how much methane could be formed by methanation of carbon oxides. These calculations show that for all conditions within the reactor tube it is possible (thermodynamically) to form methane in quantities greater than those observed.

#### SUMMARY AND CONCLUSIONS

Results of the small-scale laboratory thermobalance studies have shown that —

1. The presence of hydrogen, even at low pressure, significantly increases organic carbon recovery as compared with hydrogen-free retorting.
2. Further increases in organic carbon recovery can be achieved at an elevated hydrogen partial pressure. At 500 psia, slow heating can achieve over 95% recovery.
3. The heating rate significantly affects the organic carbon recovery. Very rapid heating to 1300°F limits recovery to about 87%.
4. The carbon dioxide generation by decomposition of  $\text{CaCO}_3$  and  $\text{MgCO}_3$  begins at about 1000°F, increasing rapidly above this temperature. Decomposition of the  $\text{CaCO}_3$  can be almost completely suppressed by the addition of small amounts of  $\text{CO}_2$  in the feed gas stream;  $\text{MgCO}_3$  decomposition cannot be suppressed at hydrogasification temperatures.

Results obtained in the 4-inch-diameter reactor have generally verified the trends observed in the laboratory study. Kerogen recoveries using hydrogen have exceeded 90% - significantly better than recoveries obtained in conventional retorting.

Constant-temperature runs (rapid shale heat-up in free fall above the bed) indicate that high temperature favors the production of gas and promotes aromatization of the liquid products.

The use of controlled shale heat-up (shale preheated in the upper portion of the bed) favors liquid production; however, the liquid products are of much higher quality.

Additional data obtained in the countercurrent tests verified the ability to suppress carbonate decomposition by adding CO<sub>2</sub> to the feed hydrogen. We also discovered that substantial methanation of carbon oxides occurs in the shale bed.

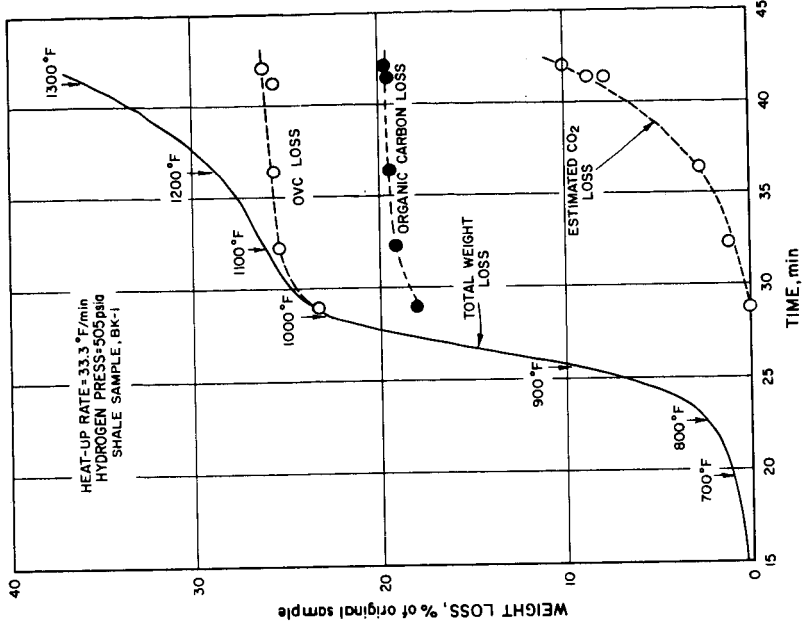
In summary, the experimental program has shown that the basic concept of countercurrent operation is technically feasible. The overall chemistry of the system is now better defined and looks very favorable.

#### ACKNOWLEDGMENT

The work described here was sponsored by the American Gas Association. The authors wish to express their appreciation to the Association for permission to publish this paper. We also wish to express our appreciation to Mr. H. W. Sohns and Mr. M. D. Smith of the U.S. Bureau of Mines who provided us with the oil shale used in this program.

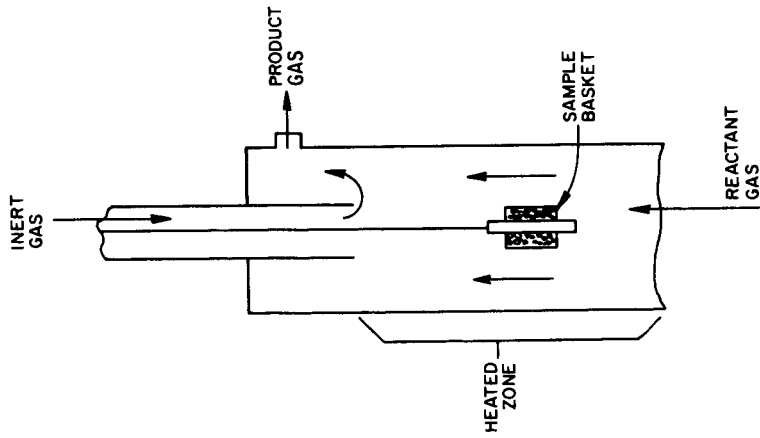
#### LITERATURE CITED

1. Dirksen, H. A. and Lee, B.S., "Balanced-Pressure Pilot Reactor," Chem. Eng. Progr. 62, 98-102 (1966) June.
2. Feldkirchner, H. L. and Johnson, J. L., "High Pressure Thermo-balance," Rev. Sci. Instrum. 39, 1227-29 (1968) August.
3. Feldman, H. F., Bair, W. G., Feldkirchner, H. L., Tsaros, C. L., Shultz, E. G., Jr., Huebler, J, and Linden, H. R., "Production of Pipeline Gas by Hydrogasification of Oil Shale," IGT Res. Bull. No. 36. Chicago, 1966.
4. Stanfield, K. E. et al., "Properties of Colorado Oil Shale," U.S. Bureau of Mines Rep. Invest. 4825. Washington, D.C., November 1971.



A-13-107

Figure 2. TYPICAL WEIGHT-LOSS CURVE FOR RICH SHALE



A-71731

Figure 1. THERMOBALANCE REACTOR

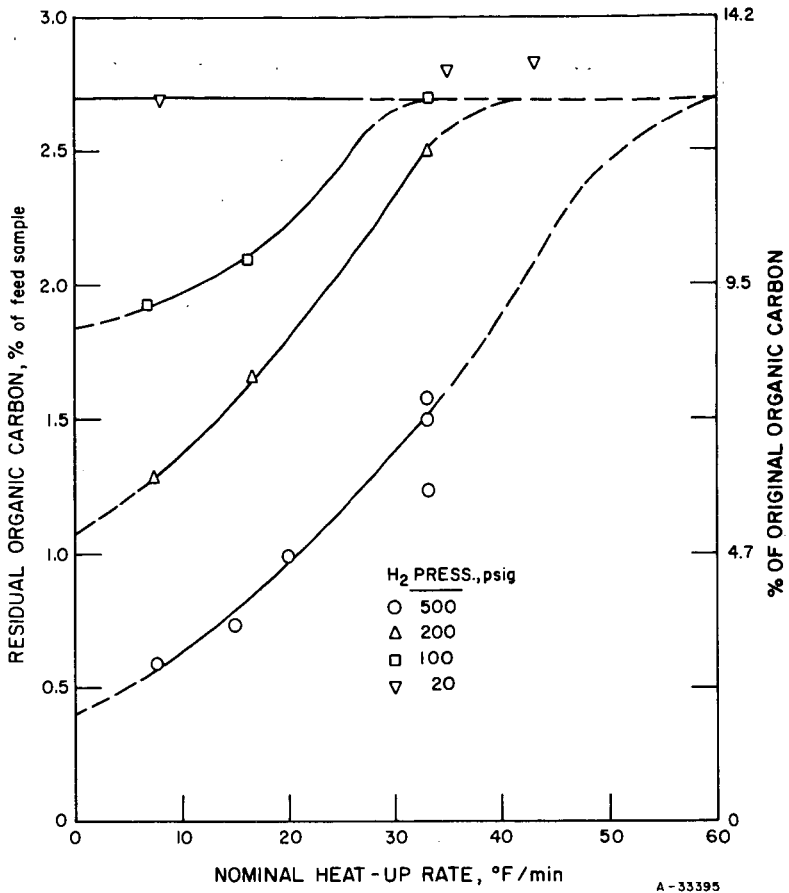


Figure 3. PRESSURE EFFECT ON KEROGEN RECOVERY FROM RICH SHALE IN PURE HYDROGEN ATMOSPHERES

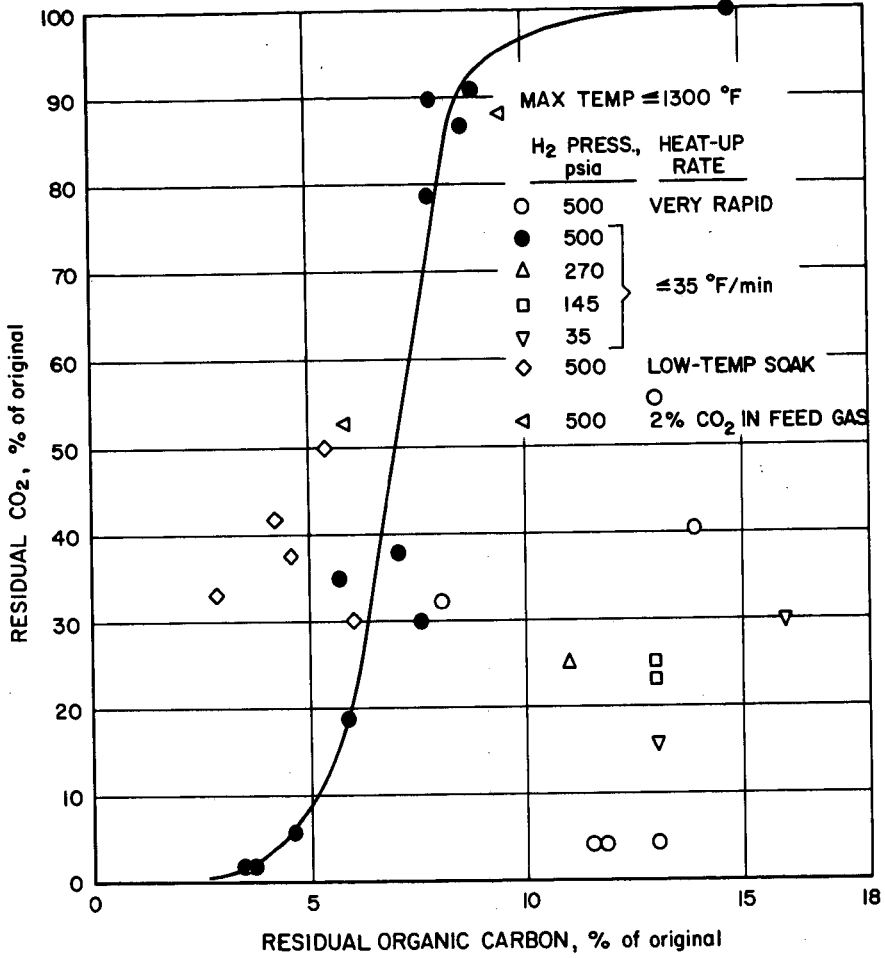
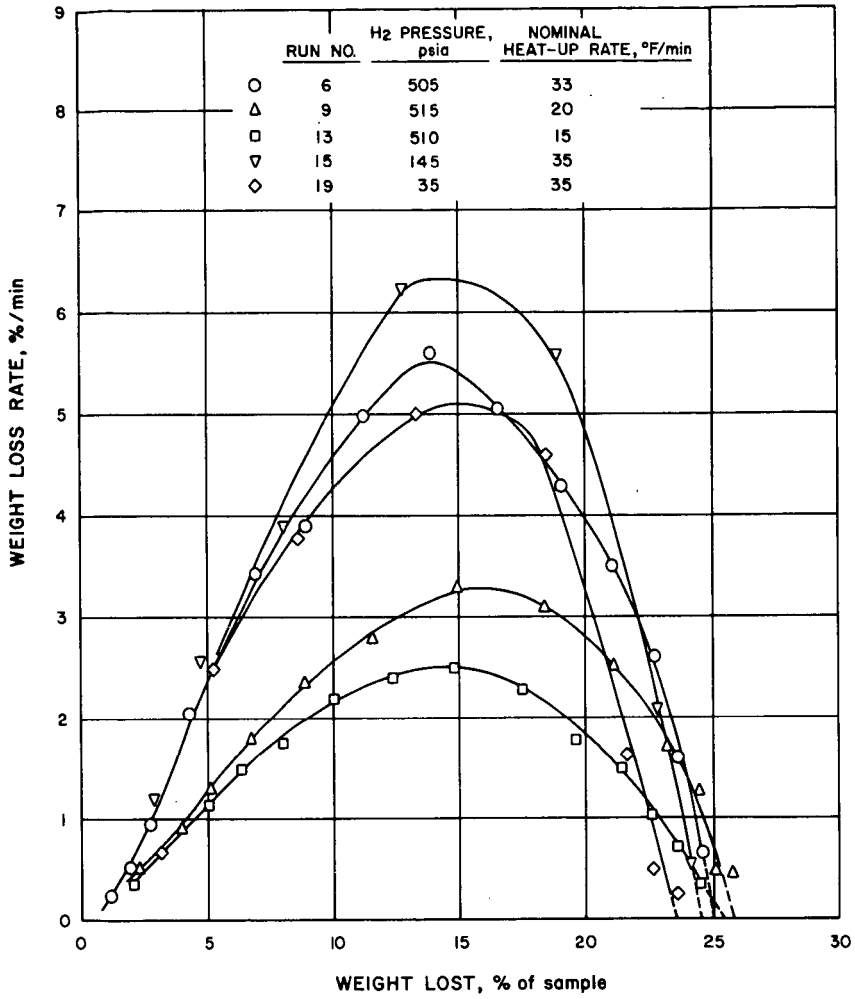
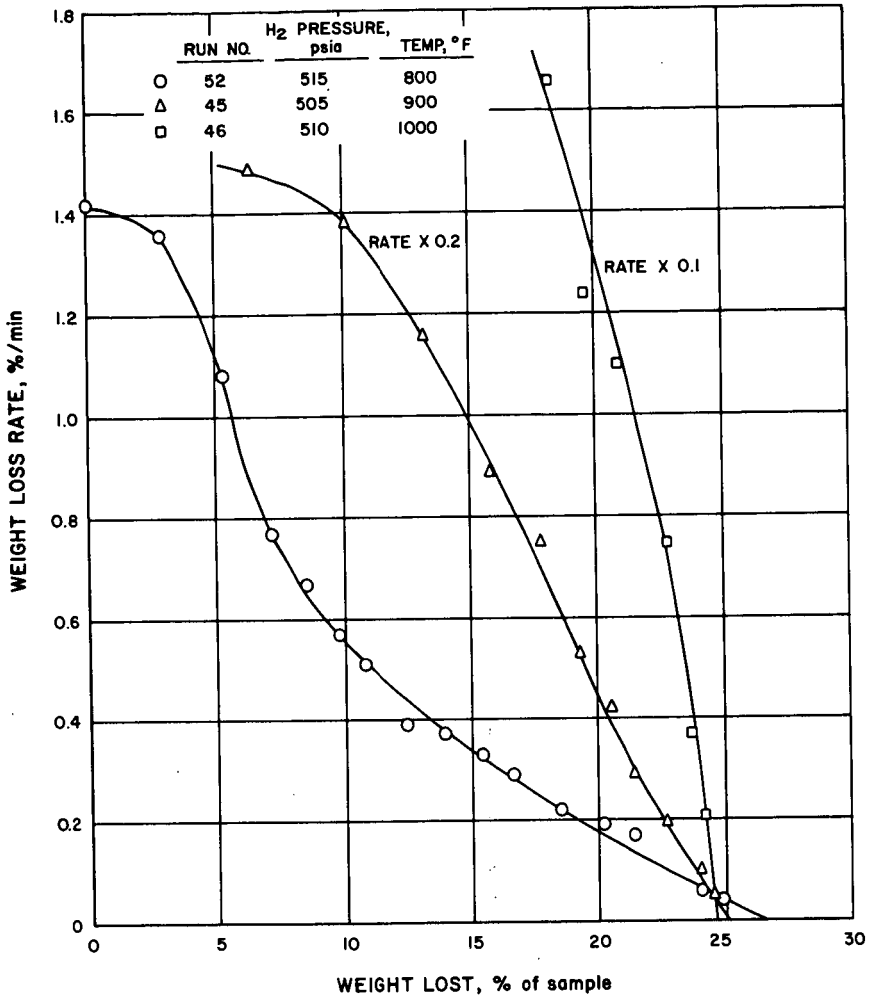


Figure 4. CORRELATION OF RICH SHALE KERGEN RECOVERY AND CARBONATE DECOMPOSITION IN PURE HYDROGEN



A-13-98

Figure 5. LOW-TEMPERATURE WEIGHT LOSS OF RICH SHALE (Heat-Up Runs)



A-13-97

Figure 6. LOW-TEMPERATURE WEIGHT LOSS OF RICH SHALE (Constant-Temperature Runs)

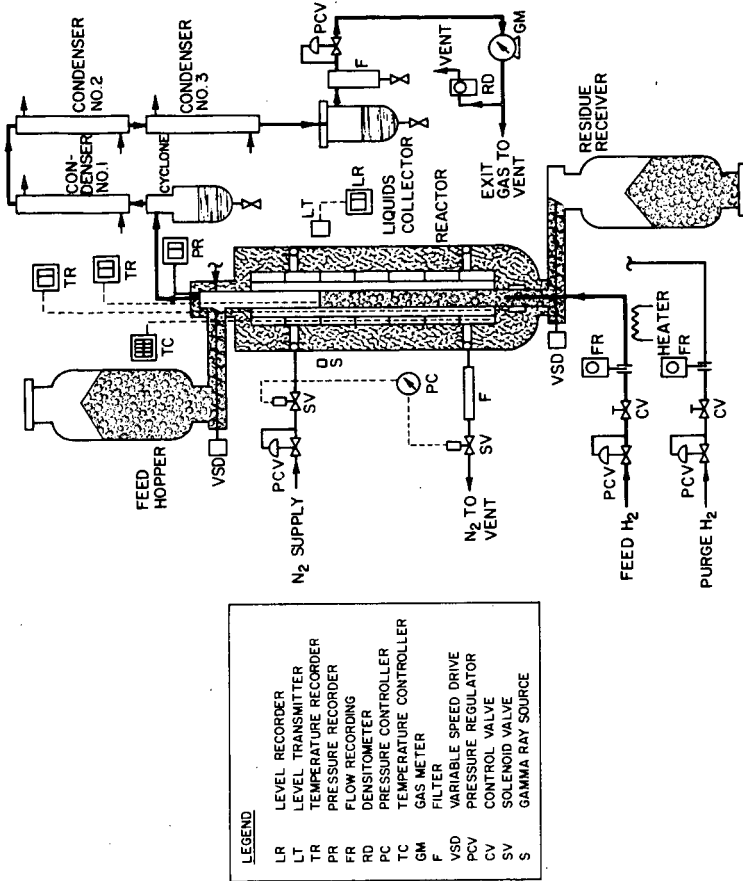


Figure 7. FLOW AND INSTRUMENTATION DIAGRAM FOR HIGH-TEMPERATURE BALANCED-PRESSURE BENCH-SCALE UNIT

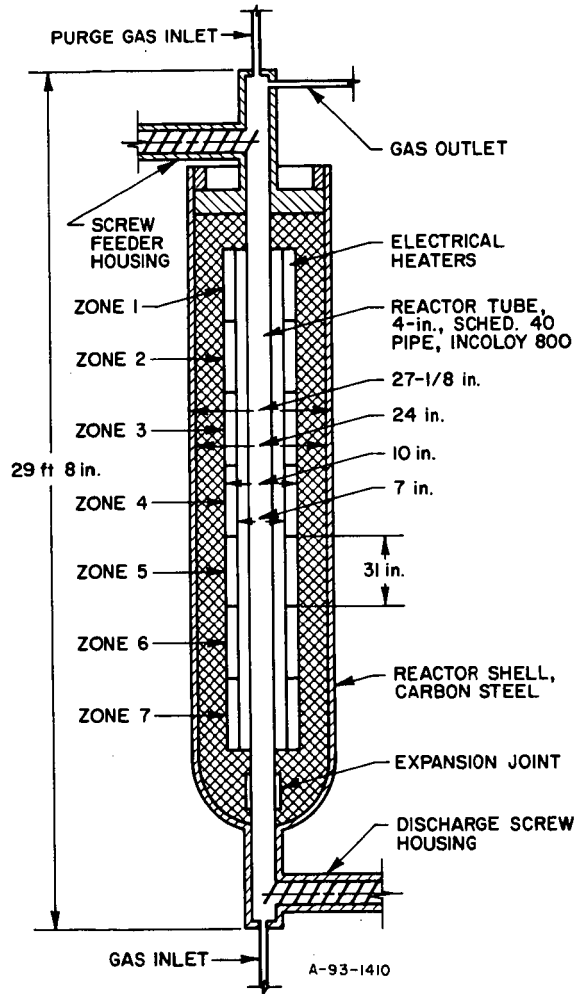


Figure 8. HIGH-TEMPERATURE BALANCED-PRESSURE REACTOR

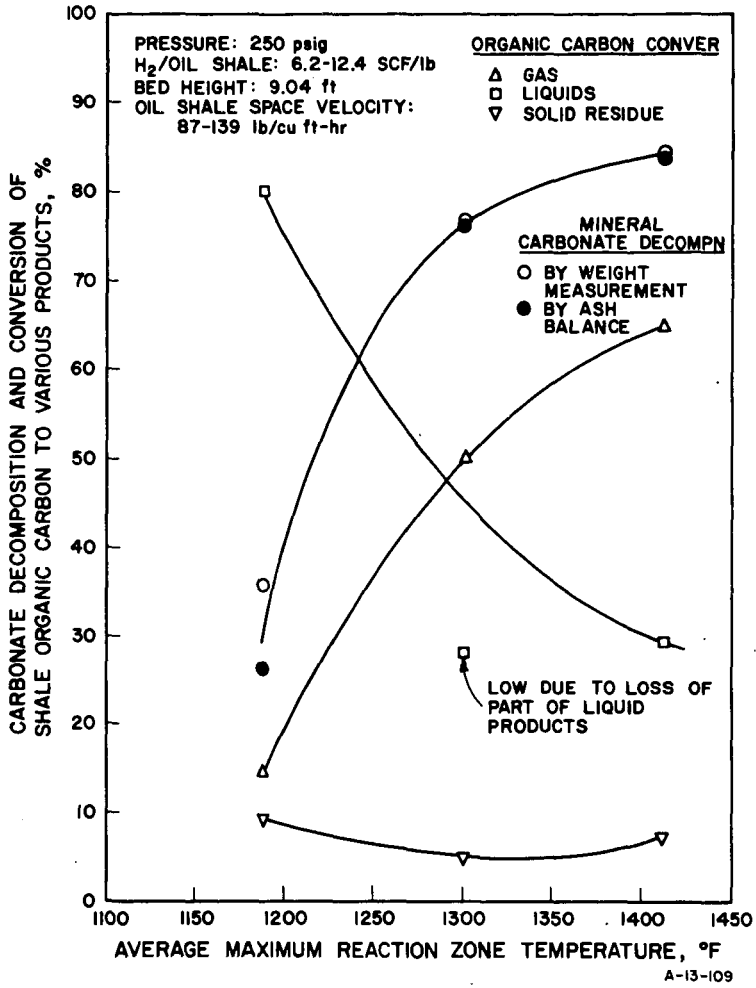


Figure 9. PRODUCT DISTRIBUTION IN BENCH SCALE TESTS

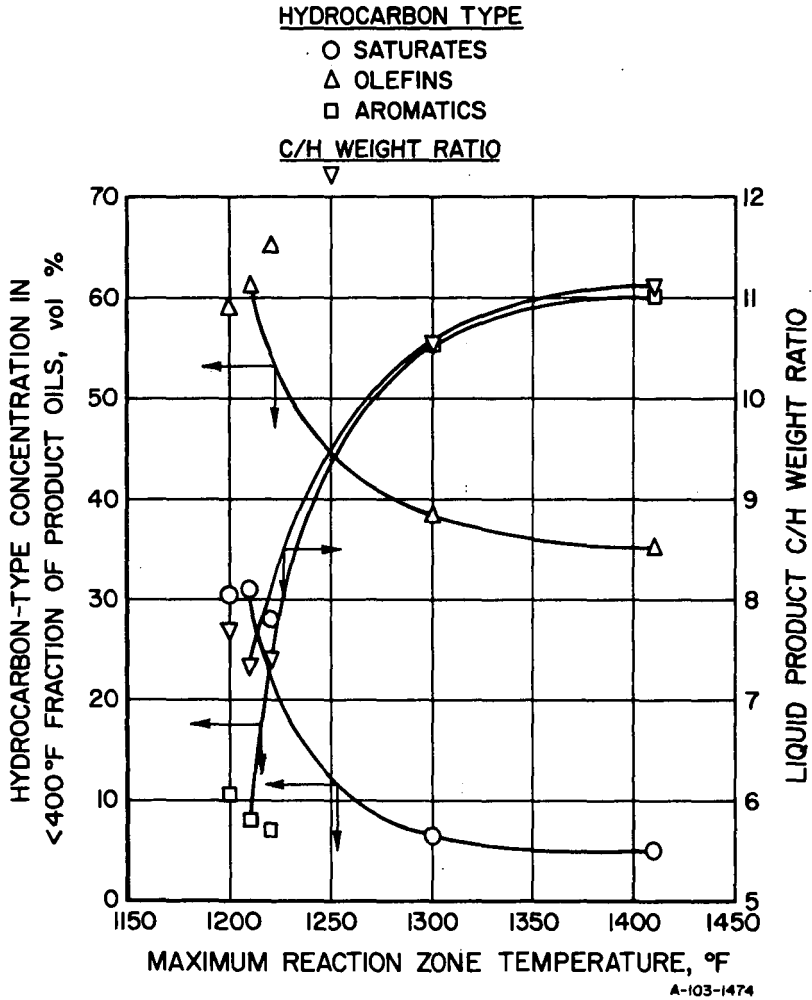


Figure 10. EFFECTS OF REACTION ZONE TEMPERATURE ON LIQUID PRODUCT PROPERTIES

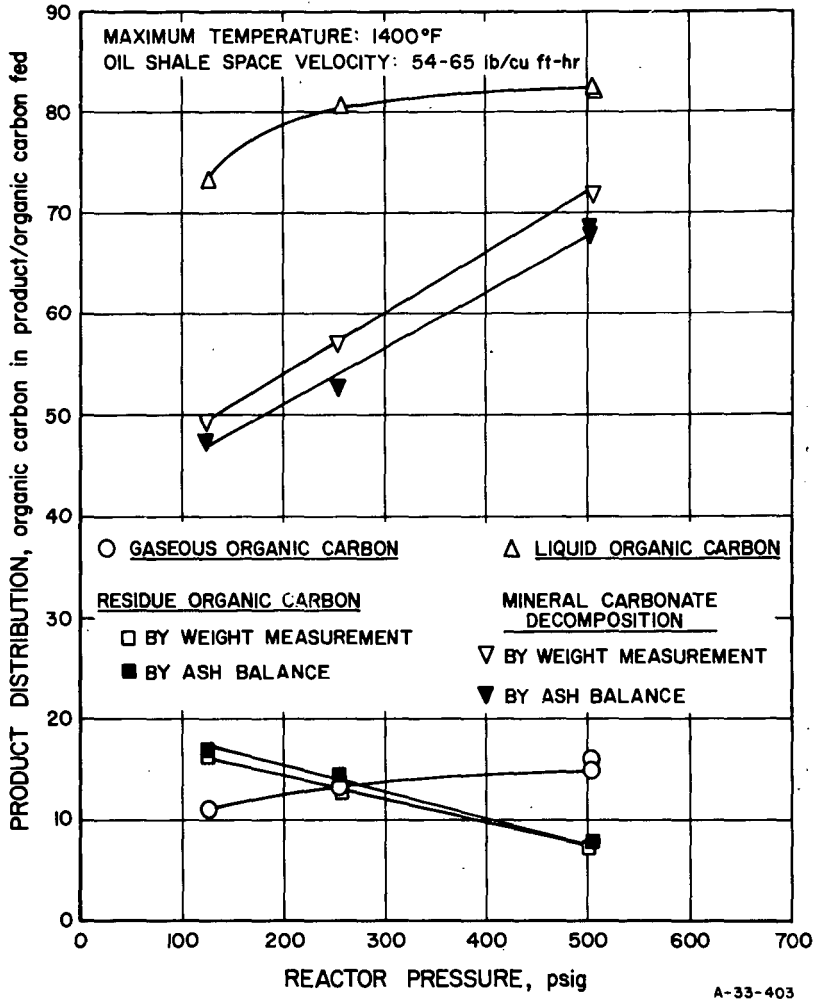


Figure 11. EFFECT OF PRESSURE ON ORGANIC CARBON DISTRIBUTION IN PRODUCTS AND MINERAL CARBONATE DECOMPOSITION

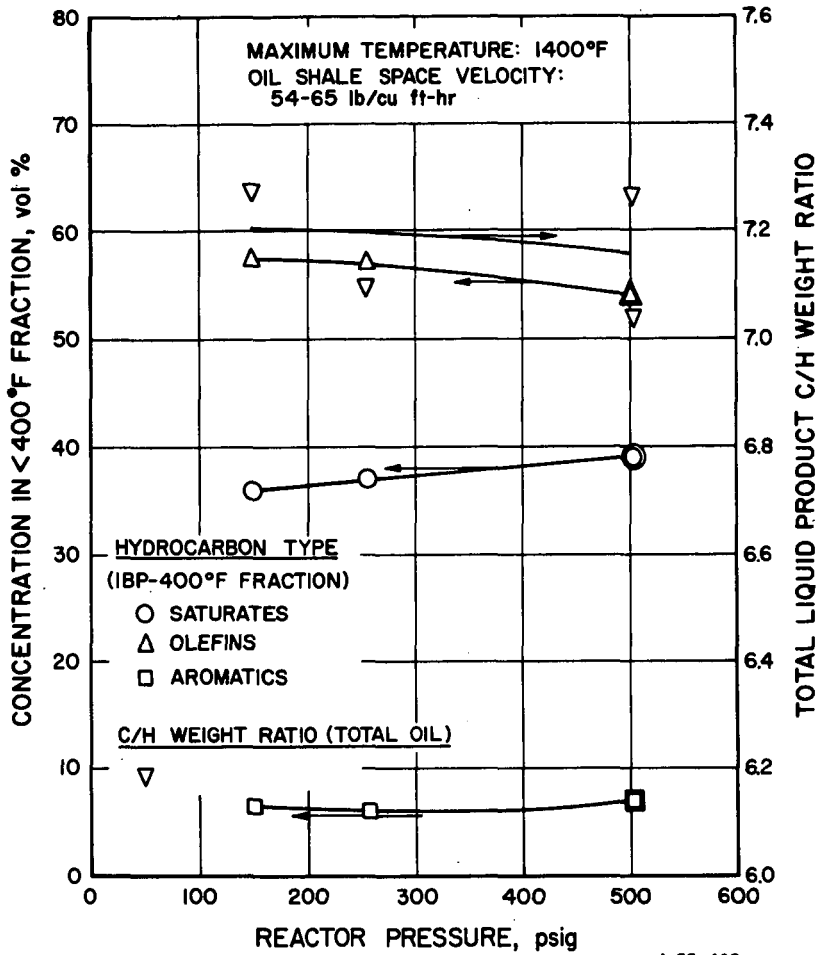


Figure 12. EFFECT OF PRESSURE ON LIQUID PRODUCT PROPERTIES

A COMPARISON OF SHALE GAS OIL DENITRIFICATION REACTIONS  
OVER Co-Mo AND Ni-W CATALYSTS

H. F. Silver and N. H. Wang

Chemical Engineering, University of Wyoming, Laramie, Wyoming 82070

H. B. Jensen and R. E. Poulson

U.S. Department of the Interior, Bureau of Mines  
Laramie Energy Research Center, Laramie, Wyoming 82070

INTRODUCTION

As the Nation's needs for additional sources of petroleum products become ever more pressing, a role of oil shale in the synthetic fuels industry becomes more probable. One of the problems in converting shale oil to hydrocarbon liquid products is the elimination of nitrogen from the shale oil. Nitrogen compounds not only impart undesirable properties to the finished products but their basic nature makes them effective poisons for the acidic catalysts used in petroleum refining.

An efficient means of eliminating nitrogen from shale oil is hydrodenitification of the oil in the presence of a dual function catalyst. In a study of the denitrification of model nitrogen compounds over an Ni-W on  $Al_2O_3$  catalyst, Flinn<sup>1</sup> reported that amines and anilines reacted readily to form ammonia, but indole was much less active, and quinoline was the most difficult to denitrify. Unfortunately, most of the nitrogen in shale oil has been found to be of the quinoline and indole types.<sup>2</sup>

In a previous study in this laboratory,<sup>3</sup> the relative rates of disappearance of the types of nitrogen compounds present in shale gas oil were studied using a Co-Mo on  $Al_2O_3$  catalyst. The present paper uses those Co-Mo results and results from experiments using Ni-W on  $Al_2O_3$  and Ni-W on  $SiO_2 \cdot Al_2O_3$  to compare the selectivity of these catalysts in denitrifying the types of nitrogen compounds in shale gas oil. These comparisons should afford insight into the role of the catalyst during denitrification reactions.

EXPERIMENTAL

A gas combustion retort shale gas oil was hydrogenated in a 2-liter, externally heated, stirred reactor for 1/2 hour and for 3 hours at operating temperatures of 600°, 700°, 750°, and 825° F. Properties of this gas oil are listed in Table I. The initial hydrogen pressure was 3,000 psig and at operating temperatures pressures varied from 3,500 psig to 5,500 psig. Details of the operating procedure have been reported previously.<sup>3</sup>

TABLE I. - Properties of shale gas oil feedstock

Gravity, °API	21.5
Nitrogen, wt pct	2.00
Sulfur, wt pct	0.60
Boiling range, °F	515 to 900

Three different catalysts were used--Co-Mo on  $\text{Al}_2\text{O}_3$  (Nalco, Nalcomo 471), Ni-W on  $\text{Al}_2\text{O}_3$  (Nalco, NT 550), and Ni-W on  $\text{SiO}_2 \cdot \text{Al}_2\text{O}_3$  (Harshaw, Ni-4301). The source and composition of these catalysts are presented in Table II and selected properties of the catalysts are presented in Table III. Although it was recognized that different catalysts require unique

TABLE II. - Source and composition of catalysts

	Catalyst		
	Co-Mo on $\text{Al}_2\text{O}_3$	Ni-W on $\text{Al}_2\text{O}_3$	Ni-W on $\text{SiO}_2 \cdot \text{Al}_2\text{O}_3$
Supplier	Nalco Chemical	Nalco Chemical	Harshaw Chemical
Trade name	Nalcomo 471	NT 550	Ni-4301
Composition, wt pct	3.5 CoO 12.5 MoO <sub>3</sub> 84.0 Al <sub>2</sub> O <sub>3</sub>	4 Ni 16 W 80 Al <sub>2</sub> O <sub>3</sub>	6 Ni 19 W 20 SiO <sub>2</sub> 55 Al <sub>2</sub> O <sub>3</sub>

TABLE III. - Selected catalyst properties

	Catalyst		
	Co-Mo on $\text{Al}_2\text{O}_3$	Ni-W on $\text{Al}_2\text{O}_3$	Ni-W on $\text{SiO}_2 \cdot \text{Al}_2\text{O}_3$
Trade name	(Nalcomo 471)	(NT 550)	(Ni-4301)
Pore volume, cc/gm	0.40	0.35	0.20
Average pore radius, Å	35.1	35.7	19.5
BET area, m <sup>2</sup> /gm	226.4	195.7	208.5
	Pore-size distribution		
Pore radius, Å	Vol pct		
300-250	1.3	1.0	1.2
250-200	2.4	1.8	.7
200-150	4.0	3.0	1.1
150-100	8.5	7.6	2.3
100-90	2.7	2.8	.8
90-80	4.0	4.7	1.1
80-70	5.0	6.9	1.4
70-60	7.0	8.3	1.8
60-50	8.8	10.0	2.0
50-45	6.1	6.9	1.5
45-40	6.6	7.0	1.9
40-35	7.6	7.5	2.4
35-30	8.0	7.5	6.0
30-25	9.1	7.9	9.7
25-20	3.9	6.8	17.5
20-15	11.6	6.1	25.6
15-10	3.6	4.1	22.9
10-7	.0	.0	.0

pretreatment before use in order to maximize their individual activities, all three catalysts were given the same pretreatment in order to reduce the number of experimental variables. On the basis of work reported by Richardson,<sup>4</sup> who indicated that the desulfurization activity of the Co-Mo catalyst could be optimized by preheating at 1,000° F, it was assumed that the same pretreatment would optimize denitrification activity and all catalysts were preheated at 1,000° F for 2 hours and allowed to cool in a desiccator. The catalysts were then added to the reactor in the oxidized state where they were partially sulfided by means of the gas-oil desulfurization reactions occurring during the period in which the reactor was heated at a rate of 4° F per minute to reaction temperature.

Samples of the product oil from the reactor were analyzed for total nitrogen using the Kjeldahl method,<sup>5</sup> and for nitrogen types using nonaqueous, potentiometric titrations and infrared analyses as suggested by Okuno<sup>6</sup> and modified by Koros.<sup>7</sup> When the titration data were combined with the data from the infrared determination of indole-type compounds, it was possible to classify the nitrogen compounds into the following types: Quinolines (including pyridines, quinolines, acridines, and tertiary amines); arylamines (including 1,2,3,4-tetrahydroquinolines, 2,3-dihydroindoles, and anilines); indoles (including pyrroles, indoles, and carbazoles); primary and secondary amines; amides (including quinolones and oxindoles); and unidentified compounds. A complete discussion of the details of this classification procedure has been previously reported.<sup>3,8</sup>

## RESULTS AND DISCUSSION

Table IV lists catalysts, temperatures, times, percent of the total nitrogen removed, and nitrogen types expressed as their weight percent of the total nitrogen remaining in the product oil. The data in Table IV show that the denitrification reactions were studied over the range of zero to 80 percent nitrogen removal and, with the exception of one instance, 90 or more percent of the total nitrogen was classified into one of the five nitrogen types.

The selectivity of each of the three catalysts toward converting each of these five types of nitrogen to either ammonia or to another nitrogen type was determined by plotting the nitrogen type in the product oil as a function of the total nitrogen removed in the denitrification reaction. If the slope of the resulting plot is positive, that nitrogen type is being converted at a slower rate than the rate at which total nitrogen is removed. If the slope is negative, the relative rate is faster.

Figure 1 is the resulting plot for the quinoline-type nitrogen using the three catalysts. The positive slope of the Co-Mo curve shows that the conversion of quinoline when Co-Mo is the catalyst proceeds at a slower rate than the rate at which total nitrogen is removed. The negative slope of the Ni-W curve shows that the quinoline is being converted at a faster, relative rate. Only one curve has been drawn through the two sets of Ni-W data because regression analyses of the Ni-W data showed very little difference when the four Ni-W on  $\text{SiO}_2 \cdot \text{Al}_2\text{O}_3$  data points were added to the eight Ni-W on  $\text{Al}_2\text{O}_3$  data points. This was true for the conversion of all five nitrogen types; hence, the Ni-W data were treated as one curve in all five cases.

Figure 2 is the resulting plot for the indole-type nitrogen. Indole-type nitrogen accounts for 15 percent of the feedstock nitrogen and at a nitrogen removal of 3 percent, when using the Co-Mo catalyst, it accounts for 19 percent of the nitrogen remaining in the liquid product. When the two Ni-W catalysts are used, indole nitrogen accounts for 18 percent of the remaining nitrogen even though there was not distinguishable removal of nitrogen from the liquid. These increased levels of indole-type nitrogen can only be accounted for by the conversion of other types of nitrogen to indole type. In a previous paper,<sup>3</sup> which reported Co-Mo results, we suggested that the amide type and unidentified type were the most likely sources of this increase in indole nitrogen. We now see the same selectivity when the two Ni-W catalysts are used.

TABLE IV. - Nitrogen types in product oils

Temp, °F	Time, hrs	Total nitrogen removed, wt pct	Nitrogen type, wt pct of total nitrogen remaining in liquid product					Unidenti- fied
			Quinoline type	Indole type	Aryl- amine type	Primary and secondary amine type	Amide type	
Feed gas oil								
-	-	-	52	16	1	2	20	9
Co-Mo on Al <sub>2</sub> O <sub>3</sub>								
600	1/2	3	53	19	5	7	11	5
	3	6	51	16	9	15	8	2
700	1/2	12	52	16	10	14	6	2
	3	32	54	14	13	12	4	3
750	1/2	26	53	13	12	14	4	4
	3	70	61	14	19	3	2	1
825	1/2	65	55	13	20	7	2	3
	3	95	-	-	-	-	-	-
Ni-W on Al <sub>2</sub> O <sub>3</sub>								
600	1/2	0	51	18	4	2	15	10
	3	0	50	18	5	3	14	10
700	1/2	3	48	17	5	10	13	7
	3	12	46	13	7	16	11	7
750	1/2	16	48	14	7	15	13	3
	3	51	46	15	16	13	3	7
825	1/2	59	44	16	18	11	1	10
	3	79	41	17	25	6	1	10
Ni-W on SiO <sub>2</sub> ·Al <sub>2</sub> O <sub>3</sub>								
700	1/2	2	49	18	4	7	16	6
	3	8	46	15	6	15	16	2
825	1/2	43	47	15	15	10	6	7
	3	75	37	15	29	3	4	12

1/ Not sufficient concentration to analyze product oil.

Figure 2 also shows that once the initial buildup of indole is over, its conversion to ammonia or to other nitrogen types is much faster than the average conversion until about 25 percent of the denitrification reaction is completed. At this point indoles are converted more slowly when the Ni-W catalysts are used than when Co-Mo is used and in both cases, the rates are slower than that for total nitrogen removal.

A conclusion that can be reached from the results shown in figures 1 and 2 is, despite the compositional differences in the two Ni-W catalysts, there is little difference in their selectivity for the conversion of quinoline types and of indole types. These results do show that the selectivity of the two Ni-W catalysts is different than the selectivity of the Co-Mo catalyst for these

two classes of compounds. The Ni-W catalysts convert quinolines faster than do the Co-Mo and above 20 percent nitrogen removal the Co-Mo converts the indoles faster than do the Ni-W catalysts.

These selectivity results might be explained on the basis of differences in the adsorption characteristics of the catalysts due to differences in the acidity of the catalyst supports. Haensel<sup>9</sup> reports that the ability of a catalyst to adsorb nitrogen compounds is largely influenced by the acidity of the catalyst. However, the Ni-W on  $\text{Al}_2\text{O}_3$  catalyst and the Ni-W on  $\text{SiO}_2 \cdot \text{Al}_2\text{O}_3$  catalyst show the same selectivity but the chemical compositions of their supports as shown in Table II, are different. Further, as shown in Table III, the Co-Mo on  $\text{Al}_2\text{O}_3$  catalyst and the Ni-W on  $\text{Al}_2\text{O}_3$  catalyst are similar in their pore distribution patterns, yet their selectivities differ. Thus, it seems more likely that in this case the observed differences in selectivity should be attributed to the differences in the active-metal components, Co-Mo and Ni-W, rather than to the differences in the catalyst supports.

Figure 3 shows the relative percentage of the unconverted nitrogen compounds which have been classified as arylamine-type compounds (including hydrogenated quinolines, hydrogenated indoles, and anilines) as a function of the extent of the denitrification reaction. Arylamines can be formed by means of hydrogenation of quinoline-type and indole-type compounds and disappear by means of hydrocracking to form ammonia. These results show that, at the high hydrogen pressures used in this study, there is little difference in the three catalysts in their selectivity for converting arylamines. Also, the rate at which arylamines are formed by hydrogenation of quinolines and indoles over all three catalysts is more rapid than the rate at which the arylamines are converted by hydrocracking. This finding is substantiated by the work of Brown,<sup>10</sup> who reported that anilines comprised about one-third of the tar bases in a shale-oil naphtha produced by recycle hydrocracking of a crude shale oil. Even though the results presented in figure 1 show that the rate of hydrogenation of quinoline-type nitrogen compounds is slower than the rate at which total nitrogen is removed over the Co-Mo catalyst, the results shown in figure 3 suggest that the hydrogenation reaction does not completely limit the overall rate of denitrification over this catalyst even at 800° F as Koros<sup>7</sup> reported and as we have reported in an earlier paper.<sup>4</sup>

Figure 4 shows the relative percentages of the unconverted nitrogen compounds which have been classified as primary and secondary amines as a function of the removal of total nitrogen. Although we have shown two curves in this figure, a regression analysis showed that there is little difference in the Ni-W and Co-Mo data. Hence, there is little difference in the selectivity of these three catalysts in their ability to effect a conversion of the primary and secondary amines. Figure 4 shows that, at nitrogen removals up to about 20 percent, the relative percentages of primary and secondary amines increase significantly, but at higher nitrogen removals, these compounds are rapidly converted to ammonia.

Figure 5 is a plot of the data for amide-type nitrogen. As shown here, the relative percentage of amide nitrogen decreases rapidly at low nitrogen removal. The Co-Mo catalyst exerts a stronger influence than do the Ni-W catalysts in the conversion of amides at low nitrogen removals, but all three catalysts are quite effective in converting amide-type nitrogen to other forms.

#### SUMMARY

The selectivity of three catalysts (Co-Mo on  $\text{Al}_2\text{O}_3$ , Ni-W on  $\text{Al}_2\text{O}_3$ , and Ni-W on  $\text{SiO}_2 \cdot \text{Al}_2\text{O}_3$ ) on influencing the conversion of five, identifiable types of nitrogen compounds has been demonstrated. The two Ni-W catalysts are somewhat more selective in converting quinoline-type compounds than is the Co-Mo catalyst. Because there is no difference in the selectivity of

the two Ni-W catalysts which differ from each other in the composition of their supports, it seems likely that the active-metal component of the catalyst is the determining factor in the selectivity of quinoline conversion. At low denitrification levels, all three catalysts are effective in rapidly converting indole-type nitrogen, but above 20 percent nitrogen removal, the Co-Mo catalyst is more effective than the Ni-W catalysts. All three catalysts show that they are less effective in converting arylamines than they are in removing nitrogen; and they show approximately the same selectivity toward primary and secondary amines. The Co-Mo catalyst converts amide-type nitrogen much faster at low levels than do the two Ni-W catalysts; but all three catalysts are highly selective in promoting conversion of amide-type nitrogen.

The results also show that the relative percentages of different nitrogen compounds change as shale gas oil is denitrified. At low and intermediate levels of nitrogen removal, all five types of nitrogen compounds are present in the liquid product. However, at higher levels of nitrogen removal, the identifiable nitrogen compounds remaining in the liquid product consist primarily of quinolines, indoles, and arylamines. Primary and secondary amines and amides are practically missing from the product at levels approaching 80 percent removal of nitrogen.

#### ACKNOWLEDGMENTS

Reference to specific trade names or manufacturers does not imply endorsement by the Bureau of Mines.

The work upon which this report is based was done under a cooperative agreement between the Bureau of Mines, U.S. Department of the Interior, and the University of Wyoming.

#### REFERENCES

1. Flinn, R. A., Larson, O. A., and Beuther, H., *Pet. Ref.* 42, 129 (1963).
2. Dinneen, G. U., Cook, G. L., and Jensen, H. B., *Anal. Chem.* 30, 2026 (1958).
3. Silver, H. F., Wang, N. H., Jensen, H. B., and Poulson, R. E., *ACS Division of Petroleum Chemistry Preprints* 17, No. 4, G74 (1972).
4. Richardson, J. T., *Ind. Eng. Chem. (Fund.)* 3, 154 (1964).
5. Lake, G. R., McCutchan, P., Van Meter, R. A., and Neel, J. C., *Anal. Chem.* 23, 1634 (1951).
6. Okuno, I., Latham, D. R., and Haines, W. E., *Anal. Chem.* 37, 54 (1965).
7. Koros, R. M., Banic, S., Hofmann, J. E., and Kay, M. J., *ACS Division of Petroleum Chemistry Preprints* 12, No. 4, B165 (1967).
8. Wang, N. H., "Hydrodenitrification Reactions in Shale Gas Oil," Master's Thesis, University of Wyoming, 1973.
9. Haensel, V., Pollitzer, E. L., and Watkins, C. H., *Proceedings for the Sixth World Petroleum Congress, Section III, Paper 17, Frankfurt/Main, Germany* (1963).
10. Brown, Dennis, Earnshaw, D. G., McDonald, F. R., and Jensen, H. B., *Anal. Chem.* 42, 146 (1970).

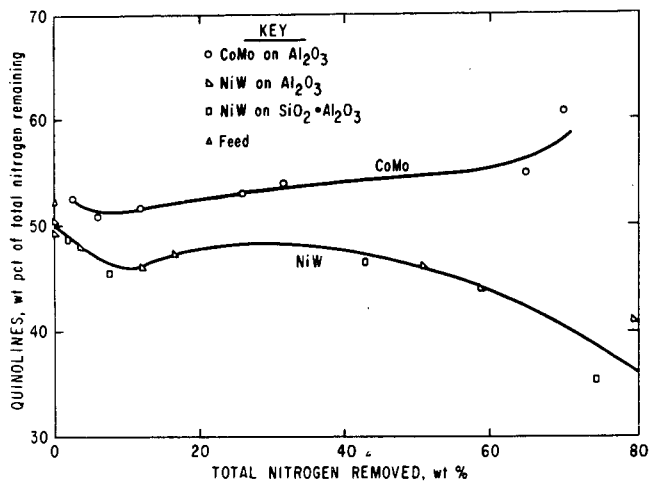


FIGURE 1.-Quinoline-Nitrogen Conversion.

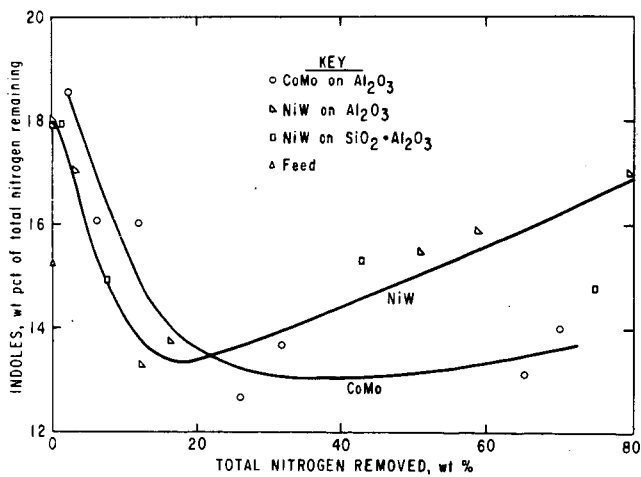


FIGURE 2.-Indole-Nitrogen Conversion.

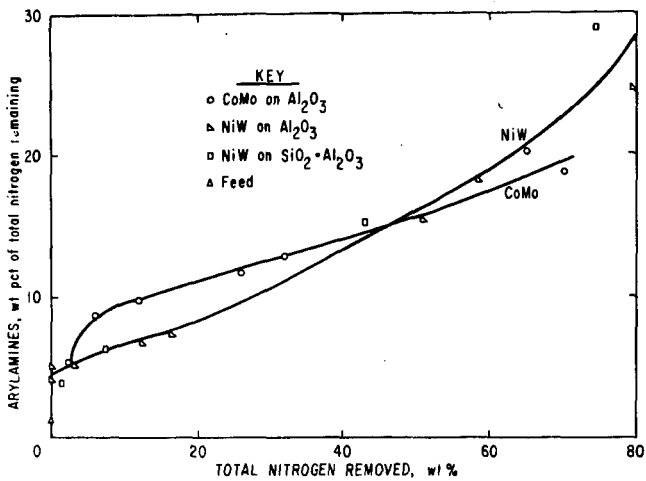


FIGURE 3.-Arylamine-Nitrogen Conversion.

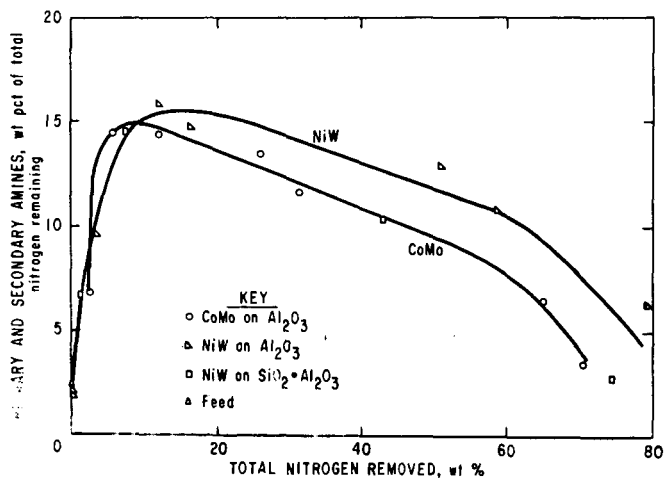


FIGURE 4.-Primary And Secondary Amine-Nitrogen Conversion.

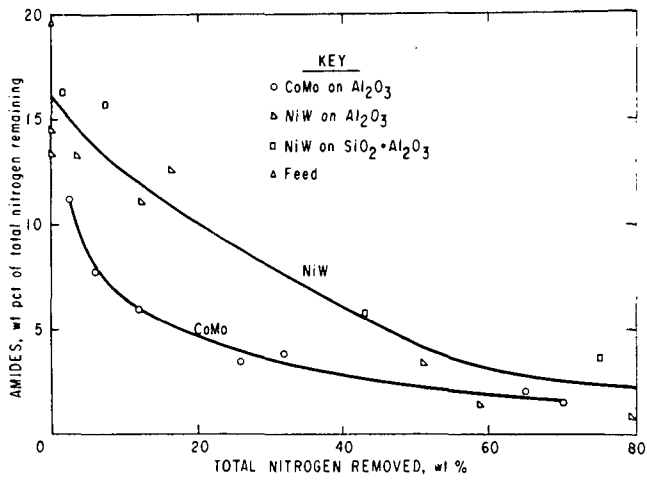


FIGURE 5.-Amide-Nitrogen Conversion.

PRODUCTION OF SYNTHETIC CRUDE FROM CRUDE SHALE OIL  
PRODUCED BY IN SITU COMBUSTION RETORTING

C. M. Frost, R. E. Poulson, and H. B. Jensen

Laramie Energy Research Center, U. S. Department of the Interior,  
Bureau of Mines, Laramie, Wyoming 82070

INTRODUCTION

Among the considerations associated with the development of a shale oil industry are the costs and environmental hazards of disposing of the spent shale that inherently is produced if any mining and aboveground retorting approach is involved. For several years the Bureau of Mines has been engaged in research in recovering shale oil by in situ combustion retorting, an approach that avoids spent shale disposal. Both actual underground (1-3) and simulated in situ retorting (4-7) are being investigated.

Crude shale oils produced by in situ combustion retorting of Green River oil shale normally have higher API gravities and lower viscosities and pour points than do crude shale oils produced in N-T-U or gas combustion retorts (8). In situ crude shale oils also contain a much higher percentage of material boiling below 1,000° F. While the nitrogen contents of in situ crude shale oils may be somewhat lower than those of crude shale oils produced in N-T-U or gas combustion retorts, they still contain more than twice as much nitrogen as high-nitrogen petroleum crudes.

Since existing refineries would not be able to cope with the high nitrogen content of raw shale oil if it were a substantial part of the refinery feed, the National Petroleum Council (NPC) (9) has suggested that crude shale oil be upgraded at the retorting site by a process of catalytic hydrogenation to produce a premium feedstock called "syncrude." In this process, the crude shale oil would be distilled to produce naphtha, light oil, heavy oil, and residuum. The residuum would be processed in a delayed-coking unit to produce petroleum coke, and a vapor stream containing gas, naphtha, light oil, and heavy oil. Vapor from the coking unit would flow back to the crude distillation facilities for separation into various fractions. The naphtha, light oil, and heavy oil would be subsequently hydrogenated to remove nitrogen and sulfur and to reduce the viscosity and pour point of the finished syncrude.

There is some disagreement in the literature as to which type of hydrotreating catalyst is the most effective for removing nitrogen from crude shale oil and/or shale oil coker distillates. Carpenter and Cottingham (10) found that, of 17 catalysts tested, a cobalt-molybdate-on-alumina catalyst was superior for removing nitrogen from crude shale oil. Benson and Berg (1) reported that of 12 catalysts tested an HF-activated cobalt-molybdate catalyst was superior for removing nitrogen from shale oil coker distillates. On the other hand, Montgomery (12) reported that catalysts containing high concentrations of nickel and tungsten were best for hydrodenitrogenation. These investigators did not report any work with nickel-molybdenum or nickel-cobalt-molybdenum catalysts.

The purpose of the present study was to test various modern hydrogenation catalysts for their effectiveness in removing nitrogen from in situ crude shale oil fractions and to determine the feasibility of producing a synthetic crude oil that would meet the specifications for syncrude suggested by the National Petroleum Council. Six modern hydrogenation catalysts were tested to compare their efficiencies in removing nitrogen from a heavy (600° to 1,000° F) in situ gas oil. The best catalyst, nickel-molybdenum-on-alumina, was used in preparing fractions of a synthetic crude using the methods suggested by NPC.

## PROPERTIES OF IN SITU CRUDE SHALE OIL

The crude shale oil used in this study was obtained from an in situ combustion retorting experiment at Rock Springs, Wyo. (1-2), during the last week of the experiment and is considered a representative "steady state" oil. Properties of the in situ crude shale oil are shown in table 1.

TABLE 1. - Properties of in situ crude shale oil

Gravity.....	° API...	28.4
Nitrogen.....	wt-pct...	1.41
Sulfur.....	wt-pct...	.72
Pour point.....	° F...	40
Viscosity.....	SUS at 100° F...	78
Carbon residue.....	wt-pct...	1.7
Ash.....	wt-pct...	.06

## EXPERIMENTAL PROCEDURES AND RESULTS

Apparatus and Operating Procedure

A simplified flow diagram of the hydrogenation unit is shown in figure 1. The reactor used in these experiments was a 1-inch-outside-diameter by 9/16-inch-inside-diameter, type 316, stainless steel tube 40 inches long. The catalyst bed was supported by a stainless steel screen 11 inches from the bottom of the reactor. A second screen was placed at the top of the catalyst bed, and the upper part of the reactor was filled with quartz chips and served as a preheater for oil and hydrogen. The reactor was surrounded by a 3-inch-outside-diameter by 1-inch-inside-diameter aluminum block and was heated by a four-zone electric furnace, each zone of which was independently controlled. Temperatures were measured by five thermocouples placed in a groove in the aluminum block adjacent to the reactor and spaced at equal intervals along the length of the catalyst bed and preheater. With proper adjustment of the heating elements, the recorded temperatures could be maintained within 5° F of each other.

At the beginning of each experiment the catalyst was heated to 700° F with air passing through the reactor at the rate of 1.1 standard cubic feet per pound of catalyst per hour (scf/lb/hr). Steam was then introduced at the rate of 0.41 pound per pound of catalyst per hour (lb/lb/hr), and these conditions were maintained for 16 hours. The reactor was then cooled to 500° F, the steam was cut off, and, after the system cooled to 350° F, the air flow was stopped. The reactor was then purged with helium and pressurized to 250 psig. A hydrogen stream containing 5 weight-percent hydrogen sulfide was passed through the reactor at a rate of 1.0 scf/lb/hr for 3 hours to sulfide the catalyst. The temperature, pressure, and hydrogen flow rate were adjusted to those required for the particular experiment, and the oil flow was started. Hydrogen (99.9 percent purity) was used directly from standard shipping cylinders without further purification.

Products from the reactor passed through a back-pressure regulator into a separator maintained at 75° F and 200 psig. Tail gas from the separator passed through a second back-pressure regulator and was metered and sampled. Liquid products were drained from the separator after each 24-hour period of operation and washed with water to remove ammonia and hydrogen sulfide before a sample was taken for analysis. At the conclusion of each experiment the oil and hydrogen flows were stopped, the reactor was depressurized, and steam was introduced at the rate of 0.41 lb/lb/hr while the reactor was cooled to 700° F. Air was then introduced at the rate of 1.1 scf/lb/hr, and these conditions were maintained until the coke burnoff was completed.

Catalyst Screening Tests

The catalysts used in these tests were obtained from commercial sources. Table 2 shows the manufacturer, manufacturer's number, active metals, and catalyst designation for each of the catalysts tested. Three of the catalysts were received in the form of 1/16-inch extrusions and were used as such. The other catalysts, obtained in larger sizes, were crushed and sized to 10-20 mesh.

TABLE 2. - Catalysts tested

<u>Manufacturer<sup>1/</sup></u>	<u>Manufacturer's No.<sup>1/</sup></u>	<u>Active metals</u>	<u>Catalyst designation</u>
American Cyanamid Co.	Aero HDS-2A	Co Mo	I Co-Mo
American Cyanamid Co.	Aero HDS-3A	Ni Mo	II Ni-Mo
Harshaw Chemical Co.	Ni 4301-E	Ni W	III Ni-W
Harshaw Chemical Co.	Ni 4303-E	Ni W	IV Ni-W
Nalco Chemical Co.	NM-502	Ni Mo	V Ni-Mo
Davidson Chemical Co.	NICOMO	Ni Co Mo	VI Ni-Co-Mo

<sup>1/</sup> Reference to specific manufacturers or trade names does not imply endorsement by the Bureau of Mines.

Charge stock for the catalyst testing experiment was prepared by topping a sample of the in situ crude shale oil to 600° F in a batch still equipped with a column having 35 trays, and then separating the 600° to 1,000° F fraction in a vacuum flash distillation unit. Properties of the 600° to 1,000° F fraction of in situ crude shale oil are shown in table 3.

TABLE 3. - Properties of 600° to 1,000° F distillate from in situ crude shale oil

Gravity.....	° API...	23.3
Nitrogen.....	wt-pct...	1.66
Sulfur.....	wt-pct...	.51
Viscosity.....	SUS at 100° F...	111
Carbon residue.....	wt-pct...	.5
Distillation		
Initial boiling point.....	° F...	579
5 pct recovered.....	° F...	611
10 pct recovered.....	° F...	620
20 pct recovered.....	° F...	648
30 pct recovered.....	° F...	666
40 pct recovered.....	° F...	681
50 pct recovered.....	° F...	699
60 pct recovered.....	° F...	732
70 pct recovered.....	° F...	768
80 pct recovered.....	° F...	809
90 pct recovered.....	° F...	867
95 pct recovered.....	° F...	914
End point.....	° F...	995

All catalyst tests were run at an operating temperature of 800° F, a space velocity of 1.0 weight of oil per weight of catalyst per hour ( $W_o/W_c/hr$ ), and a hydrogen feed rate of 5,000 standard cubic feet per barrel of feed (scf/bbl). Eighteen grams of catalyst were charged to the reactor in each test. Five of the six catalysts were

tested at an operating pressure of 1,000 psig, and all six were tested at an operating pressure of 1,500 psig. Each test was continued for 96 hours.

In figure 2 the first order denitrification rate constants at 1,000 psig expressed as the logarithm of the ratio of nitrogen in the feed to nitrogen in the liquid product ( $\ln N_0/N_t$ ) are plotted against days on stream to show the effect of operating time on catalyst activity. These curves show that the activities of all the catalysts tested decreased quite rapidly with time on stream. The catalyst with the highest denitrification activity at an operating pressure of 1,000 psig was catalyst I Co-Mo and the one with the lowest denitrification activity was catalyst IV Ni-W.

Figure 3 shows a plot of the first order denitrification rate constants versus time on stream at an operating pressure of 1,500 psig. The catalysts with the highest initial denitrification activity at 1,500 psig were catalyst II Ni-Mo and catalyst I Co-Mo. However, catalyst V Ni-Mo showed the highest activity after 96 hours, and its activity decreased very little with time on stream. Catalyst VI Ni-Co-Mo also had a high resistance to deactivation but had a much lower initial activity. Catalyst IV Ni-W again showed the lowest denitrification activity.

Composite samples of the total liquid product from each test were fractionated to determine the degree of hydrocracking attained with each catalyst. Distribution of the various distillate fractions are shown in figure 4. The distributions shown are for the tests made at 1,500 psig. Yields of naphtha and light oil were uniformly lower for tests made at 1,000 psig. The highest volume-percent yields of liquid product were attained with catalysts I Co-Mo and V Ni-Mo and the lowest yields with catalysts III Ni-W and IV Ni-W. The highest conversion--i.e., material converted to products boiling below 550° F--was attained with catalyst VI Ni-Co-Mo. The lowest conversion was attained with catalyst IV Ni-W, a hydrocracking catalyst. The highest yields of naphtha and light oil were attained with catalysts I Co-Mo and VI Ni-Co-Mo. Because of its high sustained denitrification activity, catalyst V Ni-Mo was selected for use in the preparation of syncrude by hydrogenation of the in situ distillate fractions.

#### Preparation of Synthetic Crude

The overall flow diagram for upgrading crude shale oil is shown in figure 5. A sample of in situ crude shale oil was fractionated in a Podbielniak Hypercal distillation unit to obtain a 350° F end point naphtha, a 350° to 550° F light oil, a 550° to 850° F heavy oil, and a vacuum residuum. Residuum from the fractionation was coked at atmospheric pressure in a laboratory coking unit, and the liquid product from the coker was mixed with a proportionate amount of fresh in situ crude shale oil. The mixture of crude shale oil and coker distillate was then fractionated to obtain fractions similar to those from the first distillation. Residuum from the second distillation was coked and liquid product from the coker again mixed with a proportionate amount of crude shale oil. The mixture of coker distillate and crude shale oil was fractionated to obtain a 350° F end point naphtha, a 350° to 550° F light oil, and a 550° to 850° F heavy oil to be used as charge stocks for the preparation of synthetic crude oil. Yields from the first and third distillations and coking are compared in table 4. Properties of the liquid products are shown in table 5.

The 550° to 850° F heavy oil from the third distillation was hydrogenated in a continuous 174-hour run. No deactivation of the catalyst was evident from analyses of samples of the liquid product taken during the run, and yields of liquid and gaseous products as well as hydrogen consumption were constant with time throughout the total test. Operating conditions and yields of products are shown in table 6. Approximately 40 weight-percent of the heavy oil was converted to products boiling below 550° F, of which 23.75 weight-percent was light oil boiling between 350° and 550° F, and 9.25 weight-percent was material boiling between 175° and 350° F.

TABLE 4. - Yields of products from distillation and coking

Percent of crude.....	First distillation		Final distillation	
	Weight	Volume	Weight	Volume
IBP - 350° F.....	6.20	6.86	6.30	7.00
350° - 550° F.....	43.71	45.50	37.58	39.24
550° - 850° F.....	28.89	28.60	34.62	33.50
850° F+.....	21.20	18.94	21.50	19.26
Coker distillate.....	17.21	17.50	17.30	17.47
Coke.....	2.83		3.08	
Hydrogen.....	.01		.02	
Methane.....	.26		.27	
Ethane.....	.17		.16	
Ethylene.....	.02		.03	
Propane.....	.22		.20	
Propylene.....	.11		.09	
Isobutane.....	.06	.09	.03	.05
Butane.....	.09	.14	.10	.15
Butenes.....	.09	.13	.10	.14
Carbon monoxide.....	.02		.03	
Carbon dioxide.....	.03		.02	
Hydrogen sulfide.....	.08		.07	

TABLE 5. - Properties of fractions from distillation of in situ crude shale oil

	Original crude	Final distillation
C <sub>5</sub> - 350° F naphtha:		
Gravity..... ° API...	45.4	45.8
Nitrogen..... wt-pct...	1.16	1.09
Sulfur..... wt-pct...	.52	.70
350° - 550° F light oil:		
Gravity..... ° API...	34.9	35.0
Nitrogen..... wt-pct...	1.24	1.29
Sulfur..... wt-pct...	.52	.54
550° - 850° F heavy oil:		
Gravity..... ° API...	26.8	27.2
Nitrogen..... wt-pct...	1.53	1.61
Sulfur..... wt-pct...	.46	.46
850° F+ residue:		
Gravity..... ° API...	11.3	11.2
Nitrogen..... wt-pct...	1.93	1.91
Sulfur..... wt-cpt...	.60	.56

The 350° to 550° F light oil obtained from hydrogenation of the 550° to 850° F heavy oil was combined with the 350° to 550° F light oil from the third distillation of the in situ crude shale oil and coker distillate. The combined light oils were hydrogenated in a continuous 75-hour run. Operating conditions and products yields are shown in table 7. Approximately 39 weight-percent of the 350° to 550° F material was converted to products boiling below 350° F, of which 15.7 weight-percent was naphtha boiling between 175° and 350° F.

TABLE 6. - Hydrogenation of 550° to 850° F heavy oil

## Operating conditions:

Temperature.....	° F...	800
Pressure.....	psig...	1,500
Space velocity.....	W <sub>0</sub> /W <sub>C</sub> /hr...	1.0
Hydrogen feed.....	scf/bbl...	5,000
Hydrogen consumed.....	scf/bbl...	1,320

## Yields of products:

	Percent of feed		Percent of crude	
	Weight	Volume	Weight	Volume
C <sub>5</sub> + liquid product.....	95.20	101.68	39.55	41.94
C <sub>5</sub> - 175° F.....	1.92	2.52	.80	1.04
175° - 350° F.....	9.25	10.77	3.84	4.44
350° - 550° F.....	23.75	24.92	9.87	10.28
550° F+.....	60.28	63.47	25.04	26.18
Coke.....	.12		.05	
Hydrogen.....	-2.24		-.93	
Methane.....	.77		.32	
Ethane.....	.87		.36	
Propane.....	.88		.37	
Isobutane.....	.30	.47	.12	.19
Butane.....	.90	1.36	.37	.56
Ammonia.....	1.82		.76	
Hydrogen sulfide.....	.49		.20	
Water.....	.89		.37	

TABLE 7. - Hydrogenation of 350° to 550° F light oil

## Operating conditions:

Temperature.....	° F...	750
Pressure.....	psig...	1,500
Space velocity.....	W <sub>0</sub> /W <sub>C</sub> /hr...	1.0
Hydrogen feed.....	scf/bbl...	5,000
Hydrogen consumed.....	scf/bbl...	1,050

## Yields of products:

	Percent of feed		Percent of crude	
	Weight	Volume	Weight	Volume
C <sub>5</sub> + liquid product.....	98.00	102.93	55.19	60.36
C <sub>5</sub> - 175° F.....	1.22	1.54	.69	.90
175° - 350° F.....	15.66	17.10	8.82	10.03
350° - 550° F.....	81.12	84.29	45.68	49.45
Coke.....	.19		.11	
Hydrogen.....	-1.78		-1.00	
Methane.....	.17		.10	
Ethane.....	.24		.13	
Propane.....	.20		.11	
Isobutane.....	.19	.28	.11	.17
Butane.....	.56	.82	.32	.49
Ammonia.....	1.24		.70	
Hydrogen sulfide.....	.49		.28	
Water.....	.50		.28	

The 175° to 350° F naphthas from the two previous hydrogenation runs were combined with the total naphtha from the third distillation of in situ crude shale oil

and coker distillate. The combined naphthas were then hydrogenated in a continuous 48-hour run. Operating conditions and product yields are shown in table 8. Under the conditions used, only 4.3 weight-percent of the charge was converted to products boiling below 175° F.

TABLE 8. - Hydrogenation of 175° to 350° F naphtha

Operating conditions:

Temperature.....	° F...	700
Pressure.....	psig...	1,500
Space velocity.....	$V_o/V_c$ /hr...	1.0
Hydrogen feed.....	scf/bbl...	5,000
Hydrogen consumed.....	scf/bbl...	720

Yields of products:

	Percent of feed		Percent of crude	
	Weight	Volume	Weight	Volume
C5+ liquid product.....	99.83	102.09	20.45	23.67
C <sub>5</sub> - 175° F.....	4.14	4.40	.85	1.02
175° - 350° F.....	95.69	97.69	19.60	22.65
Coke.....	.01		.00	
Hydrogen.....	-1.39		-.28	
Methane.....	.00		.00	
Ethane.....	.13		.02	
Propane.....	.24		.05	
Isobutane.....	.01	.01	.00	-
Butane.....	.02	.03	.00	-
Ammonia.....	.59		.12	
Hydrogen sulfide.....	.32		.07	
Water.....	.24		.05	

Properties of the charge stocks and liquid products from the various hydrogenation runs are shown in table 9. Hydrogenation of the 550° to 850° F heavy oil under the conditions used reduced the nitrogen content from 16,100 ppm in the charge stock to 935 ppm in the 550° to 850° F fraction of the hydrogenated liquid product. Sulfur was reduced from 4,630 ppm to 9 ppm and the gravity increased from 27.2° API to 35.6° API.

Hydrogenation of the 350° to 550° F light oil under the conditions used reduced the nitrogen content from 10,850 ppm in the charge stock to 79 ppm in the 350° to 550° F fraction of the hydrogenated liquid product. Sulfur was reduced from 4,590 ppm to 1.2 ppm and the gravity increased from 35.0° API to 41.5° API.

Hydrogenation of the 175° to 350° F naphtha under the conditions used reduced the nitrogen content from 4,900 ppm in the charge stock to less than 1 ppm in the 175° to 350° F fraction of the hydrogenated liquid product. Sulfur was reduced from 3,010 ppm to 10 ppm and the gravity increased from 47.3° API to 52.6° API.

These results indicate that nitrogen removal is considerably more efficient when the naphtha, light oil, and heavy oil are hydrogenated separately. For example, the light oil produced during hydrogenation of the 550° to 850° F heavy oil contained 1,220 ppm nitrogen; the light oil produced by hydrogenation of the 350° to 550° F light oil contained only 79 ppm nitrogen. The 175° to 350° F naphtha produced during hydrogenation of the heavy oil contained 299 ppm nitrogen and that produced during hydrogenation of the light oil contained 53 ppm nitrogen, but the 175° to 350° F naphtha produced during hydrogenation of the naphtha fraction contained only 0.8 ppm of nitrogen.

TABLE 9. - Properties of charge stocks and liquid products from hydrogenation runs

Hydrogenation of--	550°-850° F heavy oil	350°-550° F light oil	175°-350° F naphtha
Charge stock			
Gravity..... ° API...	27.2	35.0	47.3
Nitrogen..... ppm...	16,100	10,850	4,900
Sulfur..... ppm...	4,630	4,590	3,010
Liquid product			
Gravity..... ° API...	37.6	43.9	53.1
Nitrogen..... ppm...	880	70	1.3
Sulfur..... ppm...	9	7	16
C <sub>5</sub> - 175° F naphtha			
Gravity..... ° API...	77.2	77.6	60.8
Nitrogen..... ppm...	3.7	3.8	.5
Sulfur..... ppm...	22	7	3
175° - 350° F naphtha			
Gravity..... ° API...	53.3	49.6	52.6
Nitrogen..... ppm...	299	53	.8
Sulfur..... ppm...	9	3	10
350° - 550° F light oil			
Gravity..... ° API...	35.0	41.5	-
Nitrogen..... ppm...	1,220	79	-
Sulfur..... ppm...	8	1.2	-
550° - 850° F heavy oil			
Gravity..... ° API...	35.6	-	-
Nitrogen..... ppm...	935	-	-
Sulfur..... ppm...	9	-	-

In table 10 the properties of the syncrude prepared from in situ crude shale oil are compared with the properties of a syncrude listed by the NPC. Relative amounts and properties of the naphthas, light oils, and heavy oils are also compared. These data show that the nitrogen content, sulfur content, pour point, viscosity, and API gravity of syncrude prepared from in situ crude shale oil are lower than those suggested in the NPC report. The lower gravity of syncrude prepared from in situ crude shale oil may be attributable in part to the lower content of butanes and butenes and in part to the greater volumes of materials boiling above the naphtha range. The sulfur content of the naphtha is somewhat high, but the sulfur contents of the other fractions are much lower than those suggested by the NPC.

A summary of the yields from the various steps used in the preparation of syncrude from in situ crude shale oil is shown in table 11. The overall yield of syncrude was 103 volume-percent of the original crude.

#### SUMMARY AND CONCLUSIONS

Hydrogenation tests made on the 600° to 1,000° F heavy gas oil from in situ crude shale oil showed that a nickel-molybdenum-on-alumina catalyst was superior to either cobalt-molybdenum-on-alumina or nickel-tungsten-on-alumina catalysts for removing nitrogen from shale oil fractions. This nickel-molybdenum-on-alumina catalyst was used in the preparation of a synthetic crude oil by hydrogenation of various distillate fractions of an in situ crude shale oil. A high yield of premium refinery feedstock whose properties compared favorably to those of a "syncrude" described by the NPC was attained.

TABLE 10. - Comparison of NPC and in situ syncrudes and distillate fractions

	NPC	In situ
Syncrude:		
Gravity..... ° API...	46.2	43.9
Pour point..... ° F...	50	<32
Viscosity..... SUS at 100° F...	40	32
Nitrogen..... ppm...	350	250
Sulfur..... ppm...	50	5
Butanes and butenes..... vol-pct...	9.0	1.7
C <sub>5</sub> - 350° F naphtha..... vol-pct...	27.5	24.8
Gravity..... ° API...	54.5	54.7
Nitrogen..... ppm...	1	1
Sulfur..... ppm...	<1	8
Aromatics..... vol-pct...	18	14
Naphthenes..... vol-pct...	37	44
Paraffins..... vol-pct...	45	42
350° - 550° F distillate..... vol-pct...	41.0	48.1
Gravity..... ° API...	38.3	41.5
Nitrogen..... ppm...	75	79
Sulfur..... ppm...	8	1.2
Aromatics..... vol-pct...	34	24
Freezing point..... ° F...	-35	-29
550° - 850° F distillate..... vol-pct...	22.5	25.4
Gravity..... ° API...	33.1	35.6
Nitrogen..... ppm...	1,200	935
Sulfur..... ppm...	<100	9
Pour point..... ° F...	80	55

TABLE 11. - Summary of yields from preparation of syncrude

Process <sup>1/</sup> ..... wt-pct...	A	B	C	D	Totals
C <sub>5</sub> - 175° F naphtha.....	-	0.80	0.69	0.85	2.34
175° - 350° F naphtha.....	-	-	-	19.60	19.60
350° - 550° F light oil....	-	-	45.68	-	45.68
550° - 850° F heavy oil....	-	25.04	-	-	25.04
Coke.....	3.08	.05	.11	-	3.24
Hydrogen.....	.02	-.93	-1.00	-.28	-2.19
Methane.....	.27	.32	.10	-	.69
Ethane.....	.16	.36	.13	.03	.68
Ethylene.....	.03	-	-	-	.03
Propane.....	.20	.37	.11	.04	.72
Propylene.....	.09	-	-	-	.09
Isobutane.....	.03	.12	.11	-	.26
Butane.....	.10	.37	.32	-	.79
Butenes.....	.10	-	-	-	.10
Carbon monoxide.....	.03	-	-	-	.03
Carbon dioxide.....	.02	-	-	-	.02
Ammonia.....	-	.76	.70	.11	1.57
Hydrogen sulfide.....	.07	.20	.28	.07	.62
Water.....	-	.37	.28	.04	.69

<sup>1/</sup> A. Distillation and coking. B. Hydrogenation of 550° - 850° F heavy oil.  
C. Hydrogenation of 350° - 550° F light oil. D. Hydrogenation of 175° - 350° F naphtha.

## ACKNOWLEDGMENTS

The work upon which this report is based was done under a cooperative agreement between the Bureau of Mines, U. S. Department of the Interior, and the University of Wyoming.

## LITERATURE CITED

1. Burwell, E. L., H. C. Carpenter, and H. W. Sohns. Experimental In Situ Retorting of Oil Shale at Rock Springs, Wyo. BuMines TPR 16, June 1969, 8 pp.
2. Burwell, E. L., T. E. Sterner, and H. C. Carpenter. Shale Oil Recovery by In Situ Retorting--A Pilot Study. J. Petrol. Technol., 1970, pp. 1520-1524.
3. Carpenter, H. C., E. L. Burwell, and H. W. Sohns. Evaluation of an In Situ Retorting Experiment in Green River Oil Shale. J. Petrol. Technol., 1972, pp. 21-26.
4. Harak, A. E., L. Dockter, and H. C. Carpenter. Some Results from the Operation of a 150-Ton Oil Shale Retort. BuMines TPR 30, 1971, 14 pp.
5. Carpenter, H. C., S. S. Tihen, and H. W. Sohns. Retorting Ungraded Oil Shale as Related to In Situ Processing. Preprints, Div. Petrol. Chem., ACS, v. 13, No. 2, April 1968, pp. F50-F57.
6. Dockter, L., A. Long, Jr., and A. E. Harak. Retorting Ungraded Oil Shale as Related to In Situ Processing. Preprints, Div. Fuel Chem., ACS, v. 15, No. 1, 1971, pp. 2-11.
7. Jensen, H. B., R. E. Poulson, and G. L. Cook. Characterization of a Shale Oil Produced by In Situ Retorting. Preprints, Div. Fuel Chem., ACS, v. 15, No. 1, 1971, pp. 113-121.
8. Harak, A. E., A. Long, Jr., and H. C. Carpenter. Preliminary Design and Operation of a 150-Ton Oil Shale Retort. Quarterly of Colo. School of Mines, v. 65, No. 4, October 1970, pp. 41-56.
9. U. S. Energy Outlook, An Interim Report. National Petroleum Council, v. 2, 1972, pp. 80-90.
10. Carpenter, H. C., and P. L. Cottingham. Evaluation of Catalysts for Hydrogenating Shale Oil. BuMines RI 5533, 1959, 27 pp.
11. Benson, D. B., and L. Berg. Catalytic Hydrotreating of Shale Oil. Chem. Eng. Prog., v. 62, No. 8, August 1966, pp. 61-67.
12. Montgomery, D. P. Refining of Pyrolytic Shale Oil. Ind. Eng. Chem. Prod. Res. Develop., v. 7, No. 4, December 1968, pp. 274-282.

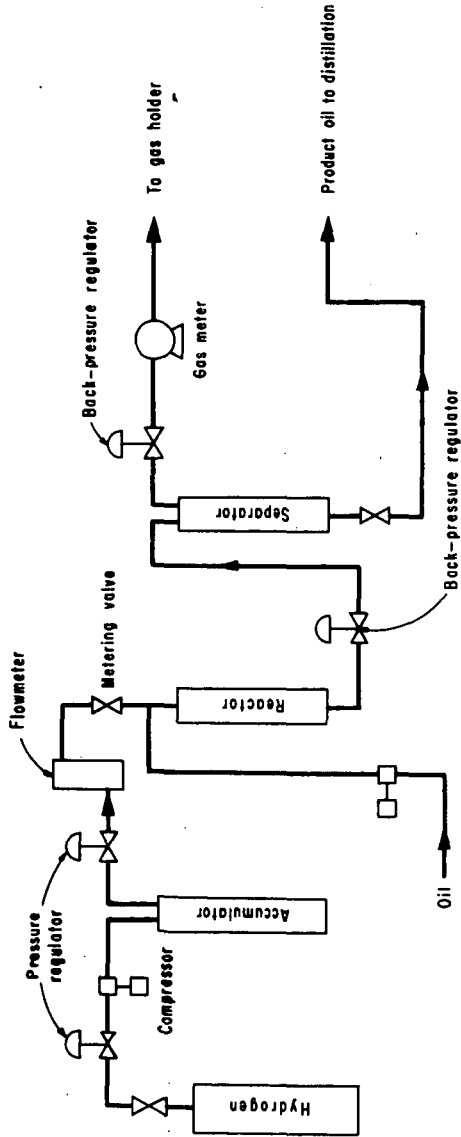


FIGURE 1. — Simplified Flow Diagram of Hydrogenation Unit.

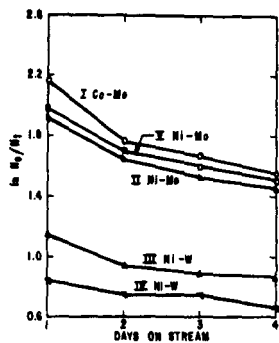


FIGURE 2.-Effect of Operating Time on Denitrification Rate Constants at 1,000 PSIG.

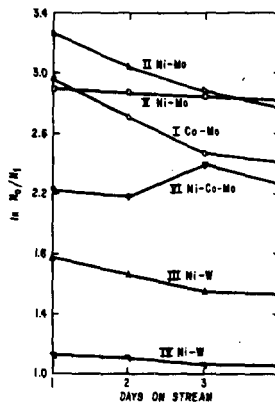


FIGURE 3.-Effect of Operating Time on Denitrification Rate Constants at 1,500 PSIG.

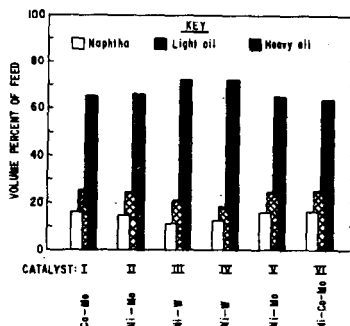


FIGURE 4.-Effect of Catalyst on Distillate Yields at 1,500 PSIG.

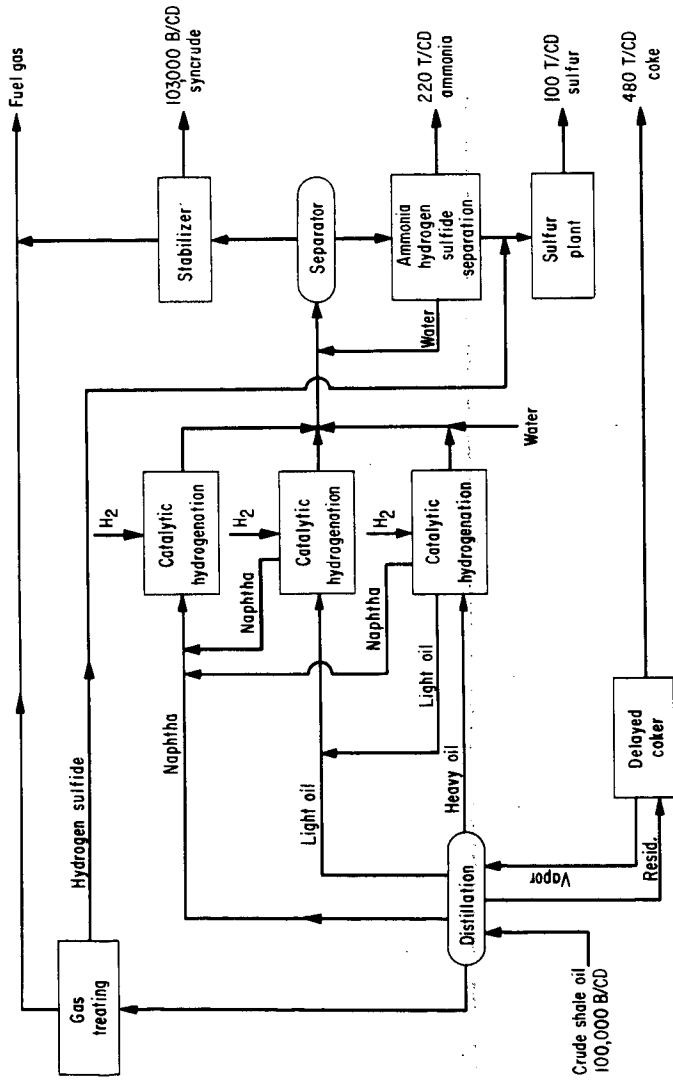


FIGURE 5.-Flow Diagram For Upgrading In Situ Crude Shale Oil.

## STEPWISE OXIDATION OF BIOLEACHED OIL SHALE

D. K. Young, S. Shih, and T. F. Yen  
Department of Chemical Engineering  
University of Southern California, University Park  
Los Angeles, California 90007

The study of organic matter present in the Green River shale formation (Eocene Age) is of considerable geochemical interest as evidenced by the reports in the past dealing with isolation and identification of the hydrocarbon fraction contained in both the solvent soluble organic portion (the bitumens) and the generally insoluble organic portion (the kerogen) of the shale. Depending on the location of the shale sample collected for analysis, the amount of organic matter is estimated to be around 15%; however, due to the extensiveness of the oil shale formation, the potential use of the entrapped organic matter, as a possible source of liquid fuel, (ca. 1.5 trillion barrels of known reserves) (1) has provided the incentive for industry to develop the most efficient process of extracting this reserve.

Destructive pyrolysis (or retorting), is the process where major industrial investigative efforts are presently centered around. The basic retorting techniques themselves are not new; they were known at least 50 years ago (2). The only industrially feasible adaptation of these basic techniques to the present problem of shale oil recovery is the in situ retorting process. The in situ technique obviates the high costs of mining, crushing, transporting, and ultimately of disposing the spent shale. To date various in situ schemes, such as injection of hot gas or steam, electrical discharge, and underground nuclear explosion, have been considered in order to provide the necessary source of heat to start the retorting process and to overcome the low permeability of the formation. Estimates of the recovery efficiency is around 50% of the organic matter with 25% burnt for the retorting process and another 25% as unrecoverable carbon-rich residue (coke).

As an alternative way of releasing the organic material, primarily the kerogen portion since the bitumens are easily extracted with solvent from the mineral matrix, we have investigated the feasibility of mild oxidative degradation. The use of oxidation as a tool for structural elucidation is well documented in the literature (3), a variety of oxidants have been used and the starting material is usually a kerogen concentrate with a major portion of the mineral matrix removed by concentrated hydrofluoric acid treatment. In the present study, the shale sample has been pretreated with dilute acid (ca. 0.1 N) for the removal of soluble mineral (dolomite and calcite) only. This can also be accomplished by leaching the shale sample with the acid medium produced by sulfur oxidizing bacteria as has been demonstrated in this laboratory (4). The shale sample, which has undergone this bioleaching process, is about 70-75% in mineral constituent, composed largely of quartz and feldspar. Starting with this 'bioleached' shale, the release of the entrapped kerogen will be carried out in mild oxidative steps using potassium permanganate solution and ozone separately. Mild stepwise oxidation is intended to prevent further fragmentation of released organic matter since it is more reactive than the still entrapped kerogenic material. Permanganate solution and ozone (5) are known to oxidize saturated hydrocarbons, however the mode of oxidation is not likely to be the same.

The basic skeletal structure of kerogen has been postulated to compose of largely cross linked aliphatic chains (3); it would be of interest to compare the effect of these two oxidants on the kerogen entrapped in a resistant mineral matrix. Results of the permanganate oxidation are presented in the rest of the report; ozone oxidation is presently in progress.

#### EXPERIMENTAL

The shale sample was collected from the Mahogany ledge of the Green River formation and was crushed to pass a 150 mesh screen. From the elemental analysis the shale was estimated to contain around 13% organic matter by weight and the solvent extractable material, the bitumens, was found to be around 2%. Direct bioleaching of the raw shale with the acid medium of the sulfur oxidizer was not done and instead it was pretreated by dilute hydrochloric acid; resulting in a similar weight loss of 40% as compared with directly bioleached shale. The dilute acid treated shale was Soxhlet extracted with a (4:1) benzene:methanol mixture for 84 hours to remove the soluble material. The hydrocarbon fraction from the soluble material was analyzed by gas chromatography (Hewlett-Packard Model 5750) on a 9 ft x 1/8 in stainless steel column, packed with 3% SE-30 on Chromosorb Q. The branched and cycloalkane components are essentially identical with early report (6).

Stepwise permanganate oxidation of 10 grams of the shale treated above was carried out in a fashion similar to Djuricic et al. (3). For each step 25 ml of a solution with 0.08 M  $\text{KMnO}_4$  and 0.2 M KOH was warmed with the shale to a temperature of 75°C. Upon completion of the oxidation the solid residue (oxidized shale and  $\text{MnO}_2$ ) was separated from the aqueous layer by centrifugation and a fresh portion of  $\text{KMnO}_4$  solution was added to continue the oxidation. The oxidation was terminated after the 28th step. The shale at this point still contains entrapped organic matter since carbon analysis showed a carbon content of 0.83% in the solid residue.

The aqueous layer from each step of the oxidation was combined and acidification with hydrochloric acid yielded a precipitate (fraction I), the precipitate turned into a lustrous dark brown material upon drying. An amount of 1.24 grams of the precipitate was isolated which corresponds to about 7.45% of the untreated raw shale. This fraction was analyzed further. The organic material that remained in the aqueous layer was isolated by first evaporating the solution to dryness with a rotary evaporator and then the residue was extracted thoroughly with diethyl ether. Evaporation of the diethyl ether left behind 0.39 grams of extract (fraction II). Together the two fractions constituted 9.78% of the raw shale.

A portion of the oxidation product (fraction I) was dissolved in pyridine- $d_5$  and subjected to NMR analysis (Varian Model TC-60) in order to characterize its overall structure (Fig. 1).  $\text{BF}_3$  esterification in methanol and subsequent heptane extraction yielded 293 mg (per gram of the material) of heptane-soluble esters. Gas chromatography, under conditions mentioned above, of the heptane soluble esters is shown in Fig. 2. The identification of the unbranched aliphatic esters (both mono-, and di-basic) was done by use of known methyl ester standards. The branched and cyclic carboxylic esters were inferred from the change of peak heights by urea clathration method which removed the unbranched esters to a considerable amount.

## RESULTS AND DISCUSSION

The products of the oxidation reaction are potassium salts of carboxylic acids. Intermediate products of consecutive oxidation were not obtained. The compounds were identified using various techniques; a comparison of the gas chromatograms with a collection of standard samples confirmed the presence of saturated unbranched aliphatic monocarboxylic acids (C<sub>11</sub>-C<sub>31</sub>), saturated straight-chained aliphatic dicarboxylic acids (C<sub>12</sub>-C<sub>18</sub>), and branched aliphatic (or naphthenic) carboxylic acid (ca. C<sub>12</sub>-C<sub>26</sub>). NMR spectra of the oxidation products in pyridine-d<sub>5</sub> solvent revealed the absence of aromatic protons. Since it has been shown that alkyl-substituted aromatic compounds are converted to aromatic carboxylic acids, one can thus conclude that Green River kerogen contains little aromatic sites which is in agreement with the results of Djuricic et al. (3). There is, however, no apparent dominance of the unbranched aliphatic dibasic acids as was observed by Djuricic and co-worker. A likely cause for this may be due to incomplete oxidation of the kerogen 'nucleus,' since the presence of mineral (e.g., quartz, feldspar and clay) that is resistant to mild chemical conditions would hinder the oxidation of the kerogen bound to it. This is consistent with the drastic increase polyfunctional aliphatic acids (especially dicarboxylics) as oxidation of kerogen concentrate progresses (Burlingame et al.) (7).

The results of the present investigation indicates that oxidative release of the entrapped organic material in an aqueous medium is possible without the necessity of disaggregating or dissolution of the resistant mineral. Under the mild oxidative conditions used a significant amount of the organic matter is released as soluble acids (ca. 9.78% of the total raw shale). If an efficient method can be devised to quickly remove the acids released, so that further oxidative degradation is prevented, a stronger oxidizing medium could be used.

Pyrolysis of Green River shale at high temperature (~500°C) tend to yield some aromatic hydrocarbons (8), possibly due to rearrangement of aliphatic hydrocarbons. Oxidation in an aqueous medium can proceed at much lower temperature (~75°C) while the product is mainly aliphatic in nature. Apparently all the available organic material present can be released by oxidation and there is no coke formation as in pyrolysis.

Permanganate is not a suitable oxidant for large scale oxidation even though it is a very effective oxidant for analytical purposes. Once the permanganate is reduced to MnO<sub>2</sub> there is no simple and economical method of oxidizing it back to MnO<sub>4</sub><sup>-</sup>, besides one must be wary of the possible environmental effects of excessive usage of a metal such as manganese. Ozone has been considered as an alternative oxidant, it can be easily generated from oxygen and excess ozone can be easily destroyed (by a catalyst) before releasing to the atmosphere as oxygen. Robinson et al. (9) have partially oxidized the Green River shale with ozone; Bitz and Nagy (10) have used ozone on coal and kerogenic materials. Results of the ozonolysis of Green River shale will be reported at a later date.

## ACKNOWLEDGEMENT

This work is supported by NSF Grant No. GI-35683.

172  
REFERENCES

1. C. A. Prien, *Ind. Chem. Eng.*, 56, 32 (1964).
2. R. H. McKee, *Shale Oil*, Chem. Catalog Co., New York, 1925.
3. M. Djuricic, M. D. Vitorovic, and K. Biemann, *Geochim. et Cosmochim. Acta*, 35, 1201 (1971).
4. J. E. Findley, Private Communication.
5. G. A. Hamilton, B. S. Ribner, and M. T. Hellman, "Oxidation of Organic Compounds III," in *Advances of Chemistry Series*, (R. F. Gould, ed.), 1967, p. 15.
6. D. E. Andres and W. E. Robinson, *Geochim. et Cosmochim. Acta*, 35, 661 (1971).
7. A. L. Burlingame and E. R. Simonet, *Nature*, 222, 741 (1969).
8. G. U. Dinneen, *Chemical Engineering Progress Symposium Series*, 61(54), 42 (1965).
9. W. E. Robinson, D. L. Lawlor, J. J. Cummins, and J. Fester, Bureau of Mines, Rept. of Invest. 6166, 1963.
10. M. C. Bitz and E. Nagy, *Proc. Nat. Acad. of Sci.*, 56, 1383 (1966).

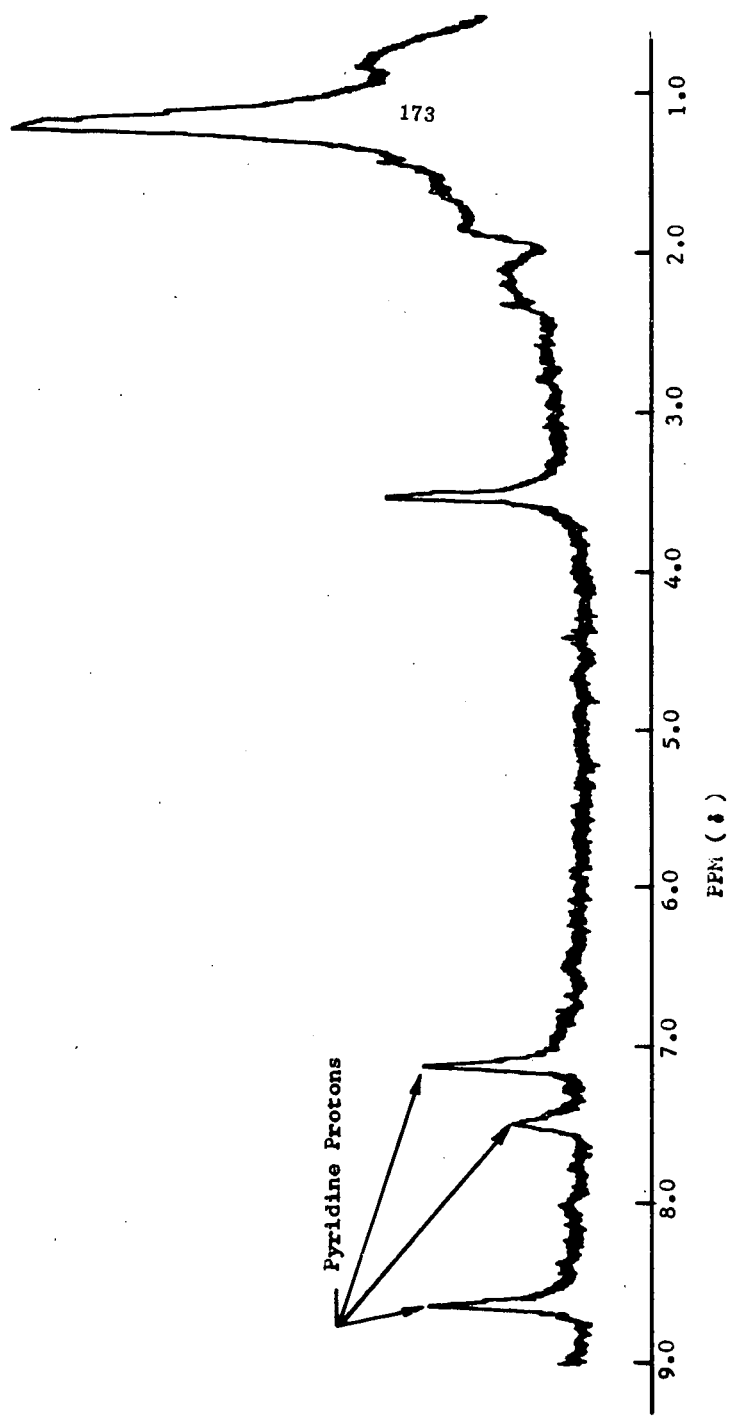


Fig. 1. NMR Spectrum of Fraction I dissolved in (99.9%) Pyridine-D<sub>5</sub>.

N - unbranched aliphatic carboxylic methyl esters.  
 D - unbranched aliphatic dicarboxylic methyl esters.  
 B - branched or cyclic acid methyl esters.  
 The numbers refer to the number of carbon atoms (not including the methoxyl carbon).

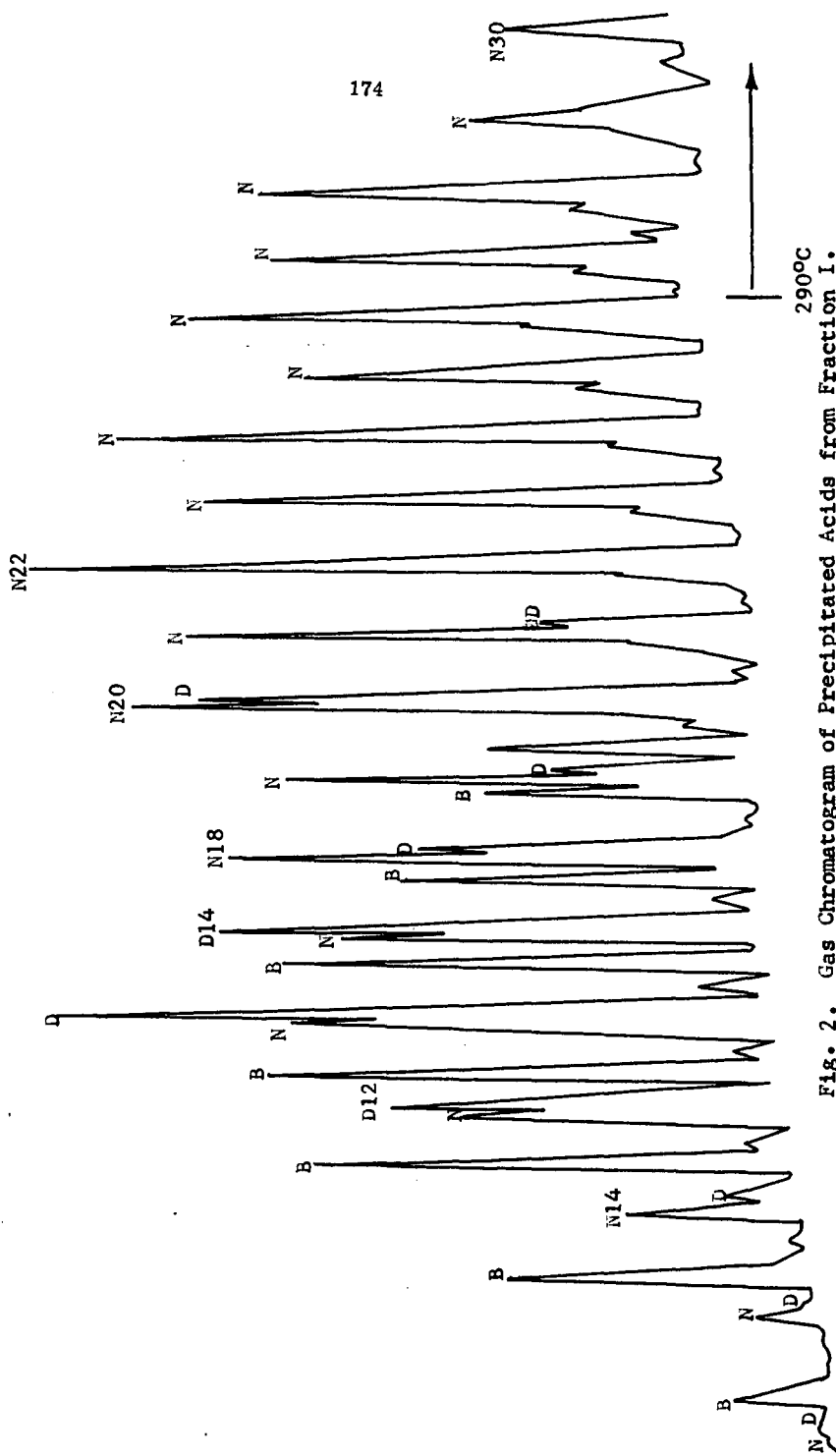


Fig. 2. Gas Chromatogram of Precipitated Acids from Fraction I.

## CHARACTERISTICS OF SYNTHETIC CRUDE FROM CRUDE SHALE OIL PRODUCED BY IN SITU COMBUSTION RETORTING

R. E. Poulson, C. M. Frost, and H. B. Jensen

U.S. Department of the Interior, Bureau of Mines  
Laramie Energy Research Center, Laramie, Wyoming 82070

### INTRODUCTION

The nitrogen contents of in situ crude shale oils may be somewhat lower than those of crude shale oils produced in other retorts;<sup>1</sup> however, these in situ oils still contain more than twice as much nitrogen as high-nitrogen petroleum crude oils. Because existing refineries would not be able to cope with the high nitrogen content of shale oil if it were a substantial portion of the refinery feed, the National Petroleum Council (NPC) has suggested<sup>2</sup> that crude shale oil be upgraded at the retorting site by a catalytic hydrogenation process to produce a synthetic, premium feedstock called "syncrude." The production of such a syncrude from in situ crude shale, a description of its bulk properties, and a comparison of its properties to those of an NPC-type syncrude have been covered by C. M. Frost<sup>3</sup> earlier in this symposium.

This paper reports the compound-type characteristics of the syncrude produced by catalytic hydrogenation of in situ crude oil. Special attention will be devoted to the nitrogen-compound types that are in a syncrude because it will be these compounds with which a refiner will have to deal if he uses this or a similar syncrude as his refinery feed.

In addition to reporting the nitrogen-compound types present in the syncrude, this paper will also report on the nitrogen types in intermediate hydrogenation products in order to relate this study to other studies<sup>4,5,6,7,8</sup> which have shown that the efficacy of nitrogen removal depends upon the nitrogen types in the charge stock. Earlier studies have been on pure compounds, or on charge stocks spiked with pure compounds, or on nitrogen-containing stocks and have been concerned with nitrogen removals approaching 80 percent. The syncrude described in the present work represents a case approaching 95 to 99 percent nitrogen removal.

### EXPERIMENTAL

#### Preparation of the Samples

The synthetic crude oil (syncrude)<sup>3</sup> used in this study was prepared by hydrogenating the naphtha (IBP-350° F), the light oil (350°-550° F), and the heavy oil (550°-850° F) fractions that had previously been obtained from in situ crude shale oil by distillation and coking of the vacuum residuum. The heavy oil used in this study was the 550° F+ material from the heavy-oil hydrogenation. The light oil was the 350° F+ material from the hydrogenation of the light oil from the distillation step combined with the 350°-550° F material from the heavy-oil hydrogenation. The 175°-350° F heavy naphtha was the 175° F+ material from the hydrogenation of the combined IBP-350° F naphtha from the distillation and the heavy naphthas from both the heavy-oil and the light-oil hydrogenations. The C<sub>5</sub>-175° F light naphtha was the material with that boiling range from each of the three hydrogenations.

In addition to using these four fractions in the characterization of the syncrude, the nitrogen compounds in three intermediate hydrogenation fractions were characterized in order to relate this denitrification study to other such studies. These materials were the light oil from the

heavy-oil hydrogenation, the 175°-350° F heavy naphtha from the heavy-oil hydrogenation, and the 175°-350° F heavy naphtha from the light-oil hydrogenation.

The heavy oil, which contained nearly 90 percent of the nitrogen in the syncrude, was fractionated by liquid displacement chromatography on Florisil. The nonpolar, nonnitrogen-containing hydrocarbons were washed from the Florisil column with *n*-heptane; a very weak-base concentrate was displaced with benzene; and a weak-base concentrate was displaced with benzene-methanol azeotrope.

### Analytical Methods

Total nitrogen values were determined with a reductive, hydrogen-nickel pyrolysis tube and an ammonia microcoulometer. Nonaqueous potentiometric titration<sup>6,9,10,11</sup> was used to classify the nitrogen compounds into weak-base (pKa -2 to +2), very weak-base (pKa +2 to +8), and neutral types. Infrared spectrometry<sup>10,11,12</sup> was used to determine the concentration of pyrrolic nitrogen (nonhydrogen-bonded N-H). Colorimetry<sup>10,13,14</sup> was used to determine pyrroles and indoles with unsubstituted  $\alpha$  or  $\beta$  positions. The aforementioned methods classified the nitrogen compounds into weak bases such as pyridines (including quinolines, 5,6,7,8-tetrahydroquinolines and acridines) and as arylamines (including 1,2,3,4-tetrahydroquinolines, 2,3-dihydroindoles, and anilines); into very weak-base pyrroles and indoles with an  $\alpha$  or  $\beta$  position unsubstituted; and into neutral carbazoles without N-substitution. Low-voltage mass spectrometry and high-resolution mass spectrometry allowed classification of the remaining nitrogen compounds into either pyrrole types with  $\alpha$  and  $\beta$  positions substituted or carbazoles with N-substitution.

Hydrocarbon types were estimated using the subtractive method of Poulson<sup>15,16</sup> for the fractions boiling above 175° F. The hydrocarbon compound composition of the C<sub>5</sub>-175° F naphtha was determined by gas chromatography. Paraffin and naphthene contents of the 175°-350° F naphtha and of the 350°-550° F light oil were calculated from mass spectra. Liquid displacement chromatography on Florisil was used to determine the amount of polar material in the 550°-850° F heavy oil.

## RESULTS AND DISCUSSION

### Hydrocarbon-Type Characterization

Table I lists the four fractions, their weight percent of the syncrude, and their hydrocarbon-type compositions. The values for polar material for the two naphthas and the light oil are estimates based on their nitrogen contents. The polar material value for the heavy oil is based on the recovered weights from the Florisil separation. As shown in Table I, all fractions of the syncrude have appreciable amounts of aromatics after the hydrogenation even though the nitrogen has been largely removed. Only the heavy oil has a detectable concentration of olefinic hydrocarbons. A reference to this olefinic nature will be made later in this paper.

### Nitrogen-Type Characterization

Syncrude Fractions.—Table II lists the microcoulometric and titration data for the four syncrude fractions. The 79 ppm nitrogen in the light oil was shown to be all pyridine-type nitrogen because it did not acetylate when acetic anhydride was used as the titration solvent. No further characterization of this nitrogen was carried out. No acetylatable arylamines were found in this fraction or in the heavy oil, although Brown<sup>7</sup> found that anilines made up nearly one-third of the tar-base concentrate from a recycle, hydrocracked shale-oil naphtha (total nitrogen in the naphtha was approximately 1,000 ppm). In addition, Silver<sup>5</sup> reports that in denitrification of

TABLE I. - Hydrocarbon types in syncrude fractions

Boiling range	Name	Wt pct of crude	Hydrocarbon type, wt pct of fraction				Polar material
			Paraffins	Naphthenes	Olefins	Aromatics	
C <sub>5</sub> -175° F	Light naphtha	3	71.8	20.5	0.0	7.7	<0.001
175°-350° F	Heavy naphtha	21	42.8	43.4	.0	13.8	< .001
350°-550° F	Light oil	49	51.5	25.0	.0	23.5	< .01
555°-850° F	Heavy oil	27	72.7		6.0	19.2	2.1

1/ Includes naphthenes.

TABLE II. - Microcoulometric and titration data for syncrude fractions

Fraction	Total nitrogen in fraction, ppm	Nitrogen type, wt pct of nitrogen in fraction			
		Weak-base	Very weak-base	Neutral	Arylamine
Light naphtha	<0.5	-	-	-	-
Heavy naphtha	.8	-	-	-	-
Light oil	79	100	0	0	0
Heavy oil	935	40.1	13.9	46.0	0

shale gas oil, to about 80 percent removal of nitrogen, arylamines appear to build up relative to the other nitrogen types in the total product oil.

**Nitrogen Concentrates.**--Table III lists the recovery of the heavy-oil nitrogen in the two Florisil concentrates and also the concentration of nitrogen types in each of these two concentrates. The weak-base and very weak-base types are determined by nonaqueous potentiometric titration, the neutral types by difference, the N-H types by infrared spectrometry, and the pyrrolic types by colorimetry. As shown in Table III, the concentrate labeled very weak base has about one-fifth very weak-base and four-fifths neutral nitrogen compounds, and the nitrogen in the concentrate labeled weak base is nearly all weak-base nitrogen with less than 3 percent being neutral nitrogen.

TABLE III. - Nitrogen distribution in heavy-oil concentrates displaced from Florisil

Concentrate	Recovery, wt pct of nitrogen in the heavy oil	Nitrogen type, wt pct of nitrogen in concentrate				
		N-H	Pyrrolic	Weak-base	Very weak-base	Neutral
Very weak-base concentrate	61.5	63.4	6.8	0.0	19.8	80.2
Weak-base concentrate	38.4	2.3	<0.01	97.4	.0	2.6

**Very Weak-Base Nitrogen Concentrate.**--Table IV is a summary of the data obtained from low-voltage mass spectrometry and from high-resolution mass spectrometry on the very weak-base concentrate from the Florisil separation. The absence of any titratable weak bases (Table III) allows an assignment of very weak-base or of neutral nitrogen types to the Z series ions as shown in Table IV. The names of the very weak-base nitrogen compounds reflect only the degree of hydrogen deficiency necessary to yield the proper Z series. The requirements for the proper Z series

TABLE IV. - Mass spectral data for very weak-base concentrate

Z series	Compound type	Percent of ionization
- 5	Cycloalkanopyrroles	<1
- 7	Dicycloalkanopyrroles	6
- 9	Indoles	7
-11	Cycloalkanoindoles	3
-13	Dicycloalkanoindoles	13
-15	Carbazoles	54
-17	Cycloalkanocarbazoles	17
-19	Dicycloalkanocarbazoles	<1

could be met by having olefinic bonds in either the cycloalkano rings or in an alkyl substituent on the ring system. For example, the Z = -13 labeled as dicycloalkanoindoles could also be correctly labeled as monocycloalkenoindoles. The inclusion of an olefinic bond in the molecule is reasonable when one considers that 6 percent of the heavy oil hydrocarbon molecules are olefinic (Table I).

Interpretation of these mass-spectral data in Table IV combined with the titration data from Table III allows additional inference concerning the characteristics of the nitrogen compounds present in the very weak-base concentrate. The sum of the compound types listed as pyrroles and indoles (Z = -7, -9, -11, and -13) amounts to 29 percent of the total. These compound types have been shown<sup>11</sup> to give very weak-base titers of about 70 percent of theoretical; thus it appears likely that the 19.8 percent titer for very weak bases in Table III may come from the titration of the pyrroles and indoles in this concentrate. In addition, they are not N-substituted because N-substituted pyrrole-type nitrogen titrates as weak-base nitrogen, and there is no weak-base titer for this concentrate.

A further characterization of these pyrrole-type nitrogen compounds in the very weak-base concentrate can be made by using the colorimetric pyrrolic nitrogen value of 6.8 percent (Table III) as the value for  $\alpha\beta$ -unsubstituted pyrrole-type compounds. This leaves 22.2 percent of the nitrogen in pyrroles and indoles which have both  $\alpha$ - and  $\beta$ -substitution. The  $\alpha\beta$ -unsubstituted pyrroles and indoles also have no N-substitution because these N-substituted compounds would titrate as weak bases and not as very weak bases. This finding of no N-substitution on the pyrroles and indoles is consistent with the research of Jacobson<sup>18,19</sup> who reported that N-alkylpyrroles and N-alkylindoles thermally and irreversibly isomerize to give the  $\alpha$  and  $\beta$  alkyl isomers and therefore would not likely be present in crude shale oil.

Table III shows that 63.4 percent of the nitrogen in the very weak-base concentrate is N-H nitrogen. Of this 63.4 percent of the nitrogen, 29 percent has already been characterized as being in pyrroles and indoles without N-substitution. This leaves 34.4 percent of the nitrogen to be in carbazoles without N-substitution. Table IV shows that 71 percent of the nitrogen is in carbazole-type compounds, and if 34.4 percent has no N-substitution then 36.6 percent has N-substitution. Table V is a summary of these findings. Thus we see that one-third of this concentrate is one- and two-aromatic-ring heterocyclics and two-thirds is three-aromatic-ring heterocyclics.

Weak-Base Nitrogen Concentrate. --Table VI is a summary of the mass spectral data on the weak-base concentrate. As was true for the very weak-base fraction, the compound types

TABLE V. - Summary of nitrogen types in the very weak-base nitrogen concentrate

Nitrogen-type compounds	Percent of fraction
Pyroles or indoles with either $\alpha$ or $\beta$ positions unsubstituted; no N-substitutions .....	6.8
Pyroles or indoles with substitutions in both $\alpha$ and $\beta$ positions; no N-substitutions.....	22.2
Carbazoles with no N-substitution .....	34.4
Carbazoles with N-substitution .....	36.6

TABLE VI. - Mass spectral data for weak-base concentrate

Z series	Compound type	Percent of ionization
- 5	Pyridines	35
- 7	Cycloalkanopyridines	25
- 9	Dicycloalkanopyridines	12
-11	Quinolines	13
-13	Cycloalkanoquinolines	8
-15	Dicycloalkanoquinolines	3
-17	Acridines	4
-19	Cycloalkanoacridines	<1

reflect only the degree of hydrogen deficiency necessary to achieve the proper Z series; and, like Table IV, this hydrogen deficiency could be achieved by olefinic bonds in the molecule. We can see from Table III that nearly all (97.4 percent) of the nitrogen in this concentrate titrates as weak-base nitrogen; hence the compound types listed in Table VI are generally consistent with that titration. However, Table III does show that 2.3 percent of the nitrogen in this fraction exhibits an N-H character. Because there is no weak-base titer, it can be assumed that this N-H character is in carbazoles either in the Z = -15 or -17 series. This indicates that there was some tailing of the carbazoles into the weak-base fraction. Contrasted to the ring structures in the very weak-base fraction in which one-ring and two-ring structures accounted for only one-third of the fraction and three-ring structures two-thirds, the weak bases are composed of two-thirds one-aromatic-ring structures and one-third two-ring and three-ring structures. Dinneen<sup>20</sup> also showed this preponderance of one-ring materials in a shale-oil gas oil as did Poulson<sup>10</sup> in a shale-oil light distillate.

**Characterization of Intermediate Fractions.**--Nonaqueous potentiometric titration was used to characterize the nitrogen compounds in three, intermediate fractions from the production of the syncrude. Table VII lists these three fractions, their source, and the results of the titrations. Also listed in this table are the syncrude fractions produced during the hydrogenation.

The first fraction listed is the 550° F+ heavy oil produced by hydrogenation of the 550°-850° F heavy oil from distillation and coking of the in situ crude oil. This is the same fraction listed in Tables I and II as the syncrude heavy oil fraction. The second fraction listed in Table VII is the 350°-550° F light oil produced in the foregoing hydrogenation and the third fraction is the 175°-350° F heavy naphtha produced in the same hydrogenation.

TABLE VII. - Microcoulometer and titration data for selected, intermediate and syncrude fractions

Fraction	Total nitrogen in fraction, ppm	Nitrogen type, wt pct of nitrogen in fraction			
		Weak-base	Very weak-base	Neutral	Arylamine
Heavy-oil hydrogenation					
Heavy oil	935	40.1	13.9	46.0	0
Light oil	1,220	78.7	11.5	9.8	1/12.3
Heavy naphtha	299	100.0	0	0	0
Light-oil hydrogenation					
Light oil	79	100.0	0	0	0
Heavy naphtha	53	100.0	0	0	0

1/ Included in weak-base nitrogen.

The fourth fraction in Table VII is the 350°-550° F light oil produced from the hydrogenation of the 350°-550° F light oil resulting from the distillation and coking of the in situ crude to which had been added an aliquot amount of the light oil shown as the second fraction in Table VII. The fifth fraction is the 175°-350° F heavy naphtha from this hydrogenation. Only the second, third, and fifth listed fractions are intermediate fractions; the first and fourth are final, syncrude ones.

There are three purposes in showing the data in Table VII. First, it is evident that when a shale-oil stock is hydrocracked to lower boiling material, the nitrogen content of the lower boiling fraction is higher than when that same boiling-range material is hydrogenated; for example, the light oil from the heavy-oil hydrogenation has 1,220 ppm nitrogen whereas the light oil from the light-oil hydrogenation is only 79 ppm nitrogen. Second, the light oil from the light-oil hydrogenation and both of the naphthas have only weak-base nitrogen, and this is all pyridine type because none of these fractions contains acetylatable amines. And, third, the light oil from the heavy-oil hydrogenation has arylamine-type weak bases, neutral nitrogen compounds, and very weak bases as well as pyridine-type weak bases. These data indicate that an unspecified but appreciable amount of hydrocracking can and does precede denitrification reactions. In general, arylamines are not found in appreciable concentrations in shale-oil distillates, but are presumed to be produced by hydrogenation of a five-membered nitrogen ring to give a 2,3-dihydroindole-type arylamine and by hydrogenation of a six-membered nitrogen ring to give a 1,2,3,4-tetrahydroquinoline-type arylamine.<sup>4,5,6,10</sup> Cracking of this saturated, nitrogen-containing ring with the nitrogen remaining attached to the aromatic moiety results in an aniline-type arylamine. The presence of arylamines in the light-oil fraction from the heavy-oil hydrogenation is consistent with Silver's<sup>5</sup> finding them in the total product from shale gas oil hydrogenation at nitrogen removals approaching the 80-percent level. The fact that the arylamines are not in either of the naphtha materials shown in Table VII nor in the naphthas shown in Table II indicates that arylamines are converted to hydrocarbons and ammonia when nitrogen conversion approaches 95 percent.

#### SUMMARY

The synthetic crude was produced by hydrogenating the 1BP-350° F naphtha, the 350°-550° F light-oil, and the 550°-850° F heavy-oil fractions obtained from in situ crude shale oil by distillation followed by coking of the 850° F+ residuum. Characterization of the syncrude was

accomplished by examining the following fractions: (1) C<sub>5</sub>-175° F light naphtha, (2) 175°-350° F heavy naphtha, (3) 350°-550° F light oil, and (4) 550°-850° F heavy oil.

The light naphtha comprised 3 percent of the syncrude and contained 72 percent paraffins, 20 percent naphthenes, 8 percent aromatics, and less than 0.5 ppm nitrogen. The heavy naphtha comprised 21 percent of the syncrude and contained 43 percent paraffins, 43 percent naphthenes, 14 percent aromatics, and less than 1 ppm nitrogen. The light oil comprised 49 percent of the syncrude and contained 51 percent paraffins, 25 percent naphthenes, 24 percent aromatics, and 79 ppm nitrogen. The heavy oil comprised 27 percent of the syncrude and contained 73 percent saturates, 6 percent olefins, 19 percent aromatics, 2 percent polar compounds, and 935 ppm nitrogen.

The nitrogen compounds in the two naphthas were not characterized. The nitrogen in the light oil was shown to be pyridine-type nitrogen with no detectable arylamine-type nitrogen.

The nitrogen compounds in the heavy oil were shown to be 40 percent weak-base, 14 percent very weak-base, and 46 percent neutral compounds. Mass spectrometry was used to classify the weak bases as 72 percent pyridines (one aromatic ring), 24 percent quinolines (two aromatic rings), and 4 percent acridines (three aromatic rings). Mass spectrometry combined with infrared analysis and pyrrolic-nitrogen determination were used to classify the very weak-base and neutral nitrogen compounds as 7 percent pyrroles or indoles with either or both of the  $\alpha$  and  $\beta$  positions open and not N-substituted; 22 percent pyrroles or indoles with substitution on both  $\alpha$  and  $\beta$  positions but no N-substitutions; 34 percent carbazoles with no N-substitutions; and 37 percent N-substituted carbazoles.

In addition to characterizing the four fractions of the final syncrude product, three intermediate fractions were also characterized. The heavy naphtha from the light-oil hydrogenation and the heavy naphtha from the heavy-oil hydrogenation both contained characterizable amounts of nitrogen compounds. These were shown to be weak bases of the pyridine type. The light oil from the heavy-oil hydrogenation had the greatest concentration of nitrogen of any of the fractions examined, 1,220 ppm. Nonaqueous titration showed these nitrogen compounds to be 66 percent weak-base pyridines, 12 percent weak-base anilines (arylamines), 12 percent very weak bases, and 10 percent neutral compounds. This material contained the only evidence of arylamines in the product from these hydrogenations, which represent removals of 95 to 99.9 percent of the nitrogen of the charge stock.

#### ACKNOWLEDGMENT

The work upon which this report is based was done under a cooperative agreement between the Bureau of Mines, U.S. Department of the Interior, and the University of Wyoming.

Reference to specific trade names or manufacturers does not imply endorsement by the Bureau of Mines.

#### REFERENCES

1. H. B. Jensen, R. E. Poulson, and G. L. Cook, Preprints, Div. of Fuel Chem., ACS, 15, No. 1, 1971, p. 113.
2. U.S. Energy Outlook, An Interim Report, National Petroleum Council, 2, 1972, p. 80.
3. C. M. Frost, R. E. Poulson, and H. B. Jensen, this symposium.

4. C. M. Frost and H. B. Jensen, Preprints, Div. of Petrol. Chem., Inc., ACS, 18, No. 1, 1973, p. 119.
5. H. F. Silver, N. H. Wang, H. B. Jensen, and R. E. Poulson, this symposium.
6. R. M. Koros, S. Bank, J. E. Hoffman, and M. I. Kay, Preprints, Div. of Petrol. Chem., Inc., ACS, 12, No. 4, 1967, p. B165.
7. R. A. Flinn, O. A. Larson, and H. Beuther, Pet. Ref., 42, 1963, p. 129.
8. J. Doelman and J. C. Vlugter, Proc. for the Sixth World Petroleum Congress, Section III, Paper 12, Frankfurt/Main, Germany, 1963.
9. B. E. Buell, Anal. Chem., 39, 1967, p. 756.
10. R. E. Poulson, H. B. Jensen, and G. L. Cook, Preprints, Div. of Petrol. Chem., Inc., ACS, 16, No. 1, 1971, p. A49.
11. H. F. Silver, N. H. Wang, H. B. Jensen, and R. E. Poulson, Preprints, Div. of Petrol. Chem., Inc., ACS, 17, No. 4, 1972, p. G74.
12. A. Pozefsky and Ira Kukin, Anal. Chem., 27, 1955, p. 1466.
13. R. B. Thompson, T. Symon, and C. Wankat, Anal. Chem., 24, 1952, p. 1465.
14. M. A. Muhs and F. T. Weiss, Anal. Chem., 30, 1958, p. 259.
15. R. E. Poulson, H. B. Jensen, J. J. Duvall, F. L. Harris, and J. R. Morandi, Analysis Instrumentation (Instrument Society of America), 10, 1972, p. 193.
16. L. P. Jackson, C. S. Allbright, and H. B. Jensen, accepted for publication by Anal. Chem.
17. Dennis Brown, D. G. Earnshaw, F. R. McDonald, and H. B. Jensen, Anal. Chem., 42, p. 146.
18. I. A. Jacobson, Jr. and H. B. Jensen, BuMines Rept. of Inv. 672, 1966, 50 pp.
19. I. A. Jacobson, Jr., BuMines Rept. of Inv. 7529, 1971, 8 pp.
20. G. U. Dinneen, G. L. Cook, and H. B. Jensen, Anal. Chem., 40, 1968, p. 1295.

RETORTING INDEXES FOR OIL-SHALE PYROLYSES FROM  
ETHYLENE-ETHANE RATIOS OF PRODUCT GASES

I. A. Jacobson, Jr., A. W. Decora, and G. L. Cook

U.S. Department of the Interior, Bureau of Mines  
Laramie Energy Research Center, Laramie, Wyoming 82070

## INTRODUCTION

The production of shale oil from oil shale is currently practical only by thermally decomposing (retorting) the organic materials in the shale and collecting the liquid products. Investigations to develop processes for retorting oil shale have resulted in many proposed designs for the equipment. However, to maintain control of any of the processes, measurements of appropriate input and output parameters are required to indicate conditions during the decomposition and the subsequent collection of products. The direct measurement of retort temperatures is not always possible. Flow rates through the retorts give only an indirect measure of residence times for material in the heated zones. Both residence times and temperature are important control parameters--related to economy of operation and quality of product.

The pyrolysis of oil-shale kerogen is a very complex reaction or group of reactions that results in the production of a myriad of hydrocarbons and hydrocarbon derivatives. These products range from compounds containing one carbon atom per molecule (methane) to compounds containing greater than 30 carbon atoms per molecule. It is not currently feasible to set forth the mathematical relationships of the pyrolysis reactions with great certainty. This inability to set down the exact mathematical relationships of the overall pyrolysis reaction should not preclude the gleanings of certain useful empirical data that can be used to assist in the interpretation or control of the retorting processes.

Shale-oil production by thermal decomposition of the organic material in the shale has been described as a pseudo first-order process.<sup>1,6</sup> In a practical process the shale is heated to the maximum temperature over a finite period of time. The products of retorting remain in a heated zone for varying periods of time. The nature of the products depends on both the temperature range over which thermal decomposition takes place and on the residence time of the products in a hot zone. Temperature measurements in a retort are not readily related to the product even if coupled with flow rates through the retort. This paper develops a parameter that combines the elements of temperature and residence time into a single number that can be used to indicate instantaneous retorting conditions or can be used to compare various thermal processing techniques for oil shale.

The parameter developed for comparison or control of the retorting process has the dimension of temperature. It could be defined as an "effective temperature" or a "Retorting Index." In the laboratory this index was developed by relating the ethylene/ethane ratio in the product gases from retorting of shale to a measured temperature in the retorting zone. Residence times of the products in the hot zone were nearly constant. In a commercial-size retort, residence times could vary over wide ranges. Residence time variation causes a change in the observed ratio. The calculated parameter also changes and so reflects the changing retorting conditions. Application of the parameter to Fischer assay retorts, gas combustion retorts, and to entrained solids retorts is illustrated with examples. The easily calculatable Retorting Index is applicable to in situ retorting as well as those retorts used as examples.

## EXPERIMENTAL PROCEDURE

Equipment

The equipment consists of an electrically heated quartz tube 2.1-cm i.d. by 83.8-cm long with 24/40 standard taper joints at the ends. A section of the tube, 15-cm minimum length, 43-cm from the inlet was heated to the desired retorting temperature. Heating was accomplished by a three-unit tube furnace, and the temperature was maintained by potentiometer controllers. Oil-shale samples were contained in a 1.25-cm by 7.62-cm boat made from stainless-steel screen. The sample boat was moved in and out of the retorting zone by means of a 1-mm stainless-steel rod which extended from the boat out through the quartz tube inlet.

A tube receiver, a U-tube trap, and an evacuated gas receiver made up the product collection system. The receiver and U-tube were cooled with liquid nitrogen when nitrogen was used for the sweep gas and with dry ice when oxygen was used in the sweep gas for oxidative retorting runs. Sweep gases into the retort tube were metered through a metering valve. Pressure in the retorting section, as monitored by an open-end manometer, was maintained at atmospheric pressure by venting gases from the U-tube through a stopcock into the gas collection system.

Oil-Shale Samples

Oil-shale samples from Colorado, Wyoming, and Utah were used in this study. The sizes of the oil shale used were (A) 20 to 30 mesh, (B) 10 to 14 mesh, (C) 1/8 in to 30 mesh, and (D) 1/4 in to 1/2 in. Most of the retorting work was performed on size C shale. Three different Colorado oil-shale samples were obtained from the Bureau of Mines mine at Rifle, Colorado and assayed 53.8, 52.5, and 22 gpt. The 53.8-gpt oil shale had been ground to sizes A and C, the 52.5-gpt shale ground to size D, and the 22-gpt shale ground to sizes B and C. Wyoming oil-shale samples were a 12.4-gpt sample from a Washakie Basin, Sweetwater County corehole and 13.4-, 19.9-, 30.5-, and 34.4-gpt shales from the Bureau of Mines Rock Springs site 6, well No. 6-2 core. The Utah shales were from the Gulf Evacuation No. 1 core drilled by Gulf Minerals, and the shale samples assayed 14.5, 20.3, 29.0, and 42.7 gpt. All of the Wyoming and Utah oil shales had been ground to size C. A summary description of the oil-shale samples used is presented in Table I.

TABLE I. - Description of oil-shale samples used in the procedure

Sample No.	Geographical source	Assay, gpt <sup>1/</sup>	Sample mesh size
1	Colorado	53.8	20 to 30 mesh
2	do.	53.8	1/8 in to 30 mesh
3	do.	52.5	1/4 in to 1/2 in
4	do.	22.0	10 to 14 mesh
5	do.	22.0	1/8 in to 30 mesh
6	Wyoming	34.4	do.
7	do.	30.5	do.
8	do.	19.9	do.
9	do.	13.4	do.
10	do.	12.4	do.
11	do.	42.7	do.
12	do.	29.0	do.
13	do.	20.3	do.
14	do.	14.5	do.

<sup>1/</sup> Potential oil yields were determined by the modified Fischer assay method (reference 10).

### Pyrolysis Procedure

Temperature profiles of the reaction tube were determined by measuring the temperature inside the tube at 2.54-cm intervals with a thermocouple and potentiometer with sweep gas flowing. Determination of temperature profiles was performed only when work at a new temperature was begun. The temperature at which the furnace was set remained constant and the temperature variation at any point within the quartz tube would fluctuate  $\pm 2^\circ \text{C}$  ( $3.6^\circ \text{F}$ ) maximum.

In making a retorting run, about 7 grams of oil shale were weighed into the sample boat, and the boat was placed at the inlet of the cold reaction tube. The entire retorting system was flushed by evacuation and filling several times with the intended sweep gas. Both the receiver and U-tube trap were cooled and the sweep gas flow adjusted to the desired rate and the vent opened to the atmosphere.

The furnace was then turned on and allowed to come to temperature. After retorting temperature was reached, the sample boat was moved into the retorting zone and kept there for 20 to 25 minutes to insure complete retorting. The boat was then moved back to the inlet, and the furnace turned off. To insure complete collection of the gaseous products, gas collection was started 10 minutes before the furnace reached temperature and continued for 10 minutes after the furnace was turned off. The coolant baths were removed from the receiver and U-tube trap, the traps were warmed to room temperature, and any liberated gases were swept into the gas collection system. When the retorting run was finished, the pressure in the gas collection system was measured and the shale oil and spent shale were weighed.

For the cracking runs the sample boat was not placed as far down the reaction tube. For these runs the boat position was generally 15.24-cm upstream from the "normal" position, and the retorting temperature was about  $100^\circ$  to  $150^\circ \text{F}$  lower.

The majority of the retorting runs were made with a nitrogen sweep through the retort tube. Gas flow was maintained at 2.5 standard  $\text{cm}^3/\text{min}$  (superficial space velocity of  $0.023 \text{ ft}^3/\text{min}/\text{ft}^2$ ). Several runs were made with the nitrogen flow increased to 20 standard  $\text{cm}^3/\text{min}$  (superficial space velocity of  $0.19 \text{ ft}^3/\text{min}/\text{ft}^2$ ). In addition to these basic retorting runs, others were made using air and nitrogen as sweep gas with the oxygen content varying from 3 to 21 percent and a total gas flow of 2.5 to 20 standard  $\text{cm}^3/\text{min}$ , steam and nitrogen as the sweep gas with the nitrogen flow at 2.5 standard  $\text{cm}^3/\text{min}$  and a steam rate of 1 g/min.

### Gas Analyses

Gas analyses were performed by gas liquid chromatography (GLC) using a 1/8-in o.d. by 10-ft stainless-steel column packed with 150 to 200 mesh Poropak Q. GLC operating conditions were a helium flow of 18  $\text{cm}^3/\text{min}$  and oven temperature programed from  $50^\circ$  to  $180^\circ \text{C}$  at  $4^\circ \text{C}/\text{min}$ . Detection was by thermal conductivity. For quantitative analyses the GLC peak areas were corrected for molar response by the method of Messner.<sup>8</sup>

## RESULTS AND DISCUSSION

Table II is a tabulation of the recoveries and ethylene-ethane ratios for retorting runs performed at  $1,064.4^\circ$  and  $1,297.5^\circ \text{F}$ . These data show the type of recovery experienced during the work. It is felt that most of the loss was due to nonrecovery of liquid, which condensed in inaccessible parts of the system. As can be seen, the ethylene-ethane ratio changes when the retorting temperature changes.

TABLE II. - Recovery and ethylene-ethane ratio for selected temperatures of laboratory retorting using nitrogen sweep gas

Source <sup>1/</sup>	Oil shale Assay, gpt		Total flow cm <sup>3</sup> /min	Retort temp., ° F	Charge, gram	Recovery, wt. pct			Wt pct ratio, ethylene/ethane	
	Size <sup>2/</sup>					Spent shale	Oil + water	Gas		Loss
C	53.8	C	2.5	1,064.4	7,6052	71.69	22.27	5.05	0.73	0.7012
C	53.8	C	20.0		7,3051	71.82	20.86	6.30	1.02	0.7124
C	53.8	A	2.5		5,9429	72.14	20.84	5.22	1.80	0.7638
C	53.8	C	2.5		7,5043	71.82	22.29	5.15	0.74	0.7207
C	52.5	D	2.5		7,4783	73.73	19.73	5.29	1.25	0.7867
C	53.8	A	2.5		6,1041	72.02	21.36	5.27	1.35	0.7565
C	52.5	D	2.5		8,2537	73.98	19.46	5.02	1.54	0.7979
C	53.8	C	20.0		7,4921	71.99	20.91	6.42	0.67	0.7213
W	12.4		2.5		7,5210	88.25	8.49	2.46	0.80	0.6968
C	3/	B+C	2.5		8,4510	80.83	14.70	3.44	1.03	0.7950
C	53.8	C	2.5	1,297.5	7,7834	66.29	13.57	15.88	4.26	1.6135
C	53.8	C	2.5		7,8141	66.13	14.97	15.85	3.05	1.7003
C	53.8	C	2.5		7,8151	66.95	13.53	16.92	2.60	1.6762
C	53.8	C	2.5		7,8141	66.38	13.59	17.32	2.71	1.6975

1/ C = Colorado, W = Wyoming.

2/ Particle size, A = 20-30 mesh, B = 10-14 mesh, C = 1/8-in to 30 mesh, D = 1/2- to 1/4-in.

3/ A mixture of 53.8- and 22-gpt oil shales to give an approximate 36-gpt oil shale.

The change in ethylene-ethane ratio is not linear with change in temperature. A linear relationship can be obtained by using logarithm of the ethylene-ethane ratio and reciprocal of the temperature. Other combinations of saturates and unsaturates, while showing similar changes with temperature, cannot be transformed to linear relationship as readily.

When a linear least-squares regression of the log (ethylene/ethane) with reciprocal temperature is performed, the resulting regression equation has a coefficient of determination ( $100 r^2$ ) of 95. This means that all but 5 percent of the variation of log (ethylene/ethane) can be explained as reciprocal temperature dependence. Data from retorting runs on oil shales from different locations, of different particle size, and of different assay richness were included in the regression.

The regression equation so derived is

$$\frac{1,000}{T} = 0.8868 - 0.4007 \log (\text{ethylene/ethane}). \quad 1)$$

where T = temperature, °F. When Equation 1 is recast for the prediction of the Retorting Index, it is

$$RI = T = 1,000/[0.8868 - 0.4007 \log (\text{ethylene/ethane})]. \quad 2)$$

When ethylene and ethane are determined with a 2 percent accuracy, it is possible to calculate the Retorting Index to  $\pm 25^\circ \text{ F}$  (95 percent confidence).

Oxygen was added to the sweep gas to determine its effects, if any, on the ethylene/ethane ratio. Total amounts of oxygen had to be kept low so the exothermic oxidation reactions would not upset the thermal balance in the retorting zone by increasing the shale temperature above the furnace temperature. In Table III are listed the results from the retorting runs made with added oxygen. These runs were made at 1,187° F using the 53.8-gpt, size C, Colorado oil shale. When the Retorting Index is calculated for the oxidation retorting runs, it is not significantly different from the furnace temperature. This shows that the presence of oxygen in the sweep gas has no effect on the Retorting Index. A similar conclusion can be drawn from the one retorting run where steam was included in the sweep gas.

Table III also lists data obtained from the cracking runs. These data produce a Retorting Index which generally is higher than the retorting temperature. The retorting temperatures for these runs were 100° to 150° F lower than the furnace temperature. This apparent anomaly can be readily explained. Both ethylene and ethane production in retorting and cracking are controlled by the laws of kinetics. The ethylene-ethane ratio is increased in a thermal cracker by increasing the temperature. The ratio can also be increased by holding the temperature constant and increasing the residence time. The same temperature-residence time control of the ethylene-ethane ratio is found in oil-shale retorting. Therefore, increasing the temperature with a small decrease in residence time or holding the temperature constant with an increase in residence time will increase the ethylene-ethane ratio, and the products of retorting will be essentially the same in either case. In most retorts the retorting products are in the high-temperature zone for only a small fraction of a second before they are swept to a cooler temperature. When the retort products were cracked in the bench retort, they spent a longer time in the high-temperature zone so more cracking could take place. Consequently, the products are the same as if they were produced at a higher temperature. Because we cannot determine the residence time for the retorting process, the composition of the retort products is compared to temperature and a higher Retorting Index is correct.



For further information on the validity of the Retorting Index, the calculations will be applied to data from four different retorting methods. Table IV lists the reported retorting temperature, ethylene-ethane ratio, and Retorting Index for (A) Fischer assay, (B) gas combustion, and (C) entrained solids retorting.

TABLE IV. - Reported retorting temperatures and Retorting Indexes

Retort	Wt pct ratio, ethylene/ethane	Reported retorting temp, °F	Retorting Index, °F
Fischer assay	0.3107	932	918
	.2585	932	892
	.3472	932	934
	$\frac{1}{2}$ .2933	932	909
	.4338	932	969
Entrained solids, steam <sup>2/</sup>	1.8884	1,000	1,287
	2.3494	1,100	1,353
	3.8667	1,200	1,532
	5.5556	1,300	1,695
	6.6316	1,400	1,787
	9.6216	1,500	2,020
Entrained solids, steam + air <sup>2/</sup>	12.9153	1,650	2,252
	5.3243	1,085	1,674
	8.4408	1,205	1,932
	5.2889	1,230	1,670
	12.9937	1,295	2,258
Gas combustion <sup>3/</sup>	13.5381	1,315	2,294
	6-ton/day, Run 311-C	$\frac{4}{5}$ 1,400	1,273
	150-ton/day, Run 25-1	$\frac{5}{5}$ 1,310	1,206
	150-ton/day, Run 25-3	$\frac{5}{5}$ 1,625	1,004

<sup>1/</sup> Reference 5.

<sup>2/</sup> Reference 9.

<sup>3/</sup> Reference 7.

<sup>4/</sup> Maximum bed temperature.

<sup>5/</sup> Maximum distributor temperature.

#### Fischer Assay

Ethylene-ethane ratios are listed for five Fischer assay runs. Four were reported in intra-Bureau reports, and the fifth was reported by Goodfellow.<sup>5</sup> The Retorting Index for these data cluster around the 932° F point, which is the maximum temperature used in the assay. In Fischer assay the oil shale is heated at a relatively slow rate to the maximum temperature of 932° F. Variation in heating rate could easily affect the Retorting Index.

#### Gas Combustion

Results from three gas-combustion retort runs<sup>7</sup> are reported. These data are for one run of the 6-ton-per-day retort and two runs of the 150-ton-per-day retort, and the reported temperatures

are for maximum bed temperature and maximum distributor temperature, respectively. Maximum distributor temperature is the highest combustion temperature in the retort and does not give an indication of the temperature of retorting any more than the maximum bed temperature does. Here the use of the calculated Retorting Index gives a meaningful value for a temperature of retorting. Reported yield data follow more closely with the Retorting Index than the maximum distributor or maximum bed temperature.

#### Entrained Solids

Retorting Indexes calculated from the data from the Bureau of Mines entrained-solids retort<sup>9</sup> deviates greatly from reported retorting temperatures. In fact, it is possible to calculate two new regression equations that have essentially the same slope as Equation 1, but different intercepts. One equation would be for the steam only entrainment, and the other for steam plus air entrainment. The fact that the entrained-solids retort data give regression equations with essentially the same slope as was obtained from the laboratory data indicates that the same kinetic mechanism producing ethylene and ethane is applicable. The steam-entrainment data show a higher ethylene-ethane ratio and therefore a higher Retorting Index because of the effect of residence time in the retort. The retort products in this retort have to pass through about 35 feet of heated retort, which would give the products a residence time of several seconds. This is considerably longer than the contact time found in most other types of retorting. At 1,000° F, for example, the residence time in the entrained-solids retort is about 2.5 to 3 seconds as compared to less than 0.5 seconds estimated for the bench retort. Severe cracking of the retorted products takes place in the entrained-solids retort producing final products that appear to have been made at a higher temperature, hence a higher Retorting Index. This argument is also borne out by the increased aromaticity of the oil produced in the entrained-solids retort. The steam plus air retorting data show even higher Retorting Index than the steam-entrained data because of the added heat from the exothermic, oxidation reactions.

#### 10-Ton Aboveground Retort

Two retorting runs of the 10-ton aboveground retort<sup>2-4</sup> provided the necessary data (unpublished) to allow the calculation of Retorting Indexes. Temperatures of the shale bed were measured every 5 hours with thermocouples placed at about 18-in intervals in bed depth. Gas analyses were performed at the same time. Retorting run 28 had an average maximum bed temperature of 1,020.9° F and an average Retorting Index of 1,070.9° F. This run suffered from extreme channeling resulting in a retorting rate of 2.28 ft/day. In this retorting run the calculated Retorting Index follows quite closely the maximum bed temperature. Retorting run 29 had no channeling, and its retorting rate was 1.59 ft/day so that the shale bed could soak and obtain a higher temperature. For this run the Retorting Index is lower than the maximum bed temperature. The average Retorting Index was 964.7° F, and the average maximum bed temperature was 1,180.3° F.

#### SUMMARY

A method of calculating a Retorting Index for oil-shale retorting has been presented. The method utilizes the relative amounts of ethylene and ethane in the retort gas and allows the determination of the Retorting Index or effective retorting temperature to  $\pm 25^\circ$  F. Calculation of the Retorting Index is possible for aboveground and in situ retorting. Factors such as particle size, rate of heating, and oil-shale assay have no apparent effect on the Retorting Index. Because of the kinetics involved, such things as retort product residence time and cracking are reflected in the Retorting Index. Thus, the Retorting Index will be more nearly associated with retort-product composition than such things as maximum temperature of the oil-shale bed.

## ACKNOWLEDGMENTS

The work upon which this report is based was done under a cooperative agreement between the Bureau of Mines, U.S. Department of the Interior, and the University of Wyoming.

Reference to specific trade names or manufacturers does not imply endorsement by the Bureau of Mines.

## REFERENCES

1. Allred, V. D., *Chem. Eng. Prog.*, 62, 55 (1966).
2. Carpenter, H. C., and Sohns, H. W., *Colo. School of Mines Quarterly*, 63, 71 (1968).
3. Carpenter, H. C., Tihen, S. S., and Sohns, H. W., *PREPRINTS, Div. of Petrol. Chem., ACS*, 13, No. 2, F50 (1968).
4. Dockter, L., Long, A., Jr., and Harak, A. E., *PREPRINTS, Div. Fuel Chem., ACS*, 15, No. 1, 2 (1971).
5. Goodfellow, L., Haberman, C. E., and Atwood, M. T., *PREPRINTS, Div. of Petrol. Chem., ACS*, 13, No. 2, F86 (1968).
6. Hubbard, A. B., and Robinson, W. E., *BuMines Rept. of Inv.* 4744 (1950).
7. Matzick, A., Dannenberg, R. O., Ruark, J. R., Phillips, J. E., Lankford, J. D., and Guthrie, B., *BuMines Bull* 635 (1966).
8. Messner, A. E., Rosie, D. M., and Argabright, P. A., *Anal. Chem.*, 31, 230 (1959).
9. Sohns, H. W., Jukkola, E. E., and Murphy, W.I.R., *BuMines Rept. of Inv.* 5522 (1959).
10. Stanfield, K. E., and Frost, I. C., *BuMines Rept. of Inv.* 4477 (1949).

THE OXIDATION OF A BITUMEN IN RELATION TO ITS  
RECOVERY FROM TAR SAND FORMATIONS

Speras E. Moschopedis and James G. Speight

Research Council of Alberta  
11315 - 87 Avenue  
Edmonton, Alberta, Canada  
T6G 2C2

The bitumen present in the Athabasca tar sand is a viscous material with a specific gravity of approximately 1.03, a viscosity at reservoir temperature, i.e., about 5° to 8°C, of several thousand centipoises and is generally located under an overburden ranging in thickness from a few feet to 200 or more feet in depth. The bitumen itself does not generally command a very high price and its separation and recovery must involve a minimum of expenditure in order to be economically attractive for commercial practice. If conventional mining forms one of the primary steps in the process for recovering bitumen from the sand, it is desirable to find locations where the overburden is light, i.e., up to 80 feet, and where the bituminous sand is relatively thick, i.e., about 150 feet. In regions where the overburden is in excess of 150 feet, the conventional strip mining method is impractical, and in situ methods have to be developed to reduce the costs.

Various methods have been attempted and proposed for the in situ extraction and recovery of oil and bitumen from formations such as the Athabasca tar sand but the majority have been found to be either ineffective in actual field operations or require the use of significant amounts of relatively expensive chemicals. Therefore, an in situ recovery method using inexpensive chemicals and simple chemical reactions to modify asphaltenes and resins in the bitumen fractions which would in turn act as emulsifying agents, would be desirable. Previous investigations in this laboratory on the chemical modification of Athabasca asphaltenes, in particular the work dealing with water-soluble derivatives (1,2) and oxidation of the bitumen fractions (3) prompted an investigation into a process for in situ recovery of bitumen from the sand. The results of our previous investigation (3) presented briefly here for convenience and illustrated in the Figure, showed that some fractions of the bitumen are more susceptible to oxidation than others and it was believed that in situ oxidation of the bitumen per se and subsequent treatment with alkali solutions of sulfites and/or bisulfites would result in water-soluble sulfonated derivatives of these fractions which would then act as emulsifying agents for dispersion and emulsification of the remaining bitumen and hence aid in its transportation to a production well.

## EXPERIMENTAL

Oxidation of the bitumen with oxygen:

A weighed amount of dry bituminous material (ca. 50 ml) was placed in a 100-ml round bottomed flask, fitted with a reflux condenser, and heated in a metal bath. Oxygen was passed into the bitumen for varying periods of time after which the product was allowed to cool and shaken with 0.1 M aq. NaOH for 24 hr. The alkaline solution was acidified to pH 2.0 and extracted with methyl ethyl ketone; soluble products were recovered by evaporation of the solvent. The results are illustrated in the Figure.

### Oxidation of the bitumen on the sand:

(a) With oxygen and air

Athabasca tar sand (50 grams) was placed in each of four columns and oxidized at 4°C with oxygen and/or air (6 cu. ft./hr.) for 240 hours. The oxidized tar sand was then extracted at 4°C for 96 hours with aqueous solutions of sodium hydroxide and sodium sulfite and bitumen was recovered by acidulation and extraction of the resulting solutions with methyl ethyl ketone. The results are presented in Table 1.

(b) With ozone

A horizontal column, 112 cm long and 5 cm internal diameter, equipped with a cooling jacket, was packed with a weighed amount of Athabasca tar sand. Oxygen containing 6-9% by volume of ozone was passed through the column (0.45 cu. ft./hr.) and, after a specified time, air was injected to flush out excess ozone still present in the sand followed by circulation (~125 ml/hr.) of an eluant to produce a dark brown solution. After acidification with concentrated hydrochloric acid, the bitumen was recovered by extraction with methyl ethyl ketone (MEK) and the product isolated by evaporation of the solvent. The results are presented in Table 2 and the analyses in Table 3. In a further experiment, Athabasca tar sand was packed in a column, placed in a vertical position, and oxygen containing ~6% ozone was passed through the column at 4°C for 48 hours. After thorough blending, 50 grams of ozonized tar sand was placed in each of eight columns and treated at 4°C for 96 hours with water, aqueous sodium hydroxide, aqueous sodium sulfite, and aqueous sodium sulfite plus sodium hydroxide solutions. The bitumen from the resulting solutions was recovered by acidulation and extraction with methyl ethyl ketone, as described above; the results are presented in Table 4.

### RESULTS AND DISCUSSION

The results of our previous work (3), outlined here in the Figure, show that whilst oxidation of the bitumen components, by oxygen, is a feasibility, the temperatures required for conversion to significant amounts of soluble materials are quite high. Nevertheless, after 8 hr., the proportions of the fractions converted to soluble products at 125°C are equivalent to ca. 3% w/w of the original bitumen. However, prolonged oxidation may lead not only to water soluble organic acids but also to extensively degraded materials with low dispersing and/or emulsifying power. To avoid this, and to increase the water solubility, the bitumen was first oxidized at temperatures similar to those that exist in the formation (~4°C). Oxidation by oxygen and air at these temperatures is slow under these conditions (Table 1) but soluble materials were produced by subsequent treatment with aqueous alkaline solutions or aqueous alkaline sulfite solutions.

The successes achieved here prompted further investigations into the use of a somewhat stronger oxidant, i.e. ozone\*, in the hope that a more rapid reaction rate would be achieved for the purposes of the current work. Accordingly, treatment of the bitumen on the sand with ozonated oxygen followed by contact with alkaline sulfite solutions did in fact produce the desired effect (Table 2). Elemental compositions and molecular weights of the original Athabasca bitumen and the different reaction products (Table 3) illustrate the pronounced changes in carbon, hydrogen and oxygen concentrations, and also the relative increase of sulfur contents in the ozonized and subsequently sulfite-treated derivatives. Confirmation that reaction (sulfonation) of the oxidized bitumen and alkali sulfite had occurred was derived from several sources.

---

\* Redford (4) has reported that ozone has a pronounced effect on the bitumen and can be used to produce communication paths within a tar sand formation.

In the first instance, sulfur analyses have shown an overall increase of sulfur contents of ozonized and subsequently alkali sulfite-treated derivatives, as compared to the sulfur contents of derivatives obtained by treating ozonized tar sand with water or sodium hydroxide solution (Tables 3 and 4). Secondly, infrared spectra of the oxidized and extracted bituminous derivatives, besides exhibiting the carbon-hydrogen absorptions at frequencies of 2900 to 3000  $\text{cm}^{-1}$  and 1450 to 1580  $\text{cm}^{-1}$ , exhibited broad absorptions centered at about 3400  $\text{cm}^{-1}$  and 1700  $\text{cm}^{-1}$ , due to hydroxyl and carbonyl groups. However, an extra absorption of moderate intensity at 1030 to 1050  $\text{cm}^{-1}$  appeared only in the spectra of the sodium sulfite-treated derivatives - attributable to the presence of sulfonic group(s) characteristic of this type of sulfonated carbonaceous material, e.g., humic acids (5). Finally, nuclear magnetic resonance spectroscopy indicated significant differences between the two extracts. Alkaline-extracted material had an aliphatic proton distribution similar to that recorded previously for the resins and low molecular weight asphaltenes extracted from the Athabasca bitumen through use of organic solvents (6,7). Material produced by sodium sulfite extraction had a more complex and less well defined aliphatic proton distribution; also evident was a region centered at 9.35 ppm (0.65  $\tau$ ) and assigned to protons in acidic locations.

The data presented in Table 4 give an indication of the extractive ability of water and aqueous solutions of sodium hydroxide and sodium sulfite on oxidized tar sand, and the surface tension-reducing powers of these bituminous derivatives are illustrated in Table 5. It is apparent that the oxidized and subsequently sulfonated bituminous derivatives have greater surface tension-reducing powers and much greater ability to extract bitumen from the oxidized tar sand than does water or sodium hydroxide solution. We presume that the fractions prone to oxidation are the dark oils and resins (Figure) leaving the bulk of the bitumen relatively unchanged.

In retrospect, we have shown that oxidation of bitumen on Athabasca sand can occur by means of an oxygen-containing gas. Furthermore, sulfur-bearing group(s) can then be introduced into the molecular structures of the oxidized materials which renders the bituminous materials more hydrophilic, increases their surface tension-reducing power, and also increases their dispersing and emulsifying power. We are of the opinion that the present method therefore provides a plausible means for recovery of bitumen from the tar sand by the following steps: (a) *in situ* oxidation of the tar sand bitumen (e.g. by injecting an oxygen-containing gas into the tar sand formation); (b) injection of an aqueous alkaline sulfite or bisulfite solution into the oxidized tar sand formation to react and form the water-soluble sulfonated asphalt-type bituminous materials; (c) formation of an aqueous emulsion between the soluble sulfonated material and the oil in the tar sand formation; (d) circulation of the emulsion formed *in situ*, with the purpose of extracting oil from the formation, and separation of the oil from the emulsion by any of the known techniques.

It is presumed that the aqueous solution of the water-soluble sulphonated materials would circulate throughout the formation and establish free flow paths. We are also inclined to believe that this process, when combined with other recovery techniques, would afford an easier, more efficient and more economic recovery of bitumen and the oxidation, with subsequent sulfonation, is compatible with other *in situ* recovery techniques, e.g., steam injection, cold emulsification, low- or high-pressure injection of fluids.

#### ACKNOWLEDGEMENTS

The authors wish to thank Messrs. A. Adam and C. van der Merwe for their technical assistance, Messrs. M. Anderson and B. Verkoczy for recording the infrared and nuclear magnetic resonance spectra, Dr. D. Redford for helpful discussions, and Syncrude Canada Ltd. for gifts of tar sand and dry bitumen.

## REFERENCES

1. Moschopedis, S.E. and Speight, J.G. , Fuel, 1971, 50, 34
2. Moschopedis, S.E. and Speight, J.G. , Fuel, 1971, 50, 211
3. Moschopedis, S.E. and Speight, J.G. , Fuel, 1973, 52, 83
4. Redford, D.A. , private communication
5. Moschopedis, S.E. , Fuel, 1970, 49, 336
6. Speight, J.G. , Fuel, 1970, 49, 76
7. Speight, J.G. , Fuel, 1971, 50, 102

## Oxidative Degradation of Bitumen Fractions

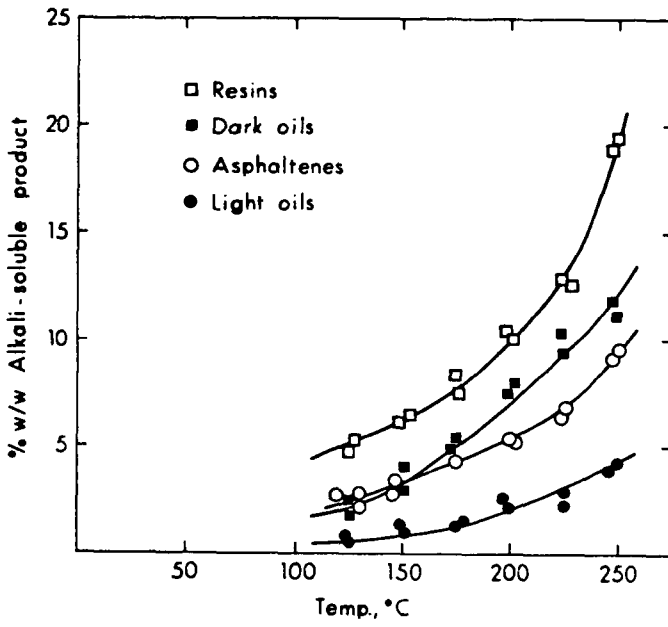


Table 1. Extractive abilities of aqueous solutions on oxidized tar sand

Column	Oxidizing agent	Eluant*	Solution pH	Weight of Extracted Bitumen (g)**	% Extracted Bitumen
1	oxygen	0.2% NaOH recycled	9.9	0.085	1.32
2	oxygen	Na <sub>2</sub> SO <sub>3</sub> (0.1M) + NaOH (0.2%) recycled	9.9	0.124	1.92
3	air	0.2% NaOH recycled	9.9	0.023	0.36
4	air	Na <sub>2</sub> SO <sub>3</sub> (0.1M) + NaOH (0.2%) recycled	9.9	0.122	1.89

\* Volume = 0.2 litre

\*\* Weight of bitumen in tar sand = 12.9%

Table 2. Ozonization of Athabasca tar sand

Method	Tar sand charged in g.	Bitumen in charge g.	Oxidation Temp. °C	Time hr.	Eluant	Circulation Temp. - Time	Solution pH (approx.)	Product Recovered g.	%	Surface tension <sup>1</sup> dynes/cm.
I	3190	412	6	48	0.05 M aq. Na <sub>2</sub> SO <sub>3</sub> /2 litre	5°C - 24 hr.	2	16.0	4	45.1
II	3530	455	25	48	{ 0.1 M aq. Na <sub>2</sub> SO <sub>3</sub> /1 litre 0.1 M aq. NaOH/1 litre	25°C - 96 hr.	2	24.8	5	46.5
						25°C - 24 hr.	9	18.5	4	45.1
III	3450	445	25	48	{ 0.15 M aq. NaOH/1 litre 0.1 M aq. Na <sub>2</sub> SO <sub>3</sub> /1 litre water/1.6 litre	a) 25°C - 72 hr.	12	45.2	10	
						b) 60°C - 24 hr.		7.2	2	
						c) 97°C - 5 hr.				
IV	3790	489	25	48	{ 0.2 M aq. NaOH/1 litre 0.2 M aq. Na <sub>2</sub> SO <sub>3</sub> /1 litre	a) 25°C - 5 hr.	12	12.5	3 <sup>a</sup>	
						b) 60°C - 48 hr.		63.0	13 <sup>a</sup>	48.0
						c) 97°C - 10 hr.				
V	3900	503	25	96	{ 0.2 M aq. Na <sub>2</sub> SO <sub>3</sub> /1 litre 0.2 M aq. NaOH/1 litre	25°C - 72 hr.	12	97.4	19	

<sup>1</sup> 0.1% solution in 0.1 N NaOH

<sup>a</sup> Toluene extract

<sup>b</sup> MEK extract

Table 3. Analysis of unozonized and ozonized-sulfonated bitumen from Athabasca tar sand

Sample Description	Carbon %	Hydrogen %	Oxygen* %	Sulfur %	Nitrogen %	Ash %	Molecular Weight	Remarks
Unozonized original bitumen	81.3	10.1	1.7	4.1	0.5	2.4	497	Toluene extract
Method I	63.2	7.4	24.4	3.8	0.3	0.8	321	Methyl ethyl ketone extract
Method II Step 1	55.7	6.4	27.9	4.8	0.2	1.7	311	Methyl ethyl ketone extract
Method II Step 2	62.7	7.5	19.1	6.0	0.3	2.6	395	Methyl ethyl ketone extract
Method III Step 1	55.6	6.4	27.7	5.4	0.2	2.7	-	Methyl ethyl ketone extract
Method IV	79.7	10.2	5.0	4.2	0.3	1.5	567	Toluene extract
Method IV	52.6	6.1	26.8	6.4	0.2	8.4	533	Methyl ethyl ketone extract
Method V	50.8	5.8	32.2	4.2	0.2	3.1	229	Methyl ethyl ketone extract
Ozonized depleted bitumen	81.1	10.1	2.2	4.0	0.5	2.0	504	Toluene extract

\* Oxygen contents were determined directly.

Table 4. Extractive abilities of aqueous solutions on oxidized tar sand

Column No.	Eluant*	Solution pH	Surface Min.	Tension Max.	Weight of Extracted Bitumen(g)**	% Extracted Bitumen	% Sulfur in Extracted Bitumen
1	H <sub>2</sub> O	5.5	64.3	68.8	0.168	2.61	0.97
2	H <sub>2</sub> O recycled	5.5	64.2	68.7	0.157	2.44	1.96
3	Na <sub>2</sub> SO <sub>3</sub> (0.1M) passed through	8.5	48.0	54.8	0.194	3.01	0.89
4	Na <sub>2</sub> SO <sub>3</sub> (0.1M) recycled	8.0	43.4	49.8	0.440	6.84	4.09
5	Na <sub>2</sub> SO <sub>3</sub> (0.1M) + NaOH (0.2%) passed through	-	41.2	50.4	0.610	9.48	6.7
6	Na <sub>2</sub> SO <sub>3</sub> (0.1M) + NaOH (0.2%) recycled	adjusted to 12-13.5	36.5	42.0	0.510	7.92	5.69
7	NaOH (0.2%) passed through	-	40.4	54.0	0.237	3.68	2.12
8	NaOH (0.2%) recycled	adjusted to 12-13	40.6	43.2	0.221	3.43	2.06

\* Volume: ≈2.2 litres; recycle = 0.2 litre

\*\* Weight of bitumen extracted by toluene from 50 g ozonized tar sand = 6.435 g

Table 5. Surface tensions of ozonized and ozonized-sulfonated bitumen

% Concentration	Ozonized bitumen	Ozonized-Sulfonated bitumen
0.1	62 dynes/cm	48 dynes/cm
0.5	62 dynes/cm	41 dynes/cm
1.0	52 dynes/cm	39 dynes/cm

SULFUR COMPOUNDS IN OILS FROM THE  
WESTERN CANADA TAR BELT

by

D.M. Clugston\*, A.E. George\*, D.S. Montgomery\*\*\*, G.T. Smiley\*\* and H. Sawatzky\*  
Fuels Research Centre, c/o 555 Booth Street, Ottawa, Canada K1A 0G1

## INTRODUCTION

In this work the sulfur compounds in the gas oil of three Cretaceous heavy oils from the edge of the Alberta sedimentary basin were investigated. These crude oils were obtained from the Athabasca, Cold Lake and Lloydminster deposits and are believed by some (1) to belong to the same oil system which implies like modes of origin. The geographic location of these deposits are shown in Figure 1. This investigation was conducted to develop the analytical capability of following the maturation of the sulfur compounds present in these oils and to permit a comparison with those in the thermally mature Medicine River oil in a reservoir of the same geological age (2).

---

\*Research Scientists, \*\*Technologist, \*\*\*Head, Fuels Research Centre, Mines Branch, Department of Energy, Mines and Resources, Ottawa, Canada.

## EXPERIMENTAL

Samples

The Athabasca bituminous sand was obtained from Great Canadian Oil Sands Ltd. and was extracted first with pentane and then with benzene. The Lloydminster oil had been taken from the "Sparky" formation at a depth of 1890 ft. and was supplied through the courtesy of Husky Oil Ltd. The Cold Lake bitumen was obtained from Imperial Oil Ltd. and had been produced by steam injection. Its depth was about 1500 ft. The Medicine River oil was produced at a depth of 7325 ft. and was donated by the Hudson Bay Oil and Gas Co. Ltd.

Molecular Distillation

The pentane extract from the Athabasca sands and the other oils without any treatment were distilled in an Arthur F Smith molecular still at pressure ranges of 75-250 $\mu$  and temperatures of 225-230°C. The light ends were obtained in the cold trap between the still and the vacuum pump.

Chromatographic Separations

The distillates from the oils were separated first by liquid chromatography, then by gas chromatographic simulated distillation according to boiling point and finally by gas chromatography on lithium chloride-coated silica, as shown in the schematic diagram.

Liquid Chromatography

The distillates were separated on a dual-packed (silica gel-alumina gel) chromatographic column according to the procedure developed by the U.S. Bureau of Mines in conjunction with API project 60 (3). The oil fractions were obtained by collecting 200 ml fractions of the eluent and evaporating the solvents by warming and using streams of nitrogen. Various fractions of

saturated, mononuclear aromatic, binuclear aromatic, polynuclear aromatic hydrocarbons and polar materials were obtained.

#### Gas Chromatographic Simulated Distillation

The fractions from the liquid chromatography were gas chromatographed according to boiling point using normal alkanes as reference compounds on non polar silicone rubber (SE-30) columns packed in 5 ft. long U-shaped glass columns of 1/4" O.D. The column effluent was split between a flame ionization detector and a trapping out assembly in a ratio of 1:9. Each collecting tube contained 10mg of chromosorb W. The helium carrier gas had a flow rate of 175 ml/min. Sulfur chromatograms were obtained with a Dohrmann microcoulometric quantitative detector which was also used for determining total sulfur contents of the samples. The carrier gas flow rate was 75 ml/min when the coulometric detector was used.

#### Gas-Solid Chromatography and Mass Spectroscopy

The cuts trapped out from the simulated distillations were rechromatographed on lithium chloride-coated silica columns as described in a previous publication (4). The column effluent was split with a portion directed to a flame ionization detector and the other to the mass spectrometer in a ratio of 1:4. This chromatographic step greatly facilitated the interpretation of the mass spectra. In many cases it appeared as though pure compounds were obtained. Only some of these gas-solid chromatograms will be discussed.

The mass spectrometer was a CEC 21-104 equipped with a Watson-Biemann type G.C. interface. The source was maintained at 250°C. An ionization potential of 70 eV was used throughout with a trap current of approximately 80  $\mu$ amp. The spectra were scanned electrically.

## RESULTS AND DISCUSSIONS

Table 1 shows the molecular distillation yields and distribution of the total sulfur contents of the first distillate in the four oils.

TABLE 1  
DISTILLATE YIELDS AND THEIR SULFUR CONTENTS  
IN THE OILS OF ALBERTA TAR BELT

	<u>Athabasca</u>	<u>Cold Lake</u>	<u>Lloydminster</u>	<u>Medicine River</u>
Light ends, wt.%	4.5	5.9	12.5	44.8
First Distillate, wt.%	37.5	31.0	36.0	43.5
Sulfur content, wt.%	2.90	2.85	2.50	0.80

The liquid chromatograms of the four gas oils are shown in Figure 2. The sulfur content of some of the fractions is also shown. The proportions of the hydrocarbon types of the oils are shown in Table 2.

TABLE 2  
HYDROCARBON TYPE DISTRIBUTION

	<u>Athabasca</u>	<u>Cold Lake</u>	<u>Lloydminster</u>	<u>Medicine River</u>
Saturates, wt.%	37.1	42.6	50.7	69.6
Monoaromatics, wt.%	21.3	22.9	22.7	13.0
Biaromatics, wt.%	15.8	14.1	13.1	7.1
Polyaromatics, wt.%	25.6	20.5	13.6	10.3

It can be seen that there is an increasing trend in the amount of saturates in the sequence Athabasca, Cold Lake, Lloydminster and Medicine River. This trend is reversed for the biaromatic and especially for the polyaromatic-polar fraction.

The saturated hydrocarbon fractions contain traces of sulfur. The gas-solid chromatography of the Lloydminster saturates boiling in the range of the C<sub>25</sub> normal alkane, with the use of a Melpar dual detector, showed the sulfur compounds to be retained much longer than the hydrocarbons which is typical for alkyl sulfides.

There was a small amount of sulfur in the mononuclear aromatic hydrocarbon fractions, which did not show any appreciable resolution on the microcoulometric trace obtained during simulated distillation. According to the U.S. Bureau of Mines report (3) describing this type separation, thiophenes and cyclic sulfides could be expected in this fraction.

Sulfur compounds in the largest binuclear aromatic fractions as well as in the largest polynuclear aromatic hydrocarbon and polar material fractions have been investigated. Also the fractions with high sulfur content in the region between the largest mono- and binuclear aromatic fractions, and between the largest binuclear and polynuclear aromatic fractions designated by the letters "A" and "B" respectively on the liquid chromatograms were investigated. The polyaromatic fraction "C" was also analyzed, Figure 2.

In Figures 3 and 4 of the fractions in region "A" the microcoulometric sulfur peaks are well resolved and appear at regular intervals as would be expected for a homologous series of compounds. Most of the sulfur peaks have matching flame ionization peaks. These chromatograms of the fractions from region "A" of both Athabasca and Lloydminster oils are so similar that only one of these fractions has been further studied by mass spectroscopy. Since the fraction from region "A" of Lloydminster oil has more material in the lower molecular weight range it was selected for more detailed study.

The material represented by the first four peaks in the flame ionization trace which have matching sulfur peaks #1 to 4 were trapped out and rechromatographed on the lithium chloride-coated silica. The resolved material was studied by mass spectroscopy. Only the data thought to be related to the sulfur compounds will be discussed. The chromatograms of the first three of these trapped out cuts with both the flame ionization and Melpar sulfur

traces are shown in Figures 5, 6 and 7. Although the Melpar sulfur trace is not quantitative, whenever matching predominant peaks were obtained on both the flame ionization and the sulfur traces they were considered to represent substantial sulfur-containing material.

The mass spectrum obtained from the material eluting at 153° in Figure 5 contained a molecular ion of  $m/e$  190 and intense fragment ions with  $m/e$  175 and 147, corresponding to a 4-carbon substituted benzothiophene. Spectra taken at higher temperatures in the chromatogram also contained these same ions but in different relative intensities. High relative intensity of the molecular ion and M-15 ion is taken to mean that the side chains on the aromatic nucleus are short - probably methyl - while low relative intensity of M & M-15 relative to the ion corresponding to the aromatic nucleus plus one methylene group is an indication of fewer and longer side chains.

The material eluting at 162° (Figure 6) produced ions at  $m/e$  204, 189 and 147 corresponding to a 5-carbon substituted benzothiophene. As before, the early eluting material appeared to have one long side chain while later in the chromatogram material having more and somewhat shorter side chains appeared. This trend appeared in all chromatograms.

The presence of molecular ions of  $m/e$  202 and 206 in some of these spectra may indicate the presence of cycloalkyl benzothiophenes and thiaindanes respectively.

In subsequent cuts from Lloydminster fraction "A" it appeared that benzothiophenes with six for cut #3 and seven alkyl carbon atoms for cut #4 were involved. On the basis of the trend that appears, it is assumed that each successive sulfur peak, obtained during simulated distillation as shown in Figures 3 and 4, represents benzothiophene with an additional alkyl carbon atom. Thus dominant benzothiophene peaks are obtained with as many as eleven substituting carbon atoms in peak #8 and then the amounts of sulfur compounds involved in these chromatograms decrease markedly which is not the case for the accompanying hydrocarbons, as shown by the flame ionization trace. High resolution mass spectral data appears to support the assumption that these compounds are benzothiophenes (5).

The microcoulometric sulfur chromatograms that were obtained during simulated distillation of the largest biaromatic fractions of the four oils are shown in Figures 8 to 11. The dominant peaks are well resolved and appear at regular intervals similar to those from a homologous series of compounds. In the case of the Athabasca fraction which had a high sulfur content the sulfur peaks had matching flame ionization peaks. It seems that the same sulfur compounds appear in all corresponding fractions of the four oils.

The sulfur compounds appear to be alkyl benzothiophenes. The mass spectra of these benzothiophenes showed very prominent molecular ions and quite limited fragmentation as though most of the alkyl groups are methyls. This is in contrast to the benzothiophenes with longer alkyl groups found in the small fractions with high sulfur content that were obtained earlier during the liquid chromatography. It would be expected that the benzothiophenes with shorter but more alkyl groups would be retained longer on the electrophilic adsorbents than those with longer but fewer electron donating groups. The fact that most of the alkyl substituents on the benzothiophenes in the largest biaromatic fraction are methyls accounts for the limited number of dominant isomers that appear to be present in these fractions as is shown by the well resolved peaks.

The chromatogram in Figure 8 of the largest biaromatic fraction from the Athabasca oil shows three dominant well resolved peaks numbered 1, 2 and 3 which appear to represent benzothiophenes with five, six and seven methylene groups. With increasing molecular weight the amounts of sulfur compounds decrease and the resolution becomes poorer as would be expected when larger substituting alkyl groups are present causing increase in the number of possible isomers.

The chromatogram from the corresponding Lloydminster fraction, Figure 9, was similar to that from the Athabasca but appears to contain considerably more lower molecular weight benzothiophenes, particularly those ones with four methylene groups represented by peak #2. The Cold Lake fraction, Figure 10, is not very well resolved but also shows peaks that match those from the other oils.

The chromatogram of the corresponding fraction from the Medicine River oil, in Figure 11, shows the best resolved peaks which appear to be the same benzothiophenes present in the other oils. This is believed to be a thermally mature oil and it is therefore expected that the alkyl side chains would be reduced to methyl residues. The alkyl naphthalenes that accompanied the benzothiophenes also appeared to possess mostly methyl substitution.

Before leaving the sulfur compounds in the biaromatic fraction it should be mentioned that only the material with well resolved sulfur peaks was examined by mass spectra. Possibly in the less resolved higher molecular weight materials other sulfur compounds besides benzothiophenes might be present.

The small fractions with high sulfur content that were obtained in the range "B" of the liquid chromatograms also gave sulfur gas chromatograms with fairly well resolved peaks in the sulfur traces of the simulated distillation. Most of the peaks had matching ones in the flame ionization trace, Figure 12. All the high sulfur content fractions in this range "B" of the four oils gave similar chromatograms. The material represented at the beginning of the chromatogram is not very well resolved. The first recognizable peak #1 appears to be due to dibenzothiophenes with mainly two methylene groups. The  $m/e$  ratio was 212 and the only fragment ion was at  $m/e$  197 which is the lowest mass fragment found in this series and is assumed to represent the aromatic nucleus, plus one alkyl carbon atom, of the dibenzothiophenes. Then there is a small peak #2 where dibenzothiophenes with three methylene groups appear to be present. Peak #3 appears to be due to mixtures of dibenzothiophenes with three and four methylene groups. In most cases the fragment ions were more abundant than the parent ions indicating that the compounds had alkyl groups larger than methyl. It would seem that the situation is similar to that of the benzothiophenes in which the material with longer chains was eluted in the liquid chromatography before the material that contains more but shorter side chains.

In this fraction mass spectra were not obtained for material of molecular weight higher than the dibenzothiophenes with four methylene groups. It is inferred that the two most prominent peaks, #5 and #6, can be ascribed to dibenzothiophene with six and seven methylene groups. With increasing molecular weight the peaks become less prominent and the amount of sulfur compounds decreases. As can be seen this is quite different from the hydrocarbons that accompany these sulfur compounds.

The first polyaromatic-polar fraction from the Athabasca oil was similar to the largest fraction in this class from the Lloydminster oil. All the simulated distillation chromatograms of the first polyaromatic-polar fractions in the "C" region of the liquid chromatograms are shown in the Figures 13 to 16. As can be seen, sulfur peaks from the three oils are fairly well resolved at least in the lower molecular weight region. It seems that the initial portion of the Athabasca chromatogram, up to Kovats Index of 2400, is due mostly to sulfur compounds. The main sulfur compounds appear to be dibenzothiophenes with three and four methylene groups which are represented by the two very predominant peaks, #2 and #3. These dibenzothiophenes constitute the major portion of the sulfur compounds in this fraction. Some dibenzothiophenes with two, five and six methylene groups represented by peaks #1, #2 and #5 respectively also appear in much smaller quantities.

The predominant sulfur peaks in the Lloydminster and Cold Lake fractions appear to be the same as in the Athabasca but there is more of the unresolved higher molecular weight material than in the Athabasca. In contrast the Medicine River fraction was quite different from the corresponding ones in the heavy oils, Figure 16.

The chromatogram of the largest polyaromatic and polar fraction from the Athabasca gas oil can be seen in Figure 17. This fraction has a sulfur content of more than 7.7% within the distillation range up to a boiling point of 500°C. Assuming the presence of one sulfur atom per molecule then about half the fraction would consist of sulfur compounds. Some of the ill-defined sulfur peaks appear, together with matching flame ionization peaks, at intervals in the boiling point suggesting a difference of a methylene group.

According to the mass spectra alkyl substituted dibenzothiophenes or possibly naphthothiophenes seem to be quite prominent in this fraction with the substitution ranging from two to eight methylene groups. It would seem unlikely that most of the alkyl groups would be larger than methyl so the poor resolution of sulfur compounds probably is due to other types of sulfur compounds in addition to dibenzothiophenes. Both dibenzothiophenes and their isomeric naphthothiophenes could also be present.

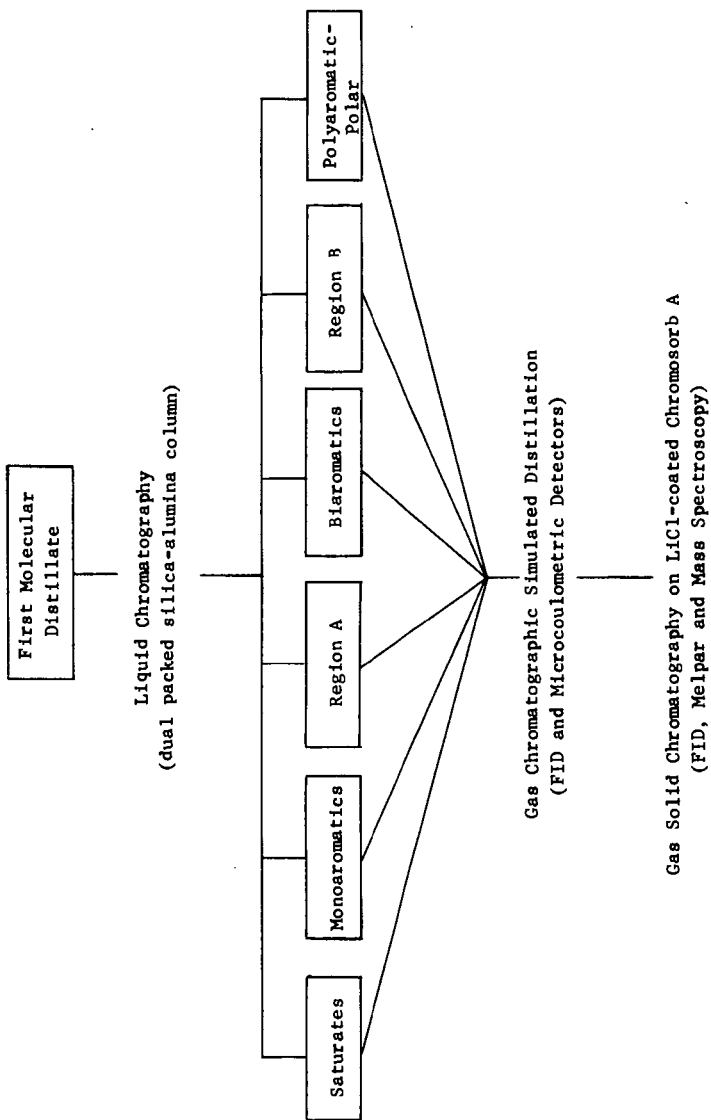
In the mass spectra there were abundant ions that might be due to naphthobenzothiophenes or phenylbenzothiophenes. The presence of small amounts of alkyl diphenylsulfides is also possible.

#### ACKNOWLEDGEMENT

We are grateful to the Husky Oil Co. Ltd. for a sample of Lloydminster oil and to the Hudson Bay Oil and Gas Co. Ltd. for a sample of Medicine River oil. We wish to thank Messrs. T.M. Potter and R.M. Evis for technical assistance.

## REFERENCES

1. Vigrass, Laurence W., Am. Assoc. Petroleum Geologists, Bull. 52, 1984 (1968).
2. Montgomery, D.S., Clugston, D.M., George, A.E., Smiley, G.T. and Sawatzky, H., pending publication Can. Soc. Petroleum Geologists Bull. 1974.
3. Hirsh, D.E., Hopkins, R.L., Coleman, H.J., Cotton, F.O., and Thompson, C.J., American Chemical Society Petroleum Preprints 17, A65 (1972).
4. Sawatzky, H., George, A.E., and Smiley, G.T., American Chemical Society Petroleum Preprints 18, 99 (1973).
5. Sawatzky, H., Smiley, G.T., George, A.E. and Clugston, D.M., American Chemical Society Fuels Preprints 15, 83 (1971).



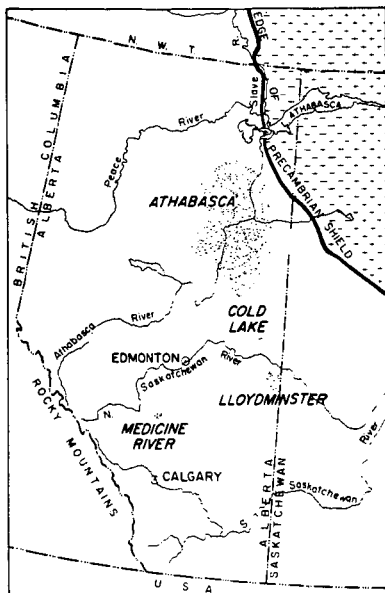
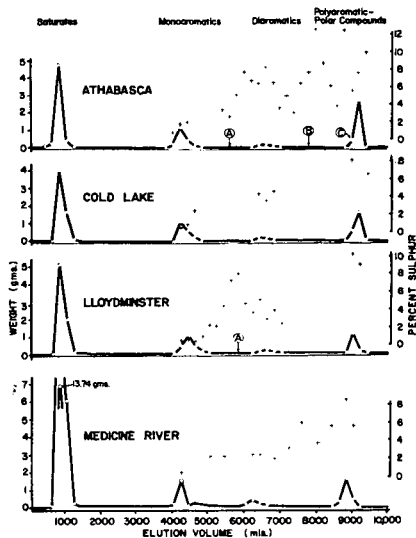
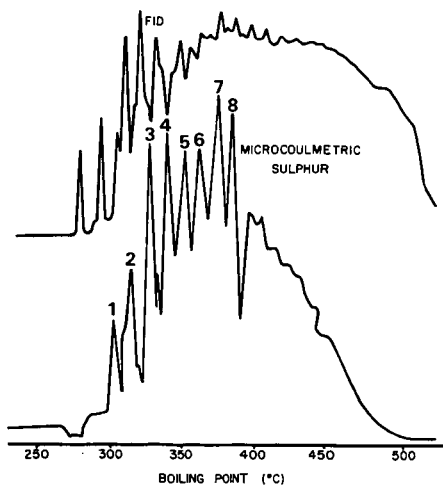


Figure 1



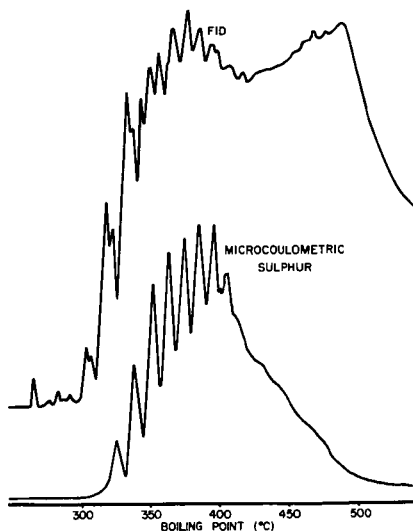
LIQUID-SOLID CHROMATOGRAPHIC SEPARATIONS

Figure 2



LLOYDMINSTER FRACTION A  
SE-30 ON CHROMOSORB W

Figure 3



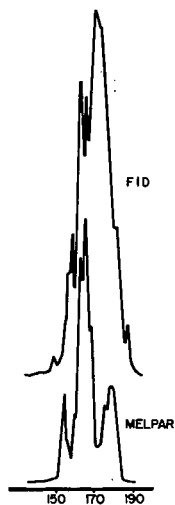
ATHABASCA FRACTION A  
SE-30 ON CHROMOSORB W

Figure 4



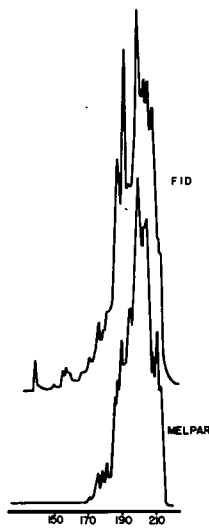
COLUMN TEMPERATURE (°C)  
LLOYDMINSTER FRACTION A  
BOILING RANGE: 275-296 °C  
LiCl ON CHROMOSORB A

Figure 5



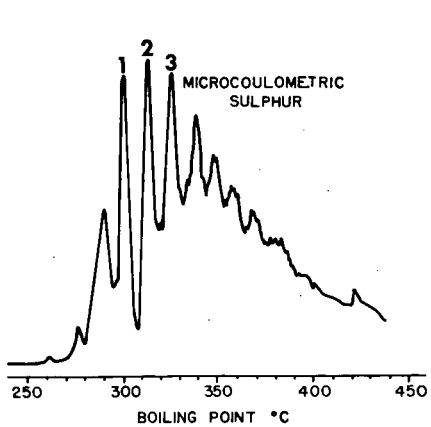
COLUMN TEMPERATURE (°C)  
LLOYDMINSTER FRACTION A  
BOILING RANGE: 296-309 °C  
LiCl ON CHROMOSORB A

Figure 6

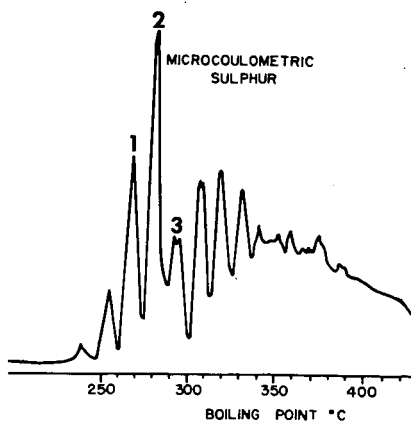


COLUMN TEMPERATURE (°C)  
LLOYDMINSTER FRACTION A  
BOILING RANGE: 309-320 °C  
LiCl ON CHROMOSORB A

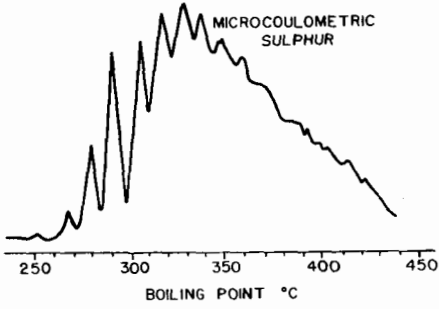
Figure 7



MICROCOULOMETRIC  
SULPHUR  
ATHABASCA BIAROMATICS FRACTION  
SE-30 ON CHROMOSORB W  
Figure 8

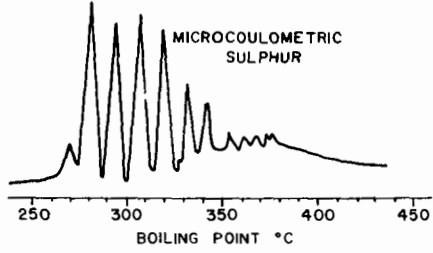


MICROCOULOMETRIC  
SULPHUR  
LLOYDMINSTER BIAROMATICS FRACTION  
SE-30 ON CHROMOSORB W  
Figure 9



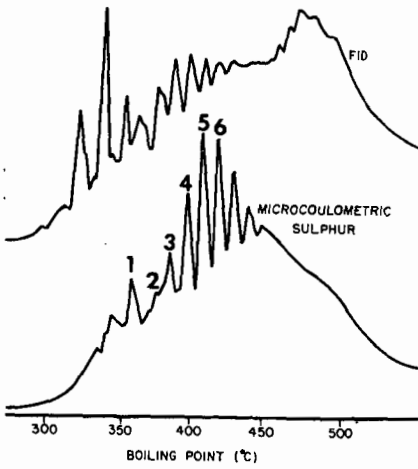
COLD LAKE BIAROMATICS FRACTION  
SE-30 ON CHROMOSORB W

Figure 10



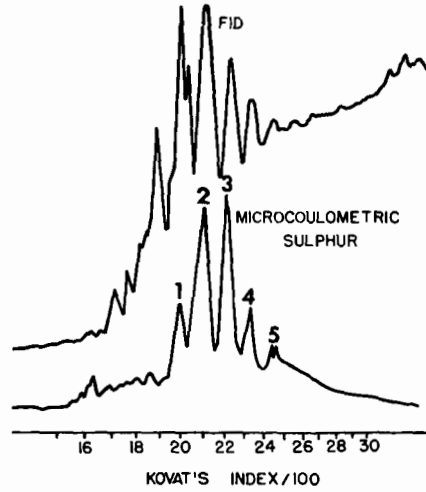
MEDICINE RIVER BIAROMATICS FRACTION  
SE-30 ON CHROMOSORB W

Figure 11



ATHABASCA FRACTION B  
SE-30 ON CHROMOSORB W

Figure 12



ATHABASCA FRACTION C  
SE-30 ON CHROMOSORB W

Figure 13

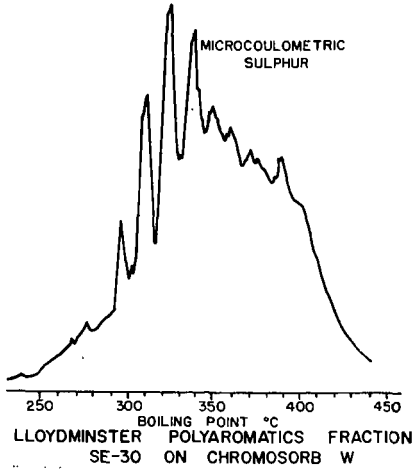


Figure 14

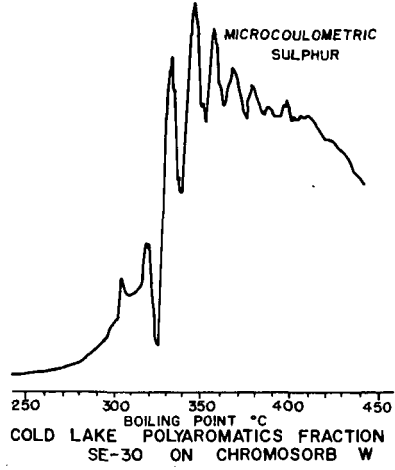


Figure 15

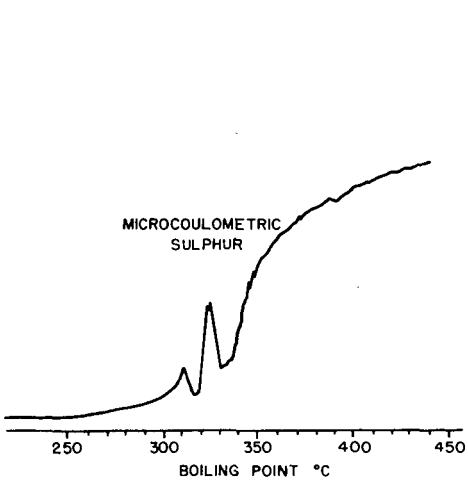


Figure 16

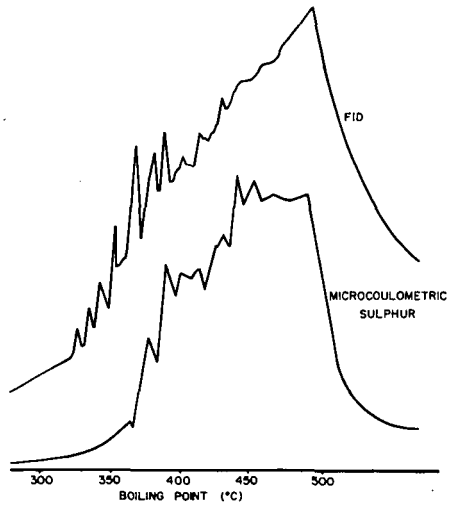


Figure 17

## DEVELOPMENT OF A BIOCHEMICAL DESULFURIZATION PROCEDURE FOR FUELS

A. J. Davis and T. F. Yen  
Departments of Biological Sciences and Chemical Engineering  
University of Southern California, University Park  
Los Angeles, California 90007

## INTRODUCTION

The removal of sulfur from high-sulfur containing petroleum has long presented a problem. With the depletion of so-called "sweet" oil (i.e., oil low in sulfur content), the problem has escalated into major proportions to contend with a clean and livable environment of our biosphere. The development of practical methods of decreasing, or eliminating the sulfur content of petroleum has repeatedly proved an economical obstacle to the industry. The amount of dollars spent on corrosion technology alone is phenomenal (1).

Rudimentary investigations of microbial desulfurization have received little attention in the literature at this time (2). A successful example is the removal of pyrite from coal by *Thiobacillus* sp. and *Ferrobacillus* sp. (3). While studies of the complex hydrocarbon-sulfur systems, being closer to in situ reality are of great value, investigations of pure systems should form the foundations of these more detailed investigations.

Our present study was intended to explore the ability of a micro-organism as a possible desulfurizing agent. To this end, a pure system was employed that would give us some idea as to the ease with which such an agent could abstract organically-bound sulfur. While this program is preliminary in scope, it is hoped that future investigations may lead to a feasible industrial application.

## MATERIALS AND METHODS

a) Media and Culture

The strain of *Thiobacillus thiooxidans* used in these experiments was originally obtained from the National Type Cultures Collection. Inoculate strain was obtained by further culture in this laboratory (4). For growth of the organisms, a variation of Waksman's medium was prepared; it contained the following concentrations of salt in grams per liter (all Mallinckrodt "AR" grade):  $(\text{NH}_4)_2\text{SO}_4$ , 0.20;  $\text{KH}_2\text{PO}_4$ , 3.00;  $\text{MgSO}_4 \cdot 7\text{H}_2\text{O}$ , 0.50;  $\text{CaCl}_2 \cdot 2\text{H}_2\text{O}$ , 0.25. The medium was prepared with distilled water. In place of the elemental sulfur substrate of Waksman's medium, different symmetric organic sulfides of the tertiary butyl class with a normalized sulfur equivalent of 10.0g/liter were utilized. In order to provide a greater surface area, the normally viscous sulfides were emulsified with 1-2 drop(s) of Triton X-100 surfactant (J. T. Baker Chemical Co.) added to the medium. The pH was then adjusted to 3.5 with 1.0 M  $\text{H}_3\text{PO}_4$  (Mallinckrodt "AR" grade). Sterilization of the media was accomplished by autoclaving and by membrane filtration.

b) Sulfide Samples

The tertiary butyl sulfide and the tertiary butyl disulfide used in these experiments were obtained from the Aldrich Chemical Company. The purity of the monosulfide, molecular weight: 146.30, was in excess of 97%. The disulfide, molecular weight: 178.36, being "technical" grade was assayed to be 88% pure disulfide with the remainder consisting of tertiary butyl trisulfide.

The tertiary butyl polysulfide employed was kindly supplied by Phillips Petroleum Company. The purity of the polysulfide whose molecular weight averaged out to be 190.00 was greater than 90%. The polysulfide contained an average of four and five sulfur atoms per molecule. No pre-treatment of the sulfides was performed.

### c) Analytical Methods

Insoluble barium sulfate precipitate, one of the two criteria by which growth of the bacteria was established was determined by standard gravimetric methods. The amount of barium sulfate is directly proportional to the amount of sulfide that has been oxidized by the sulfur bacteria.

Hydrogen ion concentration (pH) was the second criterion by which growth of the bacilli was established. Sulfuric acid is a natural metabolic by-product of the acidophilic *Thiobacillus thiooxidans* (5); and as sulfur is utilized, acid build-up in the medium is to be expected---thus lowering the pH. Studies done in this laboratory has shown that the bacteria grow well in a pH as low as 0.5.

Fernbach culture flasks (Pyrex, 2800 ml) containing 1.0 liter of modified Waksman's medium were prepared in duplicate. The first pair of flasks received 49.0 ml t-butylsulfide and one drop Triton X-100 each. The second pair of flasks received 28.0 ml t-butyl disulfide and one drop of Triton X-100 each. The third pair of flasks received 17.0 ml t-butyl-polysulfide and two drops of Triton X-100 each. In addition, flasks of elemental sulfur and flasks of organic sulfur substrates were prepared to act as controls. After sterilization, all flasks containing sulfur or organic sulfur compounds with the exception of the organic sulfur control flasks, were inoculated with 10.0 cc *T. thiooxidans* suspensions. All flasks were incubated at room temperature.

Samples for the barium sulfate determinations were prepared by removing a 5.0 ml aliquot portion from each flask and then submitting these to centrifugation on an Adams centrifuge for 15 minutes at 3,000 rpm. To the supernatant of each was added two drops concentrated HCl, an acid buffer; and eleven drops of a saturated solution of barium chloride (Mallinckrodt "AR" grade). The precipitated was filtered on a "Millipore" apparatus (Pyrex); washed with distilled water and then allowed to dry three days in an evacuated dessicator. The samples were then ignited and the weight of barium sulfate established. The organic sulfur controls were handled in the same manner to avoid discrepancy. The amount of barium sulfate produced from the organic sulfides less the controls was averaged and then plotted (Fig. 1). The pH was read directly with a Beckman "Zeromatic," SS-3 pH meter (Fig. 2).

### PROCEDURE

Modified Waksman's medium was prepared in a Fernbach culture flask. An amount of organic sulfide normalized to an equivalent sulfur content of the standard medium (10g/liter) was added; followed by the addition of an emulsifier. The medium was then autoclaved for 30 minutes at 15 psi (121°C) or subjected to membrane filtration. Upon cooling, the medium was inoculated with 10 cc pure strain *Thiobacillus thiooxidans*. The culture's initial pH value was read, and an initial gravimetric sulfate assay was performed on it. Thereafter, pH and sulfate values were determined at two day intervals for a period of 25 days.

The model was so designed as to study the ability of sulfur-oxidizing bacteria to utilize the organically bound sulfur as substrate. The symmetry of the sulfides provided an insight into the sulfur abstracting process of *T. thiooxidans*.

It can be seen that the oxidizing potential of the organism is enhanced by the availability of unshielded sulfur in the molecular structure. The sulfur-sulfur bonds of the di- and poly-sulfides are easily disrupted while the sulfur-carbon bond of the mono-sulfide seems questionable. While some sulfate ion is produced by the organism on the monosulfide, it is unknown at this point how much of the sulfate is due to residual sulfur previously incorporated by the bacteria. The values of pH seem to bear this out. There is no question that the organism is growing on the di- and poly-sulfides, as shown by sulfate ion and pH values.

DISCUSSION

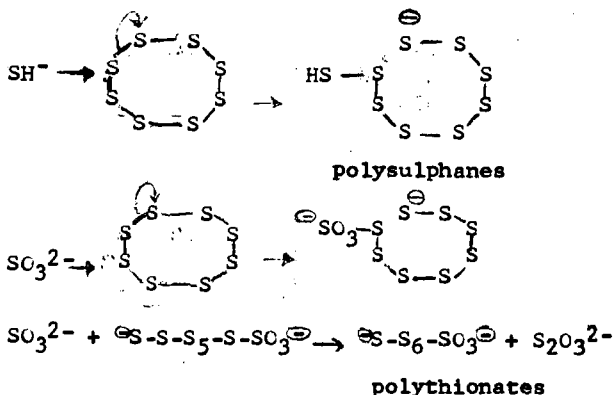
This study indicates that the sulfur of our sulfide samples was susceptible to bacterial attack in two of the three cases. The aliphatic sulfides could be ranked in the order of their ease of oxidation as: di-*n*-butyl polysulfide > di-*n*-butyl disulfide > di-*n*-butyl sulfide.

Seemingly, *T. thiooxidans* is able to attack the sulfur-sulfur bond quite readily and the sulfur-carbon bond with more time and difficulty. Since a large portion of the sulfur compounds in petroleum are of the monosulfide-aromatic type more attention will be paid to this facet.

The simplest scheme of the bacterial oxidation would be:



A few mechanisms have been postulated for this reaction (6). No matter what mechanism is considered, the oxidation of elemental sulfur or thio-sulfate is accompanied by reductive cleavage of the sulfur-sulfur bridges. In the case of sulfur, the intermediate involved is a cyclic form of sulfur, probably S<sub>8</sub>; although there is little difference observed for different allotropic forms of sulfur, such as rhombic, precipitated, and amorphous. These cyclic sulfides form the basis of polysulphanes as well as polythionates which could be metabolized readily by Thiobacilli.

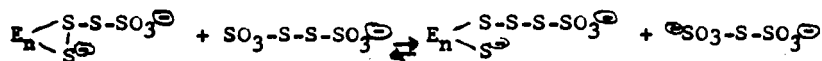
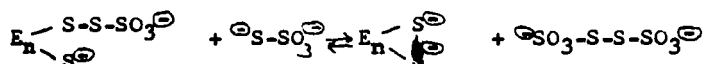
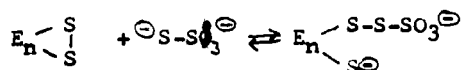


Actually, oxidation of sulfur begins with its reduction, in which the glutathione-sulhydryl groups located near the cell surface take part

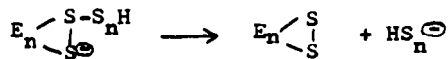
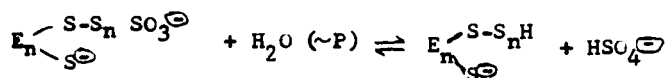


The  $\text{SH}^{\ominus}$  involved or the  $\text{SO}_3^{2-}$  performs the attack and the cleavage.

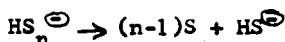
For the thiosulfate oxidation, it is hypothesized that an enzyme system on the cell surface initiates the formation of polythiosulfonic acid and consequently splits the terminal  $\text{SO}_3^-$  as sulfate. This process may evolve the intermediate of mixed anhydride  $-\text{S-O-PO}_4^-$  from phosphorylation:



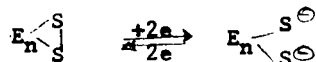
Therefore



polysulfanes



The overall reaction is one of electron transfer in the enzyme system:



The critical step in the utilization of multiple sulfur linkages is the availability of  $\text{HS}^{\ominus}$  from the reduced enzyme system. The  $\text{HS}^{\ominus}$  could possibly attack the cyclic or the acyclic multiple sulfur linkages through a nucleophilic mechanism. The sulfide linkages thus cleaved will undergo oxidation to sulfite or thiosulfate. This holds true for the present case of disulfide and polysulfide.

Finally, removal of the sulfate ion creates a new problem of contamination. In connection with this, an examination of sulfate-reducing bacteria for the complete removal of sulfur is being undertaken. The conversion of the organic sulfide into inorganic sulfide will be one future objective.

#### ACKNOWLEDGEMENT

This work is supported by NSF Grant No. GI-35683. The authors also thank Miss Judith Higa for technical help.

#### REFERENCES

1. T. A. Bertness, Personal Communication, Mobil Oil Corp., 1973.
2. D. L. Isenberg, Microbial Desulfurization of Petroleum, Ph.D. Dissertation, Louisiana State University, 1961.
3. M. P. Silverman, M. H. Rogoff, and I. Wender, Removal of Pyritic Sulfur from Coal by Bacterial Action, *Fuel*, 42, 113-124 (1963).
4. J. E. Findley, M. D. Appleman, and T. F. Yen, Papers delivered at ACS, Div. of Microbial Chemistry and Technology, Chicago, 1973.
5. A. B. Roy and P. A. Trudinger, *The Biochemistry of Inorganic Compounds of Sulfur*, Cambridge University Press, 1970, pp. 207-248.
6. G. A. Sokolova and G. I. Karavaiko, *Physiology and Geochemical Activity of Thiobacilli*, Israel Program for Scientific Translations, pp. 48-55, 1968.

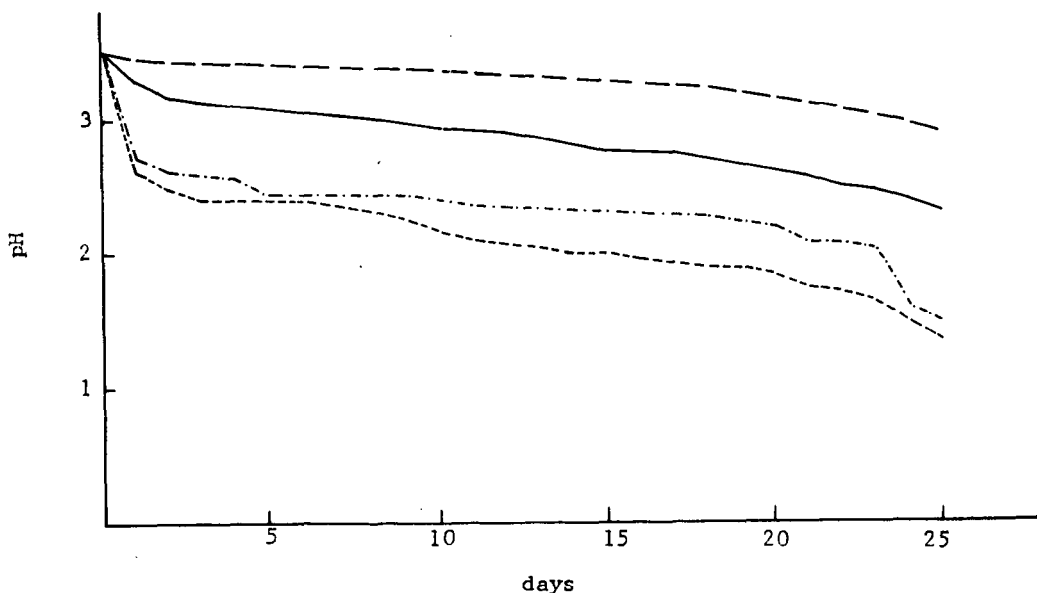


Fig. 2. Variation of pH after inoculation of sulfur bacteria: from top to bottom, the long dashed line represents di-t-butyl monosulfide; the solid line represents di-t-butyl disulfide; the dash-dot line represents di-t-butyl polysulfide, and the short dashed line represents control of elemental sulfur.

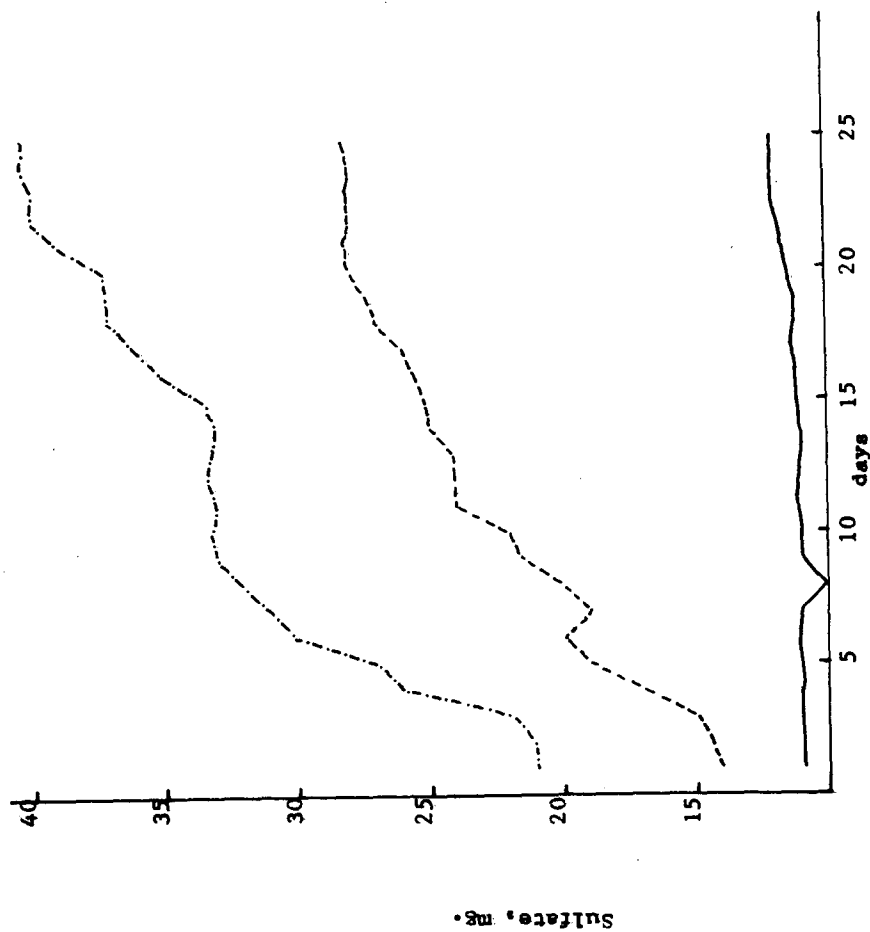


Fig. 1. Conversion of organic sulfide into sulfate in 25-day period. The amount of sulfate ion represents the difference of that produced in the inoculated flasks containing different organic sulfide and that in the controls containing the same organic sulfide without inoculation. From top to bottom, the --- represents di-t-butyl polysulfide, the - - - represents di-t-butyl disulfide and represents the di-t-butyl monosulfide.

## DEVELOPMENT OF COMMUNICATION PATHS WITHIN A TAR SAND BED

David A. Redford

Product Research and Development, Alberta Research,  
Edmonton, Alberta, Canada

Peter F. Cotsworth

Petrofina Canada Ltd., Calgary, Alberta, Canada

## INTRODUCTION

One of the first steps to understanding in situ recovery of bitumen from the Athabasca tar sands is to fully appreciate the fact that, under reservoir conditions, the bitumen in the tar sands cannot be made to flow under the influence of any reasonable or practical pressure gradient. This fact forces a change in the traditional concepts of secondary oil field recovery and necessitates the introduction of new approaches. These approaches often require that much of our traditional thinking regarding secondary oil recovery be changed, and in some cases reversed.

If, because of its extremely high viscosity the bitumen cannot be moved ahead of a front, then, it must either be changed and then moved by a front, or it must be nibbled at from one side and the products carried away to a production point. The first approach has apparently been successfully applied by Pan American Petroleum Co. in their operations at Gregoire Lake (1). There, the tar-bearing McMurray formation is first heated to about 200 °F and then the preheated bitumen is driven to production wells by a combination of forward combustion and water flooding (COFCAW process). The second approach has been demonstrated by laboratory and field work carried out by the Shell Oil Company during the period 1956-62 (2, 3, 4, 5, 6, 7, 8, 9, 10, 11). This approach, which will be referred to as the Shell process, involves three main steps:

- (a) Drilling to the base of the McMurray formation a series of production and injection wells in some suitable pattern.  
These wells are cased such that injection or production of fluids takes place only at or near the bottom of the tar-sand interval.
- (b) Achieving initial interwell communications between production and injection wells by horizontal hydraulic fracturing.  
The initial communications are then developed to the point of accepting large volumes of steam without sealing. This is done by emulsifying the bitumen along the fracture path through the action of critical concentrations of sodium hydroxide and heat, forming a low-viscosity oil-in-water (o/w) emulsion which is then transported to the production well.
- (c) Injection of large quantities of steam to the well-developed communications path to achieve principal bitumen production.  
This steam moves up the formation, heating and emulsifying the cold bitumen above it, and is itself condensed. The condensate and emulsified bitumen form an oil-in-water emulsion which trickles down the formation and is driven to the production wells by pressure of the injected steam.

Of these three steps, the most difficult to achieve in the field is the enlargement of interwell communications paths, particularly the development of a cold fracture path into a hot communications path which will accept large quantities of steam without sealing. At formation temperatures (~40 °F for 200-300 feet of overburden), the bitumen binds the formation sand together to form an almost brittle solid mass which fractures when subjected to a parting pressure. However, as the temperature increases, the formation softens and becomes an amorphous solid; still further heating causes the bitumen to flow as a viscous heavy crude (6 to 7 A Pt°). If steam is applied directly to a fracture path,

propped or otherwise, the formation first softens and tends to slump into the fracture and may result in sealing. Further heating causes the unemulsified bitumen to flow. This unemulsified bitumen is moved further along the fracture path where it contacts colder areas of the formation and cools to form a highly-viscous impermeable plug. This problem was recognized by Shell (6) during their experimental field work. Their solution (6, 9, 10) was to inject steam at a pressure above the pressure required to support the overburden (fracture propping pressure) but below the pressure which would propagate a vertical fracture. It was found that with this approach the injection pressure gradually rose, and from time to time it became necessary to replace the steam injection with injection of a hot solution of a critical concentration of sodium hydroxide. By repeating this cycle over a period of time, Shell were apparently able to develop hot communications paths which would accept large quantities of steam without sealing.

In pilot plant and field experiments in which we have been associated, this procedure has been less than satisfactory. Our experience has been that communications could not be maintained when using injection pressures below the vertical-fracture pressure. Use of pressures above the vertical-fracture pressure resulted in surface fractures and/or loss of fluids to high-lying relatively-permeable zones. This problem is particularly acute in areas where overburden is relatively light (e. g., 200-300 feet). To overcome these difficulties, it was suggested that initial emulsification should take place at formation temperature (i. e., cold emulsification) and that heating of the communications path take place at a rate such that all the bitumen entering the path would be emulsified. By this method the propped communications path would never become plugged with unemulsified bitumen and a low pressure process could be developed for obtaining a hot communications path through a tar sand bed.

## RESULTS AND DISCUSSION

Sodium hydroxide and other bases are ineffective in promoting the formation of oil-in-water emulsions below 60 °F. Their ability to promote emulsion formation gradually increases with temperature but does not become really effective until 90 °F or more. Athabasca tar sands, however, show considerable softening at 60 °F and will begin to weep bitumen at 90 °F. It was, therefore, important to find emulsifying agents which were more effective at the lower temperatures. It was found that a combination of sodium hydroxide and a nonionic surfactant (TX45, an octylphenoxy polyethylene oxyethanol in which the octyl group is branched and which contains about 5 moles of ethylene oxide) was effective in promoting low-temperature emulsification of the bitumen. Optimum concentrations of this surfactant and sodium hydroxide as a function of temperature are given in Table I. Using these concentrations and a gradual heating of the injected fluids, good hot communications were developed over a 100-foot interval near the base of the McMurray formation in a period of about 6 weeks. Pressures were maintained below the fracture-propping pressure. Stable emulsions were achieved, ranging in concentration from 3% for the cold emulsification up to 17% for the warmer emulsification.

Despite these encouraging results, it was of interest to find other agents which would cause more rapid emulsification at formation temperatures, which would be cheaper, and which would produce more concentrated cold-temperature emulsions. It was believed that the sodium hydroxide reacted with the acidic functional groups in the bitumen to form organic salts, and that these organic salts then acted as surface-active agents which caused emulsification of the bitumen. It was, therefore, hoped that the amount of these surface-active agents could be increased by oxidizing part of the bitumen to form more acidic groups. Several oxidizing agents were tried; ozone was the most successful.

Ozone (6% in oxygen) was passed for 2 days through a loosely-packed vertical column of Athabasca tar sand and the column eluted with water. The tar sand changed markedly in appearance, revealing many white sand grains, while the eluted material was a dark-brown color and foamed when lightly shaken. Evaporation of the eluent to dryness

yielded a material which analyzed: C, 45.3%; H, 5.5%; O, 40.6%; N, 1.4%; S, 7.2%. When stirred with water, under a microscope, the sand of the ozonized tar sands separated to form white water-wet grains, while the bitumen formed globules in the water phase. Similarly treated unozonized sands produced no noticeable change.

A 3-foot by 2-inch horizontal tube was then tightly packed with bitumen and a narrow path of 20/40-mesh Ottawa sand was placed at the bottom. Ozone (6% in oxygen) was passed through the tube for 2.5 days. The exit gas contained ~1% ozone. A 50-gram sample of the tar sand was extracted with water (500 ml) to yield a dark-brown solution which foamed when lightly shaken. A surface-tension curve versus concentration for this sample is given in Figure 1. Evaporation of the solution to dryness yielded 0.237 grams of material: C, 28.7%; H, 3.7%; O, 51.3%; N, 1.3%; S, 8.2%. A second similar 50-gram sample of tar sand was extracted with water and the resulting solution was neutralized to pH 7 with 0.1 N sodium hydroxide (41.4 cc required).

In sampling the tube, samples were taken from 4 equal-length sections along the tube, designated A, B, C and D starting from the ozone-inlet end. The bitumen was extracted from each of these samples and from a sample of unozonized tar sand (designated sample O) using toluene reflux. Elemental analyses of these bitumen samples and their molecular weights are in Table II. Standard S.A.R.A. analyses were conducted on each of the samples; thus dividing each of them into asphaltenes, resin I, resin II, saturates, and aromatics. Results of this analysis are given in Table III. Elemental analyses and molecular weights were carried out on each of the subsamples. Results are in Table IV. These analyses show that in general ozonolysis was limited to the asphaltene and resin fractions of the bitumen and resulted in a lower molecular weight and a decrease in the sulfur content. The saturates and aromatics were little affected; however, these fractions are of low molecular weight and viscosity. Thus, ozonolysis is attacking that part of the bitumen which is of highest molecular weight and viscosity and converting it into water-soluble or more hydrophylic material.

A second 3-foot by 2-inch horizontal tube was packed, and ozone (6% in oxygen) was passed through for 7 days (80% of the ozone was still being absorbed by the cell after 7 days). Distilled water (20 ml/hour) and ozone (6% in oxygen) were then passed through the tube for 6 days. Examination of the cell disclosed areas around the sand path and extending out around the surface of the cell which had been largely depleted of bitumen, leaving clean white sand. The initial effluent from the cell (first day's effluent after commencing water injection) was an amber color (pH 1.35) and contained about 6% water-soluble organic material. This material exhibited a surface-tension curve as given in Figure 2. The surface tension of the neutralized material as a function of concentration is also given in Figure 2. Approximately 9.5% of the bitumen originally in the cell was removed during the 6 days of water injection.

The test cell was reassembled and a solution of 0.2% sodium hydroxide was passed through the cell for 14 days (20 cc/hour). An additional 8.7% of the bitumen in the cell was removed during this period. Most of the cell effluent which was collected during the first 6 days of water injection was neutralized to pH 7, and this material was recycled through the cell 6 times. This procedure removed a further 2% of the bitumen from the cell, for a total bitumen recovery of 20.2%. When the cell was opened and the tar sand examined it became evident that the whole cross section of the tube had been affected to some extent by the combination of ozonolysis, distilled-water flush, sodium hydroxide-solution flush, and neutralized-effluent recycle, but in some areas the bitumen had been extensively removed, especially near the original sand path and extending around the glass surface.

These results indicate that ozone readily reacts with bitumen at formation temperatures (40 °F) to form water-soluble highly-oxygenated materials which have surface-active properties in both acid form and as neutralized salts. Passing of water through an ozonized formation of tar sands results in removal of part of the bitumen; in some areas this removal is extensive while in other areas it is minor. When 0.2% sodium hydroxide

solution is passed through such a bed, more bitumen is removed and the highly-depleted areas are extended. It is our intention to in future test a pilot-plant simulation of field conditions for this process to determine whether the combination of ozonolysis, water flush, 0.2% sodium hydroxide flush, and gradual heating can be used for the low-pressure development of a cold propped fracture into a hot communications path which will accept steam without sealing.

#### CONCLUSIONS

It has been demonstrated in the field and in the laboratory that by using a combination of nonionic surfactant and base (sodium hydroxide), and using pressures substantially below the propping pressure, a cold propped fracture path can be developed into a zone that will accept large volumes of steam without sealing. It has been further demonstrated in the laboratory that ozone will readily react with bitumen at formation temperatures, to form highly-oxygenated water-soluble surface-active agents. Therefore, it is anticipated that ozone together with water and/or dilute basic solutions can be used at low pressures to expand a propped fracture path into a hot communications path which will accept steam without sealing.

#### REFERENCES

- (1) Muskeg Oil Company, Application No. 4301 to the Oil and Gas Conservation Board of the Province of Alberta, Canada, October 1968; hearings January 22, 1969.
- (2) Shell Oil Company of Canada Limited, Application to the Oil and Gas Conservation Board of the Province of Alberta for the Approval of a Scheme or Operation for the Recovery of Oil or a Crude Hydrocarbon Product from the Athabasca Oil Sands, February 1963.
- (3) T. M. Doscher, Technical Problems in In Situ Methods for Recovery of Bitumen from the Tar Sands, Panel Discussion No. 13, 7th World Petroleum Congress.
- (4) T. M. Doscher, R. W. Labelle, L. H. Sawatsky and R. W. Zwicky, Steam-Drive - A Process for In Situ Recovery of Oil from the Athabasca Oil Sands, Athabasca Oil Sands K. A. Clark Volume, Research Council of Alberta Information Series No. 45, October 1963.
- (5) T. M. Doscher, Oil Recovery, Canadian patent 711,556, issued June 15, 1965.
- (6) P. J. Closmann, T. M. Doscher and C. S. Matthews, Recovery of Viscous Petroleum Materials, U.S. patent 3,221,813, issued December 7, 1965.
- (7) T. M. Doscher, et. al, Oil Recovery from Tar Sands, U.S. patent 2,882,973, issued April 21, 1959.
- (8) T. M. Doscher, et. al, Oil Recovery from Tar Sands, Canadian patent 639,050, issued March 27, 1962.
- (9) C. S. Matthews, et. al, Thermally Controlling Fracturing, U.S. patent 3,379,250, issued April 23, 1968.
- (10) T. M. Doscher, Oil Recovery, U.S. patent 3,279,538, issued October 18, 1966.
- (11) P. van Meurs and C. W. Volek, Steam Drive for Incompetent Tar Sands, U.S. patent 3,396,791, issued August 13, 1966.
- (12) D. A. Redford, Process for Developing Interwell Communications in a Tar Sand, U.S. patent 3,706,341, issued December 19, 1972; Canadian patent 933,343 related.

TABLE I

Optimum Concentrations of TX45 and NaOH  
as a Function of Temperature

Temperature (°F)	TX45 Concentration (%)	NaOH Concentration (%)
40 - 60	0.4	0.2
60 - 70	0.2	0.2
70 - 80	0.2	0.15
80 - 100	0.1	0.15
100 - 120	0.1	0.1
120 - 200	nil	0.1
>200	nil	nil

TABLE II

Analysis of Unozonized and Partly-Ozonized Bitumen

Sample	Carbon (%)	Hydrogen (%)	Oxygen (%)	Sulfur (%)	Nitrogen (%)	Ash (%)	Molecular Weight
O	81.82	10.37	0.78	5.17	1.23	-	1448
A	81.63	9.98	2.18	4.02	1.28	1.11	668
B	81.71	10.62	2.25	3.97	0.88	0.92	625
C	81.66	10.67	2.37	3.95	0.71	-	634
D	81.44	10.55	2.25	4.30	1.05	1.05	641

TABLE III

S.A.R.A. Analysis of Unozonized and Partly-Ozonized Bitumen

Sample	Asphaltenes (%)	Resins I (%)	Resins II (%)	Saturates (%)	Aromatics (%)
O	21.8	42.3	4.2	15.9	14.3
A	24.7	43.9	4.3	13.3	10.6
B	25.3	42.1	4.0	18.4	8.8
C	25.8	39.5	2.5	20.0	9.0
D	24.5	44.8	2.6	18.7	6.7

TABLE IV

Analysis of Unozone and Partly-Ozone Bitumens  
After S. A. R. A. Analysis

Sample	Carbon (%)	Hydrogen (%)	Oxygen (%)	Sulfur (%)	Nitrogen (%)	Ash (%)	Molecular Weight
<b>Asphaltenes:</b>							
O	78.84	7.83	3.03	8.48	1.34	0.64	4797
A	77.60	7.90	4.11	7.88	1.81	0.79	4722
B	76.86	7.74	4.88	7.68	0.82	1.88	-
C	76.87	7.65	4.90	7.75	0.90	1.80	-
D	77.38	7.88	4.44	7.71	0.89	1.53	3493
<b>Resins I:</b>							
O	76.89	9.72	3.97	5.48	0.73	1.01	727
A	77.27	9.48	4.23	4.77	0.77	1.31	731
B	78.53	9.73	6.05	4.65	0.25	-	563
C	78.71	9.63	6.05	4.71	0.26	-	590
D	78.67	9.73	5.97	4.64	0.17	-	617
<b>Resins II:</b>							
O	76.31	9.44	4.44	2.30	0.30	2.17	-
A	77.47	9.89	6.03	1.17	1.17	1.15	-
B	78.99	10.50	7.84	1.96	0.18	-	-
C	79.37	9.53	9.07	1.62	0.21	-	-
D	79.17	10.63	8.00	1.71	0.19	-	-
<b>Saturates:</b>							
O	85.81	13.31	0.17	0.28	0.45	-	454
A	85.92	13.34	0.14	0.27	0.41	-	433
B	86.31	13.03	0.08	0.26	0.18	-	397
C	86.57	12.88	0.22	0.36	0.21	-	395
D	86.28	13.10	0.15	0.25	0.13	-	412
<b>Aromatics:</b>							
O	85.13	10.33	0.27	3.63	0.59	-	398
A	84.94	10.25	0.19	3.75	0.64	-	397
B	85.33	10.61	0.45	3.13	0.15	-	390
C	85.30	10.45	0.48	-	0.16	-	373
D	85.29	10.48	0.50	3.22	0.26	-	379

FIGURE 1 - Surface Tension of Water Soluble Fraction of Ozonized Bitumen

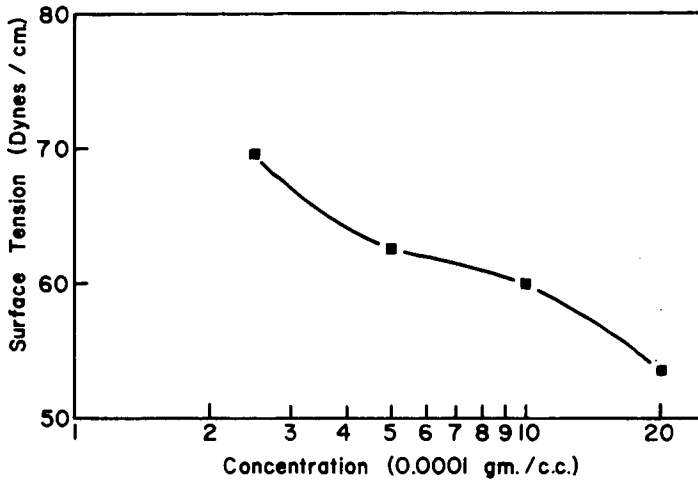
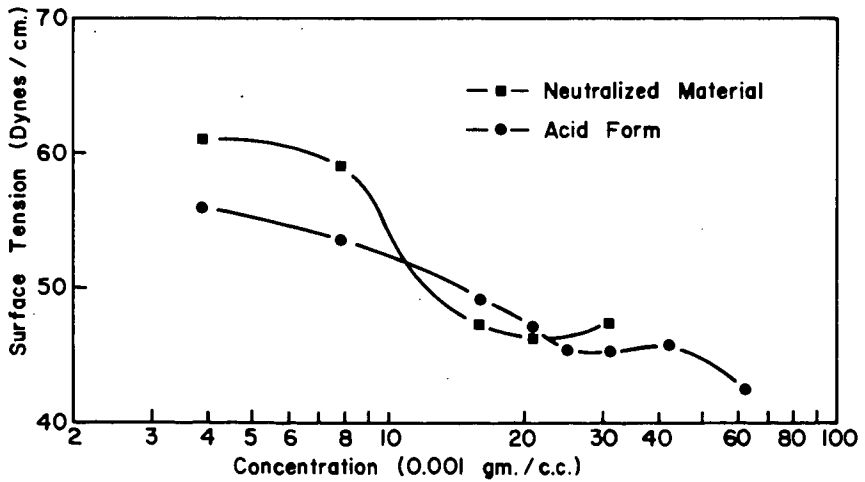


FIGURE 2 - Surface Tension of Water Soluble Ozonized Bitumen



## CHARACTERIZATION OF A UTAH TAR SAND BITUMEN

J. W. Bungler

Laramie Energy Research Center, Bureau of Mines  
U.S. Department of the Interior, Laramie, Wyo.

## INTRODUCTION

Until recently, tar sand deposits have been of relatively little importance as an energy resource. Increasing demands for energy have prompted a greater effort to utilize the energy stored in bituminous sandstone deposits. The inaccessibility of the bitumen, which is generally impregnated in subsurface sandstone, and the high viscosity of the bitumen present major problems with recovery. The high viscosity, heteroatom content, and molecular weight cause problems with utilization. Knowledge of the composition of tar sand bitumens would facilitate the accurate prediction of the chemical and physical behavior of these bitumens in recovery and refining processes.

Recently, several studies have been made to determine the properties of tar sand bitumens. Wood and Ritzma (1) and Gwynn (2) have studied several Utah bitumens. Camp (3) has made a comprehensive study of the Athabasca tar sand deposits. Speight (4) has studied the effects of thermal cracking on Athabasca bitumens. Generally, the analysis of the total bitumens included physical properties, elemental analysis, distillation, and infrared spectroscopy. Detailed analysis of the chemical composition of a total bitumen is difficult because of the complexity of these samples. Separation of the total bitumen into simpler fractions would facilitate compound-type characterization.

This study presents the results of a preliminary examination of a P.R. Spring, Utah, tar sand bitumen. Physical properties, elemental analysis, and distillation data are given and compared to literature values for other P.R. Spring samples. The separation of the bitumen, using selected techniques developed in our laboratory (5-9), into acid, base, neutral nitrogen, saturated, and aromatic hydrocarbon fractions is described. The analytical results of the separation are compared with those for high-boiling petroleum residues separated in a similar fashion. This comparative information could provide an evaluation of the bitumen for processing because more is known of the processing characteristics of petroleum fractions than of tar sand bitumens.

## EXPERIMENTAL

Description of Bitumen Sample

The core that was extracted to produce the bitumen came from Colvert No. 1, NW $\frac{1}{4}$  SE $\frac{1}{4}$ , sec. 35, T. 15 S., R. 22 E., Uintah County, Utah. The tar-bearing sand occurred in the P.R. Spring deposit, Douglas Creek Member, Green River Formation of Tertiary age. Core samples from Colvert No. 1 showed that tar-bearing sand occurred intermittently between the depths of 64 and 162 feet. Approximately 2-inch sections were taken from each foot between 84 and 117 feet, combined, and exhaustively extracted with benzene in a Soxhlet extractor. The benzene extract was filtered through a 4.0 to 5.5- $\mu$  fritted glass disk funnel, and the benzene was removed by vacuum distillation (75 to 80°C, 40 to 50 mm Hg). The recovered bitumen was used for property measurements and as the starting material for the separation into defined fractions.

### Simulated Distillation of Bitumen Sample

The boiling-range distribution of the recovered bitumen was determined by simulated distillation gas-liquid chromatography using the procedure of Poulson et al (10). Boiling points are determined by calibration with a mixture of n-paraffins ranging from C<sub>11</sub> to C<sub>42</sub>. The upper limit for boiling-point determination in this analysis is about 540°C (1000°F).

### Separation of the Bitumen into Defined Fractions

The procedure was an extension of one developed for the separation of high-boiling petroleum cuts into five fractions--acids, bases, neutral nitrogen, saturates, and aromatics (5). This separation and the further division of the first three fractions into subfractions is shown schematically in Figure 1.

A 20-g sample of the bitumen was dissolved in cyclohexane and charged to a column containing 50 g of Amberlyst\* A-29 anion exchange resin on top of 50 g of Amberlyst 15 cation exchange resin (Rohm and Haas). The column was exhaustively eluted with cyclohexane to remove nonreactive material. The resins were removed from the column, separated, and placed in individual Soxhlet extractors. The acids were extracted from the anion resin with 1) benzene, 2) 60% benzene-40% methanol, 3) 60% benzene-40% methanol saturated with carbon dioxide at < 0°C, 4) 5% acetic acid-95% benzene. These last two solvent mixtures were applied manually rather than by the usual Soxhlet reflux because they do not form azeotropes. The bases were removed from the cation resin in a similar fashion using the solvents 1) benzene, 2) 60% benzene-40% methanol, 3) 8% isopropyl amine-55% benzene-37% methanol. These seven subfractions were retained separately for analysis and labeled, respectively, acids I, II, III, and IV and bases I, II, and III.

The neutral nitrogen compounds were removed from the acid- and base-free bitumen by chromatography in cyclohexane on FeCl<sub>3</sub>/Attapulugus clay, packed in a column above Amberlyst A-29. The ratio of sample to FeCl<sub>3</sub>/Attapulugus clay to anion resin was 1:13:17. Nitrogen compounds were recovered by successive column elution with 1,2-dichloroethane and 40% methanol-60% benzene to provide two subfractions. The methanol was removed from subfraction II, after which the ferric chloride was removed from the fraction by dissolving the sample in 1,2-dichloroethane and contacting the sample with the A-29 resin.

Saturated and aromatic hydrocarbons were separated from the acid-, base-, and neutral nitrogen-free bitumen by adsorption chromatography using silica gel as the adsorbent and cyclohexane as the eluting solvent. The cutpoint was made at two bed volumes. Aromatics were desorbed with 60% benzene-40% methanol.

### Analysis of Defined Fractions

The separation procedure provided four acid subfractions, three base subfractions, two neutral nitrogen subfractions, saturated hydrocarbons, and aromatic hydrocarbons. Infrared analysis was employed for those functional groups that have definitive bands for which an average molecular extinction coefficient could be estimated. Table 1 lists the infrared bands and the apparent integrated absorption intensities used (7). Peak area was measured by planimetry. Quantitative IR spectra were measured in methylene chloride with 0.5-mm NaCl cells, using either a Perkin-Elmer 521 or 621 infrared spectrophotometer. Molecular weights of the individual fractions were determined by vapor-pressure osmometry in benzene.

\*Reference to specific brand names or models of equipment is made for information only and does not imply endorsement by the Bureau of Mines.

TABLE 1. - Infrared assignments  
and apparent integrated absorption intensity

	Wavenumber $\text{cm}^{-1}$	$\text{l/mole cm}^{-2} \times 10^4$
Phenols	3500-3640	0.5
Carbazoles	3420-3510	0.7
Carboxylic acids	1700-1790	1.5
Amides	1640-1700	1.5

Basic nitrogen was titrated according to the procedure of Buell (11). A Beckman Model 1063 potentiometric titrimeter with calomel and glass electrodes was used to titrate the bitumen solution with 70 percent perchloric acid in dioxane. The solvent system was 2:1 benzene:acetic anhydride. End points were determined at the inflection point of the curve. Calibration data allowed calculation of the percentage of titratable nitrogen in the sample. The half-neutralization potential (HNP), the potential of the curve midway through the titration, provides information on the strength of the bases.

Saturated hydrocarbons were examined with a CEC-21-110B mass spectrometer. The standard method for group-type analysis (12) was used to classify compounds according to structure.

## RESULTS AND DISCUSSION

### Properties of the Bitumen

The sandstone core from which the bitumen was extracted remained consolidated throughout the extraction. The extracted organics represented 5.27 weight percent of the core. The filtration of the bitumen to remove fine inorganic materials was adequate, as evidenced by ash content of only 0.17 weight percent. Specific and API gravities and elemental analysis for this bitumen, along with literature values for other P.R. Spring bitumens are given in Table 2.

TABLE 2. - Comparative properties of P.R. Spring bitumens

Property	Sample					
	A This study (core)	B Main canyon seep (2)	C Core 79 to 83 ft (2)	D Core 137 to 141 ft (2)	E Outcrop sample no. 69-13E (1)	F Outcrop sample no. 67-1A (1)
Specific gravity 60/60	.998	.974	.995	1.004	1.016	.969
API gravity	10.3	13.8	10.7	9.4	8.3	14.5
Elemental analysis (weight percent)						
Carbon	84.44				80.0	86.0
Hydrogen	11.05				9.5	10.9
Sulfur	.75	.34	.33	.40	.45	.36
Nitrogen	1.00	.77	.88	1.08	1.0	.67
Oxygen(a)	2.59					
C/H (atomic ratio)	.637				.702	.657
S/N (weight ratio)	.75	.44	.38	.37	.45	.54

(a)Determined by difference.

The bitumens selected for comparison are all from the P.R. Spring deposit of the Green River Formation. Samples B, C, and D were described by Gwynn (2) and E and F by Wood and Ritzma (1). Sample B is a surface seep from the Main Canyon. Samples C and D are core extracts, probably from the Douglas Creek Member. Samples E and F are outcrop extracts, again from the Douglas Creek Member. Although differences in gravity are apparent, there is no obvious correlation of gravity with surface or subsurface samples. The nitrogen content is variable among the samples and is another indicator of the variations in composition between samples. All samples are characteristically low in sulfur, as compared to bitumen samples from southern Utah or Athabasca that typically contain between 2 and 6 percent sulfur (1-4). The carbon-hydrogen atomic ratio of .637 indicates that the study bitumen is of average weight and aromaticity. Gwynn reports that the average carbon-hydrogen atomic ratio for 23 P.R. Spring samples is .635. Sulfur-nitrogen weight ratios of the P.R. Spring bitumens in Table 2 are less than 1, which is typical of both tar sand bitumens and crude oils.

The viscosity of the study bitumen was not determined. The study bitumen was semi-solid at room temperature (penetration 148) and only slightly fluid at 80°C. Thus, conventional viscosity measurements were not applicable. Standardized methods for the workup of the bitumen and the determination of viscosity have not been developed. Such methods must recognize the effect that entrained solvents and the loss of light ends during solvent removal have on viscosity. Camp (3) indicates that variations in these two phenomena are significant factors in the variations of viscosities from sample to sample.

#### Boiling-Point Distribution--Simulated Distillation

The boiling-point distribution of the material in the bitumen was determined using simulated distillation by gas-liquid chromatography. This technique has several advantages over conventional assay distillations. It is rapid and can analyze very small samples (30 mg). The boiling-point determination is extended by 120°C over that of the standard Bureau of Mines crude oil analysis (BMCOA). The relatively short contact time at higher temperatures minimizes the possibility of thermal cracking, which produces artifacts and alters the distillation curve. The amount of solvent that is entrained in the bitumen can be accurately determined so that its effects on other properties can be calculated or estimated. Complete removal of the extracting solvent is nearly impossible, and its presence in the bitumen affects the amount of recovery, the elemental analysis, and the viscosity.

Simulated distillation affords the option of choosing cutpoints for calculation of the boiling-range distribution. For purposes of comparison with other bitumens, cutpoints were chosen to coincide with the fraction for the BMCOA distillations. The GLC conditions used for the present analysis are designed to analyze the high-boiling portions and will not accurately resolve constituents boiling below 125°C. Hence, fractions 1 through 4 were combined in the calculation.

The simulated distillation results are given in Table 3, column A, along with literature values for the distillations of the P.R. Spring samples described in Table 2. The 0.4 percent material appearing in Fraction 1-4 for this study bitumen is the entrained benzene left from the extraction procedure. One advantage of the simulated distillation is quickly apparent--an additional four fractions (16 through 19) are displayed, giving more information about the bitumen. For the first 15 fractions, the simulated distillation results approximate those reported by Gwynn (2) in that no material boils below 250°C and the percentage of >420°C residue is high. The values reported by Wood (1), however, vary significantly in that substantial amounts of light ends are shown with very little material boiling between 275 and 420°C. These values

TABLE 3. - Distillation data for P.R. Spring bitumens

Fraction	Cut point, °C	Sample					
		A (a)	B	C	D	E	F
		This study (core)	Main Canyon seep (2)	Core 79 to 83 ft (2)	Core 137 to 141 ft (2)	Outcrop sample no. 69-13E (1)	Outcrop sample no. 67-1A (1)
1-4	125	0.4				2.2 <sup>(b)</sup>	
5	150					2.4	
6	175					1.2	
7	200					1.2	1.4
8	225					1.4	6.5
9	250	0.5				5.9	64.4
10	275	1.0				31.1	3.1
11	308	2.1	1.9	1.6	3.1		
12	336	2.8	2.3	2.2	2.8	0.2	
13	364	4.1	3.1	2.9	4.5	2.2	
14	392	3.2	3.4	5.6	4.1	2.5	
15	420	5.1	9.5	11.8	12.5	2.6	3.4
Residue		(80.8)	75.8	74.8	71.0	47.1	21.3
16	448	6.4					
17	476	8.1					
18	504	7.1					
19	532	8.1					
Residue		51.1					

(a) Simulated distillation data. All others are actual distillation.

(b) The total value of 2.2 was found in fraction 4.

suggest that thermal cracking occurred during the atmospheric distillation stage; thus the large fractions below 275°C are probably cracked products that do not reflect the original composition of the bitumen. These results point out the dangers and difficulties of obtaining boiling-point distributions of heavy bitumens by distillation and suggest that a different approach such as simulated distillation should be considered.

#### Separation of the Bitumen

The P.R. Spring bitumen was separated according to the flow diagram in Figure 1. Acidic compounds were isolated by using an anion exchange resin in the quaternary ammonium hydroxide form. Because the system is nonaqueous, complete ion exchange does not occur but rather an association between acidic types and the basic resin can be expected. Conversely, the bases are separated because they associate with the cation resin used in the sulfonic acid form. The acids were removed from the resin sequentially by exhaustive elution with a series of solvents with increasing polarity. The strongest acids require the most polar desorbing solvent and would appear in the later fractions. The bases were removed from the cation resin with similar elutions with solvents of increasing polarity. Thus, subfractions III and IV of the acids and sub-fraction III of the bases would contain the strongest acids and bases, respectively.

Neutral nitrogen compounds were removed by contacting the acid- and base-free bitumen with ferric chloride/Attapulgus clay in a column system. Nonreactive hydrocarbons were eluted with cyclohexane. Most nitrogen complexes were eluted from the column with

1,2-dichloroethane, and the complexes were subsequently broken when contacted with the A-29 resin in the bottom of the column. Complexes which were strongly adsorbed to the clay (subfraction II) were recovered by elution with benzene and methanol. Iron-nitrogen complexes are unstable in methanol, and so the A-29 resin does not retain the iron during the elution. Therefore, methanol had to be stripped from the sample before it was contacted with A-29 resin to remove the iron. This procedure provided two neutral nitrogen fractions for analysis.

The hydrocarbons portion, which contains some neutral oxygen and sulfur, was separated into saturates and aromatics by adsorption chromatography on silica gel. Elution of the saturates with two bed volumes of cyclohexane gave a satisfactory separation of saturates and aromatics. The UV absorbance at 270 nm for the eluant in 1-cm cells was 0.20, indicating minimal overlap of aromatics in the saturates. The aromatic hydrocarbons were recovered from the gel by exhaustive elution with 60% benzene-40% methanol.

The initial separation, which provides the percentage of total acids, bases, neutral nitrogen, saturates, and aromatics, gives information that could be useful in determining the value of a bitumen as a refining feedstock. Table 4 lists data for these five major fractions from the P. R. Spring bitumen and compares it with similar data from five petroleum residues. Data on the petroleum residues was obtained by USBM-API RP 60 as an extension of the studies of heavy

TABLE 4. - Gross composition of selected bitumens

Fraction	Residue sample					
	P.R. Spring > 225°C	Wil- mington > 485°C	Red Wash > 545°C	Recluse > 750°C	Gach Saran > 675°C	Prudhoe Bay > 675°C
Acids	15.4	10.7	6.0	5.9	12.1	10.0
Bases	12.3	13.3	10.2	8.3	14.2	15.7
Neutral nitrogen	18.5	20.4	10.8	17.4	23.2	12.6
Saturated hydrocarbons	25.7	18.4	51.8	40.8	25.6	32.9
Aromatic hydrocarbons	24.9	35.1	10.9	24.8	18.7	23.4
Recovery	96.8	97.9	94.4	97.2	93.8	94.6

distillate fractions. Comparisons of the bitumen with these residues must be made with the recognition that the residues have higher initial boiling points than the bitumen; i.e., the bitumen contains more low-boiling material. Examination of high-boiling distillate cuts (5, 6, 8, 9) has shown that nonhydrocarbons (acids + bases + neutral nitrogen) are concentrated in the high-boiling fractions. In general, the nonhydrocarbon content of the residue is twice that of the 500-600°C cut, which is in turn twice that of the 400-500°C cut. Table 4 shows that the nonhydrocarbon content of the bitumen is high--second only to the Gach Saran residue--even though the bitumen contains 30 to 50 percent material in the 275 to 500°C boiling range which is absent in the residues. This suggests that a comparable initial-boiling-point residue of the P.R. Spring bitumen would have an unusually high content of nonhydrocarbons.

An additional experiment provided semiquantitative data to show the high nonhydrocarbon content of a comparable residue from the bitumen. The hydrocarbon portion (saturates and

aromatics) of the bitumen was examined by simulated distillation, which showed that 85 percent of these hydrocarbons boiled below 532°C. Because these hydrocarbons represent 50.6 percent of the bitumen, the 85 percent below 532°C represents 43.0 percent of the bitumen. The simulated distillation of the total bitumen shows 48.9 percent boiling below 532°C (Table 3). Of this 48.9 percent, 43.0 percent is hydrocarbon, leaving 5.9 percent as nonhydrocarbon. Calculations based on these data show that a > 532°C residue of the bitumen would have a nonhydrocarbon content of 84 percent, as compared to a nonhydrocarbon content of 27 to 50% for comparable petroleum residues. The unusually high nonhydrocarbon content suggests that additional problems would be incurred in refining processes which are typically sensitive to nonhydrocarbons.

Another major difference between the tar sand bitumen and the petroleum residues is suggested in Table 4. In all the petroleum samples, the base content is higher than the acid content. In the P.R. Spring sample the acids are higher than the bases. This could be an indicator of the differences in oxidation, maturation, or origin for the tar sand bitumen as compared to crude oils.

#### Analysis of Defined Fractions

Acid, base, and neutral nitrogen compounds were eluted from their respective adsorbents by gradient elution. These fractions were examined further for functional groups by infrared spectroscopy. Only those functional groups that were characteristic and that were sufficiently resolved from other bands to be integrated could be used. These bands with their apparent integrated absorption intensities (B) are listed in Table 1. All carbonyl absorption between 1700 and 1790  $\text{cm}^{-1}$  was attributed to carboxylic acids because other carbonyl compounds such as esters and ketones are not retained by the resins and would not be present in the nonhydrocarbon concentrates. A carbonyl band that occurred about 1700  $\text{cm}^{-1}$  could be classified as either acids or amides by examining the spectrum taken in THF; THF will break up the association of acids, and the free acid carbonyl band will shift to a higher wavenumber (13).

The results of the infrared analysis of the nonhydrocarbon compounds are given in Table 5.

TABLE 5. - Infrared analysis of nonhydrocarbon concentrates

Fraction	Wt. percent of bitumen	Molecular weight	Weight percent of fraction				Unidentified by IR
			Carboxylic acids	Phenols	Carbazoles	Amides	
Acids I	4.8	1240	4	9	34	40	13
II	2.2	1161	28	20	18	33	1
III	4.0	853	60	6	7	10	17
IV	4.4	(850 est.)	39	4	17	9	31
Bases I	2.0	855			trace	67	33
II	1.5	(900 est.)				55	45
III	8.8	952				17	83
Neutral nitrogen I	10.3	982			32	55	13
II	8.2	(982 est.)			17	51	32
			-----				
Total	46.2		4.9	1.3	7.7	20.1	12.2

The accuracy of the molecular weights given, which were determined by vapor-pressure osmometry in benzene, is subject to the degree of intermolecular association exhibited in the fractions. For very polar molecules such as strong acids or bases, this association could be considerable. Along with the estimation of the apparent integrated absorption intensities, this determination is the largest source of possible error in the analysis of compound types by infrared spectroscopy. The results in Table 5 show that carboxylic acids and phenols are found only in the acid concentrates. Carbazoles (pyrrolic N-H) and amides, however, are found in all three major nonhydrocarbon fractions. The appearance of the same compound type in several fractions is presumably explained by differences in acidity or basicity which are caused by the hydrocarbon portion of the molecule. Multifunctionality could also be a factor in the distribution of compound types.

Major differences occur between the four acid subfractions. Acid subfraction I is relatively concentrated in nitrogen acids, subfraction II in phenols, and subfractions III and IV in carboxylic acids. The separations greatly facilitate infrared analysis because the high concentration of compound types results in a higher intensity of the infrared absorption bands. In addition, the separations provide fractions which are amenable to further studies such as the determination of the chemical properties and reactivity of the compound types present.

The base fractions contain substantial quantities of amides. Predictably, more amides, which are weak bases, appeared in the weak base fractions I and II than in the strong base fraction III. The neutral nitrogen compounds are largely carbazole and amide types. This, again, is expected because both types are generally nonreactive nitrogen compounds.

In order to analyze the base subfractions beyond the capabilities of infrared spectroscopy, the three fractions were titrated for basic nitrogen to determine the average strength of the bases and the amount of titratable nitrogen present. The results are given in Table 6.

TABLE 6. - Potentiometric titration of bases

Fraction	Strong bases		Very weak bases		Bases titratable <sup>(a)</sup> Wt. %
	HNP <sup>(b)</sup> (mv)	Wt. % N	HNP (mv)	Wt. % N	
Bases I			483	1.12	68
II			429	1.42	91
III	231	1.65	466	0.16	123

(a) Assuming monofunctionality and using molecular weights from Table 5.

(b) Half-neutralization potential.

The first two base fractions contain only very weak bases. These bases titrate with an HNP roughly equivalent to amides (11). Base fraction I was shown to contain 67 percent amides by IR, and thus it is likely that essentially all of the titratable nitrogen in this fraction is of the amide type. Base fraction II contains 55 percent amides (by IR analysis) and 36 percent titratable nitrogen types other than amides. This type(s) is a stronger base than the amides because of the lower HNP exhibited in this fraction than in bases I. A further indication that the unidentified bases are stronger than amides is that bases II have been defined as being stronger than bases I by the separation procedure. Bases III, which comprise over 70 percent of the total bases, contain large quantities of strong bases; essentially no weak bases are present in this fraction. An HNP of 231 could result from alkyl pyridines or quinolines (11). Strong nitrogen bases that have been found in crude oils have been predominantly of the pyridine type.

A tentative identification of condensed benzologs of pyridine has been made in this P.R. Spring bitumen by fluorescence spectroscopy. An accountability of over 100 percent could result from an inaccurate molecular weight determination caused by polar base association. Further, multifunctionality (more than one nitrogen per molecule) would cause an artificially high accountability. Of the total 1.00 percent nitrogen present in the P.R. Spring bitumen, .11 percent is found as carbazoles, .31 percent as amides, .15 percent as strong bases, and .43 percent unidentified.

A group-type analysis of the saturated hydrocarbons was obtained using a modification of the mass spectral method originally proposed by Hood and O'Neal. This method allows the determination of saturated hydrocarbons according to number of rings. Table 7 lists the results of this analysis. The data show that over 60 percent of the saturates are 2- and 3-ring compounds.

TABLE 7. - Group-type analysis of P.R. Spring saturated hydrocarbons

Number of rings	Wt. percent of saturates
0	7.1
1	12.3
2	29.4
3	31.5
4	14.1
5	4.4
6	1.3
Monoaromatics	0

Group-type analysis of aromatic hydrocarbons was not obtainable because of the wide molecular-weight ranges represented within a given series of compounds. The characterization of a bitumen sample with a discrete boiling range would allow group-type analysis of aromatics. The distillation and subsequent characterization of distillates and the residue were, however, beyond the scope of the present work.

### CONCLUSIONS

A preliminary characterization of a Utah tar sand bitumen has been made using methods developed for high-boiling petroleum fractions. The characterization includes information about the major compound types. This information can be compared with similar data for other tar sands bitumens and, more importantly, can be correlated with data from petroleum samples for which refining characteristics are known. Examination of the P.R. Spring bitumen showed that it differed significantly from representative petroleum residues, principally in its high non-hydrocarbon content. Compositional information is important because of the effects that composition has on the recovery and processing of the bitumen.

### ACKNOWLEDGMENT

The work reported in this paper was performed under a cooperative agreement between the Bureau of Mines, U.S. Dept. of the Interior, and the University of Wyoming.

## REFERENCES

1. R. E. Wood and H. R. Ritzma, "Analysis of Oil Extracted from Oil-Impregnated Sandstone Deposits in Utah." Special Studies 39, Utah Geological and Mineralogical Survey, Salt Lake City, Utah, January 1972, 19 pp.
2. John W. Gwynn, "Instrumental Analysis of Tars and Their Correlations in Oil-Impregnated Sandstone Beds, Uintah and Grand Counties, Utah." Special Studies 37, Utah Geological and Mineralogical Survey, Salt Lake City, Utah, October 1971, 64 pp.
3. Frederick W. Camp, "The Tar Sands of Alberta, Canada." Cameron Engineers, Denver, Colo., 1970, 78 pp.
4. J. G. Speight, *Fuel*, 49 (2), 134 (1970).
5. D. M. Jewell, J. H. Weber, J. W. Bungler, Henry Plancher, and D. R. Latham, *Anal. Chem.*, 44, 1391 (1972).
6. J. F. McKay, D. M. Jewell, and D. R. Latham, *Separ. Sci.*, 7, 361 (1972).
7. J. F. McKay, T. E. Cogswell, and D. R. Latham, Preprints, Div. Petrol. Chem., Amer. Chem. Soc., 19 (1), 1973. In press.
8. D. R. Latham and W. E. Haines, *Ibid.*, 18 (3), 567 (1973).
9. W. E. Haines, C. C. Ward, and J. M. Sugihara, Proc., Amer. Petrol. Inst. Div. Refining Meeting, May 1971, pp. 375-390.
10. R. E. Poulson, H. B. Jensen, J. J. Duvall, F. L. Harris, and J. R. Morandi, *Analysis Instrumentation (Instrument Society of America)*, 10, 193 (1972).
11. B. E. Buell, *Anal. Chem.*, 39, 756 (1967).
12. American Standard for Testing and Materials, Standard Method for High Ionizing Voltage Mass Spectrometric Analysis of Gas-Oil Saturate Fractions. D2786-71 in 1971 Annual Book of ASTM Standards: Petroleum Products--Fuels; Solvents; Lubricating Oils; Cutting Oils; Grease. Philadelphia, Pa., 1971, pp. 1019-1027.
13. J. Claine Petersen, *J. Phys. Chem.*, 75, 1129 (1971).

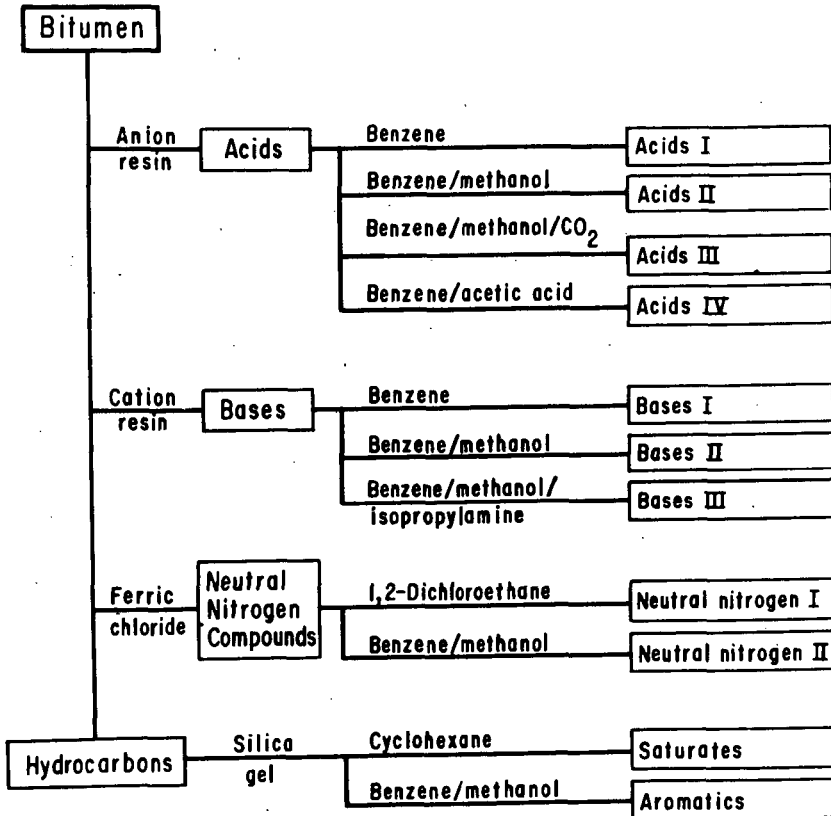


FIGURE 1. - SEPARATION SCHEME

## SOLUBILITY OF SILICA IN BASIC ORGANIC SOLVENT SYSTEM

W. C. Meyer and T. F. Yen  
 Departments of Geological Sciences  
 and Chemical Engineering  
 University of Southern California, University Park  
 Los Angeles, California 90007

The release of petroliferous organic compounds contained in Green River oil shale can be affected only after breakdown of the entrapped mineral matrix, predominantly dolomite ( $\text{CaMg}(\text{CO}_3)_2$ ) and quartz ( $\text{SiO}_2$ ) (1). Dolomite is readily solubilized in an acid medium, but removal of quartz presents a problem. On previous occasions it had been noted that during distillation, potassium hydroxide (KOH) pellets in boiling pyridine dissolved through a Pyrex flask, suggesting that basic organic solvents with potassium hydroxide may serve as good silica solvents.

Experiments were designed to test the solubility of quartz in several solvent systems, prepared as follows:

- 1) 200 ml quinoline plus 60 g potassium hydroxide pellets added directly.
- 2) 100 ml quinoline plus 100 ml saturated aqueous potassium hydroxide.
- 3) 200 ml pyridine plus 60 g potassium hydroxide pellets added directly.
- 4) 100 ml pyridine plus 100 ml saturated aqueous potassium hydroxide.
- 5) 200 ml glycerol plus 60 g potassium hydroxide pellets added directly.
- 6) 200 ml saturated aqueous potassium hydroxide.

Each of these systems were added to a measured amount ( $\approx 5$  g) of crushed ( $< 125 \mu$ ) quartz in a stainless-steel beaker, and heated to its boiling point at atmospheric pressure for a period of five hours. Quartz was chosen for these experiments because of its tight crystalline structure and relative insolubility in relation to other silica species (2). Solubility values for this mineral would represent a minimum for a given solvent system with respect to silica.

Solvent vapor was refluxed into each system by placing a volumetric flask of cold water over the mouth of the beaker. Undissolved quartz was trapped in base-resistant sharkskin filter paper and thoroughly washed with distilled water. The residue was then dried and weighed. Weight loss is expressed as percent of original weight (Table I).

TABLE I

## Quartz

<u>Solvent System</u>	<u>Temp. °C</u>	<u>Time (hr.)</u>	<u>Wt. loss*(%)</u>
Quinoline + KOH pellets	235	5	55
Quinoline + Saturated Aqueous KOH	155	5	36

TABLE I (cont.)

<u>Solvent System</u>	<u>Temp. °C</u>	<u>Time (hr.)</u>	<u>Wt. loss*(%)</u>
Pyridine + KOH pellets	130	5	3
Pyridine + Saturated Aqueous KOH	115	5	7
Glycerol + KOH pellets	179	5	29
Saturated Aqueous KOH	110	5	9
Oil Shale			
Quinoline + KOH pellets	235	5	37

\*Figures are mean values for duplicate runs.

Problems were encountered in cleaning the undissolved quartz of gummy residue and precipitated potassium hydroxide which often formed as the solution cooled during filtering. In most cases, the residue was water soluble and was eliminated by repeated washing.

#### DISCUSSION

From the accumulated data (Table I) it can be seen that, of the solvent systems investigated, quinoline plus potassium-hydroxide pellets provided the best results, followed by a mixture of quinoline and aqueous saturated potassium hydroxide. Mixtures of pyridine and potassium hydroxide. Mixtures of pyridine and potassium hydroxide did not prove effective.

It is not clear why a basic quinoline system dissolves more quartz than a basic aqueous system, especially since potassium hydroxide is not readily soluble in quinoline. Attempts to dissolve potassium hydroxide in quinoline result in a dense milky suspension. This suspension may contain the active agent, perhaps a quaternary organic salt, that in water serves as a better hydroxyl source than solid potassium hydroxide. Practical grade quinoline was used for these experiments, and this may contain enough water to dissociate a quaternary salt.

A more probable explanation is that all the studied systems are undergoing aqueous potassium hydroxide reaction with quartz, and that the different degrees of solvent efficiency is merely a direct function of the temperature at which these reactions are occurring. Siever (3) has found that the solubility of silica in water increases with temperature, and it seems reasonable to assume that this general relationship is true for aqueous potassium hydroxide systems as well. All solvents used for these experiments, with the exception of pyridine, would be expected to contain small but perhaps significant amounts of water. There seems to be a general correlation between solvent capability and boiling point of the system (Fig. 1), suggesting that the organic solvents serve merely as a substrate to elevate the temperature of aqueous reactions.

A glycerol system was chosen to test this hypothesis, because its boiling point is considerably higher than that of other solvents used

in these experiments. It was found that glycerol and potassium hydroxide form a complex with a relatively low boiling point of 179°C, nonetheless the temperature and solvent capabilities of this system are in keeping with the proposed thesis. The pyridine system produced surprisingly poor results, but since reagent grade pyridine should have a negligible water content, the possibility of a good aqueous reaction is eliminated.

Addition of aqueous potassium hydroxide to the organic solvent would be expected to provide ample water for reaction, but would also decrease the boiling point of the system. The decrease in solvent efficiency of those systems that are aqueous by design might, then, be attributable to the decreased temperature of reaction. To support or disprove this hypothesis, additional experiments are planned to ascertain the solvent capability of each of the studied systems at the same temperature.

To test the practical applicability of the quinoline solvent system, a sample of raw crushed (<125  $\mu$ ) Green River oil shale was extracted for five hours with quinoline and potassium hydroxide pellets. The sample underwent a 37% weight loss, probably representing a large portion of the quartz and other silicates contained in the rock. X-ray analysis should provide an accurate evaluation of any mineralogic changes resulting from this extraction.

#### ACKNOWLEDGEMENT

This work is supported by NSF Grant No. GI-35683. We thank Mr. Joe Yu for technical help.

#### REFERENCES

1. W. C. Meyer and T. F. Yen, The Effects of Bioleaching on Green River Oil Shale, This preprint, 1974.
2. R. K. Iler, The Colloid Chemistry of Silica and Silicates, Cornell Univ. Press, New York, p. 6, 1955.
3. R. Siever, Silica Solubility 0-200°C, and the Diagenesis of Siliceous Sediments, J. Geol., 70, 127-150 (1962).

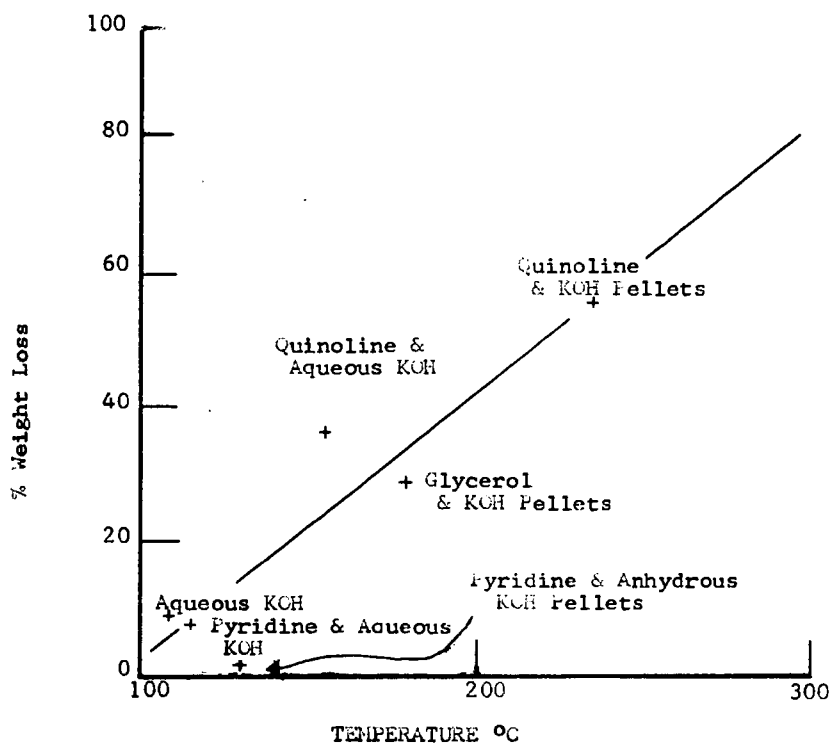


Fig. 1. Relationship of Solvent Capability to Temperature (Boiling Point of System).

DIFFERENCES AMONG OZOCERITES

Robert F. Marschner and J. C. Winters

Research and Development Department, Amoco Oil Company

Naperville, Illinois 60540

## ABSTRACT

Of the unusual organic minerals native to various parts of the world, none are more characteristic than the waxy ozocerites that occur in certain mountainous regions. n-Alkanes longer than those found in typical petroleum waxes have been recognized as the major component. Deposits are now largely exhausted, but nine samples were obtained for examination from the Field Museum and other mineral collections.

Separation by temperature-programmed gas chromatography showed that two pairs of groups of n-alkanes were most abundant: 17 to 21 carbons and 29 to 33 carbons, in which homologs of odd carbon numbers predominated, and 42 to 50 and 58 to 62 carbons, in which even-numbered homologs predominated. Galicia ozocerites belong almost exclusively to the second group, whereas Utah ozocerites are largely mixtures of the second and third.

These favored groups may relate to those previously observed in n-alkanes isolated from petroleum. There the most abundant chain lengths are 11 to 17 and 23 to 29, with odd carbons predominating. The n-alkane patterns suggest three possible sources for ozocerite.

## INTRODUCTION

Because of their usefulness and relative abundance, there are no more commonplace minerals than coal and petroleum. Oil shales and tar sands promise to become almost as familiar. A dozen other organic minerals found less frequently now seem peculiar in comparison, especially because most deposits have become depleted or exhausted. Of these, none are stranger than earth wax or ozocerite.

Ozocerite and several similar waxy minerals occur in a hundred places around the world, usually but not always in mountainous areas. Ordinarily it is associated with other organic deposits. Its densest occurrence is in Galicia, along the southwestern flank of the Carpathian Mountains, especially near Borislav. Scattered deposits are associated with the Caucasus in Russia, the Wasatch in Utah, and lesser ranges elsewhere. Cumulative world production may have reached as much as a million tons, possibly one-tenth of it in the U.S.A. The biggest use was in leather polishes.

n-Alkanes longer than those typical of petroleum are clearly the characteristic components of ozocerite. The melting points range upwards from those of petroleum waxes, the densities and refractive indices are somewhat higher, and the solubilities in various solvents are much lower. In Borislav ozocerite, at least, branched and cyclic saturates are also present (1). The high losses incurred in refining ozocerite with sulfuric acid to produce ceresins suggest gross admixture with polar substances as well.

Just enough is known about the composition of ozocerite to pose a series of interesting questions. In what manner was ozocerite formed: differently than petroleum, simultaneously with it, or subsequently from it? How can such specific structures as n-alkanes be accounted for: by biosynthesis, migration, alteration, or some other means? Do the n-alkanes in ozocerite correlate with the presence of high-melting waxes in some paraffinic crudes and their absence in some asphaltic crudes? Study of the chain-length distribution of the n-alkanes in ozocerite and comparison with that in petroleum (2) ought to suggest answers to such questions.

The n-alkane distributions of nine samples of ozocerite were accordingly obtained by programmed-temperature gas chromatography. Ozocerites were frequently refined before marketing by melting in boiling water, and are said to be commonly adulterated with cheaper waxes. Evidence for such modifications was constantly watched for.

#### EXPERIMENTAL

Although ozocerite can no longer be obtained directly from the historical sources, pieces exist in museum collections. Seven samples provided by the Field Museum of Natural History through the courtesy of Mr. B. G. Woodland made up the bulk of the material for the present study. Especially significant was the sample from the Industrial and Agricultural Museum at Warsaw, which carried the description: "Earth wax in unrefined state directly after excavation from the mine. From the Association for Earth Wax and Rock Oil Industry at Boryslaw." Further information on these and two other samples are offered in Table I.

Gas chromatograms were run on a dual Hewlett-Packard 5750 instrument temperature-programmed to 400° C at a rate of 10° per minute. Columns were 6-meter lengths of 3 mm tubing, packed with 3% OV-1 on chromosorb G-HP. Detection was by hydrogen-flame ionization. The ozocerite samples were simply dissolved in carbon bisulfide before running.

Typical chromatograms are shown in the two panels of Figure 1. Time from injection in minutes is given at the bottom and the positions of successive n-alkanes at the top. Inserts show heads and tails in greater detail. Ozocerite H-23 at the top ranged from 16 to 59 carbons, and the Russia ozocerite at the bottom ranged from 13 to 54 carbons. The hold temperature of 400° was reached near 37 carbons with both samples; at this point, about one-third of the Russia ozocerite had emerged, and about two-thirds of H-23.

Successive n-alkanes are clearly the major constituents. Two adjacent doublets near the starts of the curves locate n-heptadecane-pristane and n-octadecane-phytane, which serve as unambiguous counters for the n-alkanes. In addition, n-docosane was occasionally added to provide an internal standard at 22 carbons, and a heavy paraffinic petroleum was run daily as an external standard.

Relative amounts of individual n-alkanes were determined by measuring areas under the successive peaks above the baseline representing the background of unidentified intermediate components. Total amounts of n-alkanes given in Table I are based on estimates of the amounts of background, which increases regularly with column temperature. The n-alkane content of H-23 in Figure 1, for example, is clearly much larger than that of the Russia sample. For comparing ozocerite compositions, logarithmic plots of the amounts of the successive n-alkanes were made for each.

## DISCUSSION

Such plots for all ozocerites are presented in the three panels of Figure 2. As was evident in Figure 1, alternate n-alkanes often predominate, especially where the amounts are large and differences are most distinct. Asterisks identify n-alkanes that show clear predominance over adjacent homologs in either the original chromatograms or the logarithmic plots.

In the bottom panel, curves for all three Galicia ozocerites almost coincide. Homologs of 27 to 31 carbons each make up more than about 10% of the n-alkane mixture. The biggest differences occur near the ends: the Standard Oil sample shows a small but distinct second peak at 50 to 52 carbons; the Ward's sample shows a shoulder near 50 carbons, as well as starting three carbons lower; and the Warsaw Museum sample is narrowest and therefore tallest. The Warsaw composition might be duplicated by removing the last 1% of the other samples, perhaps by crystallization from a solvent, but there is no evidence of adulteration.

Near the 27 to 31 peak of Galicia ozocerites, odd-numbered n-alkanes predominate. By 40 to 44 carbons, however, a predominance of even carbons appears. The switch occurs between 37 and 38 carbons, suggesting that the n-alkanes derive from two overlapping sources.

In the middle panel of Figure 2, curves for the three Utah ozocerites are distinctly different. The Kyune sample peaks near 29, and plateaus at 42 to 50, much like the Galicia ozocerites. The Fort Worth sample has a large peak at 33 to 37 and a small one at 60, somewhat like a Galicia curve displaced a few carbons to the right. The Soldier Summit plateau at 33 to 37 and a small peak at 58 to 62 match Fort Worth, but the strong peak at 44 to 48 matches Kyune.

The n-alkane predominances help to sort out the Utah differences. The Fort Worth peak and Soldier Summit plateau at 33 to 37 have odd predominance, whereas the Kyune plateau and Soldier Summit peak at 44 to 48 have even. The only anomaly is that the Fort Worth sample retains its odd predominance beyond the switch at 37 carbons.

In the bottom panel of Figure 2, the three remaining ozocerites are again different. The Pennsylvania sample has a weak peak at 17 to 21 and a strong one at 29 to 33, both with odd predominance. The Russia sample has a plateau starting at 17, a peak with even predominance at 42 to 46, and what may be a shoulder with odd predominance between around 31 to 35. Finally, sample H-23 has a strong peak with odd predominance at 29 to 33 and a plateau with even predominance at 42 to 52. Only n-alkanes with 38 or more carbons show even predominance, and only those with 37 or less show odd.

Ozocerites thus have widely different patterns of n-alkane distribution, yet it is the similarities that are most remarkable. Four ranges are favored: 17 to 21 and 29 to 33-plus with odd predominance, and 42 to 50 and 58 to 62 with even predominance.

Percentages of the ranges represented in each ozocerite are summarized in Table 2. Pennsylvania and Galicia samples consist mainly of the 17-to-21 range, whereas Utah and Russia samples are largely mixtures of the 17-to-21 and 42-to-50 ranges.

## CONCLUSION

These ranges appear to relate to those previously found in petroleum, the n-alkanes in several of which show two favored ranges below 35 carbons (2). Compositions of three typical petroleum samples are plotted logarithmically in Figure 3 in the same way as the ozocerites. The n-alkanes from Darius petroleum simply diminish regularly, with no clear predominance of any carbon numbers. Although a peak occurs at 7 carbons, it probably resulted from separation of natural gas during production and perhaps losses of volatile components afterwards. n-Alkanes from John Creek petroleum peak at 11 to 17 carbons with a strong odd-carbon predominance. Uinta Basin n-alkanes show a plateau at 7 to 13 carbons, and a medium peak with odd predominance at 23 to 29.

Also shown for orientation in Figure 3 are dashed lines for three ozocerites, one from each of the panels of Figure 2. The n-alkanes in ozocerites overlap those from petroleum. Considering the entire range, at least three distinctions can be made: (A) n-alkanes of about 10 to 20 carbons, intermediate in abundance, and with a strong odd preference, relatable to natural fatty acids (2); (B) n-alkanes of almost any chain length, most abundant and without odd or even preference, for which no satisfactory explanation has yet been advanced; and (C) n-alkanes of more than 40 carbons, low in abundance and with a definite even preference, that may be associated in some way with doubling of the odd preference of shorter n-alkanes.

Answers to the questions posed earlier require a knowledge that we do not have of the interrelations among these three distinctions, if indeed three are all there are. An assumption that two independent original syntheses (A and B) and a subsequent transformation (C) occur is helpful. Ozocerite would then be formed from petroleum, in which n-alkanes already exist, probably by a biochemical process that would preserve predominance.

## LITERATURE CITED

- (1) Kastner, Moos, Schultze    Erdöl und Kohle 12 77 (1959)
- (2) Martin, Winters, and Williams    Nature 199 110 (1963)

TABLE I  
DESCRIPTIONS OF OZOCERITES  
 (obtained from Field Museum, except as noted)

<u>Original Source</u>	<u>Description</u>	<u>Original Donor</u>	<u>Approximate % n-alkanes</u>
Boryslaw, Galacia	Sample No. 110	Ward's Nat. Sci. Estab.	85
Galacia, Austria	--	Standard Oil Company	93
Baryslaw, Poland	Note attached	Ind. Ag. Museum Warsaw	82
Bedford, Pa.	Native paraffin	Standard Oil Company	80
Russia	Cast cylinder	Worlds Columbian Expos.	--
Fort Worth, Utah	--	Collected by W. J. McKay	95
Kyune, Utah	Native paraffin	Collected by H. M. Black	89
Soldier Summit, Utah	From mine	*	95
H-23 (Utah?)	Source unknown	**	93

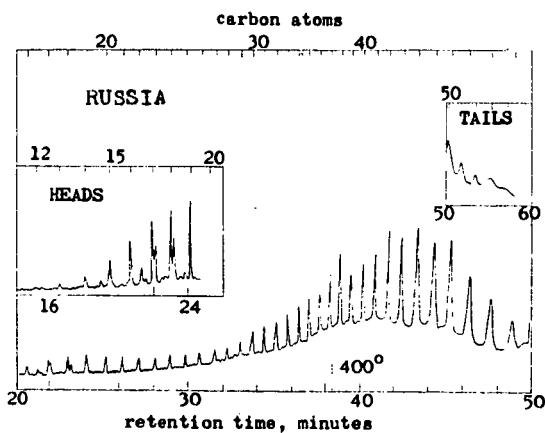
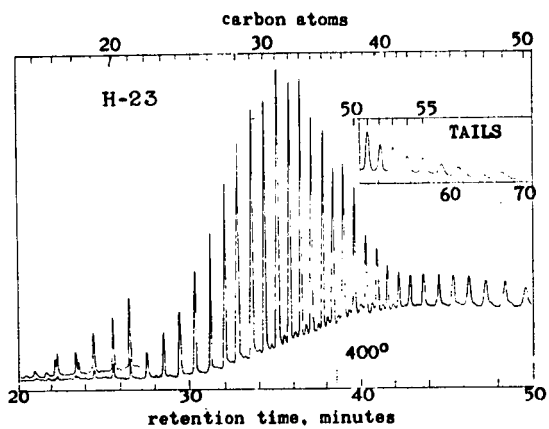
\* From University of Illinois; donated by Reino Kallio.

\*\* From Colorado School of Mines; donated by A. S. Houghton.

TABLE II  
COMPOSITIONS OF n-ALKANES IN OZOCERITES

<u>Nominal Carbon Range</u>	<u>17-23</u>	<u>29-33</u>	<u>46-50</u>	<u>58-62</u>
Predominance	Odd	Odd	Even	Even
Bedford, Pa.	16	84		
Warsaw (Galicia)		97	3	
Ward's (Galicia)		97	3	
Standard Oil (Galicia)		96	4	
Kyune (Utah)	1	92	7	
H-23	3	70	24	3
Fort Worth (Utah)		69	29	2
Russia	7	13	80	
Soldier Summit (Utah)		18	80	2

FIGURE 1  
GAS CHROMATOGRAMS OF TYPICAL OZOCERITES



256-A  
FIGURE 2

n-ALKANES IN OZOCERITES

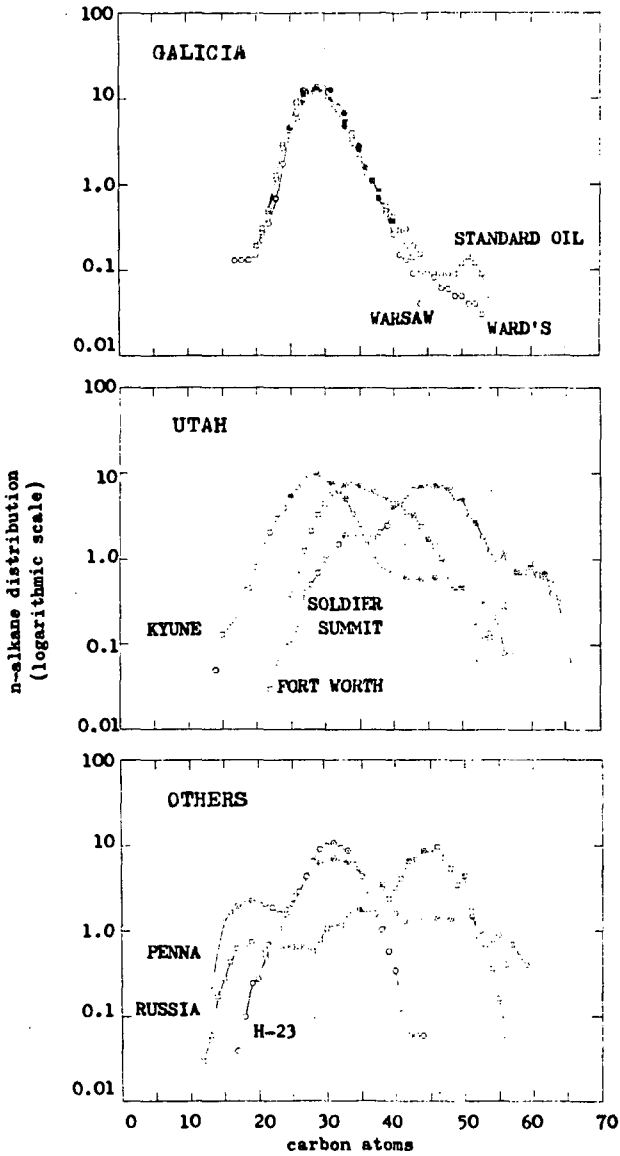
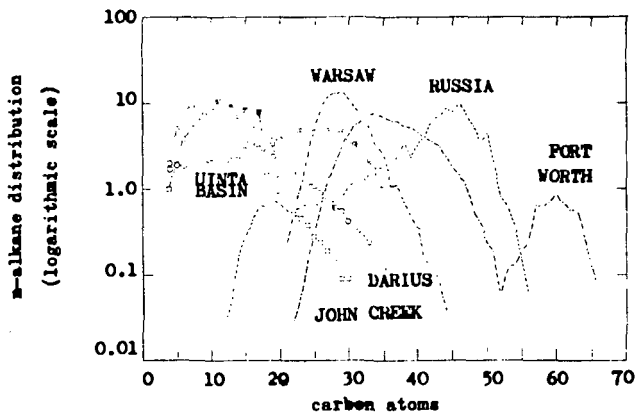


FIGURE 3  
n-ALKANES IN PETROLEUM  
OVERLAP THOSE IN OZOCERITES



## CHARACTERIZATION OF SYNTHETIC LIQUID FUELS

by

R. G. Ruberto, D. M. Jewell, R. K. Jensen\*, and  
D. C. CronauerGulf Research & Development Company  
Pittsburgh, PA 15230

## INTRODUCTION

In order to decide what is the best use of a fuel, natural or synthetic, and/or which one out of a number of fuels is the best for a specific application, it is necessary to (1) know the characteristics of each fuel, and (2) be able to compare the characteristics of one fuel directly with those of another.

Experience has shown that in order to obtain meaningful results in analyzing petroleum crudes and residues, it is necessary to separate a sample into a certain number of well-defined fractions and to analyze these fractions in detail. Conclusions as to the composition of the original sample are then arrived at by combining the results of the analyses on each fraction in a manner consistent with the steps performed to obtain them. This same approach is used for the synthetic liquid fuels and this paper reports our results obtained on such materials.

The literature on tar sands and tar sand bitumen is not very rich, as compared to that on shale oils and coal. Most of the currently available data are limited to the material of the Athabasca deposit, in the Province of Alberta, Canada, primarily because of its size and location. Detailed general information on the Athabasca tar sands and tar sand bitumen is available in References 1 and 2. In addition, the analysis of this bitumen has been reported by various workers.<sup>3-7</sup>

---

\* Present Address: Ford Motor Company, P. O. Box 2053, Dearborn, MI 48121.

The literature on oil shale and shale oils is much richer and goes back several decades. However, due to its size and location, most of the literature deals only with one oil shale formation, the Green River Formation.

Space limitations prohibit a literature survey here; however, much information on oil shales and shale oils, in general, is found in References 8 through 11, while the remainder of the available data can be divided into two general categories.

1. Data obtained on shale oils produced by various retorting methods with the purpose of obtaining a fuel.<sup>12-23</sup>
2. Data obtained on shale oils produced by solvent extraction methods for geological and geochemical studies.<sup>24-35</sup>

An enormous amount of data dealing with all aspects of the chemical and physical properties of coal is available; however, only four reviews have been referenced which are particularly comprehensive.<sup>36-39</sup>

## EXPERIMENTAL

### A. Samples Preparation

The coal liquids were derived from the catalytic liquefaction of Pittsburgh Seam bituminous and Wyoming subbituminous coals. The analysis of these coals is given in Table I. The coals were liquefied in a bench-scale catalytic unit using cyclone overhead product as recycle solvent to insure that the liquid products were derived from the coal and not the solvent. The product streams from the unit consisted of gases, water, light ends typically boiling in the range of 150-500°F, and slurry. The slurry product was filtered to remove the undissolved coal plus mineral matter prior to analysis. Based on

a calculated material balance for processing 1.0 ton of as-received Pittsburgh Seam coal, the light ends and filtrate yields were 135 and 1,350 pounds, respectively. Similarly, yields of light ends and filtrate from the subbituminous coal were 265 and 740 pounds, respectively. The term "coal liquids" as used hereafter refers to the filtered slurry product with a boiling point above 130°F.

A sample of raw bitumen recovered from Athabasca tar sands was analyzed without further upgrading. This sample was provided by Sun Oil Company.

Three distillate cuts of shale oil were obtained from The Oil Shale Corporation and were also analyzed without further upgrading.

#### B. Separation Into Fractions

The separation procedure, developed for petroleum crudes and residues,<sup>40</sup> is illustrated in Figure 1. This procedure is applicable to samples having a boiling point higher than 470°F.

The distillation step is necessary only with samples containing low boiling materials. These materials must be removed since they would be lost during the subsequent steps in which solvents are used and then evaporated to recover the fractions.

The material boiling above 470°F is separated into oils, resins, and n-pentane insoluble residue. The residue is separated into asphaltenes and benzene insolubles by extraction with benzene while the oils are separated into aromatics and saturates. The saturates can be further separated into n-paraffins and non-n-paraffins with 5 Å molecular sieves,<sup>41</sup> while the aromatics are separated into three additional fractions on alumina.<sup>42</sup> The results of the separations are listed in Table II.

### C. Method of Analyses

Unless otherwise specified, the average molecular weights were obtained by vapor pressure osmometry (VPO) in benzene according to ASTM D2503. For the aromatic fractions, an average molecular weight is also obtained by  $^1\text{H}$  NMR and reported in the respective tables.

Carbon and hydrogen were determined by a microcombustion method; nitrogen by a micro Kjeldahl method; oxygen by neutron activation or by a modified Unterzaucher method; and sulfur by a combustion method similar to ASTM D1552. Tables III and IV report all the molecular weight and elemental data.

The simulated distillation data (Table V) and the FIA analyses of the distillates (Table II) were obtained by techniques similar to those described by Mayer, et al.<sup>43</sup>

The mass spectrometric analyses of the saturates fractions (Table VI) were obtained by an in-house method similar to that of Hood and O'Neal.<sup>44</sup>

The aromatic fractions were analyzed by the proton NMR method of Clutter, et al.<sup>45</sup> and the results are reported in Tables VII and VIII.

## DISCUSSION OF RESULTS

### A. Tar Sand Bitumen

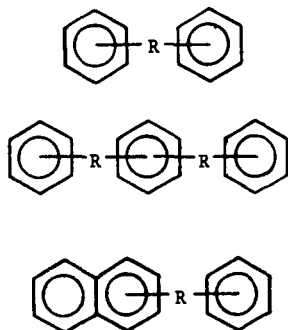
This material is very viscous, black, and contains a considerable amount of sulfur, some nitrogen and oxygen, and no light ends (see Tables II and III). The saturate fraction amounts to about 17% and is a clear colorless liquid with an average molecular weight of 365 (Table III). The carbon number ranges from about 14 to well above 44 (Figure 2) and its final boiling point is above 1,000°F (Table V). These characteristics are reconciled

by the observation that no alkanes are present as shown by: (1) the mass spectrometric data (Table VI); (2) the fact that no material was removed when this fraction was treated with 5 Å molecular sieves; and, (3) the lack of sharp peaks on the GLC of this fraction (Figure 2). In addition the inability to remove alkanes from this type of material was also reported by Speight.<sup>4</sup> The condensed and noncondensed cycloalkanes are evenly distributed, and more than half of the condensed cycloalkanes have only two rings, as indicated by mass spectrometry (Table VI).

The aromatic fraction accounts for almost half of the bitumen with the largest contribution made by the di- + triaromatics (Table II). The aromatic fractions were further characterized by a <sup>1</sup>H NMR spectroscopic technique. This method, developed for petroleum crudes and fractions, calculates from the NMR spectrum a set of average parameters used to describe an "average molecule". In this method, three assumptions are necessary which place constraints on its applicability. The assumptions are: (1) no aromatic fused ring systems larger than three are present; (2) the resonances of the unsubstituted non-bridge aromatic ring carbon protons are sufficiently separated in the proton NMR spectrum so that the ratio of mono- to di- to triaromatics can be determined; and, (3) the number of substituent groups, on the average, is the same for mono-, di-, and triaromatics. The last two assumptions are probably as valid for synthetic liquid fuels as for petroleum. The first assumption is partially satisfied by the separation steps which provide three fractions two of which (the monoaromatics and the di + triaromatics) are free of fused ring systems larger than three rings. The proton NMR analysis of the third fraction (the polyaromatics), which does contain four or more rings, condensed and noncondensed, is then only qualitative.

Figure 3 shows the spectra of the three aromatic subfractions and Table VII the results of the calculations. The monoaromatic subfraction is shown by NMR to be free from other aromatic types and to have many short alkyl substituents and at least one naphthene ring per molecule. The average molecular weight obtained by NMR agrees very well with that determined by VPO.

The di- + triaromatic subfraction analyzes as 54% "monoaromatics" and 47% "diaromatics" by proton NMR. The average molecule also contains many short alkyl substituents, more than one aromatic ring and one naphthene ring. The average molecular weight calculated from NMR is lower than that obtained by VPO. These data indicate that noncondensed di- and triaromatics are present in this subfraction. Compounds such as



are di- and triaromatics and are all separated as such by the alumina column. Proton NMR, however, will see the first two as monoaromatics and the last one as a monoaromatic and a diaromatic, and all the calculations are affected

accordingly. There is no way to circumvent this problem until the condensed and noncondensed aromatics can be separated from each other. It must be pointed out, however, that the presence of noncondensed systems could not have been detected by separation or spectroscopic techniques alone. Both must be used and one must support the other.

The molecular weight of the polyaromatic fraction as calculated by NMR is well below that determined by VPO. As pointed out earlier the NMR analysis of this fraction can only be semiquantitative because tetra- and higher aromatic systems will be calculated as mono- and diaromatics and all the calculations will be affected accordingly. In our separation scheme all of the polar non-hydrocarbons are concentrated in the resin fractions. Only ethers and thioethers are included in the oil and are eventually concentrated in the di + triaromatics and polyaromatics, as the data in Table III show. Also only half of the saturates are condensed cycloalkanes, mainly of two and three rings. These observations are indirect evidence that no significant amounts of large condensed systems are present, and that at least part of the polyaromatic fraction consists of noncondensed mono-, di-, and triaromatic units.

The resins and asphaltenes have not been analyzed beyond the extent shown by the tables. The resins can be fractionated and analyzed in more detail using methods developed for petroleum resins by Jewell<sup>46</sup> and McKay<sup>47</sup>. This analysis, however, is beyond the scope of this work.

#### B. Coal Liquids

The two coal liquids contain about the same amount of material boiling below 470°F very little saturates, and substantial amounts of aromatics, mainly di- + triaromatics (Table II). The liquids from the Big Horn coal, however, contain more aromatics and less resins, asphaltenes,

and benzene insolubles than the liquids from Pittsburgh Seam coal. This is not surprising considering the fact that higher rank coals are harder to hydrogenate and that the liquefaction process is believed to follow the path:



The distillates were fractionated into saturates, aromatics, and olefins by FIA as already mentioned. Attempts to further characterize the FIA fractions by GLC were not successful.

By GLC methods, it is possible to obtain detailed quantitative analyses of saturates up to  $C_9$ , of mono-olefins up to  $C_7$ , and of aromatics up to  $C_{10}$ .<sup>43</sup> The liquid chromatographic steps cannot handle materials boiling below  $n-C_{12}$ . Therefore, there is a gap in the analysis of the distillate fractions on which a detailed analysis cannot be readily, routinely and inexpensively obtained. This gap includes all the  $C_8$  to  $C_{12}$  saturates, all the  $C_{11}$ - $C_{12}$  aromatics, and all the heterocompounds and olefins that are present in this fraction.

The saturates boiling above  $470^\circ\text{F}$  were analyzed by mass spectrometry and appear to contain alkanes but predominantly cycloparaffins. The alkanes appearing in these liquids may not be part of the coal network, but may simply be embedded in it. The primary coal structure is generally believed to be formed of small aromatic units held together by short links, mainly methylene, ethylene, propylene, and ethers.<sup>48-55</sup> However, the alkanes present in these fractions have a carbon range between 12 and 30, as shown

by the chromatogram in Figure 4, and should not be the result of the decomposition of coal. Vahrman, et al., have shown that small molecules can be extracted from coal by non-destructive methods.<sup>56-61</sup>

The cyclic saturates can also be entrained in the coal pores, but they can also be the result of the hydrogenation and liquefaction process. In order to establish the actual origin of these saturates, it would be necessary to carry out a considerable amount of work which would be valuable but is beyond the present scope.

The aromatic fractions were also examined by  $^1\text{H}$  NMR and examples of spectra are shown in Figure 5. The liquids are derived from coals of different ranks and this is reflected in the size of each fraction as already pointed out. However, at least for these materials, the characteristics of corresponding fractions are very similar regardless of their origin. This is evident from the mass spectrometric analysis of the saturates and is further shown by the analysis of the aromatic fractions. The NMR spectra of corresponding fractions from the two coal liquids are almost superimposable, and for this reason only one set of spectra is shown here, that for the Big Horn coal liquids. The similarity of the aromatics from the two coals is made quite clear by the NMR data shown in Table VII.

The two monoaromatic and di- + triaromatic fractions are practically indistinguishable from each other except for a slightly higher molecular weight of the fractions from the Pitt Seam coal liquids. The spectra of the polyaromatic fractions were too weak and unresolved, and no meaningful calculations could be made from them. Similar problems were encountered when it was attempted to analyze the asphaltenes by NMR; methods have to be developed in order to analyze polyaromatic and asphaltene fractions.

### C. Shale Oils

As indicated by the data in Table II, only Cut I of the shale oils contains a considerable amount of material boiling below 470°F, as would be expected from the low boiling range of this fraction (Table V). This distillate was fractionated into saturates, aromatics, and olefins by preparative FIA techniques, but a GLC analysis of these fractions proved unfruitful for the same problems mentioned above in the case of the coal liquids.

A large portion of the remainder of the shale oil consists of resins with smaller contributions from the saturates and aromatics. The amount of asphaltenes is really insignificant, and a larger contribution would actually be surprising since these are retorting products.

The shale oils are rich in olefins; in our separation scheme free olefins are concentrated in the saturate fractions. The IR spectra of all three saturate fractions show the characteristic olefin bands at 6.1, 10.1, 10.35, and 11.0 microns. However, no attempt has been made to characterize these olefins in detail, mainly because they are easily hydrogenated.

The mass spectrometric analyses of the saturate fractions are reported in Table VI. These fractions appear to be composed mostly of alkanes and noncondensed cycloalkanes with smaller amounts of condensed cycloalkanes, mainly two- and three-ring systems. However, due to the presence of olefins in these fractions the analyses are only semiquantitative. In fact, an olefin should make a contribution to the cycloalkane group type which has the same molecular weight. That is, a mono-olefin will contribute to the cycloalkanes, a diolefin or a cyclic olefin will contribute to the bicycloalkanes, etc. However, the extent of these contributions has never been determined.

No carbon number predominance was detected in the saturate fraction from Cut I and Cut II. The chromatogram of the saturates from Cut III is shown in Figure 6 and an odd-over-even carbon number predominance is evident for the higher carbon number region.

The aromatic subfractions have also been analyzed by proton NMR, and Figure 7 shows the spectra obtained with the fractions from Cut II, and the results of the calculations for all of the fractions are shown in Table VIII. The monoaromatics are free of other aromatic types, have a very low aromaticity, are highly substituted, and at least two of the substituents are naphthene rings. Anders, et al.,<sup>34</sup> and Gallegos<sup>35</sup> have isolated and identified a large number of alkylbenzenes, alkyltetralines, dinaphthenebenzenes, and trinaphthenebenzenes from Green River shale oils.

The di- + triaromatics contain large amounts of non-condensed systems and a much higher aromaticity due to a decrease in the number and size of the substituents. The apparent decrease in the average molecular weights (calculated) is due in part to the presence of the noncondensed systems. As pointed out earlier, one molecule of 1,4-diphenylbutane, for example, will be detected by  $^1\text{H}$  NMR as 2 molecules of ethylbenzenes, and the calculation will be affected accordingly. An apparent decrease in the average molecular weight is then seen and this decrease will be even more marked if the concentration of noncondensed triaromatics is significant. Anders and Robinson<sup>28</sup> have reported the evidence of large amounts of perhydrocarotenes, and Gallegos<sup>35</sup> has isolated and identified various phenyl (cyclohexyl) alkanes. By complete dehydrogenation of these materials, during maturation, noncondensed systems would be formed.

The  $^1\text{H}$  NMR analyses of the polyaromatic fractions present the same problems already mentioned in the discussion of the corresponding fractions from the other synthetics. While noncondensed systems are certainly present, no conclusion can be drawn from these data as to the true composition of these fractions.

#### D. Comparison of Fuels

The separation data of Table II show immediately some gross differences and similarities among the various fuels analyzed. Both coal liquids have a considerable amount of low boiling material which is made up of saturates and aromatics in about equal concentration. Similarly, the shale oil contains low boiling material, while the tar sand bitumen does not.

Of the material boiling above 470°F, the tar sand bitumen contains more saturates than the other fuels. As pointed out above, these saturates are unique in that they do not contain free alkanes, while the saturates from the other fuels contain from 22 to 40% alkanes as determined by mass spectrometry (Table VI).

Only the Big Horn coal liquids have more condensed cycloalkanes than noncondensed cycloalkanes. The tar sands have an equal distribution of the two types of saturates, and the remaining fuels have a higher concentration of noncondensed cycloalkanes; the effect of the olefins on the mass analysis of the saturates from the shale oils must, however, be kept in mind in making this comparison.

The fact that only the coal liquids show condensed systems with up to six rings, and that the Pitt Seam coal liquids (products from a higher rank coal) have a higher concentration of these condensed systems is also worth pointing out. However, the amount of the total saturates in the coal liquids is insignificant from a production and refining point of view.

The aromatic content of the fuels ranges from about 15% to 58%, and in every case the largest contribution is made by the di- + triaromatics. In addition to the differences in the quantity of the aromatic fractions, as shown by the data in Table II, the characteristics of each fraction vary depending on its origin. The variations are shown pictorially by the NMR spectra, and more tangibly by the NMR data listed in Tables VII and VIII. The tar sand bitumen fractions have, in general, a lower aromaticity than the shale oil and coal liquid fractions. This is due to a higher number and a larger size of the substituents. The coal liquids have the highest concentration of condensed di- + triaromatics, and the tar sand bitumen the lowest. Conversely, the amount of noncondensed systems is highest in the tar sand bitumen and lowest in the coal liquids.

Perhaps, where these fuels differ most is in the amount of resins, asphaltenes, and benzene insolubles. The shale oils contain a very large amount of resins from 12 to 69%, or approximately 50% by weight on a total shale oil basis. The tar sand bitumen contains only half as much resins and the coal liquids contain much less. On the other hand, the asphaltenes are significant in the tar sand bitumen and in the Pitt Seam coal liquids. These latter materials are the only ones to contain a significant amount of benzene insolubles.

#### CONCLUSION

Coal liquids and other synthetic liquid fuels can be analyzed by a modification of the methods normally used for petroleum crudes and products. These methods of analysis are relatively fast, require only a few grams of

sample, provide discrete fractions which can be characterized in as much detail as desired with available techniques, and provide comparative compositional profiles for fuels from various sources, natural and synthetic. The methods have limitations, as indicated throughout the paper. However, as new procedures are developed to take care of these limitations, they can readily be incorporated.

RGR;qrc/mag

ACKNOWLEDGMENTS

The authors wish to thank A. V. Vayda for aid in preparing the coal liquids; W. E. Magison for help in obtaining the NMR data; W. Hubis and H. P. Malone for helpful discussions; The Oil Shale Corporation and Sun Oil Company for providing the samples of shale oil and tar sand bitumen, respectively, and for their permission to publish the data obtained on them.

## REFERENCES

1. Camp, F. W., ENCYCLOPEDIA OF CHEMICAL TECHNOLOGY, Vol. 19, "Tar Sands", Second Edition (1969), page 682.
2. Carrigy, M. A. (editor), Athabasca Oil Sands: A collection of papers presented to K. A. Clark on the 75th anniversary of his birthday, Research Council of Alberta, Edmonton, Alberta, Canada, October 1963.
3. Boyd, M. L. and Montgomery, D. S., "Composition of Athabasca Bitumen Fractions as Determined by Structural-Group Analysis Methods", a paper in Reference 2, above.
4. Speight, J. G., Fuel, London 49, 76 (1970).
5. Speight, J. G., ibid 50, 102 (1971).
6. Moschopedis, S. E. and Speight, J. G., ibid 50, 34 (1971).
7. Moschopedis, S. E., ibid 50, 211 (1971).
8. Special Section, "Shale Oil--The Problems and Prospects", Oil Gas J., March 9, 1967, pages 65-80.
9. Gustafson, R. E., ENCYCLOPEDIA OF CHEMICAL TECHNOLOGY, Vol. 18, "Shale Oil", Second Edition (1969), page 1.
10. Robinson, W. E. and Dinneen, G. U., Proc. 7th World Petrol. Congr., New Mexico (1967), American Elsevier Publishing Co., Inc., New York, NY, Vol. 3, page 669.
11. Cane, R. G., ibid, Vol. 3, page 681.
12. Ball, J. S., et al., Ind. Eng. Chem. 41, 581 (1949).
13. Dinneen, G. U., et al., ibid 44, 2632 (1952).
14. Cady, W. E., et al., ibid 44, 2636 (1952).
15. Dinneen, G. U., et al., ibid 44, 2647 (1952).
16. Dinney, I. W., et al., Anal. Chem. 24, 1749 (1952).
17. Van Meter, R. A., et al., ibid 24, 1758 (1952).
18. Dinneen, G. U., et al., ibid 27, 185 (1955).
19. Dinneen, G. U., et al., ibid 30, 2026 (1958).
20. Heady, H. H., et al., Bureau of Mines RI 5662 (1960).

21. Morandi, J. G. and Jensen, H. B., J. Chem. Eng. Data **11**, 81 (1966).
22. Jensen, H. B., et al., PREPRINTS, Div. Fuel Chem., ACS, 12(1), F98 (1968).
23. Jensen, H. B., et al., ibid **15**(1), 113 (1971).
24. Robinson, W. E., et al., Geochim. Cosmochim. Acta **29**, 249 (1965).
25. Gelpi, E., et al., Anal. Chem. **43**, 1151 (1971).
26. Gelpi, E., et al., J. Chromatogr. Sci. **9**, 147 (1971).
27. Gallegos, E. J., Anal. Chem. **43**, 1151 (1971).
28. Anders, D. E. and Robinson, W. E., Geochim. Cosmochim. Acta **35**, 661 (1971).
29. Simoneit, B. R., et al., Chem. Geol. **7**, 123 (1971).
30. Douglas, A. G., et al., Tetrahedron **27**, 1071 (1971).
31. Djuricic, M., et al., Geochim. Cosmochim. Acta **35**, 1201 (1971).
32. Hang, P., et al., Chem. Geol. **7**, 213 (1971).
33. Maxwell, J. R., et al., Geochim. Cosmochim. Acta **37**, 297 (1973).
34. Anders, D. E., et al., ibid **37**, 1213 (1973).
35. Gallegos, E. J., Anal. Chem. **45**, 1399 (1973).
36. Lowry, H. H., (editor), CHEMISTRY OF COAL UTILIZATION, Supplement Volume, John Wiley and Sons, Inc., New York (1963).
37. Van Krevelen, D. W., COAL, Elsevier, New York (1961).
38. Seglin, L. and Eddinger, R. T., ENCYCLOPEDIA OF CHEMICAL TECHNOLOGY, Supplement Volume, "Coal (To Synthetic Crude Oil)", Second Edition, (1971), page 178.
39. Speight, J. G., APPLIED SPECTROSCOPY REVIEWS, Vol. 5, Brame, E. G., Jr., Editor, Marcel Dekker, Inc., New York (1972), page 211.
40. Jewell, D. M., et al., PREPRINTS, Div. Petrol. Chem., ACS, No. 2, F81 (1972).
41. O'Connor, J. G., et al., Anal. Chem. **34**, 82 (1962).
42. Jewell, D. M., et al., ibid **44**, 2318 (1972).

43. Mayer, T. J., et al., PREPRINTS, Div. Petrol. Chem., ACS, 17(4), F14 (1972).
44. Hood, A. and O'Neal, M. J., ADVANCES IN MASS SPECTROMETRY, J. D. Waldron (Editor), Pergamon Press, New York (1959), page 175.
45. Clutter, D. R., et al., Anal. Chem. 44, 1395 (1972).
46. Jewell, D. M., et al., ibid 44, 1391 (1972).
47. McKay, J. F. and Latham, D. R., ibid 44, 2132 (1972).
48. Herdy, L. A., et al., Coal Sci., ACS, "Advances in Chemistry Series", 55, 493 (1966).
49. Heredy, L. A., et al., Fuel, London 44, 25 (1965).
50. Chatterjee, A. K. and Mazundar, B. K., ibid 47, 93 (1965).
51. Ouchi, K. and Brooks, J. D., ibid 46, 367 (1967).
52. Bartle, K. D. and Smith, J. A., ibid 44, 109 (1965).
53. Lawson, G. J. and Purdie, J. W., ibid 45, 115 (1966).
54. Davies, L. and Lawson, G. J., ibid 46, 95 (1967).
55. Chakrabarthy, S. K. and Kretschmen, H. O., ibid 51, 160 (1972).
56. Vahrman, Mark, ibid 49, '5 (1970).
57. Rahman, M. and Vahrman, M., ibid 50, 318 (1971).
58. Palmer, T. J. and Vahrman, M., ibid 51, 14 (1972).
59. Palmer, T. J. and Vahrman, M., ibid 51, 22 (1972).
60. Vahrman, M. and Watts, R. H., ibid 51, 130 (1972).
61. Vahrman, M. and Watts, R. H., ibid 51, 235 (1972).

TABLE I  
ANALYSIS OF COAL SAMPLES

Coal Sources	Pittsburgh Seam	Big Horn, Wyoming
Rank	Bituminous	Subbituminous
<b>Proximate Analysis(wt. %)</b>		
Moisture	2.5	19.6
Volatile Matter	33.4	34.0
Fixed Carbon	57.4	41.2
Ash	6.7	5.2
<b>Chemical Analysis(wt. %)</b> (Moisture Free Basis)		
Carbon	78.68	69.15
Hydrogen	4.96	4.69
Nitrogen	1.57	1.23
Oxygen (Difference)	6.29	17.75
Sulfur	1.65	0.72
Ash	6.87	6.46

TABLE II

Sample Description	SEPARATION DATA (Weight Percent)									
	Tar Sands		Coal Liquids		Coal		Shale Oils			Cut III
	Bitumen	Big Horn	Coal	Pitt Seam	Coal	Cut I	Cut II	Cut III		
Boiling Range, °F	600+	130+	130+	130+	100.0	100.0	140-540	540-680	660+	57.0
Fraction of Total Sample	100.0	100.0	100.0	100.0	100.0	100.0	32.6	10.4	66.5	0.0
Distillate (B.P. <470°F)	0.0	28.3	25.2	25.2	0.0	0.0	66.5	2.7	14.3	0.0
Saturates*	0.0	14.0	14.2	14.2	0.0	0.0	14.3	-	33.9	0.0
Aromatics*	0.0	14.2	10.8	10.8	0.0	0.0	18.3	-	18.3	0.0
Olefins*	0.0	0.1	0.2	0.2	0.0	0.0	33.5	97.3	6.0	12.3
Residue (B.P. >470°F)	100.0	71.7	74.8	74.8	100.0	100.0	14.7	27.0	14.7	15.8
Saturates	16.5	3.6	1.8	1.8	0.0	0.0	8.3	8.0	4.2	5.3
Aromatics	47.8	58.3	36.2	36.2	0.0	0.0	2.3	5.6	12.1	68.6
Monoaromatics	7.0	9.0	5.9	5.9	0.0	0.0	0.7	0.8	0.7	3.3
Di- + Triaromatics	30.1	42.0	26.7	26.7	0.0	0.0	<0.1	<0.1	<0.1	<0.1
Polyaromatics	10.7	7.3	3.6	3.6	0.0	0.0	5.5	38.6	5.5	5.5
Resins (Non-hydrocarbons)	25.9	8.3	11.1	11.1	0.0	0.0	0.0	0.0	0.0	0.0
Asphaltenes	9.8	1.5	20.3	20.3	0.0	0.0	0.0	0.0	0.0	0.0
Benzene Insolubles	<0.1	<0.1	5.5	5.5	0.0	0.0	0.0	0.0	0.0	0.0

\* By FIA, ASTM D 1319.

TABLE III

CHEMICAL ANALYSIS AND MOLECULAR WEIGHTS OF TAR  
SANDS BITUMEN, COAL LIQUIDS, AND THEIR FRACTIONS

	<u>Mol.</u> <u>Wt.</u>	<u>C</u> <u>Wt. %</u>	<u>H</u> <u>Wt. %</u>	<u>N</u> <u>Wt. %</u>	<u>O</u> <u>Wt. %</u>	<u>S</u> <u>Wt. %</u>
<u>Tar Sands Bitumen</u>	-	82.98	10.42	0.42	1.15	4.60
Saturates	365	86.00	14.00	--	--	--
Aromatics	460	--	--	--	--	--
Monoaromatics	360	88.55	11.36	--	--	--
Di- +Triaromatics	365	85.04	9.45	0.02	1.14	3.80
Polyaromatics	1,400	79.36	9.57	0.42	3.40	6.89
Resins	1,300	81.15	9.04	1.34	3.35	5.31
Asphaltenes	5,100	78.84	7.80	1.19	4.53	8.46
 <u>Big Horn Coal Liquids</u>	 -	 89.18	 8.97	 0.40	 1.03	 0.04
Saturates	300	86.12	13.65	--	--	--
Aromatics	222					
Monoaromatics	285	88.09	10.10	0.06	1.82	0.00
Di- +Triaromatics	220	92.38	7.13	0.01	0.80	0.15
Polyaromatics	-	84.19	6.60	0.20	7.80	0.97
Resins	380	83.84	7.09	1.62	7.15	0.30
Asphaltenes	-	87.37	6.06	1.25	4.92	0.62
Benzene Insolubles	-	--	--	--	--	--
 <u>Pitt Seam Coal Liquids</u>	 -	 89.05	 8.18	 0.82	 1.47	 0.17
Saturates	-	85.40	14.17	--	--	--
Aromatics	240	--	--	--	--	--
Monoaromatics	290	--	--	--	--	--
Di- +Triaromatics	235	92.52	7.20	0.01	0.67	0.35
Polyaromatics		--	--	0.05	7.75	0.34
Resins	440	81.30	7.33	1.37	5.77	0.42
Asphaltenes	775	87.73	6.86	1.76	3.92	0.38
Benzene Insolubles	-	85.87	5.46	2.12	5.64	0.57

TABLE IV

 CHEMICAL ANALYSIS AND MOLECULAR WEIGHTS OF  
 SHALE OIL FRACTIONS

	Mol. Wt.	C Wt. %	H Wt. %	N Wt. %	O Wt. %	S Wt. %
<u>Cut I, Total</u>	145 <sup>a</sup>	85.30	12.12	0.98	0.98	0.80
Distillate	130 <sup>a</sup>	85.99	12.50	0.63	0.99	0.75
Saturates	230 <sup>a</sup>	85.84	14.31	--	--	--
Aromatics	170 <sup>b</sup>	85.44	10.09	0.25	2.17	2.05
Monoaromatics	240 <sup>b</sup>	83.26	11.65	<0.01	4.80	<0.01
Di- +Triaromatics	190 <sup>b</sup>	86.35	8.27	0.02	5.06	<0.01
Polyaromatics	200 <sup>b</sup>	76.89	9.76	0.35	10.52	2.46
Resins	445	75.89	8.38	1.28	10.82	3.44
<u>Cut II, Total</u>	260	84.68	11.07	2.10	1.23	0.68
Saturates	266 <sup>a</sup>	85.99	14.34	--	--	--
Aromatics	325	--	--	--	--	--
Monoaromatics	390	86.61	12.07	<0.01	1.67	<0.01
Di- +Triaromatics	290	87.79	9.26	<0.01	1.70	1.84
Polyaromatics	-	78.97	9.58	0.71	9.12	0.39
Resins	420	78.44	8.66	2.63	7.36	2.04
Asphaltenes	-	--	--	--	--	--
<u>Cut III, Total</u>	420	84.65	10.17	2.97	1.68	0.78
Saturates	390	85.61	14.25	--	--	--
Aromatics	-	84.35	10.40	<0.01	4.44	0.90
Monoaromatics	-	84.14	11.85	<0.01	4.49	<0.01
Di- +Triaromatics	370	86.23	9.54	0.08	1.75	1.73
Polyaromatics	-	--	--	0.84	6.25	0.50
Resins	950	79.95	8.56	2.50	3.58	0.93
Asphaltenes	c	83.12	7.45	4.63	4.23	0.49

<sup>a</sup>From GLC data.<sup>b</sup>From low voltage mass data.<sup>c</sup>Will not dissolve in benzene.

TABLE V  
SIMULATED  
DISTILLATION DATA

IBP, °F	COAL LIQUIDS						SHALE OILS					
	Tar Sand Bitumen Saturates	Big Horn		Pitt Seam		Distill- late From	Saturates		Distill- late From	Saturates		
		Total Distillates	Heavy Saturates	Total Distillates	Heavy Saturates		Cut I	Cut II		Cut I	Cut II	
1% off at	402	136	460	132	440	118	433	481	491	433	481	491
5	460	170	480	170	457	146	443	517	545	443	517	545
10	504	197	520	195	501	174	463	562	621	463	562	621
20	557	223	539	215	532	204	480	576	659	480	576	659
30	601	273	569	247	563	235	498	600	697	498	600	697
40	629	326	598	289	592	261	515	613	749	515	613	749
50	670	367	622	335	633	289	531	624	779	531	624	779
60	706	394	647	371	667	312	545	630	806	545	630	806
70	743	420	690	404	710	342	557	641	824	557	641	824
80	786	450	728	431	760	361	565	657	848	565	657	848
90	828	483	769	470	798	391	572	682	879	572	682	879
95	870	532	814	520	858	435	585	703	918	585	703	918
99	891	564	849	551	897	465	594	736	956	465	594	736
FBP	940	623	894	602	984	516	615	797	1,014	615	797	1,014
	954*	696	917*	664	1,016*	563	634	831	1,094	563	634	831

\* GLC trace does not return to base line indicating material boiling higher than 1,000°F.

Table VI  
 MASS SPECTROMETRIC ANALYSIS OF SATURATES  
 (Volume Percent)

Weight % of Frac. in Sample	Tar Sand Bitumen	COAL LIQUIDS			SHALE OILS		
		Big Horn Coal	Pitt Seam Coal	Coal	Cut I	Cut II	Cut III
16.5	3.6	1.8			6.0	31.0	12.3
Alkanes	0.0	39.9	22.0		42.2	34.4	29.4
Noncondensed Cycloalkanes	48.0	23.8	43.9		40.8	47.1	46.2
Condensed Cycloalkanes	47.9	32.2	30.4		15.4	16.6	22.5
2 Rings	26.7	16.3	16.2		11.3	11.8	8.9
3 Rings	14.0	9.5	7.2		3.8	4.0	11.1
4 Rings	6.5	4.1	4.2		0.3	0.9	2.5
5 Rings	0.7	1.4	1.7		0.0	0.0	0.0
6 Rings	0.0	0.9	1.1		0.0	0.0	0.0
Benzenes*	4.0	3.8	3.3		1.6	1.8	1.8
Napthalenes*	0.1	0.2	0.4		0.0	0.0	0.1

\*Artifacts due to the fragmentation of certain cycloparaffins.

TABLE VII

<sup>1</sup>H NMR ANALYSIS OF AROMATIC FRACTIONS

Sample Fraction	Tar Sands Bitumen			Big Horn Coal		Pitt Seam Coal	
	Mono-	Di- + Tri-	Poly-	Mono-	Di- + Tri-	Mono-	Di- + Tri-
Wt. % of Fraction in Sample	7.0	30.1	10.7	9.0	42.0	5.9	26.7
Monoaromatics, Mole %	100.0	53.7	49.1	100.0	16.4	100.0	15.6
Diaromatics, Mole %	0.0	46.3	50.9	0.0	69.7	0.0	63.5
Triaromatics, Mole %	0.0	<0.1	<0.1	0.0	13.8	0.0	21.0
Aromaticity, C <sub>A</sub>	0.24	0.37	0.27	0.39	0.76	0.37	0.73
Average Molecular Weight*	339	284	404	204	169	218	181
Alkyl Substituents/Molecule	3.5	3.5	4.4	3.4	1.8	4.0	2.1
Carbons/Alkyl Substituents	5.3	3.7	4.9	2.7	1.7	2.6	1.8
Aromatic Rings/Molecule	1.0	1.5	1.5	1.0	2.0	1.0	2.1
Naphthene Rings/Molecule	1.4	0.9	1.5	1.3	0.3	1.5	0.4

\*Does not account for O, N, S, etc.

TABLE VIII

<sup>1</sup>H NMR ANALYSIS OF AROMATIC SHALE OIL FRACTIONS

Sample Fraction	Cut I			Cut II			Cut III		
	Mono-	Di-+Tri-	PNA	Mono-	Di-+Tri-	PNA	Mono-	Di-+Tri-	PNA
Wt. % of Fraction in Sample	8.3	4.2	2.3	8.0	13.4	5.6	5.3	9.3	1.3
Monoaromatics, Mole %	100.0	38.2	81.0	100.0	52.8	84.3	100.0	55.0	56.4
Diaromatics, Mole %	0.0	61.8	19.0	0.0	47.2	15.7	0.0	35.5	28.5
Triaromatics, Mole %	0.0	0.0	0.0	0.0	0.0	0.0	0.0	9.5	15.1
Aromaticity, CA	0.20	0.61	0.32	0.26	0.51	0.29	0.18	0.44	0.44
Average Molecular Weight*	413	183	283	316	204	311	448	248	248
Alkyl Subst./Molecule	4.4	3.3	4.6	4.0	3.6	5.2	5.4	3.9	5.5
Carbons/Alkyl Subst.	5.5	1.6	3.1	4.3	2.1	3.2	5.0	2.7	1.9
Aromatic Rings/ Molecule	1.0	1.6	1.2	1.0	1.5	1.2	1.0	1.5	1.6
Naphthene Rings/Molecule	2.5	0.4	1.1	1.5	0.5	1.2	2.2	0.7	0.3

\*Does not account for N, O, S, etc.

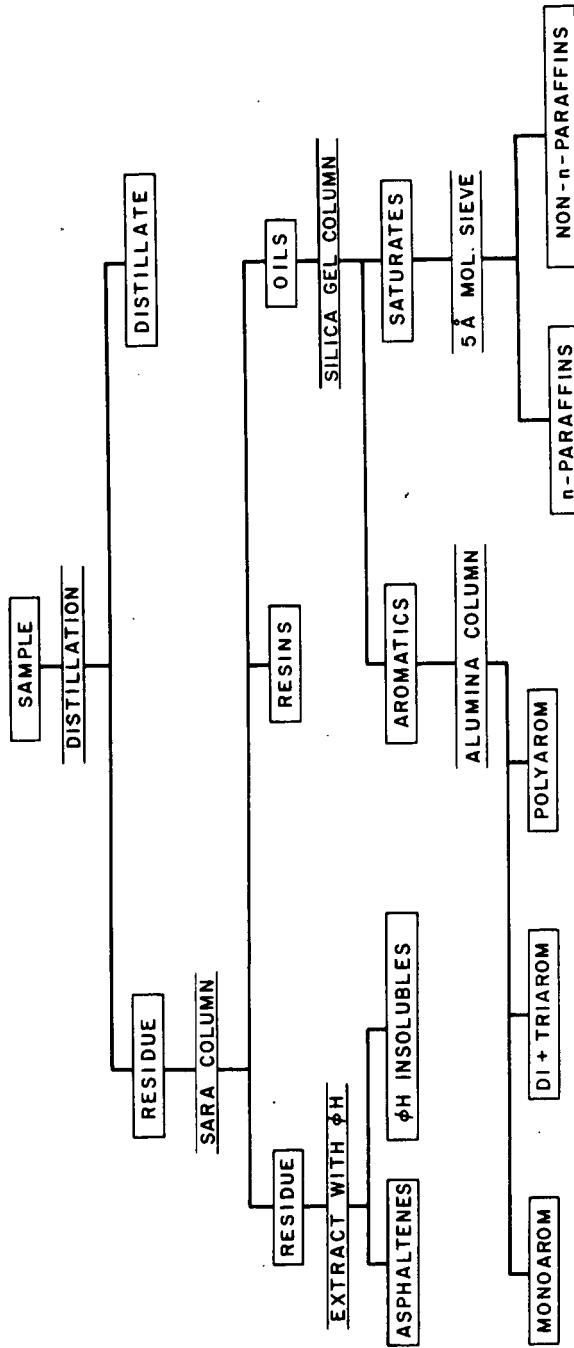
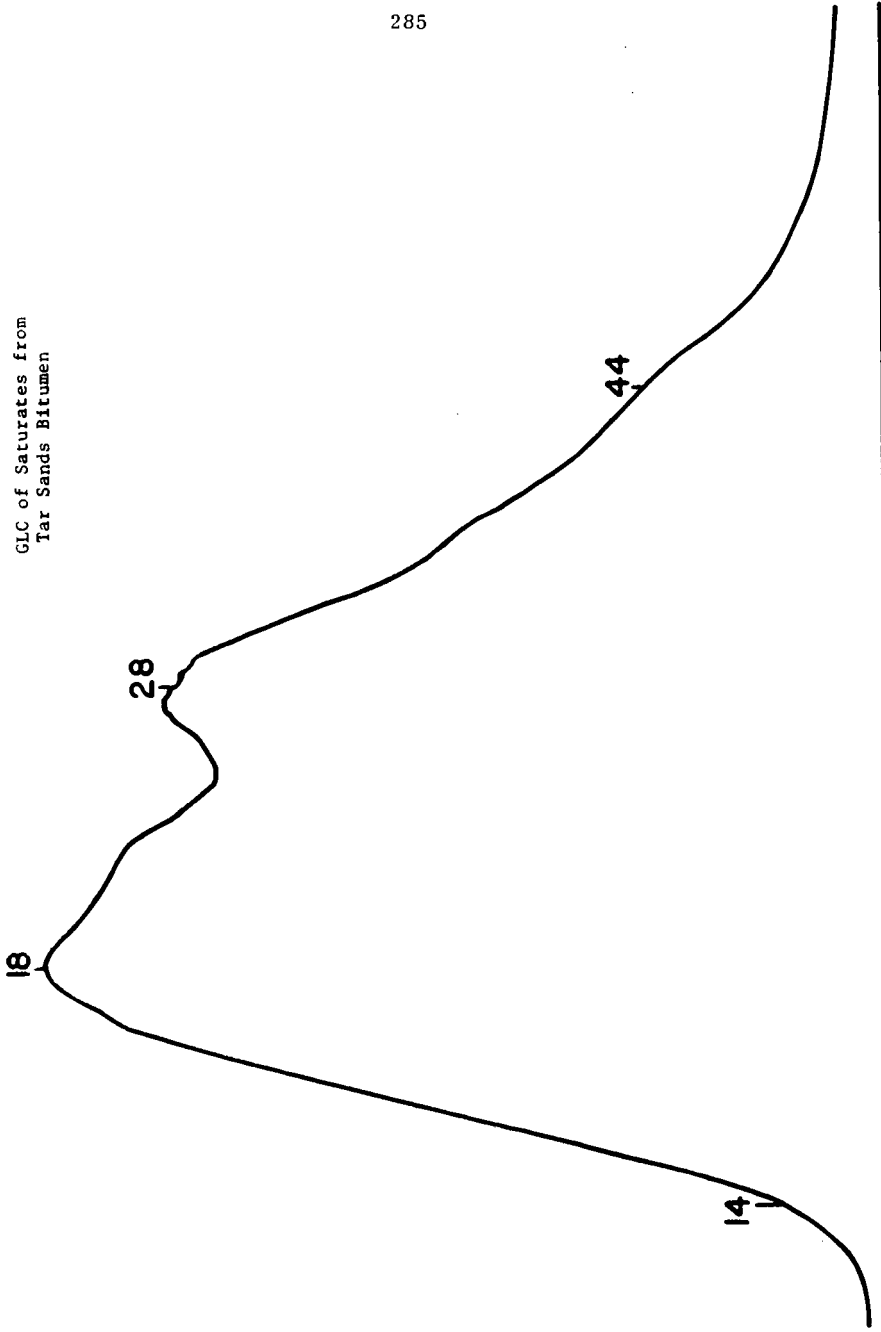
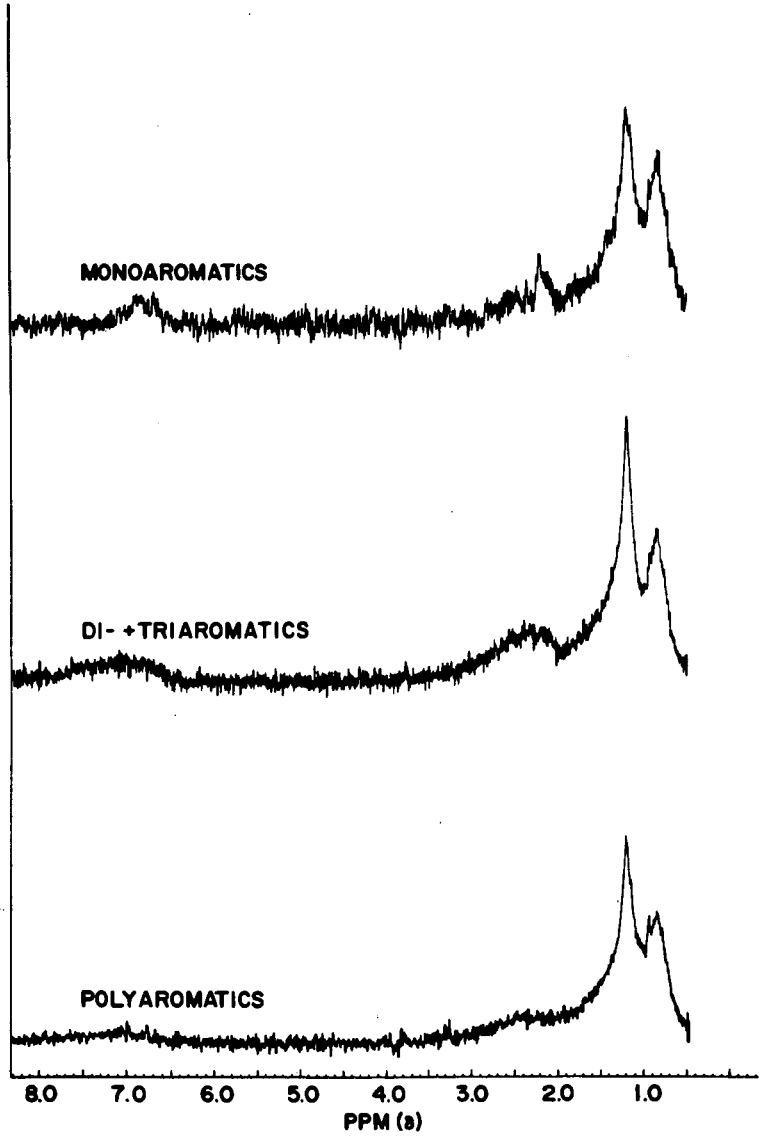


FIGURE 1.

Separation Scheme

FIGURE 2.  
GLC of Saturates from  
Tar Sands Bitumen



**<sup>1</sup>H NMR SPECTRA OF AROMATIC FRACTIONS  
FROM TAR SANDS BITUMEN**

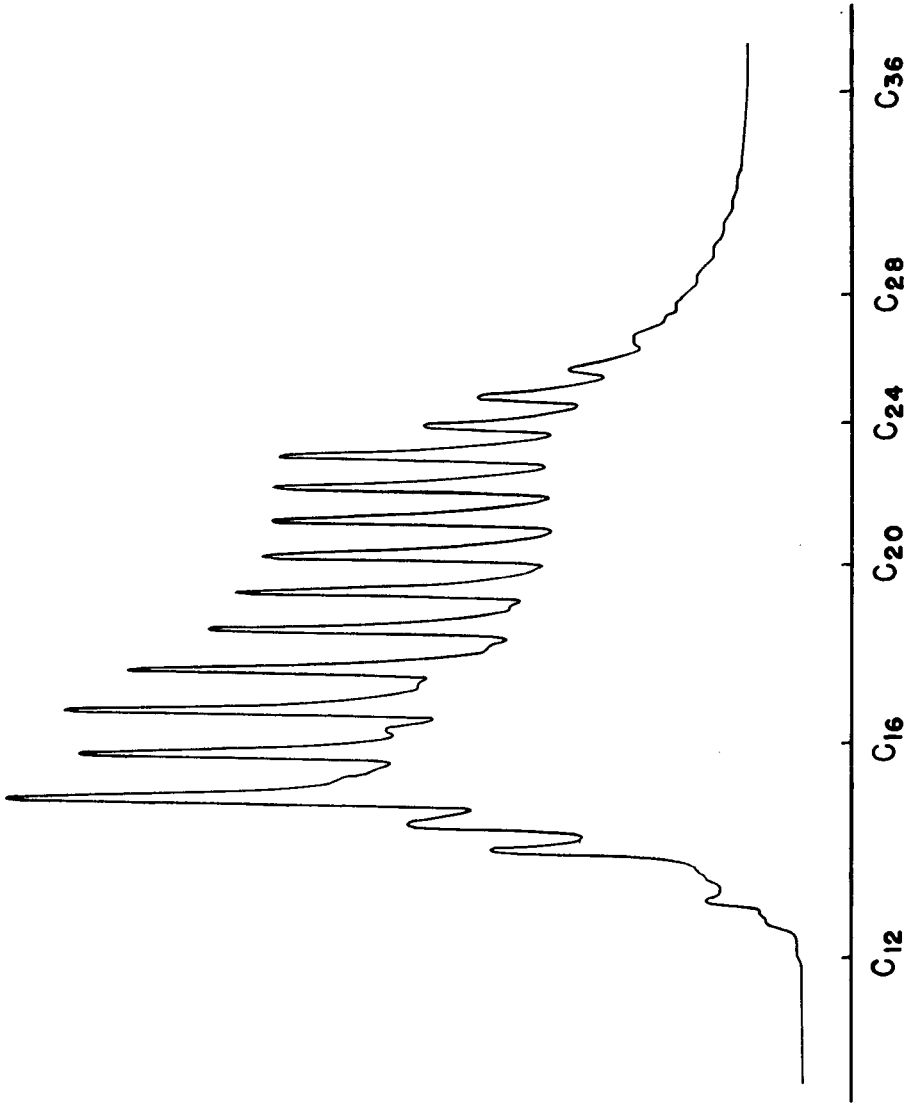


FIGURE 4.  
GLC of Saturates from Big  
Horn Coal Liquids

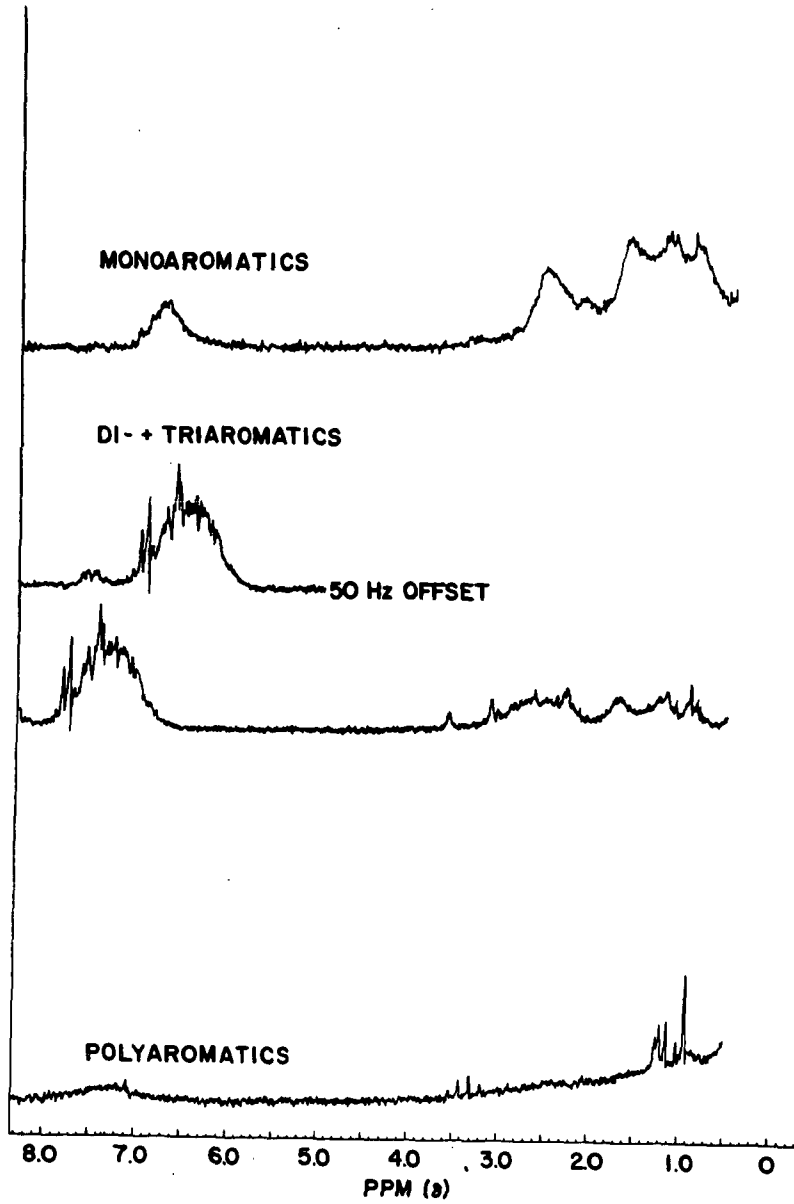
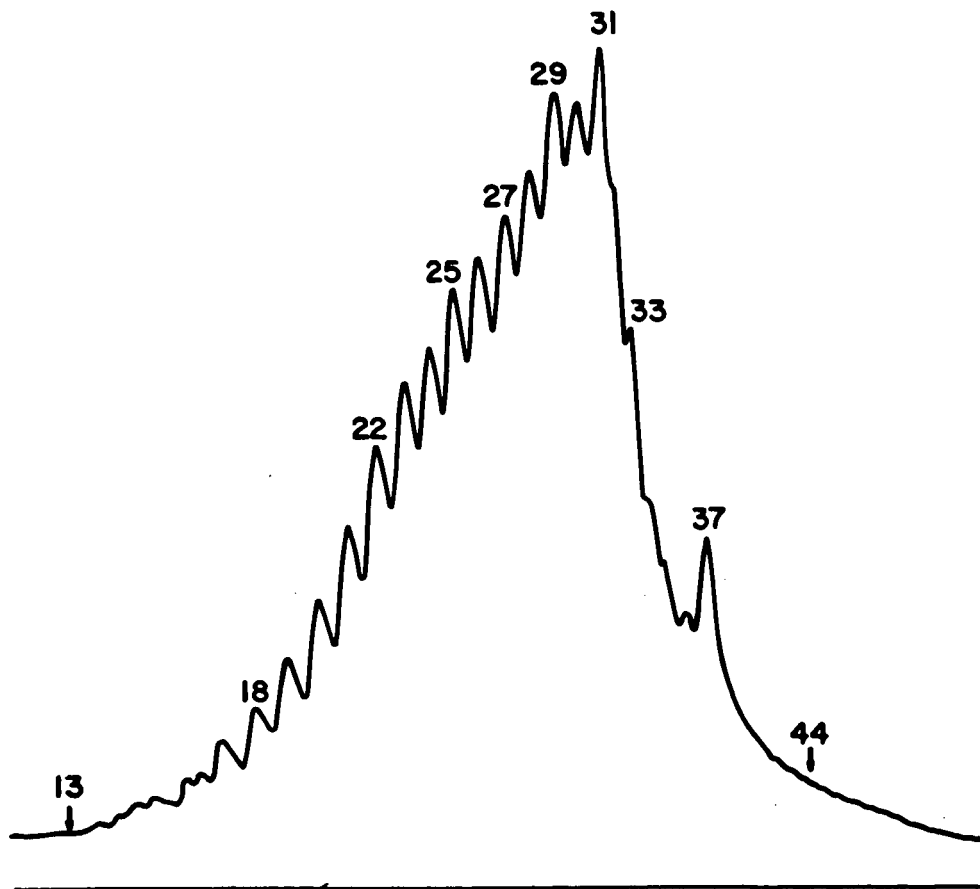
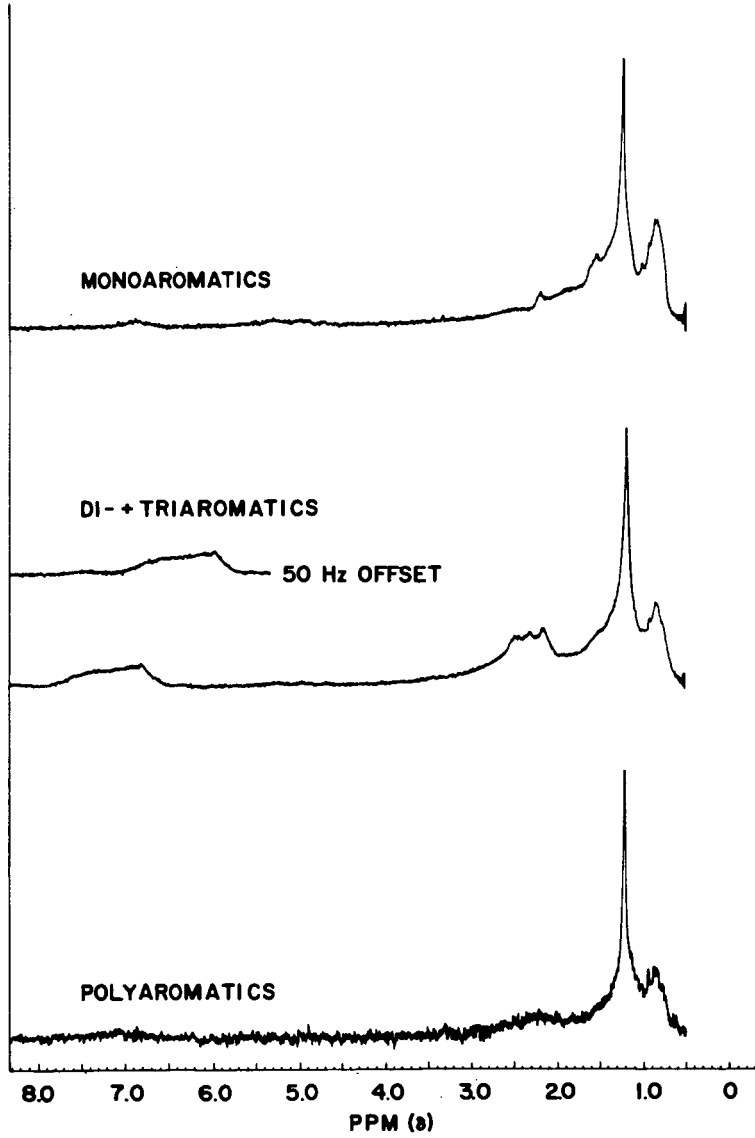
**<sup>1</sup>H NMR SPECTRA OF AROMATIC FRACTIONS  
FROM COAL LIQUIDS**

FIGURE 6.

# GLC OF SATURATES FROM SHALE OILS



**<sup>1</sup>H NMR SPECTRA OF AROMATIC FRACTIONS  
FROM SHALE OILS**



THE CHEMICAL MODIFICATION OF A BITUMEN  
AND ITS NON-FUEL USES

Speros E. Moschopedis and James G. Speight

Research Council of Alberta  
11315 - 87th Avenue  
Edmonton  
Alberta T6G 2C2  
Canada

The development of the Athabasca tar sands has become one of the major advances of the petroleum industry. However, it is evident that the production of materials from the bitumen is only just beginning and with the introduction of gas turbine, electric, propane autos and the like, it is possible that the future of the tar sands lies not in the production of gasoline but in the use of the bitumen as a chemical raw material. In the present communication, we report some simple chemical conversions that may be employed to introduce functional groups into the bitumen\* and some preliminary investigations on the uses of the products.

## CHEMICAL REACTIONS

As a result of structural studies, it is evident that petroleum asphaltenes are agglomerations of compounds of a particular type (1, 2). Thus, it is not surprising that asphaltenes will undergo a wide range of interactions, of chemical and physical nature, based not only on their condensed aromatic structure but also on the attending alkyl and naphthenic moieties. In the following discussion, we will again rely heavily on the evidence accumulated, for the major part, in our own laboratories, which has either been published elsewhere or is in preparation.

Oxidation

Oxidation of Athabasca asphaltenes with a series of common oxidising agents, i.e., acidic and alkaline peroxide, acidic dichromate, and alkaline permanganate, is a slow process there being < 10% of the product soluble in alkali after treatment with the oxidant for ca. 30 hr. (4). It is evident, however, from the elemental ratios in the products that some oxidation has occurred. Moreover, the occurrence of a broad band centred at  $3420\text{ cm}^{-1}$  and a weaker band at  $1710\text{ cm}^{-1}$  indicates the formation of phenolic and carboxyl groups on the asphaltene molecules. The H/C ratios of the partially-oxidised products indicate that there are two predominant oxidation routes, notably (i) the oxidation of naphthene moieties to aromatics and active methylene groups to ketones which would reduce the H/C ratios and (ii) more severe oxidation of naphthene and aromatic functions resulting in partial degradation of these systems to carboxylic acid functions whereby the overall effect is diminishing aromatic, but increasing alkane, moieties. Investigation of the partially oxidised materials by proton magnetic resonance spectroscopy (4) provides information about the structural changes which occur during the oxidation processes and an overall picture of these effects is a decrease in size of the condensed aromatic sheet as well as a slight decrease in the degree of substitution of the sheet and a decrease in average chain lengths of the alkyl substituents.

Use of a more severe oxidising agent, i.e. concentrated nitric acid, brings about good conversion of the asphaltenes to water- and alkali-soluble materials (5).

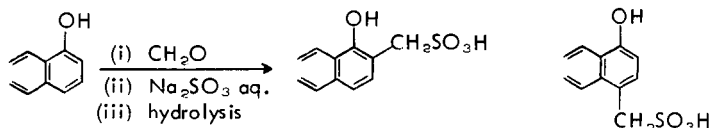
---

\* For convenience, we describe the reactions of the asphaltenes - a fraction considered somewhat useless (except for fuel purposes) by many workers.

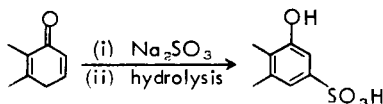
### Sulphonation and Sulphomethylation

Sulphomethylation and/or sulphonation of the asphaltenes are not feasible processes because of the lack of functional groups within the asphaltene molecule. Nevertheless, oxidation of the asphaltenes does produce the necessary functional groups and subsequently sulphomethylation and sulphonation can be conveniently achieved (5). Confirmation that sulphomethylation and sulphonation of the oxidized asphaltenes occurs can be obtained from three sources, namely, (i) overall increases in the sulphur contents of the products relative to that of the starting material; (ii) the appearance of a new infrared absorption band at  $1030\text{ cm}^{-1}$  attributable to the presence of sulphonic acid group(s) in the molecule(s) (6); and (iii) the water-solubility of the products – a characteristic of this type of material (7, 8). These sulphomethylated and sulphonated oxidized asphaltenes even remain in solution after acidification with 5% aqueous hydrochloric acid to a pH of 2.5–3.0, while the parent oxidized asphaltenes can be precipitated from alkaline solution by acidification to a pH of 6.5.

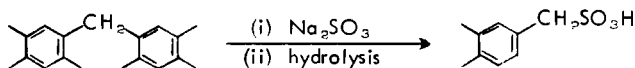
The facile sulphomethylation reaction indicates the presence in the starting materials of reactive sites ortho or para to a phenolic hydroxyl group, e.g.:



while the comparative ease of sulphonation suggests the presence of quinoid structures in the oxidized materials, e.g.:



Alternatively, active methylene groups in the starting materials would facilitate sulphonation by:



since such groups have been known to remain intact after prolonged oxidation (9).

### Halogenation

Halogenation of the asphaltenes occurs readily to afford the corresponding halo-derivatives (10) and is accompanied by weight increases in the products. The physical properties of the halogenated materials are markedly different from those of the parent asphaltenes. For example, the unreacted asphaltenes are dark brown, amorphous, and readily soluble in benzene, nitrobenzene, and carbon tetrachloride but the products are black, shiny, and only sparingly soluble, if at all, in these solvents.

There are also several features whereby the individual halogen reactions differ from one another. For example, during chlorination there is a cessation of chlorine uptake by the asphal-

tenes after 4 hours. Analytical data indicate that more than 37% of the total chlorine in the final product is introduced during the first 0.5 hour, reaching the maximum after 4 hours. Furthermore, the H/C ratio of 1.22 in the parent asphaltenes [ (H + Cl)/C ratio in the chlorinated materials ] remains constant during the first two hours of chlorination, by which time chlorination is 88% complete. This is interpreted as substitution of hydrogen atoms by chlorine in the alkyl moieties of the asphaltenes while the condensed aromatic sheets remain unaltered since substitution of aryl hydrogens only appears to occur readily in the presence of a suitable catalyst, e.g.  $\text{FeCl}_3$ , or at elevated temperatures. It is only after more or less complete reaction of the alkyl chains that addition to the aromatic rings occurs as evidenced by the increased (H + Cl)/C ratios in the final stages of chlorination.

Bromine uptake by the asphaltenes is also complete in a comparatively short time (< 8 hr.). However, in contrast to the chlorinated products, the (H + halogen)/C ratio remains fairly constant (1.23 and 1.21 in the bromo-asphaltenes, cf. 1.22 in the unreacted asphaltenes) over the prolonged periods (up to 24 hr.) of the bromination.

Iodination of the asphaltenes is different insofar as a considerable portion of the iodine, recorded initially as iodine uptake, can be removed by extraction with ether or with ethanol whilst very little weight loss is recorded after prolonged maintenance of the material in a high vacuum. The net result is the formation of a product with a (H + I)/C ratio of 1.24 after 8 hr. reaction whilst a more prolonged reaction period affords a product having a (H + I)/C ratio of 1.17. This latter result may be interpreted as iodination of the alkyl or naphthenic moieties of the asphaltenes with subsequent elimination of hydrogen iodide. Alternatively, oxidation of naphthenic moieties to aromatics or oxidative coupling of asphaltene nuclei would also account for lower (H + I)/C ratios. In fact, this latter phenomenon could account, in part, for the insolubility of the products in solvents which are normally excellent for dissolving the unchanged asphaltenes.

Halogenation of the asphaltenes can also be achieved by use of sulphonyl chloride, iodine monochloride, and N-bromosuccinimide or via the Gomberg reaction (11), whereby products similar to those described above are produced.

Attempted water-solubilization of the asphaltenes by treatment of the halo-derivatives with aqueous sodium hydroxide or with aqueous sodium sulphite is not a feasible process (11). Indeed, the hydrolyzed products remained insoluble in strongly alkaline solution. That partial reaction occurs is evident from the decreased (H + Cl)/C ratios and the increased O/C ratios of the products relative to those of the parent halo-asphaltenes. The infrared spectra of the products showed a broad band centered at  $3450 \text{ cm}^{-1}$ , assigned to the presence of hydroxyl groups in the products, but it was not possible to establish conclusively the presence of sulphonic acid group(s) in the product from the sodium sulphite reaction by assignment of infrared absorption bands to this particular group.

#### Reactions with Metal Salts

Interactions of asphaltenes with the metal chlorides yield products containing organically-bound chlorine but the analytical data are indicative of dehydrogenation processes occurring simultaneously (12). There is, of course, no clear way by which the extent of the dehydrogenation can be estimated but it may be suggested that it is a dehydrogenation condensation rather than elimination with olefin formation; infrared spectroscopy did not show any bands that could be unequivocally assigned to  $\text{C}=\text{C}$  bond vibrations, nor did proton magnetic resonance (p.m.r.) spectroscopy show any olefinic protons. Thus, the mode of dehydrogenation is assumed to involve predominantly inter- or intramolecular condensation reactions insofar as the solubilities and

apparent complexities of the products varied markedly from those of the starting materials and these differences could not be attributed wholly to the incorporation of chlorine atoms into the constituents of the asphaltenes or heavy oil. Indeed, the data accumulated are indicative of a condensation dehydrogenation or, in part, loss of alkyl substituents as, for example, lower molecular weight hydrocarbons during the reactions. As an illustration of the former, the cokes produced during the thermal cracking (450°C) of the asphaltenes or heavy oil have H/C ratios in the range 0.59 - 0.77 (16), while the majority of the insoluble materials produced in the asphaltene/metal chloride reactions have only slightly higher (H + Cl)/C ratios (0.88 - 1.10).

#### Reactions with Sulphur and Oxygen

Reactions of asphaltenes with sulphur and oxygen have also received some attention and have yielded interesting results (13). For example, treatment of the asphaltenes with oxygen or with sulphur at 150 - 250°C yields a condensed aromatic product [H/C = 0.97, cf. H/C (asphaltene) = 1.20] containing very little additional oxygen or sulphur. The predominant reaction here appears to be condensation between the aromatic and aliphatic moieties of the asphaltenes effected by elemental oxygen and sulphur which are in turn converted to hydrogen sulphide and water. In the former case, i.e. with oxygen, condensation appears to precede in preference to molecular degradation but we note that prolonged reaction times afford lower molecular weight products. Treatment of the condensed products at 200 - 300°C for 1-5 hr. again affords good grade cokes (H/C = 0.54 - 0.56). In all instances the final products contained only very low amounts of elements other than carbon and hydrogen (i.e.  $\Sigma \text{NOS} < 5\%$  w/w) - a desirable property of good grade coke.

#### Phosphorylation

Attempts to phosphorylate asphaltenes with phosphoric acid, phosphorous trichloride or phosphorous oxychloride were partially successful insofar as it is possible to introduce up to 3% w/w phosphorous into the asphaltenes (14). However, application of these same reactions to oxidised asphaltenes increases the uptake of phosphorous quite markedly there being up to 10% w/w in the products (14). Subsequent reaction of the phosphorous-containing products are necessary to counteract the acidity, where necessary, of the phosphorous moieties.

#### Hydrogenation

Montgomery and his co-workers (15, 16) studied the reduction products of tar sand asphaltenes and noted that considerable amounts of hydrogen could be added to the asphaltenes whilst some sulphur was removed. Other studies of the hydrogen processes have been performed mainly with the effects of additional hydrogen on the cracking when increased yields of paraffins were observed (3).

#### Miscellaneous Chemical Conversions

Other reactions of the asphaltenes have also been performed but the emphasis has mainly been on the formation of more condensed materials to produce good grade cokes. For example, thermal treatment of the halogenated derivatives affords aromatic cokes [H/C = 0.58, cf. coke from the thermal conversion of asphaltene at ~ 460°C has H/C = 0.77] (13, 17) containing less than 1% w/w halogen. Other investigations (13) also show that treatment of the halo-asphaltenes with suitable metal catalysts, e.g. copper at 200 - 300°C/1-5 hr. or sodium at 80 - 110°C/1-5 hr., yield aromatic (H/C = 0.55 - 0.86, respectively) coke-like materials having 0.5 - 3% w/w halogen. Residual halogen may finally be removed by treatment at 300°C for 5 hr. The implications of these investigations to the petroleum industry are many-fold but

perhaps the most significant are (a) the comparatively lower temperatures required for coking due to the presence of bonds in the asphaltenes which are relatively labile and (b) the use of oxygen or sulphur as condensing and aromatising agents without being significantly incorporated into the ensuing coke. Further work on the catalytic effects of other readily available inorganic and organic materials on the coking process are still under investigation and all of the data will be reported in detail in due course.

Other chemical modifications pursued in our laboratories include metallation of the asphaltenes or halo-asphaltenes using metal or metallo-organics followed by, for example, carboxylation to the end product. Interaction of the asphaltenes with *m*-dinitrobenzene affords an oxygen-enriched material which, when treated with hydroxylamine or an amine yields materials containing extra nitrogen. Similarly, reaction of the asphaltenes with maleic anhydride and subsequent hydrolysis yields products bearing carboxylic acid functions.

### APPLICATIONS

The traditional uses of petroleum involve the derivation of chemicals from the oil during a refinery operation. It is usual that at some stage during the operation any asphaltenes are removed either as a sludge to be discarded later or to serve as a fuel. In the foregoing discussion we have attempted to show how the asphaltenes may be regarded as chemical entities which are able to undergo a variety of chemical or physical conversions to, perhaps, more useful materials. The overall effects of these modifications is the production of materials which either afford good grade aromatic cokes comparatively easily or the formation of products bearing functional groups which may be employed as a non-fuel material. To date, our main tests have centred around the sulphonated and sulphomethylated materials and their derivatives which have satisfactorily undergone investigations for drilling mud thinners giving results comparable to those obtained with commercial mud thinners (Table 1). In addition, their ability to lower surface tension in aqueous solution indicates that these compounds may also find use as emulsifiers for the in situ recovery of the Athabasca bitumen (Table 2) (18). There are also indications that these materials and other similar derivatives of the asphaltenes, especially those containing functions such as carboxylic or hydroxyl will readily exchange cations and could well compete with synthetic zeolites. Other uses of the hydroxyl derivatives and/or the chloro-asphaltenes include high temperature packings or heat transfer media.

The reactions incorporating nitrogen and phosphorus into the asphaltenes are particularly significant at a time when the effects on the environment of many materials containing these elements are receiving considerable attention. Here we have potential slow-release soil conditioners which will only release the nitrogen or phosphorus after considerable weathering or bacteriological action. One may proceed a step further and suggest that the carbonaceous residue remaining after release of the hetero-elements may be a benefit to humus-depleted soils such as the grey-wooded and solonchic soils found in Alberta. It is also feasible that coating a conventional quick-release inorganic fertiliser with a water-soluble or water dispersible derivative will provide a slower-release fertiliser and an organic humus-like residue. In fact, variations of this theme are multiple.

Only further work will tell how practical these projected uses may be and none should be discounted as long as research continues and the need for new uses of petroleum remains.

### ACKNOWLEDGMENTS

The authors are indebted to Syncrude Canada Ltd. for gifts of bitumen.

TABLE I  
Thinning Properties and Comparison of Water-Soluble Asphaltenes with Commercial Thinners

Designation	lb/bbl	NaOH lb/bbl	CaO lb/bbl	pH	Viscosity 600 rpm	Plastic viscosity centipoise	Yield Point lb/100 sq. in.	--Gel Strength-- 10 sec	10 min
• Base Mud		2	5	12.4	77	7	63	20	32
Sulphomethy- lated asphaltene	2	-	-	11.6	17	5	7	2	3
	4	-	-	11.5	21	6	9	1	4
	6	-	-	11.5	19	7	5	0	4
Sulphonated asphaltenes	2	-	-	11.5	22	10	2	1	2
	4	-	-	11.5	18	8	2	0	1
	6	-	-	11.5	18	8	2	0	1
UNI-CAL	2	-	-	12.6	13	6	1	0	4
	4	-	-	12.6	13	6	1	0	0
	6	-	-	12.6	13	6	1	0	0
SPERCENE	2	-	-	12.6	14	5	4	3	5
	4	-	-	12.6	14	6	2	0	2
	6	-	-	12.6	19	7	5	0	7
PELTEX	2	-	-	12.5	12	5	0	0	0
	4	-	-	12.5	13	6	1	0	0
	6	-	-	12.5	12	5	2	0	2

• Aqueous suspension of 25 lb/bbl Wyoming bentonite, 5.0 lb/bbl lime, and 2.0 lb/bbl sodium hydroxide.

TABLE 2

Surface tensions of ozonised and ozonised-sulphonated bitumen

Concentration % w/w	Surface tension, dynes/cm	
	Ozonised bitumen	Ozonised-sulphonated bitumen
0.1	62	48
0.5	62	41
1.0	52	39

297  
REFERENCES

- (1) J. G. Speight, Fuel, 49, 76, (1970).
- (2) J. G. Speight, Fuel, 50, 102 (1971).
- (3) J. G. Speight, Fuel, 52, (1973) in press.
- (4) S. E. Moschopedis and J. G. Speight, Fuel, 50, 211 (1971).
- (5) S. E. Moschopedis and J. G. Speight, Fuel, 50, 34 (1971).
- (6) C.N.R. Rao, "Chemical Applications of Infrared Spectroscopy", Academic Press Inc., New York, p. 305 (1963).
- (7) S. E. Moschopedis, Canadian Patent, 722,720 (1965).
- (8) S. E. Moschopedis, U.S. Patent, 3,352,902 (1967).
- (9) S. E. Moschopedis, Fuel, 41, 425 (1962).
- (10) S. E. Moschopedis and J. G. Speight, Fuel, 50, 58 (1971).
- (11) S. E. Moschopedis and J. G. Speight, Fuel, 49, 335 (1970).
- (12) J. G. Speight, Fuel, 50, 175 (1971) and unpublished data.
- (13) S. E. Moschopedis and J. G. Speight, Fuel, 50, 332, (1971).
- (14) J. G. Speight, unpublished data.
- (15) H. Sawatzky and D. S. Montgomery, Fuel, 43, 453 (1964).
- (16) H. Sawatzky, M. L. Boyd, and D. S. Montgomery, J. Inst. Petroleum, 53, 162 (1967).
- (17) J. G. Speight, Am. Chem. Soc., Div. Fuel and Petrol. Chem., Reprints, 15, 57 (1971).
- (18) S. E. Moschopedis and J. G. Speight, companion paper presented at Symposium on "Oil Shale, Tar Sands and Related Fuel Sources, Div. Fuel Chem., Am. Chem. Soc., Los Angeles, March 31 - April 5, 1974.

TABLE I  
Thinning Properties and Comparison of Water-Soluble Asphaltenes with Commercial Thinners

Designation	lb/bbl	NaOH lb/bbl	CaO lb/bbl	pH	Viscosity 600 rpm	Plastic viscosity centipoise	Yield Point lb/100 sq. in.	--Gel Strength-- 10 sec	--Gel Strength-- 10 min
* Base Mud		2	5	12.4	77	7	63	20	32
Sulphomethy- lated asphaltrene	2	-	-	11.6	17	5	7	2	3
	4	-	-	11.5	21	6	9	1	4
	6	-	-	11.5	19	7	5	0	4
Sulphonated asphaltenes	2	-	-	11.5	22	10	2	1	2
	4	-	-	11.5	18	8	2	0	1
	6	-	-	11.5	18	8	2	0	1
UNI-CAL	2	-	-	12.6	13	6	1	0	4
	4	-	-	12.6	13	6	1	0	0
	6	-	-	12.6	13	6	1	0	0
SPERCENE	2	-	-	12.6	14	5	4	3	5
	4	-	-	12.6	14	6	2	0	2
	6	-	-	12.6	19	7	5	0	7
PELTEX	2	-	-	12.5	12	5	0	0	0
	4	-	-	12.5	13	6	1	0	0
	6	-	-	12.5	12	5	2	0	2

\* Aqueous suspension of 25 lb/bbl Wyoming bentonite, 5.0 lb/bbl lime, and 2.0 lb/bbl sodium hydroxide.

TABLE 2

Surface tensions of ozonised and ozonised-sulphonated bitumen

Concentration % w/w	Surface tension, dynes/cm	
	Ozonised bitumen	Ozonised-sulphonated bitumen
0.1	62	48
0.5	62	41
1.0	52	39

CORRELATION OF OIL SHALE PARTICLE SIZE  
TO RATE OF DISSOLUTION OF MINERAL MATRIX

Mohsen Mousavi, D. K. Young, and T. F. Yen  
Departments of Chemical Engineering and Environmental Engineering,  
University of Southern California, University Park,  
Los Angeles, California 90007

The kerogenic material present in the Green River shale (Eocene Age) is bound to a mineral matrix composed of carbonates, quartz, clays, and other minor minerals. The isolation of this organic material can, therefore, be carried out in two ways: 1) The complete disaggregation and dissolution of the mineral material, thereby freeing the largely intact kerogen. Concentrated hydrofluoric acid is the most widely used reagent in this case (1,2) since it is still the only reagent that can effectively solubilize the silicate mineral (clay and quartz) that is resistant to most chemical treatments, 2) The partial cracking of the kerogen into smaller more soluble components while leaving the majority of the mineral matrix intact. Processes such as oxidation (3), pyrolysis (4), and hydrogenation (5) all belong to the latter category.

Methods whereby the kerogen can be isolated, preferably in the form of a more directly usable fuel, from raw shale with a minimal amount of pretreatment and handling, is of obvious economic interest. Knowledge of the physical structure of the intact raw shale would supplement in the design of such methods. In particular, increase of the porosity of the raw shale, without causing extensive disaggregation of the mineral matrix, would facilitate the movement of materials through the mineral matrix. For instance in oxidation and hydrogenation the reactants (i.e., the oxidant or hydrogen) must somehow come in contact with the kerogen entrapped in the mineral matrix, while smaller organic fragments that have been broken off from the kerogen 'nucleus' (6) must somehow be released to the outside.

Scanning electron micrographs (SEM) of bioleached shale (e.g., shale that has been leached with the acid produced by sulfur oxidizing bacteria) have revealed a more pitted, spongy-appearing surface texture (7). Bioleaching removes, primarily, the carbonate minerals (dolomite and calcite) which are apparently deposited in pits (7) throughout the rest of the mineral matrix; the removal of the carbonate would therefore be expected to increase the porosity of the raw shale. The results of SEM reveal the surface effect of bioleaching only, however, the effect of bioleaching on the structure inside the raw shale could only be inferred from such results. In order to increase the understanding of the internal structural changes we have measured the kinetics of this dissolution process using several different mesh sizes of oil shale.

## EXPERIMENTAL

All shale samples used are collected from the Mahogany Ledge of the Green River formation. The shale rock was crushed and sized into three ranges, 42/60, 60/100, and 150/200. Since the effect of bioleaching is essentially that of dilute acid reaction with the carbonate material, hence for better accuracy in monitoring the acid concentration reagent grade hydrochloric acid was used instead of the acid produced by the sulfur oxidizing bacteria. The rate of dissolution of the carbonate mineral was followed by direct measurement of the weight loss and by atomic absorption measurement.

For each of the mesh size used several containers, each with 0.3 gm of raw shale and 50 ml of a HCl-KCl buffer (ionic strength ~0.1, pH ~1.28), were prepared. The reaction was allowed to progress; after a specific period of time the shale from one of the containers was quickly separated from the acid by vacuum filtration and washed thoroughly with deionized water. The shale was then dried at 100°C for at least 2 hours before weighing. The results of the weight loss in time for 42/60, 60/100, and 150/200 mesh size shale are presented in Fig. 1. Atomic absorption measurement, at 285 mμ, of the magnesium ions released, as a result of the breakdown of the dolomite portion of the raw shale, was also followed in order to confirm the results obtained from direct weight loss measurements.

#### RESULTS AND DISCUSSION

The results shown in Fig. 1 can be fitted, empirically, to the following equation

$$\frac{F}{P_0 - P} = Kt \dots\dots\dots 1)$$

where P is the percent weight loss at time, t, P<sub>0</sub> is the maximum percent weight loss, and K is a constant. By rearranging this equation into the form  $P = P_0 - P/Kt$  and plotting P versus P/t, straight lines are obtained (Fig. 2). The values of P<sub>0</sub> and K for each of the mesh ranges, as can be estimated from the y-intercept and the slope respectively, are listed below:

<u>Mesh Ranges</u>	<u>P<sub>0</sub></u>	<u>K</u>
42/60	40.7	0.59
60/100	41.0	1.10
150/200	42.8	13.3

The maximum amount of carbonate mineral (P<sub>0</sub>) that can be removed by dilute acid is apparently independent of the size of the shale particles, this is evident from the closeness of the value of P<sub>0</sub> for the different mesh ranges. The increase of the surface area, by mechanical crushing, seems only to accelerate the rate of carbonate removal while the maximum amount eventually removed by dilute acid remains relatively constant. This would indicate that the carbonate mineral is deposited at sites, presumably interspersed in the rest of the 'dilute acid resistant' mineral matrix, which are not inaccessible to chemical species (such as hydrogen ions and water molecules) in an aqueous medium. These carbonate deposit sites are therefore not isolated but can perhaps be thought of as interconnected by channels built from the 'dilute acid resistant' mineral.

The dilute acid (hydrogen ion) could come into contact with the carbonate minerals through these channels and the products (carbon dioxide, magnesium ion and calcium ions) can likewise be released to the outside. The rate of reaction of the acid with the carbonate mineral would be controlled by diffusion, of the reactant into and the products out of the shale particles, and not only by the availability of the surface of contact between the acid and carbonate. If the reaction is controlled by surface availability then the rate of carbonate removal is, for spherical particles of pure carbonate mineral, proportional to 2/3 powers of the amount of still unreacted mineral or  $dP/dt \propto (P_0 - P)^{2/3}$ . However, the presence of the 'dilute acid resistant' mineral, which separates the carbonate mineral into isolated sites connected by channels, would retard the rate of carbonate

removal so that  $dP/dt \propto (P_0 - P)^n$  where  $n > 2/3$ . The empirical Equation (1) used to fit the data for carbonate removal can be derived from  $dP/dt \propto (P - P_0)^2$ .

Atomic absorption measurements of the magnesium released, as a result of carbonate removal from shale, can also be fitted to the empirical equation  $P = P_0 - P/Kt$ , (Fig. 3). Therefore the rate of carbonate removal by diluted acid is not dependent on the surface of contact alone (such as a mothball sublimation model would predict) but that other controlling factors could be involved (diffusion was suggested as one such possible factor). Due to the obvious complexity of the controlling factors that may be involved, we shall not attempt at present to elucidate them. The existence of interconnecting channels was postulated from scanning electron micrographs of bioleached shale surface (7) and is supported by evidence from the present study. The increase of porosity by removing the carbonate mineral with dilute acid would, presumably, improve the permeability of certain chemical species into and out of the remaining shale structure.

#### ACKNOWLEDGEMENT

This work is supported by NSF Grant No. GI-35683.

#### REFERENCES

1. W. E. Robinson, in Organic Geochemistry, (G. Elington and H. F. J. Murphy, eds.), Springer-Verlag, Berlin, 1969, Chap. 6, pp. 181-195.
2. J. D. Saxby, Chem. Geol., **6**, 173-184 (1970).
3. W. E. Robinson, D. L. Lawlor, J. J. Cummins, and J. I. Fester, Bureau of Mines Rept. of Invest. 6166 (1963).
4. G. U. Dinneen, Chemical Engineering Progress Symposium Series, **61(54)**, 42-47 (1965).
5. E. B. Shultz, Jr., Chemical Engineering Progress Symposium Series, **61(54)**, 48-59 (1965).
6. M. Djuricic, R. C. Murphy, D. Vitorovic, and K. Biemann, Geochimica et Cosmochimica Acta, **35**, 1201 (1971).
7. W. C. Meyer and T. F. Yen, The Effects of Bioleaching on Green River Oil Shale, this preprint, 1974.

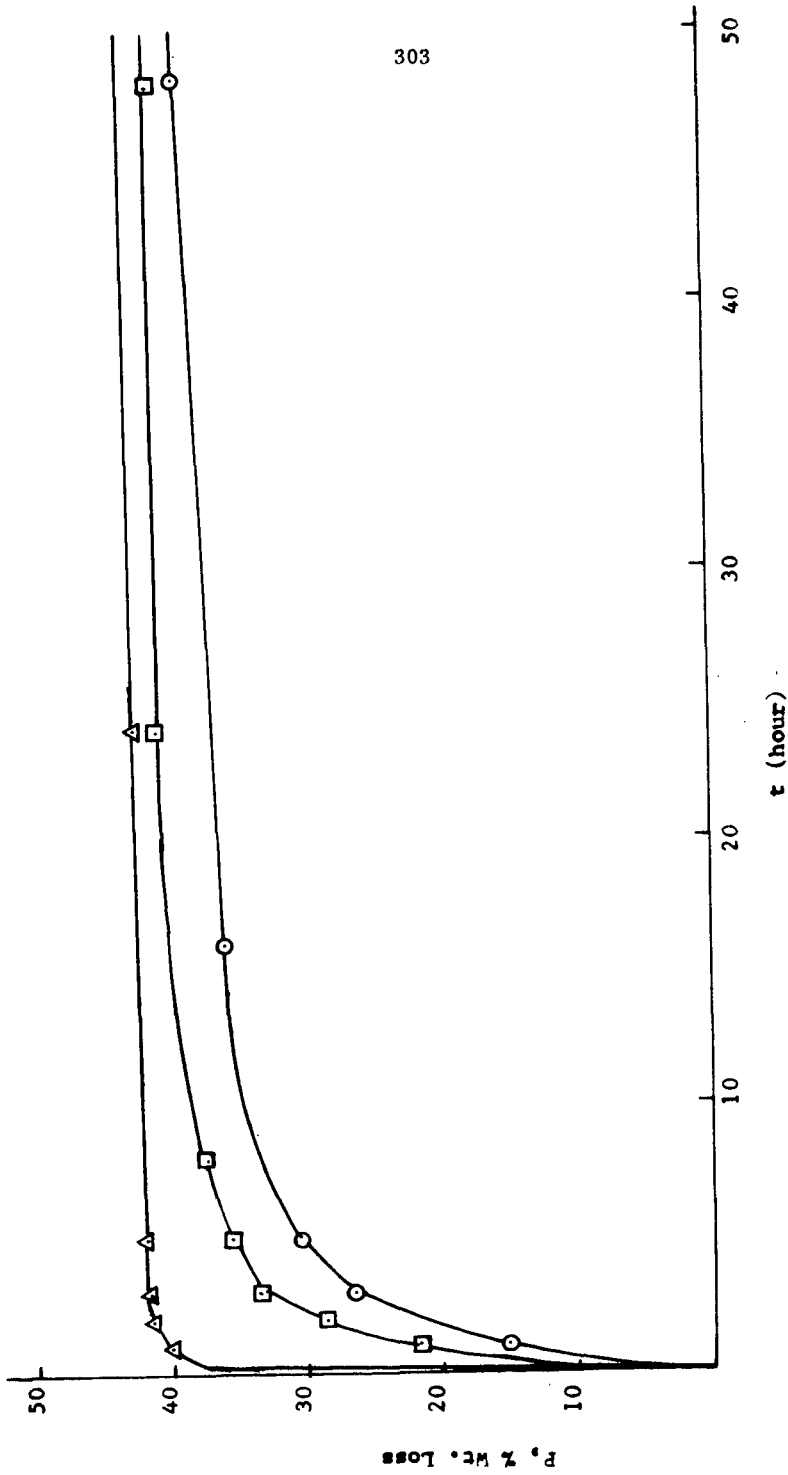


Fig. 1. Rate of weight loss of Green River Oil Shale in dilute acid (the round points indicate 42/60; the square points indicate 60/100; and the triangular points indicate 150/200; all in mesh sizes).

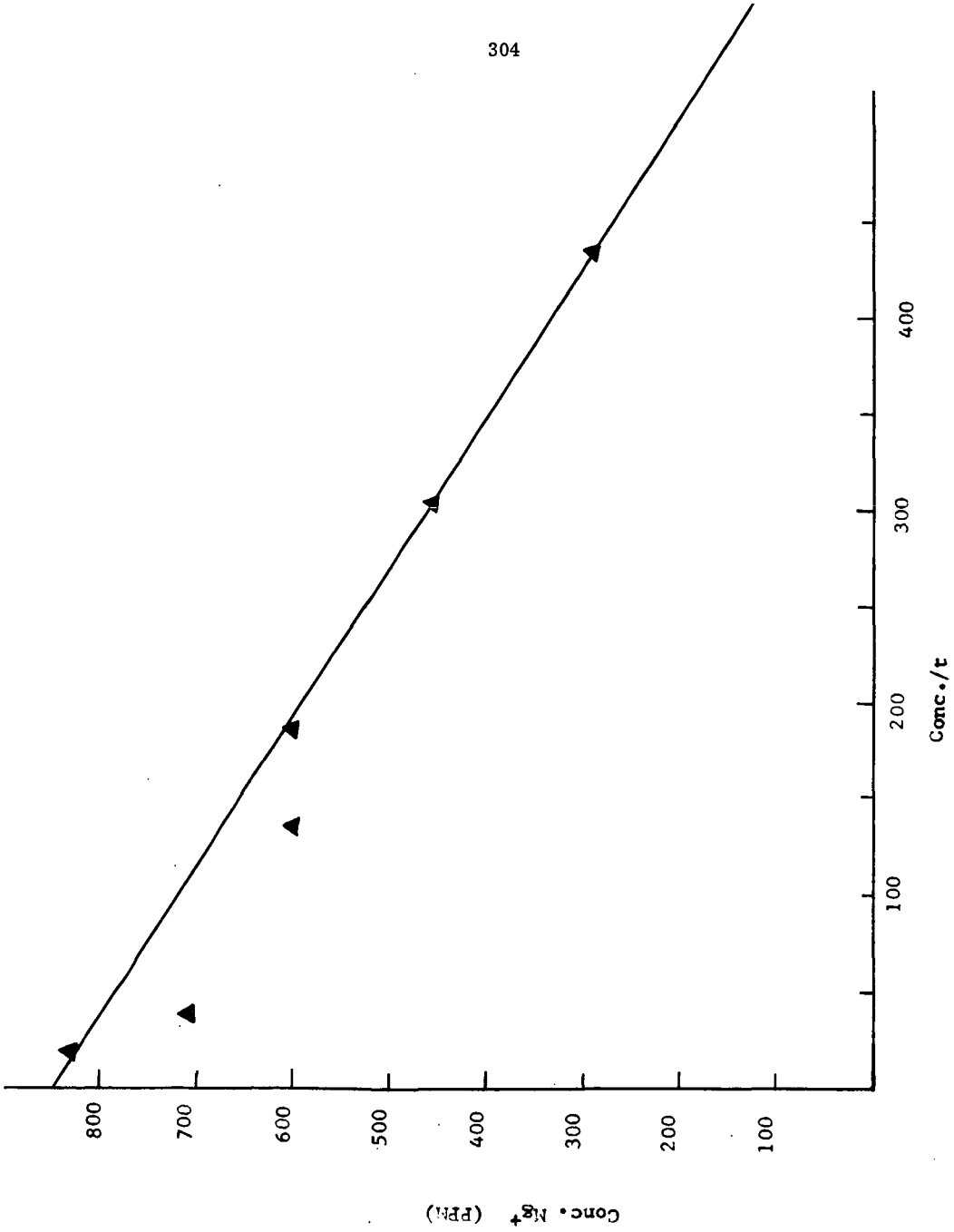


Fig. 3. Magnesium ion released from Green River oil shale by leaching with HCl. The mesh size used is 16/42. Concentration is determined by atomic absorption method.

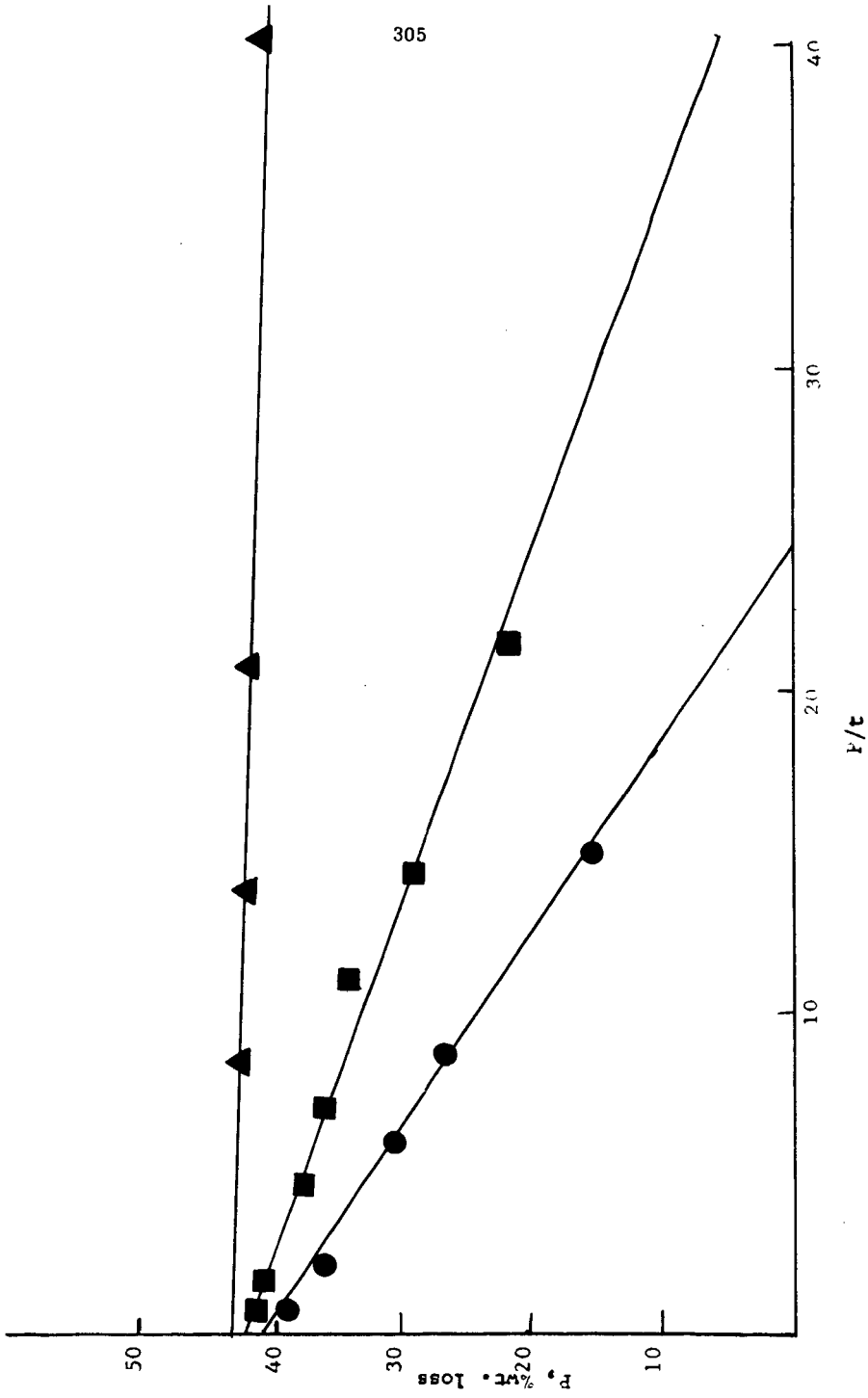


Fig. 2. Rate of dilute acid leaching fitted to the equation  $P = F/\sqrt{kt}$ , where  $F$  is maximum percent weight loss. (The round points denote 42/60; the square points denote 60/100; and the triangular points denote 150/200; all in mesh sizes).

DIRECT  $ZnCl_2$  HYDROCRACKING OF SUBBITUMINOUS COAL  
- REGENERATION OF SPENT MELT

C. W. Zielke, W. A. Rosenhoover and Everett Gorin

Research Division  
Consolidation Coal Company  
Library, Pennsylvania 15129

INTRODUCTION

The use of molten metal halides of the Lewis acid type for the hydrocracking of coal and coal extract was extensively investigated by Consol Research in the period 1964-1967 under a research contract with the Office of Coal Research. A complete description of the work is available in reports to the OCR.<sup>(1,2)</sup> Summary papers dealing with some of this work have also been presented.<sup>(3)</sup>

The above work concentrated most of its attention on the use of  $ZnCl_2$  as the molten halide and on the use of bituminous coal extract as feed to the process. Hydrocracking of the extract<sup>(1)</sup> and regeneration by a fluidized-bed combustion technique of the spent catalyst melt<sup>(2)</sup> from the process were both demonstrated in continuous bench-scale units.

A substantial program was also previously conducted in batch autoclaves on the direct hydrocracking of bituminous coal<sup>(1)</sup> with zinc chloride melts, but no work was done in either batch or continuous units on regeneration of spent melts from direct hydrocracking of coal.

Other workers have also examined direct hydrocracking of coal with molten metal halide catalysts. A large number of metal halide catalysts, for example, were examined for the direct hydrocracking of bituminous coal (Illinois No. 6) by Wald<sup>(4)</sup> and co-workers and by Kiovsky.<sup>(5)</sup> However, little or no data are available either on the direct hydrocracking of lower rank coals with  $ZnCl_2$  catalyst or on the regeneration of spent melts from such an operation. A large number of different coals ranging in rank from lignite to bituminous have more recently been tested in unpublished work at Consol Research. Almost all coals tested responded well to the  $ZnCl_2$  hydrocracking technique.

The present paper presents batch autoclave data on the direct hydrocracking of a single subbituminous coal only from the Powder River basin of Southeastern Montana. Comparative data were also obtained with the Pittsburgh Seam bituminous coal that was used in the previous work.<sup>(1)</sup> Data on the regeneration of simulated spent melts from such an operation are also given in a continuous bench-scale, fluidized-bed combustion unit.

EXPERIMENTAL

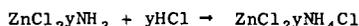
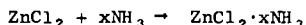
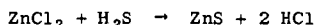
A.  $ZnCl_2$  Hydrocracking - Batch Autoclave Work

All tests were made in a 316 stainless steel, 300 ml rocking autoclave. The equipment, the product workup, analytical and calculational procedures employed are all identical to those previously described.<sup>(1)</sup> A constant hydrogen partial pressure was used in each run by monitoring it with a palladium-silver alloy probe within the autoclave. The sensitivity of the probe response was increased as compared with prior work by heat treating at 1100°F for four hours before use. Subbituminous coal from the Colstrip Mine in Southeastern Montana was used in this work. Its analysis is given in Table I. The residence time at temperature was 60 minutes in all the runs reported here.

## B. Regeneration by Fluid Bed Combustion

### 1. Preparation of Feedstock

During the hydrocracking process, the  $ZnCl_2$  catalyst becomes contaminated with  $ZnS$ ,  $ZnCl_2 \cdot NH_3$  and  $ZnCl_2 \cdot NH_4Cl$  that are formed by the  $ZnCl_2$  catalyst partially reacting with the sulfur and nitrogen liberated from the feed in the hydrocracking step:



The proportions of  $ZnCl_2 \cdot xNH_3$  and  $ZnCl_2 yNH_4Cl$  depend on the ratio of nitrogen and sulfur in the feed. In addition to these inorganic compounds, the catalyst leaving the hydrocracker also contains residual carbon that cannot be distilled out of the melt. In the case of direct coal hydrocracking, the catalyst also contains the coal ash.

The melt used in this work was prepared from the residue of hydrogen-donor extraction of Colstrip coal with tetralin solvent in such a way as to simulate the composition of an actual spent melt. The extraction was conducted in the continuous bench-scale unit previously described<sup>(2)</sup> at 775°F and 50 minutes residence time. The residue used was the solvent-free underflow from continuous settling<sup>(6)</sup> of the extractor effluent. The residue was then precarbonized to 1250°F in a muffle furnace. The melts were blended to simulate the composition of a spent melt from the direct hydrocracking of the Colstrip coal by blending together in a melt pot  $ZnCl_2$ ,  $ZnS$ ,  $NH_4Cl$ ,  $NH_3$  and the carbonized residue in appropriate proportions. Analysis of the feed melt used in this work is given in Table II.

### 2. Equipment and Procedure

Figure 1 is a diagram of the continuous, 2-7/8" ID fluidized bed combustion unit that was used. The melt is fed via syringe feeders and is dropped from a remote drip tip into a batch bed of fluidized solids that is fluidized by feed air that enters at the apex of the reactor cone. The carbon, nitrogen and sulfur are burned out in the fluidized bed and the  $ZnCl_2$  is vaporized. The gas,  $ZnCl_2$  vapor and elutriated solids leaving the reactor pass through the cyclone where the solids are collected. The cyclone underflow solids derive solely from the melt since the sizing of the bed solids is such that there is essentially no elutriation of this material. The solids collected at the cyclone then include coal ash, zinc oxide formed by hydrolysis of zinc chloride, and any unburned carbon or zinc sulfide. The gas then passes to the condenser where  $ZnCl_2$  is condensed out, then to the electrostatic precipitator to remove  $ZnCl_2$  fog and then to sampling and metering.

The analytical methods and calculational procedures are substantially the same as those previously described.

## RESULTS AND DISCUSSION

### Hydrocracking

A series of experiments were carried out at a relatively low temperature and hydrogen partial pressure of 358°C and 103 atms, respectively. Comparison runs were carried out with the Pittsburgh Seam coal from the Ireland Mine used in the previous work. Selected results are given in Table II.

The previous work with bituminous coal at these mild conditions was carried out without a hydrocarbon vehicle. These data are reproduced in the last column of Table II.

Attempts to run with the subbituminous coal at the above mild conditions without a vehicle were not successful due to a formation of a high viscosity mix which made temperature control very poor and yielded erratic results.

Methylnaphthalene was then used as a vehicle, but even in this case very poor results were obtained, i.e., conversion to MEK solubles and distillate products was very low. Results of this run are not reported since they are obscured by extensive cracking of the solvent.

The use of tetralin as a hydrogen-donor solvent, however, gave a very good conversion to MEK soluble products as shown in Table II. In this case, also some cracking of the solvent occurred, but the hydrogen consumption and gaseous products are calculated neglecting any contribution made to these quantities by hydrogenation and cracking of the tetralin.

The addition of a hydrogen-donor solvent to the subbituminous coal at these mild conditions, appear to be required to assist in melting of the coal to permit access of the molten halide catalyst.

The highly fluid Pittsburgh Seam coal, on the other hand, does not require addition of a vehicle as the data of Table II show. As a matter of fact, superior results were obtained in the absence of a vehicle although the difference may be due to the fact that in one case a cleaned coal was used, i.e., the poorer results with the vehicle may reflect some adverse effect of the mineral matter on the hydrocracking process. Also, a somewhat lower catalyst/coal feed ratio was used in the run without a vehicle.

Operation at these mild conditions are of interest where the objective is to produce low-sulfur fuel oil in major amounts as a co-product with gasoline. Previous work has shown that 65-80% of the MEK solubles may be recovered from the spent melt by extraction with a fraction of the distillate oil product. The data of Table IV, interestingly enough, show that the MEK soluble oil contains less than 0.2 wt % sulfur even when the high sulfur Pittsburgh Seam coal is used as feedstock.

The total liquid yield, i.e., C<sub>4</sub> through MEK soluble hydrocarbons at these mild conditions is almost as high with the subbituminous coal, i.e., 74.4 wt % of the MAF coal as with the bituminous coal, i.e., 75.5 and 76.7 wt % of the MAF coal with and without the use of a vehicle, respectively. The hydrogen consumption, on the other hand, is significantly lower for the subbituminous case. This is primarily because of the lower gas and distillate yields. The yield of heavy fuel oil, i.e., MEK soluble oil is significantly higher in the case of the subbituminous coal.

If the temperature and pressure is increased, then a vehicle is no longer necessary even in the case of the subbituminous coal. A series of experiments were carried out without a vehicle using a hydrogen partial pressure of 205 atm and at temperatures ranging from 370 to 427°C. The ZnCl<sub>2</sub>/MF feed ratio and the reaction time were held constant at 2.5/1 and 60 minutes, respectively, in these runs.

The above series of runs showed that two optimum temperatures existed. The first at about 385°C gave a maximum conversion to MEK soluble and lighter products of about 95%. The second at about 410°C gave a maximum conversion to gasoline expressed as C<sub>4</sub> x 200°C distillate of about 60 wt % of the MAF coal.

More detailed results of two runs, each near the above two optimum temperatures are given in Table III. Comparison is also given with results obtained with Ireland Mine coal at the lower of the above two temperatures.

It is noted that the conversions and hydrogen consumptions are very nearly the same for both coals. The yield of hydrocarbon distillates and particularly gasoline is about 20% higher for the bituminous coal case. The hydrogen consumption per unit of liquid distillate hydrocarbons produced is about 15% higher for the subbituminous coal case. The above differences are to be anticipated and are a result of the higher hydrogen and lower oxygen contents as noted in Table I of the bituminous coal.

The sulfur content of the MEK soluble oil is again as noted in Table IV very low.

#### Regeneration via Fluid Bed Combustion

Table V gives the conditions of runs presented here - essentially atmospheric pressure, superficial residence time of one second, excess air, i.e., 115% of stoichiometric, silica bed solids. Temperatures of 1800 and 1900°F were investigated. No operability problems such as ash agglomeration or defluidization of the bed were encountered at these conditions.

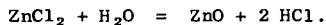
Table VI gives the distribution of carbon, sulfur and nitrogen in the products for runs at 1800 and 1900°F. One-hundred fifteen percent of stoichiometric air was used in both runs. The feed gas was pure air. It is apparent that the carbon, nitrogen and sulfur impurities almost completely burned out, i.e., 89% or more burn-out was achieved. The effluent melt contains less than 3% of the carbon and sulfur in the feed melt and 11% or less of the nitrogen.

Table VII shows the distribution of total coal ash as well as the coal ash components, silica and alumina, in the products in two runs at 1800°F. In Run 3, the feed gas was 100% air while in Run 11, the feed gas was 94.5% air and 5.5% anhydrous HCl. The HCl was added to prevent hydrolysis of the ZnCl<sub>2</sub>. This will be discussed further later. Eighty-nine percent or more of the total coal ash and silica and alumina were removed from the melt in the regeneration process. The ashes were either trapped in the bed or collected at the cyclone.

Table VIII shows the distribution of the ash components, iron, calcium, and magnesium in the products of the same two runs as in Table VII. Again, it is apparent that the large majority of these ash components were removed from the melt and that they were either trapped in the combustor bed solids or collected at the cyclone.

The distribution of sodium and potassium is not given in the tables. Essentially all of the sodium and potassium in the feed appears in the effluent melt. This is likely due to the potassium and sodium being converted into the chlorides which are sufficiently volatile to be vaporized along with the ZnCl<sub>2</sub>. This chlorine is considered to be irrecoverable. Hence, this method of regeneration is chiefly useful with coals that have relatively low alkali concentrations.

Table IX shows the distribution of zinc and chlorine among the products in Runs 3 and 11. The feed gas in Run 3 was pure air. In this run, about 10% of the feed zinc was found in the bed solids and cyclone solids as ZnO while 90% is in the melt as ZnCl<sub>2</sub>. The large amount of ZnO is formed by hydrolysis of ZnCl<sub>2</sub> in the combustor,



Because of the hydrolysis, a large amount of the chlorine in the feed melt is found in the gas as HCl. For the process to be economically feasible,  $ZnCl_2$  would have to be reformed from the ZnO and HCl products.

To preclude such a step, the HCl can be recycled with the feed air to prevent hydrolysis. Run 11 was made to test this concept where the feed gas contained 5.5% anhydrous HCl. The chlorine in the feed HCl amounted to 14.8% of the chlorine in the  $ZnCl_2$  feed. It is apparent that hydrolysis was almost completely suppressed and that the Zn in the feed melt was almost totally converted to and recovered as  $ZnCl_2$ .

Before starting this work, it was feared that considerable chlorine would be lost as  $CaCl_2$  by interaction of the calcium in the coal ash with the  $ZnCl_2$ , but it appears that essentially no chlorine is lost in this manner. It will be noted in both Runs 3 and 11, that the bed solids contain substantially no chlorine whereas they contained a large percentage of the calcium that was fed. Since  $CaCl_2$  is molten but nonvolatile at combustion temperature, it would be expected that any calcium chloride would be retained in the bed solids. Since none was, it is concluded that no calcium chloride was formed. (It also appears that no magnesium chloride was formed.)

Table X shows some pertinent reactions in the regeneration system. We determined the equilibrium constant for reaction (3) and obtained  $P_{ZnCl_2}$  of 57 torr whereas  $P_{ZnCl_2}$  in the combustor was about 120 torr. Hence, it might be expected that some  $CaCl_2$  would be formed. It is believed that the reason we didn't get  $CaCl_2$  is because of reactions such as (4) and (5) whose equilibria are probably far to the right. Kuxmann and Oder<sup>(7)</sup> have reported recovering zinc as pure  $ZnCl_2$  vapor from impure ores by reaction (4) carried out at about 1650°F.

It appears that some  $FeCl_2$  is formed but not in the amount that would be expected if equilibrium had been established in reaction (2). Reactions analogous to (4) and (5) with  $FeCl_2$  substituted for  $CaCl_2$  may be the reason for this. In any case, the equilibrium constant indicates that the amount of  $FeCl_2$  that can be formed is limited to 1 mol per 9 mols of  $ZnCl_2$ . We have unpublished data that indicates that  $FeCl_2$  does not affect catalyst activity.

We believe, based on the results just presented as well as other results, that fluid bed combustion provides a workable process for regenerating  $ZnCl_2$  from direct hydrogenation of western subbituminous coals. Other work not presented here indicates that the process can also be successfully applied to melts from direct hydrogenation of eastern bituminous coals also. The process is, however, restricted to coals having relatively low sodium and potassium contents so that economically prohibitive amounts of chlorine are not lost to these alkali metals. Lignites are the major type of coal that would be ruled out by the above restriction.

LITERATURE CITED

1. Consolidation Coal Co., R&D Report No. 39 to the Office of Coal Research, U.S. Dept. of the Interior, Under Contract No. 14-01-0001-310.  
  
Interim Report No. 2, "Research on Zinc Chloride Catalyst for Converting Coal to Gasoline - Phase I - Hydrocracking of Coal and Extract with Zinc Chloride - Vol. III, Book 1, March 1968.
2. Ibid.,  
  
Interim Report No. 2, "Pre-Pilot Plant Research on the CSF Process - Phase I - Regeneration of Zinc Chloride Catalyst" - Vol III, Book 2, March 1968.
3. a. Zielke, C.W., Struck, R.T., Evans, J.M., Costanza, C.P. and Gorin, E., Ind. Eng. Chem., Process Design Develop., 5, 151 (1966).  
  
b. Ibid., 158 (1966).  
  
c. Struck, R.T., Clark, W.E., Dudd, P.J., Rosenhoover, W.A., Zielke, C.W. and Gorin, E., Ibid., 8, 546 (1969).  
  
d. Zielke, C.W., Struck, R.T. and Gorin, E., Ibid., 8, 552 (1969).
4. Wald, M.M., British Patent 1,310,283, March 14, 1973. Assigned to Shell International Research Maatschappij, N.V.
5. Kiofsky, T.E., U.S. Patent 3,764,515, October 9, 1973. Assigned to Shell Oil Company.
6. Gorin, E., Lebowitz, H.E., Rice, C.H., and Struck, R.T., Proceedings of 8th World Petroleum Congress, PD10, 5 (1971).
7. Kuxmann, V. and Oder, F., Z. Erzbergbau Metallhüttenwesen, 19, 388 (1966).

TABLE I

Analysis of FeedstocksA. Proximate & Ultimate

	←———— Coals —————→			Regeneration Feedstock "Spent" Melt
	<u>Colstrip</u>	<u>Cleaned Ireland Mine</u>	<u>Ireland Mine</u>	
<u>Wt % MF Basis</u>				
Volatile Matter	37.3	43.4	42.5	--
Non Oxidized Ash	9.7	6.4	9.1	1.78
Organic (Hydrogen)	4.4	5.3	5.3	0.11
Carbon	68.0	76.5	74.5	5.03
Organic (Nitrogen)	1.1	1.6	1.1	0.09
Oxygen (by Diff)	16.1	8.3	7.7	0.24
Organic Sulfur	0.5	1.9	2.3	0.04
Pyritic Sulfur	0.2	0.9	1.7	--
Sulfate Sulfur	0.04	0.0	0.08	--
ZnCl <sub>2</sub>	--	--	--	85.34
ZnS	--	--	--	2.92
NH <sub>4</sub> Cl	--	--	--	3.20
NH <sub>3</sub>	--	--	--	1.25
<u>B. Ash Composition (Oxidized &amp; SO<sub>3</sub> Free Basis)</u>				
P <sub>2</sub> O <sub>5</sub>	--	--	--	0.15
S <sub>1</sub> O <sub>2</sub>	43.9	41.0	43.5	42.2
Al <sub>2</sub> O <sub>3</sub>	26.0	20.4	24.6	25.3
Na <sub>2</sub> O	0.25	0.6	0.5	0.47
K <sub>2</sub> O	0.15	1.5	1.6	0.21
CaO	17.3	2.8	1.7	18.7
MgO	6.7	0.7	0.7	7.1
Fe <sub>2</sub> O <sub>3</sub>	4.7	29.6	22.8	4.6
TiO <sub>2</sub>	1.0	1.1	1.0	1.4

TABLE II

Hydrocracking at "Mild" ConditionsA. Constant Conditions for All Runs

Temperature	358°C
Time at Temperature	60 minutes
Total Time Above 315°C	70 minutes (approx.)
H <sub>2</sub> Partial Pressure During Hydrocracking	103 atm. abs.
Coal Particle Size	-100 mesh

B. Variable Conditions and Yields

Coal	<u>Colstrip</u>	<u>Ireland Mine</u>	<u>Cleaned Ireland Mine</u>
<u>Gms Feed/gm MF Coal</u>			
ZnCl <sub>2</sub>	2.5	2.5	2.0
Solvent	0.5	0.5	0.0
Solvent Used	Tetralin	Tetralin	None
<u>Yields, Wt % MAF Coal</u>			
(C <sub>1</sub> -C <sub>3</sub> ) Hydrocarbons	1.7	5.1	5.2
(CO + CO <sub>2</sub> ) Gas	5.5	0.8	0.1
(H <sub>2</sub> O)	12.3	7.2	8.7
C <sub>4</sub> x 400°C Distillate	27.5	43.8	56.4
+400°C MEK Soluble	46.9	31.3	20.3
+400°C MEK Insoluble	10.5	16.5	12.8
N,O,S + H to Catalyst	<u>1.5</u>	<u>2.8</u>	<u>3.0</u>
Total	105.9	107.5	106.5
H <sub>2</sub> Consumed, Wt % MAF Coal	5.9	7.5	6.5
<u>Wt. % Conversion MAF Coal</u>			
To - 400°C Products	42.6	52.2	66.9
To - 400°C + MEK Solubles	89.5	83.5	87.2

TABLE III  
Hydrocracking at "Severe" Conditions

A. Constant Conditions for All Runs

Time at Temperature	60 minutes
Total Time Above 315°C	70 minutes
ZnCl <sub>2</sub> /MF Coal Feed Ratio	2.5
H <sub>2</sub> Partial Pressure	205 atm. abs.
Coal Particle Size	-100 mesh

B. Yields and Conversions, Wt. % MAF Coal

Coal	<u>Colstrip</u>	<u>Colstrip</u>	<u>Ireland Mine</u>
Temperature, °C	385	413	385
CH <sub>4</sub>	0.6	1.3	0.4
C <sub>2</sub> H <sub>6</sub> + C <sub>3</sub> H <sub>8</sub>	4.8	8.6	8.3
C <sub>4</sub> x 200°C Distillate	55.6	59.0	66.4
200 x 400°C Distillate	3.1	1.2	2.2
+400°C MEK Soluble	17.1	9.2	13.9
+400°C MEK Insoluble	5.2	8.7	6.0
CO + CO <sub>2</sub> + H <sub>2</sub> O	19.9	19.3	8.6
N, O, S + H to Catalyst	<u>2.4</u>	<u>2.2</u>	<u>3.3</u>
Total	108.7	109.5	109.1
H <sub>2</sub> Consumed, Wt. % MAF Coal	8.7	9.5	9.1
<u>Wt. % Conversion MAF Coal</u>			
To - 400°C Products	77.7	82.1	80.1
To - 400°C + MEK Solubles	94.8	91.3	94.0
Total - 400°C Hydrocarbons	64.1	70.1	77.3
<u>Total - 400°C Hydrocarbons</u>			
H <sub>2</sub> Consumed	7.4	7.4	8.5

TABLE IV  
Sulfur Content of +400°C MEK Soluble Oil

Coal	<u>Colstrip</u>		<u>Ireland Mine</u>	
Temperature, °C	358	385	358	385
H <sub>2</sub> Partial Pressure, atm	103	205	103	205
% Sulfur in MEK Solubles	0.17	0.04	0.17	0.18

TABLE V

GENERAL CONDITIONS

PRESSURE, PSIG	2.0
SUPERFICIAL AIR VELOCITY, FPS	1.0
SUPERFICIAL RESIDENCE TIME, SEC.	1.0
MELT FEED RATE, LB/HR.-FT. <sup>2</sup>	73
% OF STOICHIOMETRIC AIR	115
FLUIDIZED BED DEPTH, INCHES	12
TYPE OF BED SOLIDS	28 x 48M SILICA

TABLE VI

DISTRIBUTION OF C, S AND N IN THE PRODUCTS

RUN NUMBER	3	4
TEMP. , °F	1800	1900
% of STOICH. AIR	115	115
<u>DISTRIBUTION of C, %</u>		
BURNED to CO <sub>2</sub> (+ LOSS)	92.7	92.9
BURNED to CO	5.9	4.2
IN CYCLONE SOLIDS	0.4	0.5
IN MELT	1.0	2.4
<u>DISTRIBUTION of S, %</u>		
BURNED to SO <sub>2</sub> (+ LOSS)	91.3	96.4
IN BED	1.8	0.4
IN CYCLONE SOLIDS	3.8	1.4
IN MELT	3.1	1.8
<u>DISTRIBUTION of N, %</u>		
NH <sub>3</sub> BURNED to N <sub>2</sub> + H <sub>2</sub> O (+LOSS)	89.3	100.0
N IN MELT	10.7	0.0

TABLE VII

## DISTRIBUTION OF TOTAL COAL ASH, Si, Al, AMONG THE PRODUCTS

RUN NUMBER	3	11
TEMP., °F	1800	1800
<u>FEED GAS COMP., MOL %</u>		
AIR	100	94.5
ANHYDROUS HCl	-	5.5
<u>DIST. OF TOTAL ASH, %</u>		
BED SOLIDS (+ LOSS)	19	34
CYCLONE SOLIDS	70	59
MELT	11	7
<u>DIST. OF Si, %</u>		
BED SOLIDS (+ LOSS)	29	28
CYCLONE SOLIDS	67	68
MELT	4	4
<u>DIST. OF Al, %</u>		
BED SOLIDS (+ LOSS)	94	31
CYCLONE SOLIDS	}	64
MELT	6	5

318  
TABLE VIII

DISTRIBUTION OF Fe , Ca , Mg  
 AMONG THE PRODUCTS

<u>RUN NUMBER</u>	<u>3</u>	<u>11</u>
TEMP. , °F	1800	1800
<u>FEED GAS COMP. , MOL %</u>		
AIR	100	94.5
ANHYDROUS HCl	-	5.5
<u>DIST. OF Fe , %</u>		
BED SOLIDS (+ LOSS)	73 }	0
CYCLONE SOLIDS		61
MELT	27	39
<u>DIST. OF Ca , %</u>		
BED SOLIDS (+LOSS)	29	53
CYCLONE SOLIDS	48	42
MELT	23	5
<u>DIST. OF Mg , %</u>		
BED SOLIDS (+LOSS)	44	57
CYCLONE SOLIDS	43	41
MELT	13	2

TABLE IX

## DISTRIBUTION OF ZINC AND CHLORINE IN THE PRODUCTS

RUN NUMBER	3	11
TEMP., °F	1800	1800
<u>FEED GAS COMP., MOL %</u>		
AIR	100	94.5
ANHYDROUS HCl	-	5.5
<u>Cl DIST., % OF Cl IN FEED MELT</u>		
BED SOLIDS	.02	.01
CYCLONE SOLIDS	.44	.30
GAS	9.10	14.50
MELT (+LOSS)	<u>90.40</u>	<u>100.00</u>
TOTAL	100.00	114.80
<u>Zn DIST., % OF Zn IN FEED MELT</u>		
BED SOLIDS	5.5	.40
CYCLONE SOLIDS	4.4	.74
MELT (+LOSS)	90.1	98.90

TABLE X

SOME PERTINENT REACTIONS

K at 1800°



FIGURE 1

# FLUIDIZED COMBUSTION UNIT

